

**USDA-NRCS CONSERVATION INNOVATION GRANT
Final Report**

| | |
|--|--|
| Grantee Name: University of Nebraska Board of Regents-Extension | |
| Project Title: Demonstrate and adapt remote sensing technology to produce and utilize consumptive water use maps for the Nebraska Panhandle | |
| Agreement Number: 68-3A75-6-154 | |
| Project Director: Gary W. Hergert | |
| Contact Information: | Phone number: 308-632-1372, E-mail: ghergert1@unl.edu |
| Period covered by report: 1 August 2006 to 1 June 2011 | |
| Project end date: 31 August 2010 | |

Acknowledgements:

I wish to express our sincere appreciation to the USDA Natural Resources Conservation Service, the North Platte Natural Resources District, and the South Platte Natural Resources District, for providing financial support for this project. The collaboration in this study with the University of Idaho with Dr. Richard Allen of the Kimberly Research and Extension Center and Dr. Jeppe Kjaersgaard (now at South Dakota State) provided the initial training on the METRIC model, provided initial computer code, and provided advice and review during the study. Drs. Allen and Kjaersgaard worked closely with UNL faculty to advance the development of methods to integrate ET between satellite image dates that better account for impacts of precipitation events between image dates. They provided valuable advice on the implementation of spatial ET products the NRDs and NRCS might be able to implement with additional resources.

Dr. Ayse Irmak was a good choice as a younger faculty member who had the background and personnel to undertake learning METRIC. During the project, many of the things she learned and discovered, helped advance the state of processing within METRIC, especially her work on cloud-filling. Her GIS technician Ian Ratcliffe spent countless hours processing data to develop precise information and maps, as well as her graduate student Parikshit Ranade.

I would like to acknowledge the work of Peggy Penrose, GIS technician on the project at Scottsbluff who provided local GIS expertise and processing of crop mix maps. Part of this project was to see how 'transferable' the technology was and if it could be 'taught' to personnel with less than a PhD in evapotranspiration and energy balance education. It turned out to be much more complex than we envisioned when we started the project, but we also realized that any agency that does undertake to learn and use METRIC needs strong GIS technical support in addition to scientific guidance on interpretation of Landsat images and data omissions (primarily cloud masking).

I would like to acknowledge Gary Stone's work with the NRDs as the practical application part of this project to establish the soil water monitoring network (atmometers and WaterMark sensors) in the NE panhandle and his work with others at UNL on the development of the water management web site (<http://water.unl.edu/web/cropswater/nawmdn>). His

presentations, workshops and one-on-one contact with growers are having an impact on improving irrigation management in this area

Project Objectives:

The goal of the project was to accurately quantify net Consumptive Water Use (CWU) for different crops and range land vegetation by processing LANDSAT images using Mapping EvapoTranspiration with High Resolution and Internalized Calibration (METRIC™) algorithms for a portion of the Nebraska panhandle. The CWU maps were to be developed initially by the University of Idaho (UI) in conjunction with the University of Nebraska-Lincoln (UNL) for training purposes. The next step was to have UNL develop maps from the remaining years with checking by UI. The team of UI and UNL was to develop, test and demonstrate tools that would take the CWU maps and turn them into usable products for planning, managing and regulating groundwater resources. UI was to provide training to UNL in applying the METRIC equations, as they are critical to understand the data process including assumptions, and to make consistent and dependable decisions. These CWU maps were to be used to estimate net water use during the 1997, 2002 and 2005 growing seasons

Project Background:

Recurrent droughts across the High Plains and Inter-Mountain West have magnified the problem of declining ground water resources. The High Plains Aquifer (HPA), often referred to as the Ogallala aquifer, underlies parts of Colorado, Kansas, Nebraska, New Mexico, Oklahoma, South Dakota, Texas, and Wyoming. Nearly 30 percent of the ground water used for irrigation in the United States is extracted from the HPA.

A significant proportion of the HPA is located within Nebraska. Ground water-levels began declining in some parts of Nebraska after extensive irrigation development began in the 1960's (Figure 1)

Groundwater-level Changes in Nebraska - Predevelopment to Spring 2010

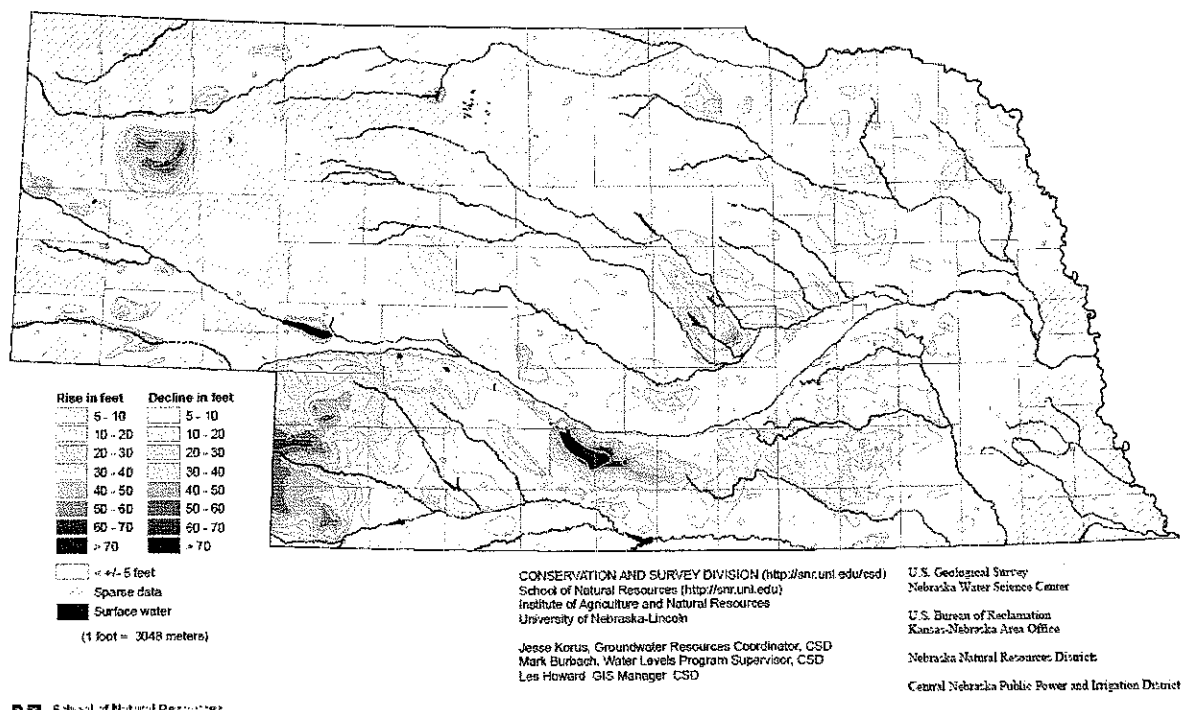


Figure 1. Groundwater level changes in Nebraska from predevelopment to spring 2010

The passage of Nebraska LB 108 in 1996 recognized the relationship between ground and surface water and LB962 (2004) provided new regulatory measures to conjunctively manage ground water and surface water. This legislation has led to changes in the way water resources are managed. In the North Platte and South Platte River Basins, surface water deliveries were reduced during the drought and the NPNRD and SPNRD have adopted groundwater pumping allocations that took effect during the life of this project.

Actual CWU from irrigated agriculture is almost exclusively the principal consumer of irrigation in the High Plains. CWU demands by irrigated crops in the HPA generally exceed natural precipitation and require supplementation from ground and surface water. Understanding and quantifying actual CWU across NRD management areas is essential to manage water resources. However, considerable uncertainty exists regarding the spatial and temporal distribution and variability of CWU estimates. The variation comes from differences in weather, precipitation timing and quantity, soils, crops and cropping systems, irrigation methods, their management and efficiencies, and consumptive use of water by natural vegetation.

Remote sensing technology has been used in land use mapping, geology, mineral exploration, to locate river beds and lakes, and to assess water resources, coastal environments, and forestry and rangeland resources. Application of algorithms to compute CWU by assessing the energy balance using Surface Energy Balance Algorithm for Land (SEBAL) (Bastiaanssen et al., 1998) and Mapping Evapo Transpiration with High Resolution and Internalized Calibration

(METRIC) (Allen et al., 2007a) have been used. Accurately quantifying CWU is necessary to provide prediction of the timing and the spatial extent of potential depletions or gains in both the short-term and in the long-term management of surface and ground water used for irrigated systems. This information is also required to support hydrologic modeling such as the Cooperative Hydrology Study (COHYST) model which is used extensively in Nebraska.

List of deliverables/products from project activities:

The primary product of this project was to be CWU maps developed from LANDSAT images by applying METRIC algorithms. The tools and products that were to be developed and demonstrated for the North and South Platte Natural Resource Districts (NPNRD & SPNRD) include: (1) Developing CWU maps for areas irrigated by groundwater sources and by surface water supplies. (2) Sampling of CWU data across the project area to develop locally calibrated Crop Coefficient (Kc) curves for specific crops [alfalfa, wheat, corn, dry bean and sugar beet]. (3) Produce maps of net differences in CWU from irrigated agriculture and CWU from rainfed agriculture and; (4) Produce maps of net differences in CWU from irrigated agriculture and CWU from natural vegetation. The products were to be shared between UNL, the NRDs, and the area NRCS offices.

University of Idaho Efforts

The final report for the part of the project conducted by UI is included as Attachment 1. It describes the setup and processing of Landsat satellite imagery covering a portion of the Nebraskan Panhandle for year 1997 using METRIC. Eight Landsat images from path 33 row 31 for 1997 were processed to produce estimates of monthly and growing season (April – October) ET. Counties within the area contained by the Landsat path 33 row 31 image includes Cheyenne, Kimball, western Deuel, Banner, Morrill, Scotts Bluff, southern Sioux and western Garden Counties. In addition, for training purposes and comparison to ET products generated in parallel with the University of Nebraska, an additional seven images from 1997, 2002 and 2005 were processed. In conjunction with the University of Idaho applications, the University of Nebraska has generated monthly and seasonal ET estimates from paths 32 and 33, row 31, for the study years 2002 and 2005, covering the entire geographical domain of the NPNRD and SPNRD.

University of Idaho Summary

ET was calculated with a spatial resolution of 30 m. However, because the thermal information contained in the Landsat 5 images was 120 m resolution and because the METRIC process relies heavily on the thermal information, the 'real' spatial resolution or spatial accuracy and representativeness of the final ET images is probably somewhere between 30 and 120 m. It is, nevertheless, presented as 30 m for ease of handling and sampling. The daily ET maps from 1997 were extrapolated into monthly and seasonal (April 1-October 31) ET estimates. The images processed from 2002 and 2005 were used for training and comparison to images being processed in parallel by the University of Nebraska. The primary focus areas for the METRIC processing were irrigated agricultural areas in the project area. Land areas adjacent to the project

area including surrounding rangeland, forest and wilderness areas, agricultural and wetland areas were additionally processed.

Developments were made to the METRIC model during this project to improve performance under the specific conditions of the western Nebraska study area. These specific conditions included the substantial amount of late spring and summer rainfall events and large amounts of clouds in some images that complicated the estimation of monthly and seasonal ET. Improvements included a new cloud gap filling procedure for the ETrF estimates which automatically adjusts for background evaporation from recent precipitation, gap filling of NDVI, the generation of grids of precipitation and ETr used to estimate distributed bare soil evaporation and to adjust the satellite date ET estimates for background evaporation, and using evaporative fraction, EF, rather than ETrF, as the vehicle to extrapolate from the instantaneous, at-satellite overpass time ET estimates to daily values for rangeland.

Since some degree of cloudiness is present within some portions of the images, those areas of some images had to be masked out. The resulting gaps were filled with data from previous and following image dates which increased uncertainties in the ET and ETrF estimates for the mountain areas. Evaporation from open water bodies within the image was estimated using a function developed for larger, clear lakes in southern Idaho. As a result, the ET estimates from small water bodies, including small shallow lakes, canals, rivers and cattle ponds may have an increased uncertainty compared to larger water bodies.

Monthly and growing season (April-October) ET and ETrF (fraction of alfalfa reference ET) from 1997 was calculated by splining the ET fraction determined for each satellite image over each month and multiplying by reference each day, following adjustment of background evaporation to better represent the periods between satellite image dates.

Differencing of April – October ET and reported precipitation for the image area show areas of substantial recharge where $P > ET$, and areas of irrigation, where $ET > P$. All ET data products are available for each image date, month, and growing season as ERDAS Imagine (.img) files.

A list of ‘value-added’ products that could be developed from this and further METRIC calculations was developed to give to the NRDs (Attachment 2). This information was presented when the final oral report was presented to a combined meeting of the NPNRD and SPNRD March 28, 2011. A follow-up technical session was held with NRD, NE DNR and other NE state agency personnel on March 29, 2011. Bill Sabatka, NE State Water Management Engineer with NRCS attended the meeting. The consensus was that further funding would be required to provide the ‘value-added’ products. With current decreased state and local budgets, the NPNRD and SPNRD did not feel they could provide additional funding. All data files (500 GB drive) from the project and procedures were shared with the NPNRD, SPNRD and with Mr. Sabatka.

University of Nebraska Efforts

Data Processing and Protocol

Weather data

The final report for the part of the project conducted by the University of Nebraska is included as Attachment 3. It describes the setup and processing of Landsat satellite imagery covering a portion of the Nebraskan Panhandle for years 2002 and 2005 using METRIC. METRIC utilizes alfalfa reference ET (i.e., ET_r) as calculated by the ASCE standardized Penman-Monteith equation (ASCE-EWRI 2005). Weather data at a single weather station from each Landsat Path/Row were used for the internal calibration of METRIC for the area of interest. High Plains Regional Climate Center (HPRCC) Automated Weather Data Network (AWDN) weather stations were used from the Scottsbluff (Landsat path 33, row 31) and Sidney (Landsat path 32, row 31) stations. The AWDN stations record hourly data for air temperature, humidity, soil temperature, wind speed and direction, solar radiation, and precipitation.

The generation of final METRIC products for monthly periods was produced from the individual images using daily reference ET maps derived from reference ET data from all AWDN stations in and surrounding the two Landsat paths. The daily reference ET maps were developed via interpolated maps of reference ET for the project area and were used to develop the monthly and seasonal ET maps. The weather data quality control is described in Appendix A of Attachment 3. A daily soil water balance model was used to determine whether any residual evaporation existed from exposed soil at the time of each satellite image due to recent rainfall events. The residual evaporation was considered when assigning a value for ET from the 'hot' anchor pixel during the METRIC calibration process, where the hot anchor pixel was generally a bare soil. The FAO-56 (Allen et al., 1998) soil evaporation model was used to estimate residual evaporation from the upper 0.125 m soil layer. Soil properties of the area were obtained from Soil Survey Geographic (SSURGO) Database from Natural Resources Conservation Services (NRCS).

Satellite Imagery

Individual satellite images were selected by the project PIs from the University of Idaho and the University of Nebraska based on a list of available Landsat 5 and Landsat 7 preview images for the years 1997-2007 prepared by the University of Idaho. Representatives from the North Platte and South Platte NRDs approved the list. The principles of the image selection are described in Appendix B of Attachment 3. METRIC can only estimate ET in satellite imagery free of major atmospheric disturbances such as clouds, jet contrails and smoke and cloud shadows. The major image selection criteria were therefore based on whether 1) the irrigated agricultural areas along the South Platte River and along Pumpkin Creek were relatively cloud free, and, of secondary importance, that 2) rangeland areas within the NRDs were free from clouds. Most imagery had some degree of cloud cover.

Gap-filling of Landsat 7 ETM+ due to the failure of the Scan Line Corrector (SLC)

On May 31, 2003, image data from the ETM+ sensor onboard the Landsat 7 satellite began exhibiting "striping" artifacts. It was determined that the problem was a result of the failure of the Scan Line Corrector (SLC) which compensates for the forward motion of the satellite. Due to the SLC failure, about 22% of the scene area is missing in SLC-off images. Processing of SLC-off images for 2005 required replacing the missing data. Because Landsat 7 was still able to acquire imagery, the USGS developed new image products to fix the striping problem by combining two separate dates or by interpolation to fill in the data gaps.

We carried out our own correction to the scan line correction for Landsat7 datasets by using convolution filtering (nearest neighborhood method) with a 5X5 pixels majority function (Sing and Irmak, 2009).

Digital Elevation Model

A digital elevation model (DEM) is required input for METRIC. A DEM is used for the calculation of DEM-corrected surface temperature, determination of hot and cold pixel elevations, and the calculation of air density for use in sensible heat estimation. A DEM of the study area was obtained from the EROS Data Center Seamless Data Distribution System (<http://seamless.usgs.gov>).

Land Use Data

A land use map was used for the parameterization and estimation of the aerodynamic roughness parameter and soil heat flux in the METRIC model. A composite land use map was generated by combining (1) the 1991-1993 Nebraska Gap Analysis Program (GAP), (2) the 1997, 2001, or 2005 Nebraska Cooperative Hydrology Study (COHYST), and (3) the 2001 National Land Cover Dataset (NLCD). Three land use maps were created for the Nebraska Panhandle by University of Nebraska: 1997, 2001, and 2005. These maps correspond to the years the COHYST land use maps were generated. The land use maps were reprojected into NAD 83 GRS 1980 UTM 13 using nearest neighbor resampling.

Due to the different land use systems having the same values for different classes, NE GAP and NE COHYST values were reclassified. The 2001 land use data, used for input to ET estimation for 2002, was considered acceptable because for agricultural areas, the surface roughness parameter is a function of LAI not specific crop type. By combining the classification strengths of both maps, the surface roughness estimation was improved.

Calibration of METRIC Model

METRIC version 2.0.4 was used for UNL processing (Allen et al., 2010). The primary focus for this project was to generate estimates of ET from agricultural areas. Because of this, METRIC was calibrated with a focus on accurate estimation of ET from agricultural areas. However, because the entire Landsat scenes were processed, efforts were made to minimize uncertainty in ET estimates from other land cover types present within the imagery, including forests, riparian vegetation, and rangeland.

Refinements to METRIC during this work

To better account for impacts of local precipitation events and image cloudiness in the study area on the final ET estimates, new methods were developed and implemented, especially during integration of ET between satellite images, to account for conditions that deviate from the description of the standard Level 1 METRIC model application. Some of these adjustments are referred to as Level 2 processing (Allen et al., 2010).

Improvements to METRIC that were advanced during this study include a new cloud gap filling procedure for the ETrF estimates that automatically adjusts for background evaporation from recent precipitation, gap filling of NDVI, the generation of grids of precipitation and ETr used to estimate distributed bare soil evaporation that is, in turn, used to adjust the satellite date

ET estimates for background evaporation. In addition, UNL collaborated with UI to explore the use of evaporative fraction, EF, rather than ET_rF, to extrapolate from the instantaneous, at-satellite overpass time ET estimates to daily values for rangeland portions of scenes. These new developments and their applications are described in Appendix E of Attachment 3.

Calibration Philosophy

The METRIC model calculates actual ET by utilizing satellite images containing both short wave and thermal bands. METRIC uses what are termed cold and hot pixels. These should be located near the weather station (~within 50 km). The cold pixel is used to define the amount of ET occurring from the well-watered and fully vegetated areas of the image which represent instances where the maximum (or near maximum) amount of available energy is being consumed by evaporation. For this study, we selected a number of cold pixel candidates for each image representing an agricultural area under center pivot irrigation system that has vegetation at full cover (LAI is usually greater than 4.0 m² m⁻²) to estimate ET at the cold pixel. We assumed that $ET = 1.05 ET_r$ at the cold pixel. The ET_r is the rate of ET from the alfalfa reference calculated using the ASCE Standardized Penman-Monteith equation for alfalfa. H for the cold pixel was then calculated as $H = R_n - G - 1.05 ET_r$.

The selection of the hot pixel followed the same procedure as for the cold pixel. The hot pixel should be located in a dry and bare agricultural field where one can assume evaporative flux is 0. We selected the hot pixel candidates with a surface albedo similar to dry and bare fields (0.175-0.2) with very low LAI (usually less than 0.1). In western Nebraska, we found that the hot pixels could not be assumed to have zero evaporation because of high variability of rain in the region that tended to supply some residual evaporation over extended periods. Therefore, H was estimated as $R_n - G - ET_{bare\ soil}$, where $ET_{bare\ soil}$ was obtained by running a daily soil water balance model of the surface soil using ground-based weather measurements (Allen et al., 1998). The METRIC model was then run for each of the cold and hot pixel candidates. The best suitable anchor pixels were determined based on the distribution of ET_rF over the image.

Daily Soil Water Balance Model to check METRIC calibration

A daily soil water balance model was applied for 2002 and 2005 using precipitation and ET_r from the Sidney and Scottsbluff AWDN stations. The model is based on the two-stage daily soil evaporation model of the United Nations Food and Agriculture Organization's Irrigation and Drainage Paper 56 (Allen et al., 1998). The soil water balance is a 'slab' model, where the soil is assumed to dry uniformly. The results from the soil water balance were used to determine ET_rF for hot pixel selection, an internal calibration step for running METRIC.

UNL Results

Reference Evapotranspiration

Reference evapotranspiration used for estimating ET_c has been based either on grass (ET_o) or alfalfa (ET_r) reference surfaces (ASCE-EWRI 2005). The ET_r values for each of the weather station under the study area were estimated using the standardized American Society of Civil Engineers Penman-Monteith (ASCE-PM) equation (ASCE-EWRI 2005) on an hourly time step. Hourly time steps are needed to produce ET_r for calibration of the METRIC energy balance

estimation process at the time of the Landsat overpasses. The hourly ET_I values are summed to daily totals to provide a basis for producing daily and monthly ET.

We used the RefET software (version 3) of the University of Idaho (Allen, 2010). Automatic weather station (AWS) data, obtained from the High Plain Regional Climate Center (HPRCC), were used for ET_I calculations. The datasets measured at the stations included daily maximum and minimum temperature (T_{max} and T_{min}), relative humidity (RH), wind speed (u), and solar radiation (R_s). Since estimates of ET_{ref} can only be as good as the weather data quality, a rigorous data quality check was carried out on the climatic data. The details of data quality check are described in Appendix A.

Daily Fraction of Reference Evapotranspiration (Relative ET or Crop Coefficient)

ET_{rF} maps were generated from Landsat 5 and Landsat 7 satellite imagery. Each satellite image for 2002 and 2005 was processed on a pixel by pixel basis using METRIC to estimate land surface energy balance fluxes. Meteorological data used for the model inputs came from the respective AWDN weather stations. Maps of reflectance of short wave radiation, vegetation indices (NDVI and LAI), surface temperature, net radiation, and soil heat flux were generated as intermediate products during the METRIC processing. Daily (24-h) ET_I totals for the processed Landsat 5 and Landsat 7 image were developed. When the ET_{rF} images were interpolated over time to create monthly ET images, daily ET_{rF} was determined by spline and multiplied by daily ET_I . During the interpolation process, daily ET_I 'surfaces' were created over the image area, as described in Appendix A, using HPRCC and NWS COOP weather stations from within and outside the image footprint.

The final output from the METRIC model was images showing instantaneous ET_{rF} (fraction of alfalfa based reference ET, ET_I) at the satellite overpass time. The ET_{rF} is defined as the ratio of instantaneous ET (ET_{inst}) for each pixel to the alfalfa-reference ET calculated using the standardized ASCE Penman-Monteith equation for alfalfa (ET_I) following the procedures given in ASCE-EWRI (2005). The ET_{rF} serves as a surrogate for K_c (basal crop coefficient) and has been used with 24-hour ET_I in order to estimate the daily ET at each Landsat pixel. The ET_{rF} values range from 0 to about 1.05. The ET_{rF} of well-irrigated and fully vegetated agricultural crops usually have an ET_{rF} of 1.0 on average, while the dry and bare agricultural fields have little evaporative flux and range from 0 to 0.15 unless there is a recent precipitation event prior to satellite overpass. Daily ET in mm/day was calculated by multiplying ET_{rF} by daily ET_I values. Procedures for obtaining daily estimates of ET and ET_{rF} are further explained in Appendix E.

Contrasting ET for 2002 and 2005

Comparing growing season ET for 2002 and 2005 showed substantial differences in ET for rangeland and non-irrigated (rainfed) agricultural areas. Rainfed regions around Scottsbluff averaged about 12 inches of ET during April-October 2002, whereas these same areas averaged about 18 inches of ET for 2005. These differences in ET are consistent with precipitation recorded at the Scottsbluff station, where recorded rainfall was only 8 inches during 2002 and was 20 inches during 2005. It is recognized that these rainfall totals are for point locations and can contain some error. However, 2002 was a dry year and 2005 a wet year, which is exhibited by the ET images produced during this study.

Summary and Discussion of UNL Efforts

The METRIC model was used to estimate surface energy fluxes at the same scale as the input imagery, which is 30x30 m pixel size in the case of Landsat 5 and/or 7 satellite images (Allen et al., 2010). The METRIC algorithms were applied over a crop growing season (April to October) for 2002 and 2005 for the North Platte and South Platte NRDs using Landsat 5/7 TM images. The project area consists of Landsat path 32-33, row 31 for 2002 and path 33, row 31 for 2005. Meteorological information from automated weather stations (AWS) was used during the calibrations of METRICTM. AWS data from Scottsbluff were used in for path 33 row 31 and the Sidney AWS was used for path 32, row 31. Extensive data quality analyses were conducted on climate data. A distributed daily water balance model was used to estimate residual moisture from the bare soil for 2002 and 2005.

Images were acquired as systematic terrain-corrected (Level 1T) with a 30m spatial resolution and the thermal band was re-sampled to 30m pixels. The satellite overpass times were acquired from the image meta data files to estimate zenith angle of the sun, instantaneous values of wind speed at 200m, air humidity, and reference evapotranspiration (ET_r).

Creating maps of ET that are useful in management and in quantifying and managing water resources requires the computation of ET over monthly and longer periods such as growing seasons or annual periods. Interpolation between images involves treatment of clouded areas of images, accounting for evaporation from wetting events occurring prior to satellite overpass. Daily ET maps of the Nebraska Panhandle are shown in Appendix B. The images shown there have not had cloud masks applied. Innovative cloud filling methods developed to reconstruct clouded areas of images to acceptable ranges, and monthly and seasonal ET map were generated for each path and row. The monthly and seasonal ET for 2002 was completed by combining (mosaicking) Landsat paths 32-33.

Our results show that ET is highly variable in space and time due to variability in land use, climatic conditions, soil properties, and management practices. Spatial variation in soil properties affect surface soil evaporation and surface energy balances, and cause within-field and across field variability in ET. Satellite remote sensing provides an opportunity for representing spatial and temporal variation of ET.

METRIC ET Mapping Summary

The original goal and objectives of the project were mostly accomplished. What we were not able to accomplish was taking a very technical process and developing practical end-use products that could be used by water management entities. Those products could be developed, but it would take much more work, time and money than we had for this project. I imagine that at least an additional 2 years of work from Drs. Allen or Irmak with local NRDs or DNR would be required to get to that stage.

When this project was initiated, there was the hope and expectation that once we were able to develop expertise in NE, that we would have a 'trainer' who could further train other NRD and or NRCS personnel to use METRIC and develop the products we proposed. The METRIC processing turned out to be much more involved and complicated than we originally estimated. Processing requires a well-trained individual with adequate background and knowledge about ET, GIS modeling capability plus an understanding of energy balance (soil and

atmosphere) and a full-time GIS technician to manipulate all the data from the images discussed in the reports from Drs Allen and Irmak. I believe we have a good start and we now have expertise in Nebraska with Dr Ayse Irmak and her GIS technician Ian Ratcliffe to move forward. Dr. Allen also has this capability, but my sense is that it requires an expert 'in the area' to work closely with those who want to develop the capabilities of METRIC. This has been done in the state of Idaho with Dr. Allen consulting with the ID Department of Water Resources.

University of Nebraska Educational Efforts

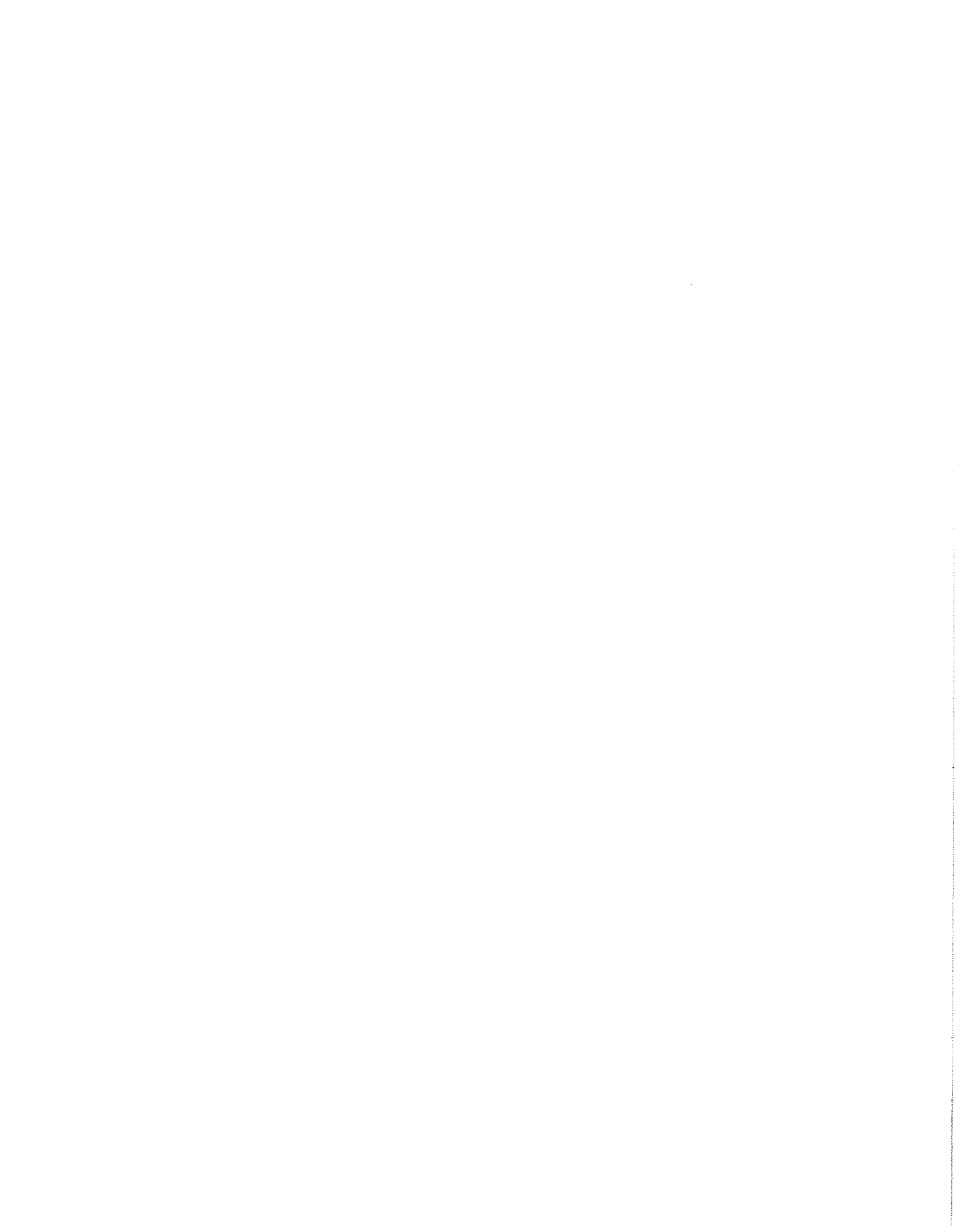
Another aspect of this project addressed the practical application. Early on, we realized that it would be several years before METRIC might be developed to a stage that it would actually assist producers with real-time irrigation management. Gary Stone was hired as an extension educator on this project to work on training, installation and maintenance of the atmometers (ET gages) and WaterMark™ soil moisture sensors with the cooperators in each of the NRDs. An educational program on using the atmometers and WaterMark sensors was developed by the extension educator and presented to cooperators in the NRDs and NRCS clientele, to educate and expand the grower base in irrigation water management practices. Presentations on the METRIC™ project were made to various organizations across the state and included the Nebraska Unicameral Agriculture and Natural Resources joint subcommittee hearing, Nebraska Natural Resources Commission, Nebraska Department of Natural Resources, Nebraska Golf Course Superintendents and weed managers. Data was collected throughout the season from the atmometers in each of the hydrologic units that are part of the North Platte and South Platte NRDs.

The data from the different monitoring sites was entered in the NE Agricultural Water Management Data Network (NAWMDN) web site (<http://water.unl.edu/web/cropswater/nawmdn>) for the 2009 and 2010 growing seasons. Using this as a base and with the help of an additional grant from NE DNR and the NP, SP and UNW NRDs, the educator expanded the cooperator base utilizing ET gages. Eighteen additional ET gage sites were installed across the Panhandle of Nebraska, six ET gages in each of the Panhandle NRDs respectively. Additional meetings were conducted with the new cooperators to educate them in irrigation water management practices utilizing the ET gages and WaterMark™ soil moisture sensors. Cooperative assistance was provided by NRD staff and NRCS staff when required for meetings or cooperator contacts. The data from these ET gages are also being collected and posted to the NAWMDN web site for grower utilization in irrigation water management during the growing season across the area. The data collected from these ET gage sites may also be utilized by the North and South Platte NRDs in the Nebraska COHYST hydrology study. As progress continues with the project, updates will be made to the METRIC website (<http://www.panhandle.unl.edu/metric/index.htm>).

REFERENCES

- Allen, R. G., Pereira, L. S., Raes, D., and Smith, M. 1998. Crop evapotranspiration: Guidelines for computing crop water requirements. United Nations FAO, Irrigation and Drainage, N.Y., Paper No. 56. (<http://www.fao.org/docrep/X0490E/X0490E00.htm>) February 5, 2007.
- Allen, R. G., M. Tasumi, and R. Trezza. 2005. Benefits from Tying Satellite-based Energy Balance to Ground-Based Reference Evapotranspiration. International Conference on Earth Observation for vegetation monitoring and water management. Naples, Italy, 10-11 Nov. 2005
- Allen, R. G., M. Tasumi, R. Trezza, 2007a Satellite-Based Energy Balance for Mapping Evapotranspiration with Internalized Calibration (METRIC) – Model J. *Irrig. Drain. Eng.*, 133(4), 380-394.
- Allen, R. G., M. Tasumi, A. Morse, R. Trezza, J. L. Wright, W. Bastiaanssen, W. Kramber, W. Lorite, I. Robison, C. W., 2007b Satellite-Based Energy Balance for Mapping Evapotranspiration with Internalized Calibration (METRIC) – Applications. *J. Irrig. Drain. Eng.*, 133(4), 395-406.
- Allen, R. G. 2010. Procedures for adjusting METRIC-derived ET_{IF} Images for Background Evaporation from Precipitation Events prior to Cloudfilling and Interpretation of ET between Image Dates. Report, University of Idaho. 11 pages. Version 7, last revised April 2010.
- ASCE-EWRI, 2005. The ASCE Standardized Reference Evapotranspiration Equation. R. G. Allen, I. A. Walter, R. L. Elliot, T. A. Howell, D. Itenfsu, M. E. Jensen, and R. L. Snyder (eds). Environmental and Water Resources Institute (EWRI) of the Am. Soc. of Civil. Engrs, ASCE, Standardization of Reference Evapotranspiration Task Committee Final Report. ASCE, Reston, Virginia
- Bastiaanssen, W. G. M., Menenti, M., Feddes, R. A. and Holtslag, A. A. M. 1998. "A remote sensing surface energy balance algorithm for land (SEBAL): 1. Formulation" *J. Hydrol.*, 212-213, 198-212
- Ranade, P. 2010. Spatial Water Balance for Bare Soil University of Nebraska Report, 10 pp
- Singh, R. K., A. Irmak, S. Irmak and D. L. Martin. 2008. Application of SEBAL for mapping evapotranspiration and estimating surface energy fluxes in south central Nebraska. *J. Irrig. and Drain. Eng.*, ASCE 134(3):273-285.
- Singh R., and A. Irmak. 2009. Estimation of Crop Coefficients Using Satellite Remote Sensing. *J. Irrig. and Drain. Eng.*, ASCE 135(5): 597-608.

Attachment 1



Remote Sensing Technology to Produce Consumptive Water Use Maps for the Nebraska Panhandle

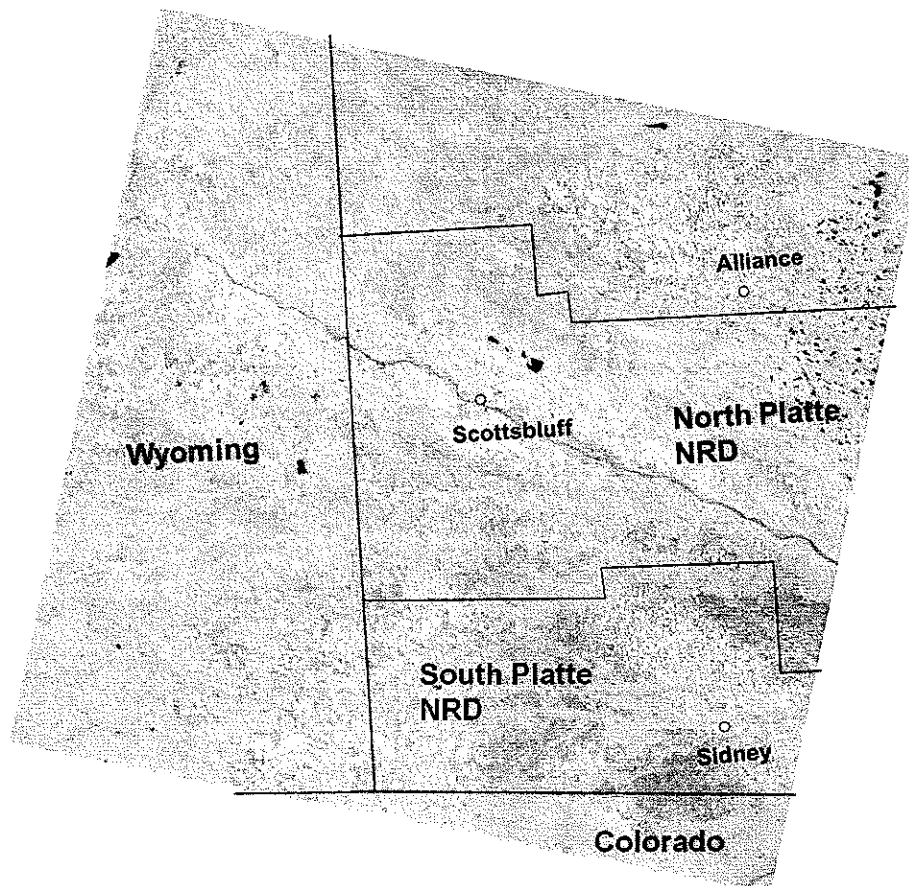
Dr. Jeppe Kjaersgaard and Dr. Richard Allen
University of Idaho
Kimberly, Idaho

Final Research Completion Report

Submitted to

University of Nebraska

August 2010



Acknowledgements. This work by the University of Idaho was funded by the University of Nebraska who was, in turn, funded by the USDA Natural Resources Conservation Service (NRCS) and by the North Platte and South Platte Natural Resources Districts. The University of Idaho acknowledges the fruitful, collaborative working relationship established during this study between the Univ. Idaho and Univ. Nebraska research faculty and staff, notably with Dr. Ayse Irmak, College of Natural Resources, Dr. Gary Hergert, Scottsbluff Research Center, Ian Ratliffe, College of Natural Resources, Gary Stone and Peggy Penrose, Scottsbluff Research Center. Drs. Darrell Martin, Sashi Verma, Suat Irmak and Ron Yoder of the Dept. of BioResources Engineering at UNL also guided and encouraged this research and developments. Mr Clarence Robison, Univ. Idaho, provided IT and GIS support at Kimberly.

Introduction

This report describes the setup and processing of Landsat satellite imagery covering a portion of the Nebraskan Panhandle for year 1997 using the University of Idaho METRIC (Mapping Evapotranspiration with high Resolution and Internalized Calibration) procedure for determining evapotranspiration (ET). Evapotranspiration is calculated within METRIC using a surface energy balance that produces instantaneous (at approximately 1100 overpass time) and daily values for ET. The objective of the study was to produce spatial estimates of monthly and growing season ET for irrigated agriculture, dryland agriculture and rangeland for the area covering the western portions of the North Platte and the South Platte Natural Resource Districts (NRD).

ET was calculated with the same spatial resolution as the satellite image which is 30 m in the case of Landsat. The geographic location of the western portion of the North Platte and South Platte NRDs is contained within a single Landsat scene, as shown in Figure 1, and the entire Landsat scene (approximately 150 x 150 km), which also includes portion of south east Wyoming and north east Colorado, was processed by METRIC

Eight Landsat images from path 33 row 31 for 1997 were processed to produce estimates of monthly and growing season (April – October) ET. Counties within the area contained by the Landsat path 33 row 31 image includes Cheyenne, Kimball, western Deuel, Banner, Morrill, Scotts Bluff, southern Sioux and western Garden Counties. In addition, for training purposes and comparison to ET products generated in parallel with the University of Nebraska, an additional seven images from 1997, 2002 and 2005 were processed. The dates of the satellite images processed for ET using METRIC are listed in Table 1. In conjunction with the University of Idaho applications, the University of Nebraska has generated monthly and seasonal ET estimates from paths 32 and 33, row 31, for the study years 2002 and 2005, covering the entire geographical domain of the North Platte and South Platte NRDs.

The METRIC procedure utilizes the visible, near-infrared and thermal infrared energy spectrum bands from Landsat satellite images and weather data to calculate ET on a pixel by pixel basis. Energy is partitioned into net incoming radiation (both solar and thermal), ground heat flux, sensible heat flux to the air and latent heat flux. The latent heat flux is calculated as the residual of the energy balance and represents the energy consumed by ET. The topography of the region was incorporated into METRIC via a digital elevation model (DEM), and used to account for impacts of near surface air temperature gradients in the energy balance. METRIC was calibrated for each image using ground based meteorological information and identified 'anchor' conditions (the cold and hot pixels of METRIC) present in each image. A detailed description of METRIC can be found in Allen et al. (2007a,b; 2010)

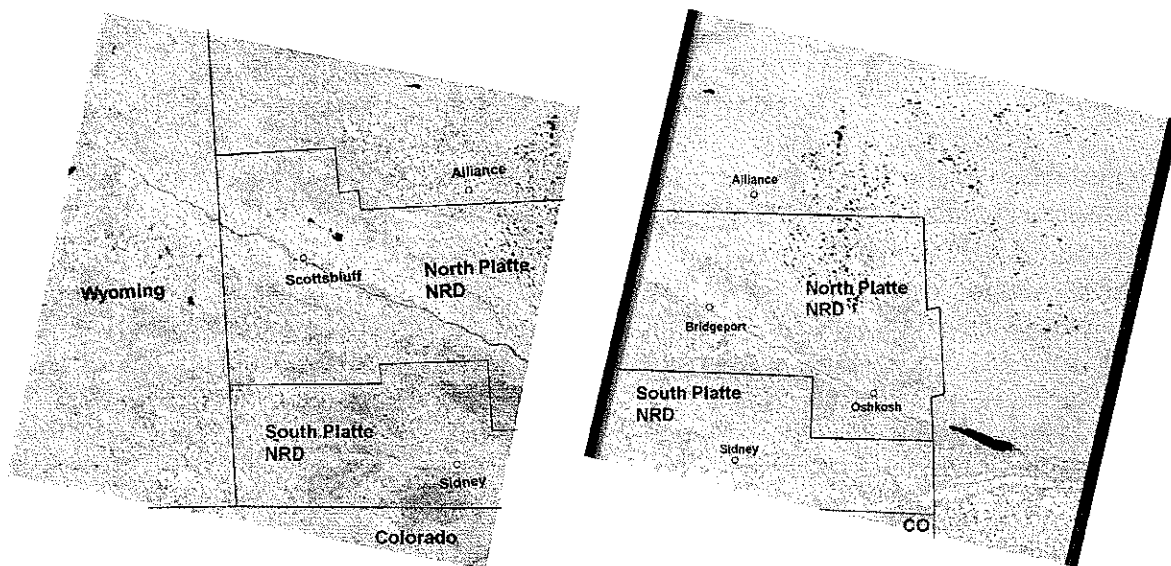


Figure 1. The Landsat image domain for Landsat path 33 row 31 (from June 26, 1997) and path 32 row 31 (from June 8, 2002) showing the state boundaries (red lines) and the approximate boundaries of the North Platte and the South Platte Natural Resource Districts (NRDs) (black lines)

Table 1 Dates, satellite platform and path/row processed using METRIC by the University of Idaho.

| Date | Satellite | Path | Row |
|------------|-----------|------|-----|
| 04/23/1997 | Landsat 5 | 33 | 31 |
| 05/09/1997 | Landsat 5 | 33 | 31 |
| 06/26/1997 | Landsat 5 | 33 | 31 |
| 07/12/1997 | Landsat 5 | 33 | 31 |
| 08/13/1997 | Landsat 5 | 33 | 31 |
| 08/22/1997 | Landsat 5 | 32 | 31 |
| 09/30/1997 | Landsat 5 | 33 | 31 |
| 10/16/1997 | Landsat 5 | 33 | 31 |
| 12/03/1997 | Landsat 5 | 33 | 31 |
| 03/28/2002 | Landsat 7 | 33 | 31 |
| 06/08/2002 | Landsat 5 | 33 | 31 |
| 07/03/2002 | Landsat 5 | 32 | 31 |
| 05/15/2005 | Landsat 5 | 33 | 31 |
| 08/19/2005 | Landsat 5 | 33 | 31 |
| 10/14/2005 | Landsat 7 | 33 | 31 |

The primary focus during METRIC processing was to estimate ET from agricultural areas within the geographical domain of the North Platte and South Platte NRDs during 1997. Therefore, satellite image dates were selected that were especially free of clouds over these areas. Clouds were present on some image dates over some rangeland areas and sometimes along Pumpkin Creek. Because METRIC is unable to compute valid ET estimates for areas impacted by clouds, smoke or other conditions of greatly reduced transmissivity of the atmosphere, ET estimates were not available for portions of some image dates.

Work by the University of Idaho during this project included further development of the METRIC model to perform more accurately under the specific conditions of the western Nebraska study area. These specific conditions included the substantial amount of late spring and summer rainfall events and large amounts of clouds in some images that complicated the estimation of monthly and seasonal ET. Improvements to METRIC included a new cloud gap filling procedure for $ET_r F^1$ images that automatically adjusts for background evaporation occurring from recent precipitation, the gap filling of normalized difference vegetation index (NDVI) images used to estimate expected $ET_r F$, the generation of gridded precipitation surfaces and gridded ET_r used to estimate distributed bare soil evaporation and to adjust the satellite date ET estimates for background evaporation, and using evaporative fraction, EF, rather than $ET_r F$, as the vehicle to extrapolate rangeland ET from the instantaneous, at-satellite overpass time ET estimates to daily values.

This report is organized to describe the setup and calibration of the satellite image processing and to present some of the results from the application of METRIC. Descriptions of the quality control of supporting meteorological information, Landsat image selection, selection of supporting information and the extrapolation of daily estimates to monthly and seasonal estimates of ET and $ET_r F$ are provided in Appendices A through G as outlined in Table 2.

Table 2. Overview of the appendices

| Appendix | Subject |
|----------|---|
| A | Quality control of weather data |
| B | Selection of Landsat images for METRIC processing |
| C | Shift of the thermal band relative to the shortwave bands |
| D | Selection of a digital elevation map and a land use map |
| E | Cloud masking and estimating monthly and seasonal $ET_r F$ and ET from daily values |
| F | Estimating distributed soil evaporation and adjustment for background evaporation |
| G | Extrapolating ET Estimates from instantaneous to daily Time Steps |

¹ $ET_r F$ is the fraction of alfalfa reference ET_r and represents the relative amount of reference ET occurring on any particular pixel of an image. $ET_r F$ is a direct product from METRIC. ET_r is also used to calibrate the METRIC process and is calculated using hourly meteorological information from a weather station. Typical ranges for $ET_r F$ are 0 to about 1.1. $ET_r F$ is synonymous with the crop coefficient

1. Data processing

Weather data

METRIC utilizes alfalfa reference ET (i.e., ET_r) as calculated by the ASCE standardized Penman-Monteith equation (ASCE-EWRI 2005) for calibration of the energy balance process and to establish a daily soil water balance to estimate residual soil evaporation from bare soil following precipitation events (Allen et al. 2007a). The ET_r is used as a means to 'anchor' the surface energy balance by representing the ET from locations having high levels of vegetation and cooler surface temperatures. Therefore, high quality estimates of ET_r are needed, which, in turn, require high quality weather data. Therefore, before processing the satellite images, the quality and accuracy of the meteorological data were assessed. The weather data used during the calibration of METRIC were from the Scottsbluff, Sidney and Alliance North High Plain Regional Climate Center (HPRCC) weather stations located within the area of interest. The weather data quality control is described in Appendix A.

Hourly weather data time steps are needed to produce ET_r for calibration of the METRIC energy balance estimation process at the time of the Landsat overpasses. The hourly ET_r values are summed to daily totals to provide a basis for producing daily and monthly ET. ET_r was calculated using the RefET software (version 3) of the University of Idaho (Allen, 2008).

A daily soil water balance was parameterized and used to determine whether any residual evaporation existed from exposed soil at the time of each satellite image due to recent rainfall events. The residual evaporation was considered when assigning a value for ET from the 'hot' anchor point during the METRIC calibration process, where the hot anchor point was generally a bare soil condition located within about 20 km of the weather station. The FAO-56 (Allen et al 1998) soil evaporation model was used to estimate residual evaporation from the upper 0.125 m soil layer and using soil water holding capacity for a Tripp very fine sandy loam soil typical in the agricultural regions of the North Platte valley in the Scottsbluff vicinity. The simulated soil water balance was initiated several months before each image date, hence meteorological data from the full years 1997, 2002 and 2005 were used as input.

Selection and setup of satellite images, land use map and digital elevation map

The satellite images to be processed were selected by the PIs from the University of Idaho and University of Nebraska based on a list of available Landsat 5 and Landsat 7 image candidates for the years 1997 - 2007 prepared by University of Idaho. Representatives from the North Platte and South Platte NRDs approved the list. Normally, one satellite image per month is required to establish monthly and seasonal ET estimates. The principles behind the image selection are described in Appendix B. The Landsat images were ordered from the USGS Earth Resources Observation Systems (EROS) in Sioux Falls, S.D by University of Nebraska (prior to the free-data policy of EROS) The images were ordered as an L1T product, which includes both radiometric, geographic and terrain correction. Based on advice from the NRDs, the geographic projection of the images was specified as GRS 1980, NAD83, UTM zone 13, and resampling of the thermal band to 30 m pixel size was done by EROS using nearest neighbor resampling.

Only areas free from major atmospheric disturbances (including cirrus clouds, jet contrails, smoke etc) and cloud shadows can be processed to ET with METRIC. The main image selection criteria were therefore based on whether 1) the irrigated agricultural areas along the South Platte River and along Pumpkin Creek were cloud free, and, or secondary importance, that 2) rangeland areas within the NRDs were free from clouds. Most of the selected images had some degree of cloud cover within the image.

It was previously noted by Trezza and Allen (2008) that the thermal band (band 6) of L1T terrain-corrected Landsat 5 images processed by EROS using the NLAPS preprocessing system during the 2007 to 2009 period was typically shifted 60 m in the southerly direction relative to the visible and near-infrared bands. The shift was found to be consistent throughout the image. It is important that the pixels of all bands in the Landsat image 'line up' in order to perform a correct solution to the surface energy balance during the METRIC process. Therefore, prior to METRIC processing, images were screened and the shift corrected. The shift and its remedy are described in Appendix C. The shifting procedure is no longer needed with post Jan. 2010 images obtained from EROS due to their use of an updated process.

Landsat 7 images acquired after May 2003, although from a newer satellite than Landsat 5, are less preferred than Landsat 5, due to an anomaly with the Landsat 7 satellite caused by the malfunction of the scan line corrector. As a result, Landsat 7 images processed for year 2005 are "SLC-off" images where wedge shaped gaps exist in the images, extending from the edges of the image and stretching towards the centers. To obtain as complete coverage as possible, the gaps in ET_F maps produced by METRIC are generally filled in during post processing using the natural neighbor tool of Arc-GIS. However, because during this study, the 2005 images were used for training purposes, the gaps were not filled in.

A digital elevation map (DEM) is used during METRIC processing to adjust surface temperatures for lapse effects caused by elevation variation. A DEM with 30 m resolution was obtained from the USGS seamless server and was resampled into the projection of the Landsat images using cubic convolution resampling. Maps of slope and aspect (aspect is the cardinal direction of an inclined surface) at 30 m resolution used during the METRIC processing were created using the tools of the ERDAS Imagine processing system based on the DEM. More information about the DEM is provided in Appendix D.

A land use (LU) map was used to support the estimation of aerodynamic roughness and soil heat flux during METRIC processing. A composite land use map was generated from land use maps from the CALMIT Cooperative Hydrology Study (COHYST), NE GAP and from the USGS National Land Cover Database (NLCD). COHYST land cover maps are available for years 1997, 2001 and 2005; the NE GAP land use map is based on data collected during 1991 – 1993 and the NLCD is based on classification performed on 2001 Landsat imagery. These land cover maps offer different degrees of resolution for different categories of land cover. Greatest detail for natural vegetation and riparian zones are found in the NE GAP map, while the greatest detail in agricultural crop diversity is found in the COHYST maps. Land use generally only changes very little from year to year, except for agricultural lands where crops are often rotated every year.

A composite land use map based was created based on the NE GAP land use map. Pixels defined as agricultural (excluding rangeland) in the COHYST map (for each project year) were used to distinguish between crop types during ET image reviews. For areas not covered by the COHYST and NE GAP maps (in SE Wyoming and NE Colorado) the NLCD map was used. More detail about the land use maps and land use classes is provided in Appendix D.

The ET information from the path 33 row 31 images from 1997 was used to assemble monthly ET images by interpolating relative ET fractions between image dates using a cubic spline interpolation model and multiplying by daily reference ET that was based on weather data.

Calibration of METRIC

METRIC version 2.0.4 was used for the UI processing. This version was released by the University of Idaho in June 2008 (Allen et al., 2008). A detailed description of METRIC can be found in Allen et al. (2007a,b; 2008).

The main focus for the processing was to generate estimates of ET from lands having agricultural production, so that METRIC was calibrated with primary focus on accurate estimation of ET from the agricultural areas. However, because the full Landsat images were processed, efforts were made to minimize uncertainty in ET estimates from other land cover types present within the image, including forests, riparian vegetation and rangeland.

Refinements to METRIC during this work.

To better account for impacts of local precipitation events and image cloudiness in the study area on the final ET estimates, the METRIC model was adjusted and new methods were developed and implemented to account for conditions that deviate from the description of the standard Level 1 METRIC model application. These adjustments are referred to as Level 2 processing (Allen et al., 2010). Improvements to METRIC that were advanced during this study include a new cloud gap filling procedure for the ET_rF estimates that automatically adjusts for background evaporation from recent precipitation, gap filling of NDVI, the generation of grids of precipitation and ET_r used to estimate distributed bare soil evaporation that is, in turn, used to adjust the satellite date ET estimates for background evaporation, and using evaporative fraction, EF , rather than ET_rF , as the vehicle to extrapolate from the instantaneous, at-satellite overpass time ET estimates to daily values for rangeland. These new developments and their application are described in Appendix E.

Calibration Philosophy.

METRIC uses a vertical near surface-to-air difference, dT , to estimate sensible heat flux. Sensible heat flux (H) is the amount of heat that is convected from a surface into the air, thereby reducing the amount of available energy for evaporation. The dT function is generally assumed to be linearly proportional to surface temperature and is defined using the properties of two user selected anchor pixels, the "cold" and the "hot" pixels, that represent the extreme conditions encountered within the image (a condition having nearly complete conversion of available energy into evapotranspiration and a condition having nearly zero conversion of available energy into evapotranspiration). The cold anchor pixel generally represents a fully

vegetated and actively transpiring vegetation, while the hot anchor pixel represents a bare and dry or nearly dry agricultural soil with little or no vegetation. The selection of cold and hot anchor pixels by the user is described by Allen et al., (2007b, 2008). These pixels are generally selected from agricultural fields for consistency and to match assumptions made in the estimation of soil heat flux, for example, where that algorithm was developed for agricultural soils. The surface temperature used to estimate dT was 'delapsed' to account for differences in surface temperature occurring as a result of elevation differences.

During the internal calibration of sensible heat flux in METRIC, a fraction of ET_r , $ET_{r,F}$, is assigned to the hot and cold conditions. $ET_{r,F}$ is equivalent to the crop coefficient (K_c) based on full-cover alfalfa as the reference crop. $ET_{r,F}$ at the cold pixel is normally assigned a value of 1.05 (Allen et al., 2007a,b) unless vegetation cover is insufficient to support this assumption (for example, early in spring and during winter when full, robust vegetation cover is rare). The 1.05 assignment to $ET_{r,F}$ is used to account for the variation in ET inherent within a large population of fully vegetated fields. Previous applications of METRIC and comparisons against lysimeter measurements of ET at Kimberly, Idaho show that the "nearly coldest", or wettest, agricultural fields having full vegetation cover tend to have ET rates that are typically 5% higher than that of the alfalfa reference ET_r . This is because, for a large population of fields, some fields may have a wet soil surface beneath the canopy, or the canopy may be wet from recent (sprinkler) irrigation or precipitation, that tend to increase the total ET rate to about 5% above ET_r . In addition, when viewing a large population of fields containing full cover alfalfa, a specific subpopulation of fields will have somewhat wetter conditions and therefore slightly higher ET and slightly cooler temperature than the "mean" full cover condition represented by the alfalfa reference. When the METRIC image is calibrated using an $ET_{r,F}$ of 1.05 at the cold pixel, sampling of $ET_{r,F}$ over a large population of full cover, irrigated fields tends to produce, on average, an $ET_{r,F}$ value of 1. The cold pixel is selected from a population of fields having full cover and relatively cold temperatures. Ideally, an alfalfa field is preferred for calibration, since the ASCE Penman-Monteith equation is calibrated to an alfalfa reference. However, Wright (1982) has shown that most agricultural crops, when at full cover, transpire at levels very similar to those of alfalfa. Therefore, the selected location for the cold pixel does not need to be alfalfa, but can be any pixel from within the interior of a fully vegetated, cool, field (crop type is generally unknown when applying METRIC).

During calibration of METRIC via the assignment of $ET_{r,F}$ values for the cold and hot pixel conditions, normally only a single weather station is utilized in the calibration. A single station is used during calibration for several reasons. One, the locations for the cold and hot conditions are selected as close as possible to the single calibration weather station (usually within 20 km) so that wind speed and reference ET from the station can be assumed to closely approximate that for the selected calibration pixels. The internal calibration of the sensible heat flux function within METRIC is tied to the wind speed occurring at the calibration locations. Secondly, the internal calibration of the sensible heat flux function within METRIC generally requires the use of the same wind speed as was used in its determination, throughout the image. Third, the assignment of the $ET_{r,F}$ at the hot pixel is closely tied to any recent precipitation occurring at the calibration weather station. Fourth, the assignment of $ET_{r,F}$ at the cold and hot pixel conditions

and the application of the METRIC process to the image should create (if calibrated and applied correctly) an ET_rF surface over the image that has general limits of 0 and 1, and that can be later applied to an ET_r surface that may vary over the image

When processing path 33 row 31, the Scottsbluff weather station was selected for use in the METRIC calibration due to its proximity to large irrigation areas and centrality to the general areas of interest. When processing path 33 row 31, the Sidney weather station was selected for use. The ET_rF image created by METRIC can be applied using ET_r from the Scottsbluff or Sidney weather stations, or any other reference weather station in the image domain

Special Calibration Cases.

For the April 4 1997, December 3 and March 28 2002 images, we were unable to locate fields that appeared to have full vegetation cover. Therefore, the ET from the agricultural fields evaluated on those dates and assigned as the cold pixel is expected to be lower than that from the alfalfa reference. ET_rF for the cold pixels on those three dates was calculated using the following relationship between ET_rF and the normalized difference vegetation index (NDVI) as $ET_rF_{cold} = 1.25NDVI$ (Tasumi et al., 2005, Burnett, 2007). NDVI generally ranges from about 0.1 to 0.2 for bare soil to 0.75 to 0.85 for full vegetation cover.

The hot pixel is generally considered to be a dry, bare soil having no residual evaporation (i.e. $ET_rF=0$) This is generally true if there have been no precipitation events for several weeks prior to the image overpass date. In the case where there have been recent precipitation events, the soil may not be dry and there will likely be some residual evaporation from the soil that must be accounted for during calibration of energy balance parameters and processing of ET for satellite images. In addition, there can often be residual evaporation from tilled agricultural soils that have substantial water storage at depth, In these situations, an $ET_rF=0.05$ to 0.10 may be appropriate

Using a daily soil water balance model to check the METRIC calibration.

A daily soil water balance was applied to the entire years 1997, 2002 and 2005 using precipitation and ET_r from the Scottsbluff and Sidney weather stations. The water balance estimates residual evaporation on each of the image dates. The soil water balance is based on the two-stage daily soil evaporation model of the United Nations Food and Agriculture Organization's Irrigation and Drainage Paper 56 (Allen et al. 1998). Fig. 2 shows a simulation of evaporation from the upper 0.125 m of soil at Scottsbluff

The August 13 1997 and October 2005 images fell immediately after several days where substantial rainfall was recorded at the Scottsbluff weather station. As a consequence, the soil water content at all bare fields around Scottsbluff were near to or exceeding field capacity, and the ET_rF value predicted by the soil water balance, for the hot pixel, was near 1 leaving a narrow span in ET_rF values for the calibration. The soil water balance is a 'slab' model, where the soil is assumed to dry uniformly.

As a means to verify the calibration of the hot pixel in METRIC, based on the Scottsbluff soil water balance, the soil water balance model was also set up using meteorological information

from the Alliance North weather station, which is about 50 km NE of Scottsbluff, and where the water holding capacity of the soil is lower (due to sandy soils) compared to Scottsbluff. When rainfall timing and magnitudes are different between the two locations, similarity between estimated ET_rF by METRIC at Alliance, using a calibration based on Scottsbluff, and the evaporation model estimate for Alliance provides good indication of appropriate calibration and estimation over the image.

During the drying cycle after a wetting event, a typical bare agricultural soil can be expected to continue to evaporate at a small rate beyond the first several weeks due to diffusion of liquid water and vapor from beneath the upper soil layer. This evaporation can continue at very low rates for several additional weeks, provided no new wetting events occur, especially from tilled soils that have a moderate amount of water stored within the soil profile. This is typical of agriculture.

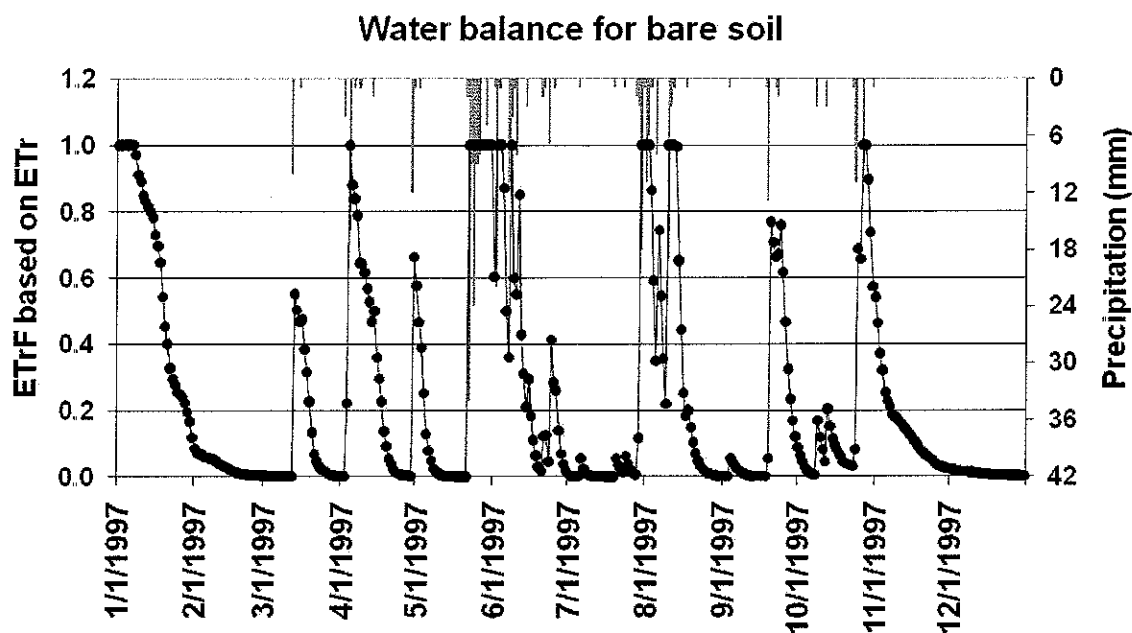


Figure 2. Daily ET_rF for bare soil estimated from the soil water balance for 1997 using weather data from the Scottsbluff HPRCC weather station.

The medium-term, low-level residual evaporation is not simulated by the FAO soil water balance model. Because wetting events greater than a few millimeters generally occurred every 2 -3 weeks in the study area, a minimum ET_rF value of 0.1 was generally used to estimate the minimum rate of evaporation from bare soil conditions, representing agricultural fields, and selected as the hot calibration pixels for all image dates (desert and range soils having low water profiles are expected to go lower than the $ET_rF=0.1$ residual). If the soil water balance suggested a higher ET_rF value for bare soil than the residual evaporation rate of 0.1, the higher value was used as shown in Eq. 1:

$$ET_r F_{\text{bare soil for the hot pixel}} = \text{Maximum}(\text{Soil water balance model estimate}, 0.1) \quad (1)$$

One exception from Eq. 1 was for the July 3 2002 image date, where only trace amounts of precipitation had been recorded for four weeks. As a consequence, the $ET_r F$ value was set to 0.05 (Allen et al. 2010). Table 3 lists the $ET_r F$ assigned to and location of the hot and cold pixels for the image dates.

Table 3 $ET_r F$ values assigned to and locations (X, Y coordinate) of the hot and cold pixels for each image date.

| Image date | $ET_r F$ | $ET_r F$ | Hot pixel X | Hot pixel Y | Cold pixel X | Cold pixel Y |
|------------|----------|----------|-------------|-------------|--------------|--------------|
| 04/23/1997 | 0.1 | 0.84 | 599527 | 4649696 | 602341 | 4655976 |
| 05/09/1997 | 0.1 | 1.05 | 620620 | 4637886 | 599816 | 4640942 |
| 06/26/1997 | 0.26 | 1.05 | 582435 | 4655494 | 645603 | 4675289 |
| 07/12/1997 | 0.1 | 1.05 | 620206 | 4637902 | 600843 | 4641990 |
| 08/13/1997 | 0.75* | 1.05 | 585477 | 4637010 | 623642 | 4635630 |
| 08/22/1997 | 0.32 | 1.05 | 705877 | 4561107 | 672058 | 4606772 |
| 09/30/1997 | 0.12 | 1.05 | 616112 | 4634056 | 592139 | 4644722 |
| 10/16/1997 | 0.1 | 1.05 | 620109 | 4637992 | 641461 | 4628879 |
| 12/03/1997 | 0.1 | 0.83 | 659013 | 4608330 | 611129 | 4638869 |
| 03/28/2002 | 0.28 | 0.80 | 664351 | 4616148 | 591987 | 4653786 |
| 06/08/2002 | 0.1 | 1.25 | 647760 | 4624229 | 614672 | 4651108 |
| 07/03/2002 | 0.05 | 1.05 | 676692 | 4566371 | 677520 | 4600469 |
| 05/15/2005 | 0.16 | 1.05 | 594556 | 4650278 | 628565 | 4629509 |
| 08/19/2005 | 0.37 | 1.05 | 595773 | 4641419 | 672148 | 4659170 |
| 10/14/2005 | 0.8* | 1.05 | 603668 | 4655372 | 593253 | 4644895 |

*These calibrations were verified using soil ware evaporation information from Alliance North

Other model calibration exceptions.

Desert and range soils typically run 'hotter' in terms of surface temperature than bare agricultural soils. Reasons for this include effects of organic mulches, shielding of the soil surface by sparse live or dead vegetation, delamination of soil crusts, and increased soil porosity caused by animals and roots that is common to these land uses, but not to bare agricultural soils. To prevent the higher temperatures in desert and range from overestimating the near surface air temperature gradient (dT) and thus H, thereby causing ET from the energy balance to even go negative at times, adjustments were made to the dT estimation and estimation of soil heat flux when surface temperature exceeded a threshold temperature. On all image dates the soil heat flux and the slope of the dT function were reduced for those pixels where the surface temperature exceeded the surface temperature of a dry agricultural pixel as described by Allen et al. (2008).

A surface temperature lapse rate is used during the METRIC process to normalize the surface temperature image for changes in temperature caused by normal lapse effects associated with elevation changes within the image. This normalization is needed in any energy balance process before estimating near surface air temperature gradients and the associated sensible heat flux (Allen et al., 2007a). A lapse rate of 6.5 K/km elevation change was used. However,

this lapse rate can be custom fitted to an image when the range in surface temperatures across an image varies for the same evaporative conditions (wet or dry).

2. Results

The sample images shown below have been included in the image files transferred to the University of Nebraska. A complete list of the files provided is given in Appendix E.

Reference ET

Daily ET_r was calculated by summing hourly ET_r , computed using the ASCE standardized Penman-Monteith equation, over 24-h periods. For calibration, hourly ET_r was calculated using meteorological information from the Scottsbluff and Sidney weather stations. Daily (24-h) totals for the processed image dates are listed in Table 4. When the ET_rF images were interpolated over time to create monthly ET images, daily ET_rF was determined by spline and multiplied by daily ET_r . During the interpolation process, daily ET_r 'surfaces' were created over the image area, as described in Appendix A, using 14 HPRCC and CoagMet weather stations from within and outside the image area.

Table 4. Day of year and calculated alfalfa based ET, ET_r for the satellite image dates

| Image date | Day of year | ET_r (mm/day) |
|------------|-------------|--------------------|
| 04/23/1997 | 113 | 5.53 ¹ |
| 05/09/1997 | 129 | 7.34 ¹ |
| 06/26/1997 | 177 | 8.51 ¹ |
| 07/12/1997 | 193 | 8.18 ¹ |
| 08/13/1997 | 225 | 6.24 ¹ |
| 08/22/1997 | 234 | 7.07 ² |
| 09/30/1997 | 273 | 4.87 ¹ |
| 10/16/1997 | 289 | 3.01 ¹ |
| 12/03/1997 | 337 | 1.30 ¹ |
| 03/28/2002 | 87 | 5.66 ¹ |
| 06/08/2002 | 159 | 11.19 ¹ |
| 07/03/2002 | 184 | 11.43 ² |
| 05/15/2005 | 135 | 7.34 ¹ |
| 08/19/2005 | 231 | 5.74 ¹ |
| 10/14/2005 | 287 | 3.53 ¹ |

¹Calculated from Scottsbluff HPRCC weather station data; ²Calculated from Sidney HPRCC weather station data

Daily ET_rF

Maps of reflectance of short wave radiation, vegetation indices (NDVI and LAI), surface temperature, net radiation and soil heat flux were generated as intermediate products during METRIC processing. The final output from the METRIC energy balance model were images showing instantaneous ET_rF (fraction of alfalfa based reference ET, ET_r) at the satellite overpass time. For land covers other than rangeland, the estimate of daily ET_rF was set equal to the instantaneous at the satellite overpass time, based on extensive ET measurements made using precision weighing lysimeters at Kimberly, Idaho (Allen et al. 2007b, 2008). For rangeland, the evaporative fraction was used to extrapolate from instantaneous to daily values of ET, rather than ET_rF , since, by definition, no net transfer of advective energy exists with rangeland systems. The ET_r estimated by the Penman-Monteith method generally accounts for the influence of advective energy into vegetation systems having an external water source such as irrigation or shallow ground-water, and thus the use of ET_rF to transfer from instantaneous to 24-hour ET tends to convey the impact of

advection. On the other hand, the evaporative fraction, $EF = \frac{ET}{R_n - H}$, the ratio of ET to the difference of net radiation and soil heat flux, tends to not account for influences of advection occurring during afternoon. Daily ET in mm/day was calculated by multiplying the ET_rF by daily ET_r or by multiplying the EF by daily net radiation. In both cases, a daily ET_rF was computed by dividing daily ET by daily ET_r . The procedures for obtaining daily estimates of ET and ET_rF are further explained in appendix E

Maps of ET_rF for the area north of Scottsbluff for the 05/09-1997, 07/12-1997 and 09/30-1997 image dates are shown in Fig. 3. Contrasts in spatial ET_rF and changes over time are apparent. On 05/09-1997 most fields had no or only little vegetation cover and the soil generally were relatively dry, thus the ET_rF was quite low for most fields and rangeland. Fields with winter cereals or alfalfa had some vegetation transpiring some water, with some fields likely irrigated prior to and after planting. By 07/12-1997 the desert soils were quite dry and the ET_rF for rangeland was decreasing to relatively low values due to the soil drying. The agricultural fields were mostly covered by crops having apparently good vigor, and many were evapotranspiring at close to the reference level (so that $ET_rF \sim 1.0$). Some of these crops were cut for hay or started to senesce by 09/30-1997, causing lower ET rates, while other fields retained high vegetation cover and therefore maintained high ET_rF .

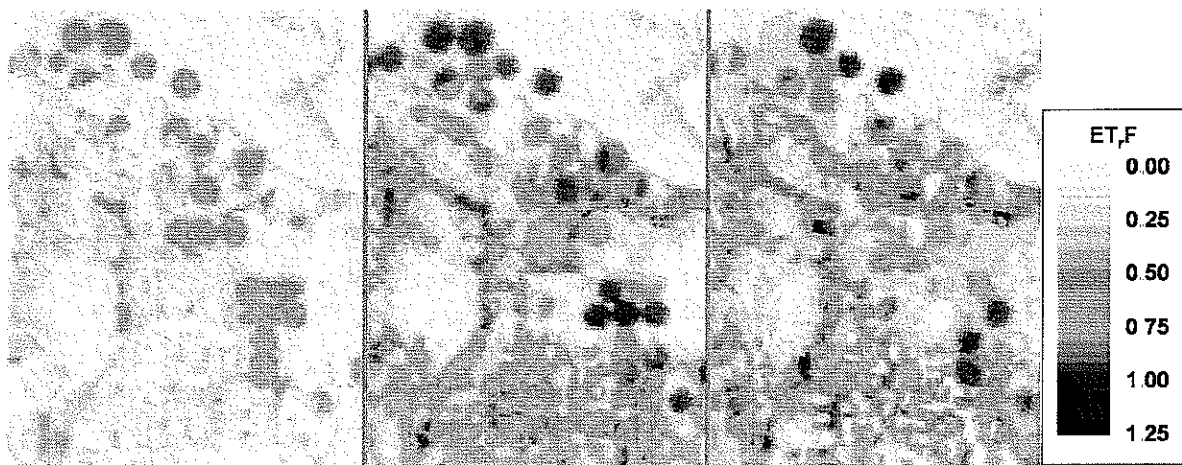


Figure 3. Daily ET expressed as ET_rF for 05/09-1997 (left), 07/12-1997 (center) and 09/30-1997 (right) for the area north of Scottsbluff.

Treatment for cloud cover.

Some images had cloud cover in portions of the images, usually away from the irrigated agricultural areas in the study area. Prior to integration of ET over months and growing season for year 1997, the clouded areas were manually identified, masked, and then filled in by interpolating ET_rF information from adjacent images in time as described in Appendix E. Prior to the interpolation for clouded areas, the ET_rF transferred was adjusted for background evaporation stemming from rainfall. Areas masked for cloud cover are shown in Figure 4 for each image date (except December 3) of 1997.

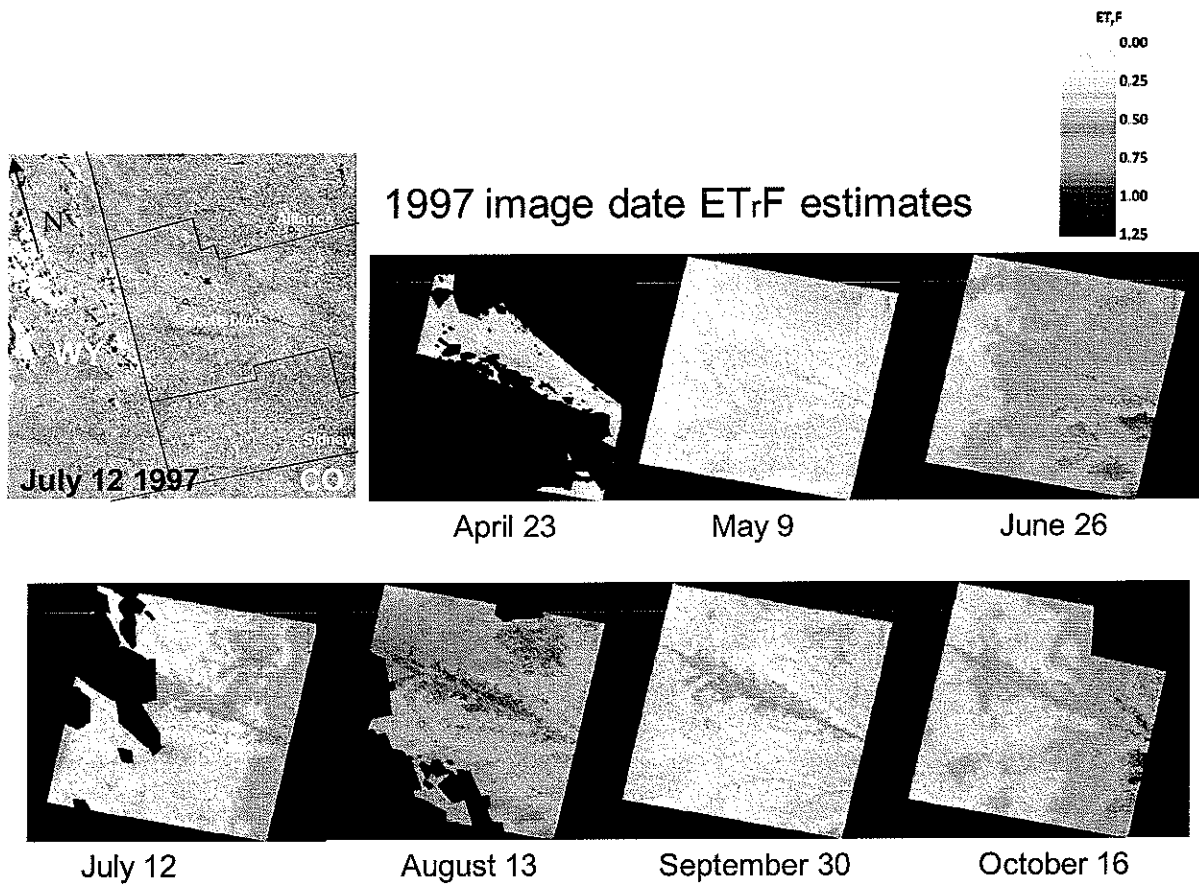


Figure 4 Maps of cloud masked ET_rF from seven 1997 images dates. The geographical extent of the NP and SP NRD boundaries is shown on the image in the top left corner

Figure 5 shows the June 26 1997 Landsat image in true color with some geographical features indicated. This area is the same as shown in the following Figures 6 and 7

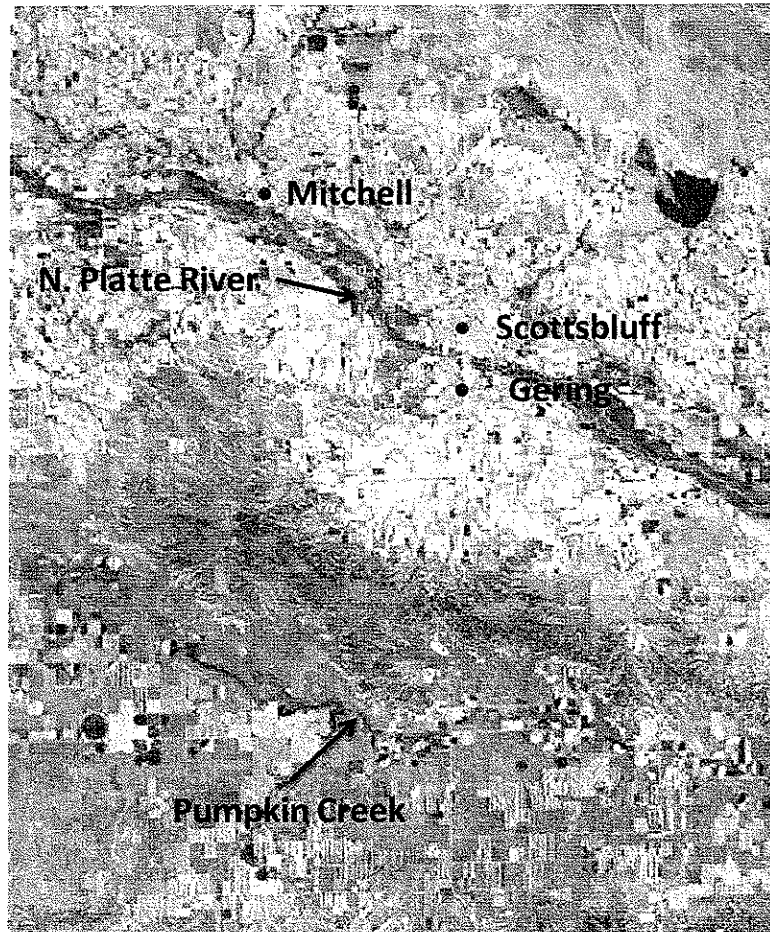


Figure 5. The 06/26-1997 Landsat 5 image in true color with some geographical features indicated.

The ETrF maps in the following Figure 6 show the ET_rF on the satellite overpass dates for the Scottsbluff area for the 1997 image sequence. The values and ranges of ET varies with time of year, with peak values reached during early summer for many crops, with low values during spring and late fall when most vegetation is dormant and evapotranspiration potentials were low. The values for ET reflect the weather data on the satellite overpass date, and therefore do not paint as clear a picture of ET evolution as do the images of ET_rF . The ET_rF images show a progressive increase in ET_rF through spring and early summer and subsequent decrease into the fall and winter.

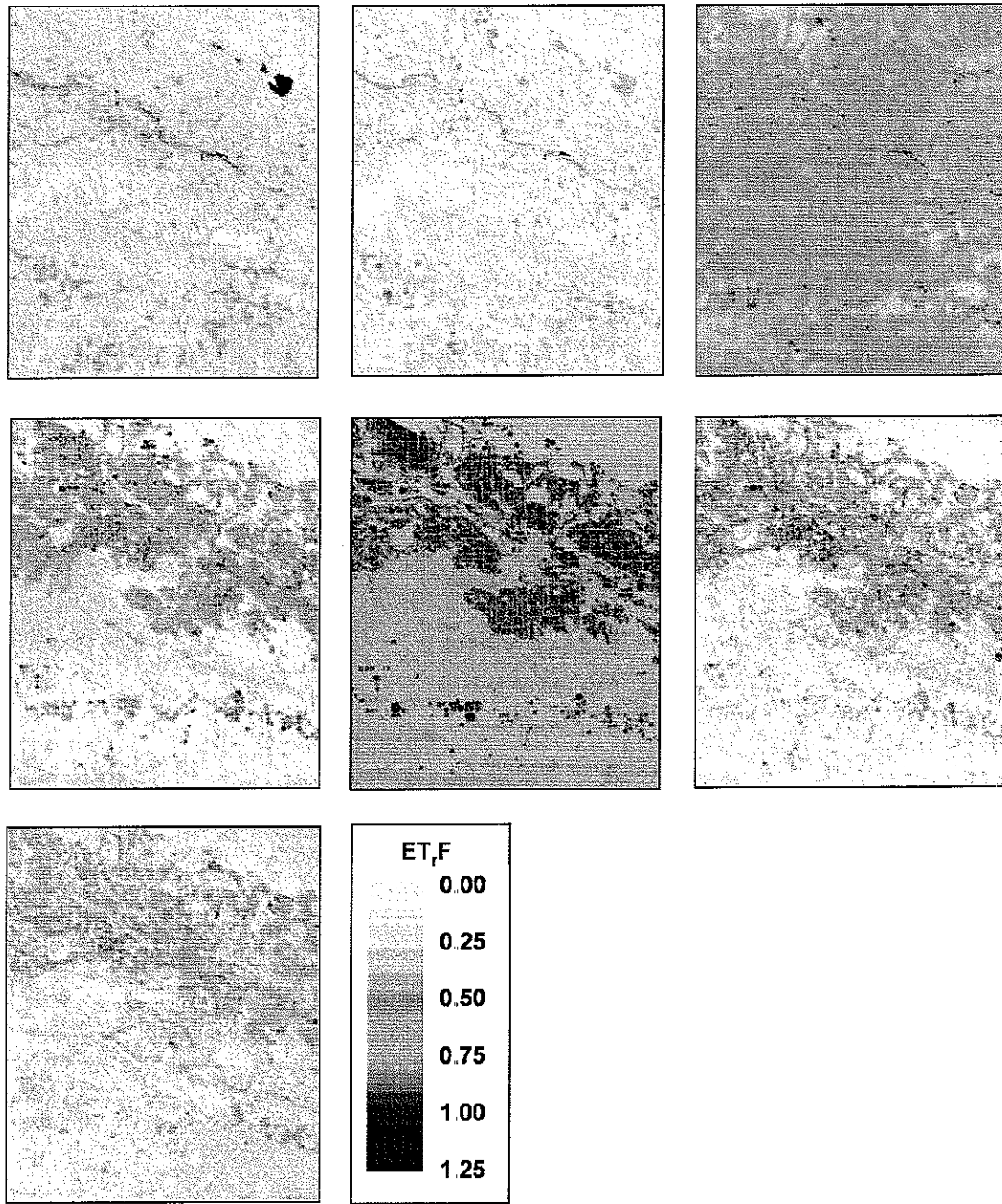


Figure 6. ET,F estimated for April 23 1997 (top left), May 9 1997 (top center), June 26 1997 (top right), July 12 1997 (middle row, left), August 13 1997 (middle row, center), September 30 1997 (middle row, right) and October 16 (bottom, left) for the area indicated in Figure 5.

Adjustment of ET_rF for background Evaporation

When setting up the METRIC satellite-based surface energy balance model, the evaporation from bare soil is normally estimated for the area immediately around a single weather station located within the image. These estimates of residual evaporation from antecedent rainfall are used during the calibration of the estimates of sensible heat flux from the surface. The energetic of the METRIC process produce estimates of evaporation across the image that generally agree with evaporation estimates, for that image date, that are derived from a daily simulation model using spatial precipitation data as input.

Because the evaporation from bare soil and sparsely vegetated areas at the satellite overpass dates may not be representative for a longer period, such as one month, an adjustment for the average ET_rF for that period is made prior to estimating monthly ET. The primary approach developed during this study is to remove impacts of wetting events that occurred immediately prior to the image date, and thus impacted the Landsat image processed, and then add back in background evaporation that is more similar to the average evaporation expected for the averaging period, which in many cases is approximately one month. The averaging period length is defined by the period midway, in time, between the previous image date and the current image date, and extending forward in time to midway between the current and the following image date.

Spatially distributed estimates of daily soil evaporation are needed to make this adjustment. The parameterization of a spatially distributed soil water balance using the FAO56 method is described in Appendix F. In the University of Idaho applications, an ERDAS based gridded evaporation model was developed using daily calculation time steps. A similar model was developed by the University of Nebraska (Ranade, 2010) using Arc-GIS.

An example of the adjustment for background evaporation is shown in Figure 7 for an image date where the adjustment increased the ET_rF for bare soil and partially vegetated areas. Figure 8 shows an example of an image date where the ET_rF from bare soil and partially vegetation cover was decreased by the adjustment.

The 'adjusted' images no longer represent the actual ET fluxes experienced on the day of the Landsat images, especially for areas having low amounts of vegetation. Instead, the adjusted images represent the ET_rF averaged over the approximately monthly period represented by the particular image so that, when ET_rF is splined between image dates, the resulting monthly ET calculations include all evaporation associated with precipitation events occurring during that month, even if not 'seen' by the Landsat image. Therefore, these adjusted images should be considered to be intermediary products for use in splining ET_rF to actual monthly average values.

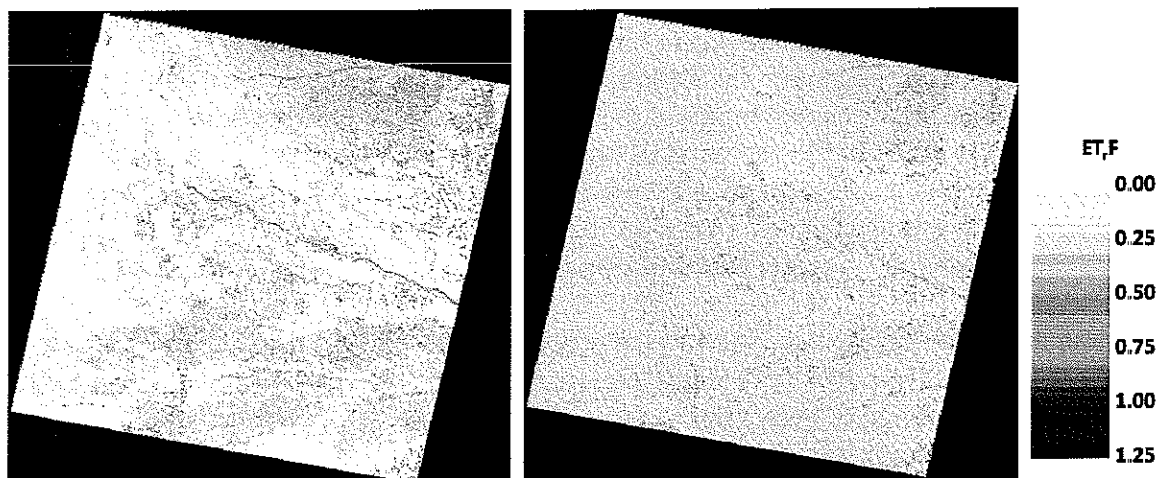


Figure 7. ET_r,F from May 9 1997 before (left) and after (right) adjustment for background evaporation representing the time period (\sim month) represented by that image.

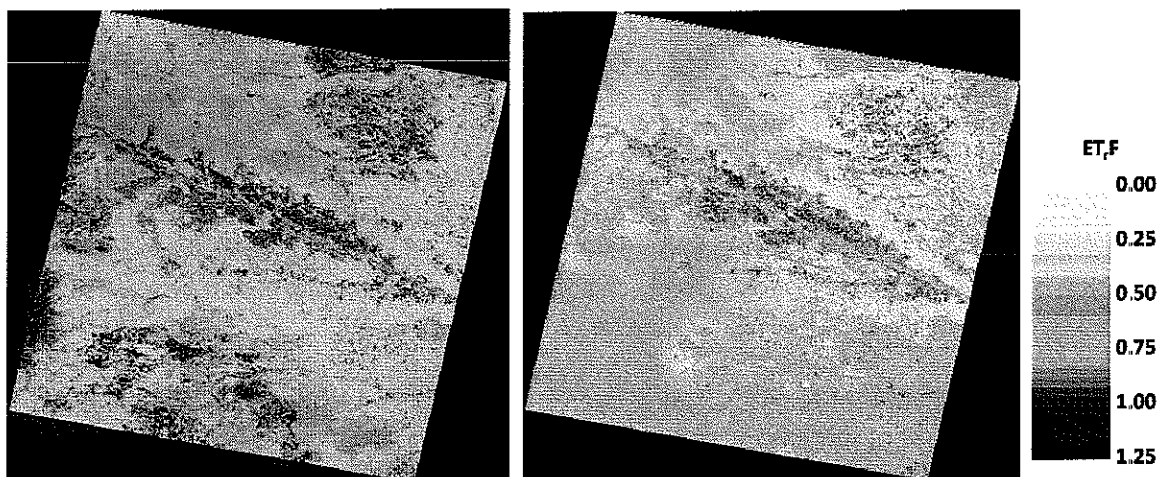


Figure 8. ET_r,F on August 13 1997 before (left) and after (right) adjustment to reflect soil evaporation occurring over the time period (\sim 1 month) represented by that image. Note that irrigated fields with full vegetation cover having a substantial transpiration component were not affected by the adjustment.

Monthly and seasonal ET_r,F and ET

Maps showing monthly and seasonal ET in mm from 1997 were produced by interpolating the values of daily ET_r,F on satellite overpass dates between dates using a cubic spline function. Values for ET_r,F for each day between images were multiplied by ET_r for that day and then integrated over the specific month. The splining and integration process is described in Appendix E and the creation of ET_r surfaces is described in Appendix A.

The December 3 1997 Landsat 5 image was a cloud free image processed using METRIC. The image did have partial snow cover, and the soil surface was very cold. Since the properties of the snow layer were unknown with regard to snow density, water content, thickness etc., ET estimates from METRIC for this snow layer have a great deal of uncertainty. Because the temperature differences were very small across the image, and because it was partially covered

by snow the December 3 image was not included in the estimation of monthly and seasonal ET estimates.

ET during April 1997. Because the first satellite image date was at the end of April, producing an estimate of the monthly ET_rF for April was challenging, since no direct information was available for the beginning of the month. Because of the cold temperatures experienced in this area, very little crop development is expected to occur until May. Therefore, ET_rF and ET estimates for April were made using daily simulated bare soil evaporation over the April period, which in most cases provided a reasonable estimate of the ET during the non-growing season portion of the year. Evaporation estimates, described in Appendix F, were based on daily ET_r and precipitation grids and soil information from the STATSGO data base. Grid size was 900 m. The evaporation from bare soil represents 'average' bare soil conditions regarding drainage, soil type and texture for the specific area. As a consequence, some uncertainty in the ET_rF and ET estimates for April exists for fields having soil and drainage properties different from those for the soil types simulated, and for fields that were covered by a layer of senesced plant material, mulch or having a relatively dense cover of green plant cover that might reduce evaporation rates. Users are cautioned to consider these factors on a field-to-field basis before using the estimates of ET_rF and ET for the month of April. A similar approach was employed when estimating the ET for the month of October 1997.

Impacts of clouds. Because of the high degrees of cloudiness within some image areas, some of the monthly and the seasonal estimates of ET are based on values that had to be interpolated and scaled from the previous and/or following month. This interpolation increases the uncertainties in the estimates of ET and ET_rF for the affected areas, since the estimates are based on interpolated values and not on actual values for that month. Therefore, users are encouraged to review the data availability section of Appendix E as summarized in Figure 4, and use caution before using the ET estimates for areas outside of the agricultural fields in the study area.

Evaporation from Water. The surface energy balance of water bodies varies substantially, depending on their properties, especially depth, temperature profiles and turbidity. The version of METRIC applied in this study attempts to account for variations among open water bodies, provided the water bodies are classified and partitioning algorithms between water heat storage and net radiation are adjusted accordingly. The partitioning can change with time of year. Because such classification and description of partitioning were not available for water bodies in the study area, and because the primary project goal was to estimate ET from agricultural crops and not evaporation from open water, the evaporation from open water bodies (lakes, rivers, canals, reservoirs, farm ponds etc) was estimated using a single algorithm that is calibrated to southern Idaho lakes (Allen et al., 2010), regardless of body size, depth and turbidity. The algorithms used to estimate open water ET represents assumed "large" water body properties, which may increase the uncertainty of ET from the water within the image (Allen and Tasumi, 2005). This algorithm may underestimate the ET from small water bodies such as cattle ponds, shallow lakes etc. For this reason, users are cautioned if extracting estimates of open water evaporation from the maps of ET or ET_rF . Current research

developments with METRIC are testing the use of an aerodynamic function for evaporation from water, which may have better accuracy in future applications

Figure 9 shows the monthly ET_F products for the period April 1 – October 31 for the same subarea illustrated in Figure 5. Figure 10 shows the average ET_F from April 1 through October 31, 1997 estimated using METRIC and Figure 11 shows the summed ET in mm from April 1 through October 31, 1997. The images have resolution of 30 m, so that monthly and seasonal ET data can be extracted for each 30 m on a grid.

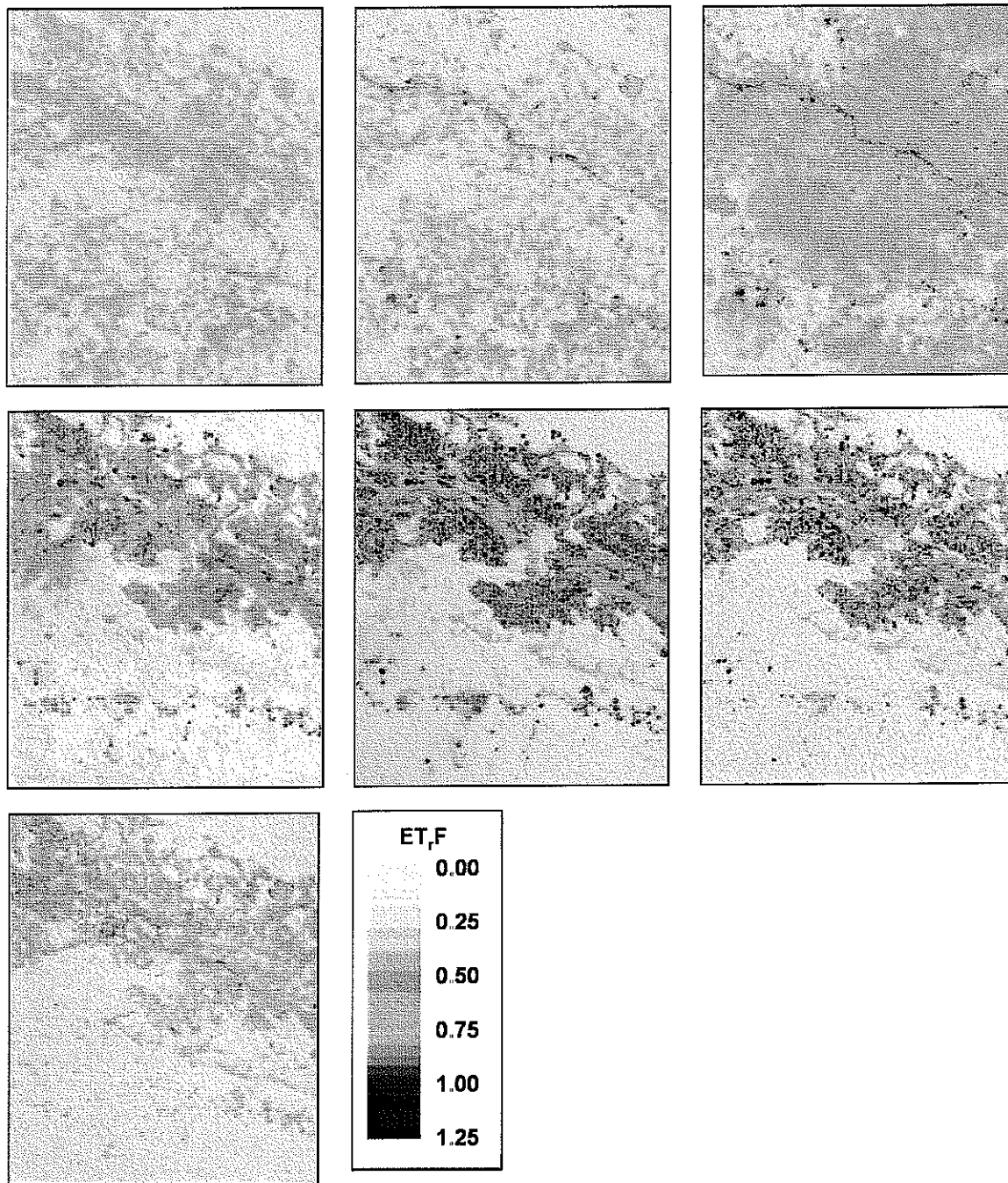


Figure 9. ET,F estimated for April (top left), May (top center), June (top right), July (middle row, left), August (middle row, center), September (middle row, right) and October (bottom, left) for the area indicated in Figure 5.

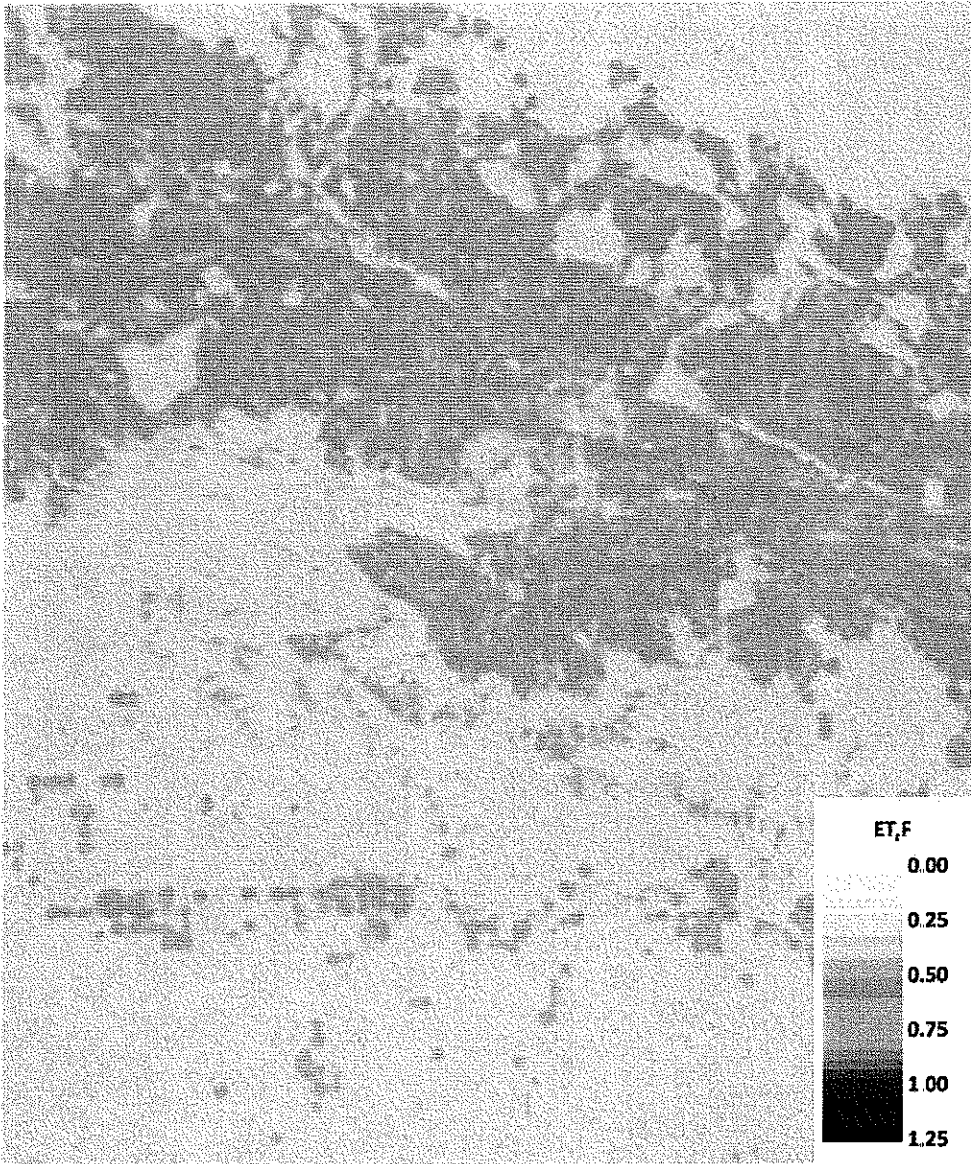


Figure 10. Average ET,F from April 1 through October 31 1997 estimated using METRIC.

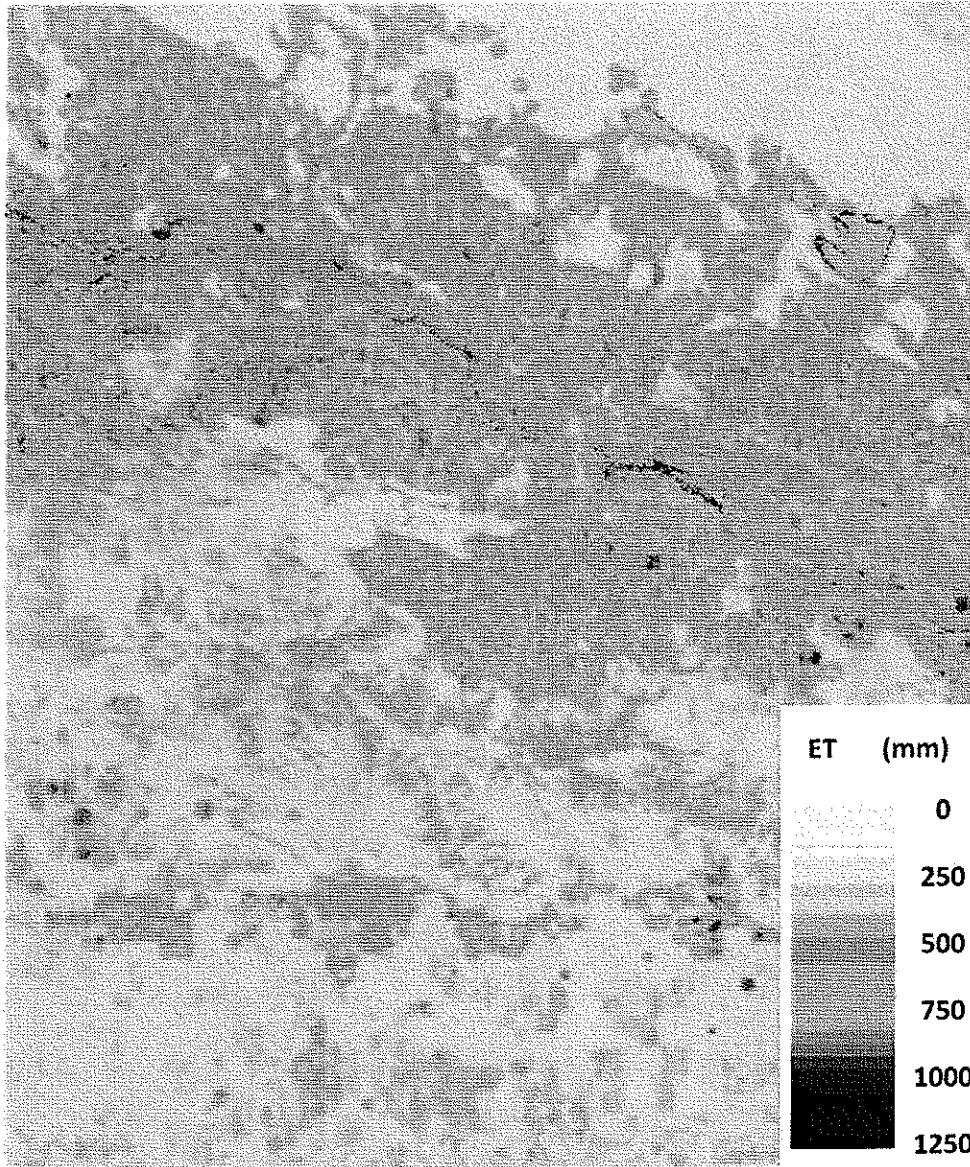


Figure 11. ET in mm estimated for April 1 through October 31 1997 using METRIC.

The seasonal (April 1 –October 31) precipitation subtracted from the seasonal (April 1 –October 31) ET, in mm, estimated from METRIC is shown in Figures 12 and 13. Negative values in the figure indicate that precipitation exceeds the ET. ET from desert areas surrounding the agricultural areas in the project area is typically similar to or slightly higher than reported rainfall amounts. If real, the additional ET from these areas may have been derived from the change in stored soil moisture between April 1 and October 31. On April 1 there was still residual moisture in the soil from winter precipitation, and the soil profile dried as the summer progressed.

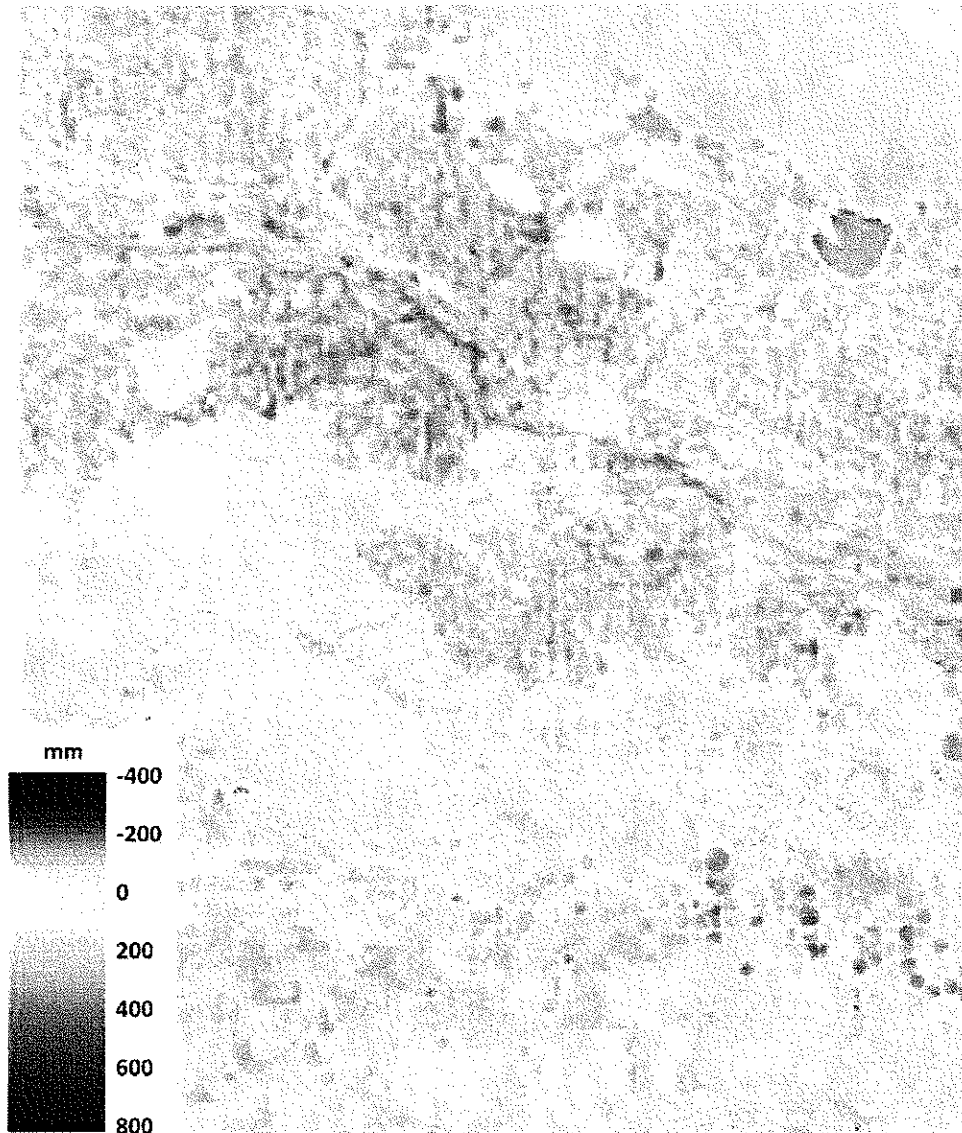


Figure 12. Seasonal (April 1 – October 31 1997), distributed precipitation subtracted from seasonal (April – October 31 1997) ET estimated from METRIC for the area indicated in Figure 5. Negative values indicate where precipitation exceeded the ET.

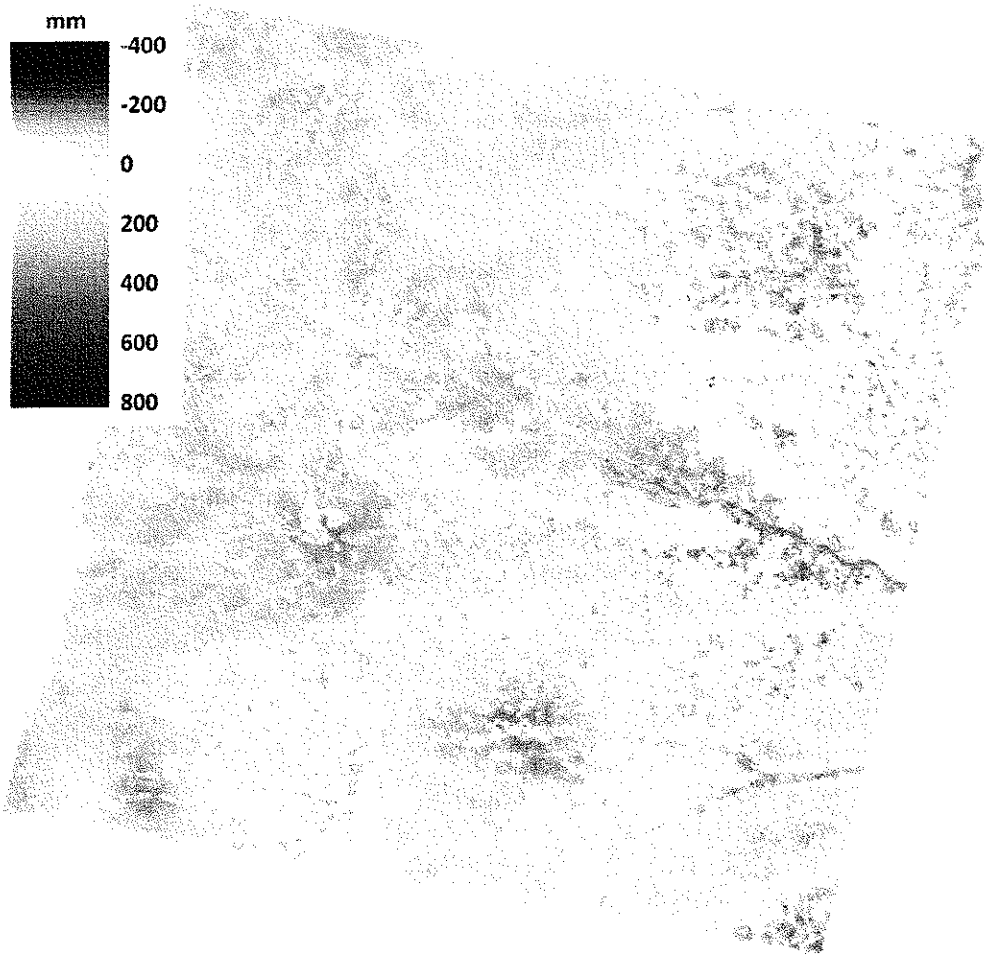


Figure 13. Seasonal (April 1 – October 31 1997), distributed precipitation subtracted from seasonal (April – October 31 1997) ET estimated from METRIC for the entire Landsat scene path 33 row 31. Negative values indicate where precipitation exceeded the ET.

3. Summary

The METRIC (Mapping Evapotranspiration with high Resolution and Internalized Calibration) procedure for determining evapotranspiration (ET) from satellite imagery was applied to the south-west portion of the Nebraskan Panhandle. ET was calculated within METRIC using a surface energy balance applied to Landsat images and augmented by local weather data. Processing was conducted for eight Landsat image dates from 1997, three image dates from 2002 and three image dates from 2005.

ET was calculated with a spatial resolution of 30 m. However, because the thermal information contained in the Landsat 5 images was 120 m resolution and because the METRIC process relies heavily on the thermal information, the 'real' spatial resolution or spatial accuracy and representativeness of the final ET images is probably somewhere between 30 and 120 m. It is, nevertheless, presented as 30 m for ease of handling and sampling. The daily ET maps from 1997 were extrapolated into monthly and seasonal (April 1-October 31) ET estimates. The images processed from 2002 and 2005 were used for training and comparison to images being processed in parallel by the University of Nebraska. The primary focus areas for the METRIC processing were irrigated agricultural areas in the project area. Land areas adjacent to the project area including surrounding rangeland, forest and wilderness areas, agricultural and wetland areas were additionally processed.

Developments were made to the METRIC model during this project to improve performance under the specific conditions of the western Nebraska study area. These specific conditions included the substantial amount of late spring and summer rainfall events and large amounts of clouds in some images that complicated the estimation of monthly and seasonal ET. Improvements included a new cloud gap filling procedure for the ET_rF estimates which automatically adjusts for background evaporation from recent precipitation, gap filling of NDVI, the generation of grids of precipitation and ET_r used to estimate distributed bare soil evaporation and to adjust the satellite date ET estimates for background evaporation, and using evaporative fraction, EF, rather than ET_rF , as the vehicle to extrapolate from the instantaneous, at-satellite overpass time ET estimates to daily values for rangeland.

Since some degree of cloudiness is present within some portions of the images, those areas of some images had to be masked out. The resulting gaps were filled with data from previous and following image dates which increased uncertainties in the ET and ET_rF estimates for the mountain areas. Evaporation from open water bodies within the image was estimated using a function developed for larger, clear lakes in southern Idaho. As a result, the ET estimates from small water bodies, including small shallow lakes, canals, rivers and cattle ponds may have an increased uncertainty compared to larger water bodies.

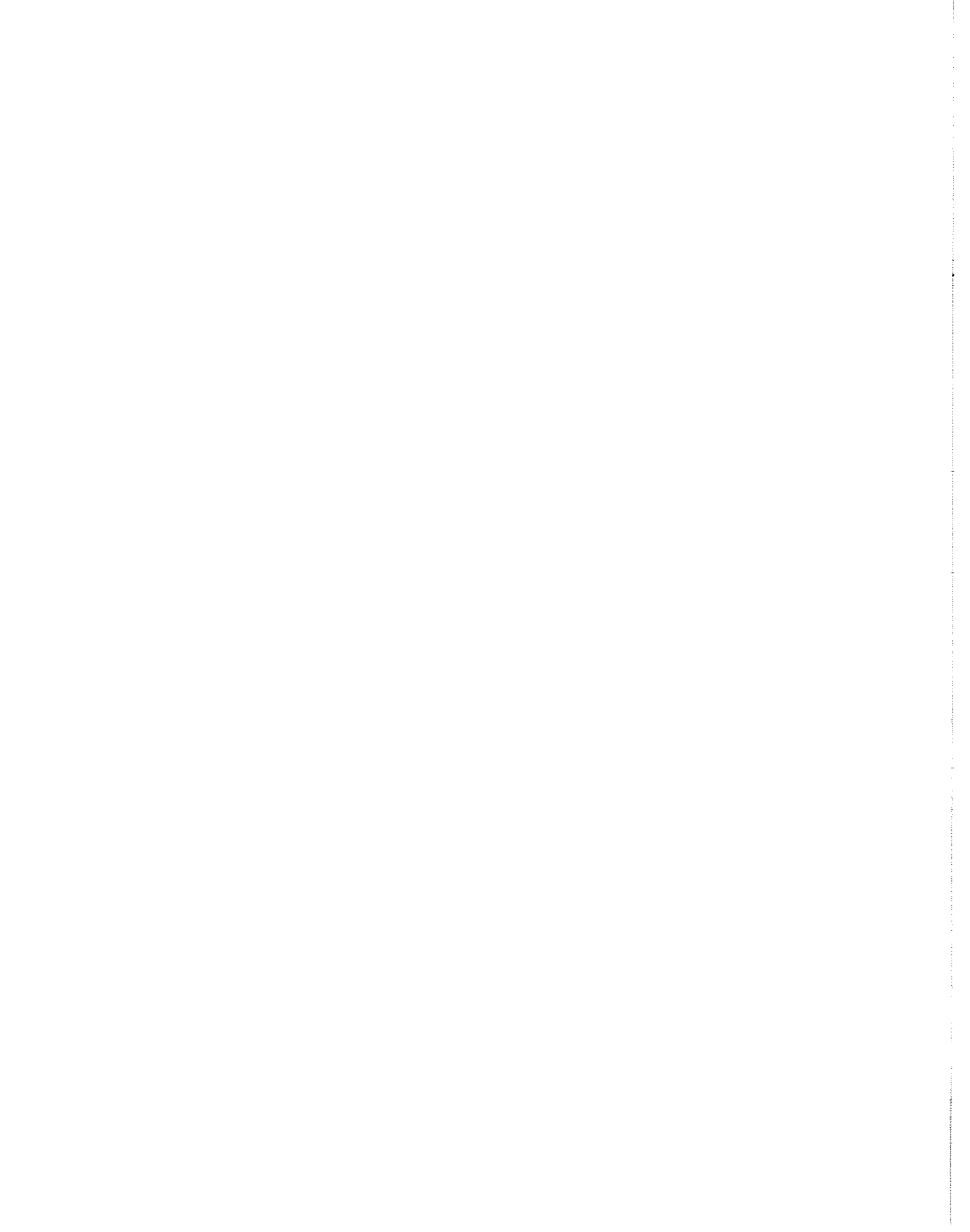
Monthly and growing season (April-October) ET and ET_rF (fraction of alfalfa reference ET) from 1997 was calculated by splining the ET fraction determined for each satellite image over each month and multiplying by reference each day, following adjustment of background evaporation to better represent the periods between satellite image dates.

Differencing of April – October ET and reported precipitation for the image area show areas of substantial recharge where $P > ET$, and areas of irrigation, where $ET > P$. All ET data products are available for each image date, month, and growing season as ERDAS Imagine (.img) files.

4. References

- Allen, R G , 2008. REF-ET: Reference Evapotranspiration Calculation Software for FAO and ASCE Standardized Equations. University of Idaho, 82 pp. [<http://www.kimberly.uidaho.edu/ref-et/index.html>]. Contact author for updates.
- Allen, R.G., Pereira, L.S., Raes, D., Smith, M., 1998. Crop Evapotranspiration. Guidelines for computing crop water requirements. FAO Irrigation and Drainage Paper 56. FAO, Rome, 300 pp.
- Allen, R.G., Pereira, L.S., Raes, D., Smith, M., Wright, J.L., 2005. FAO-56 Dual Crop Coefficient Method for Estimating Evaporation from Soil and Application Extensions. *J. Irrig. Drain. Engr.*, 131(1), 2-13.
- Allen, R.G., Tasumi, M., 2005. Evaporation from American Falls Reservoir in Idaho via a Combination of Bowen Ratio and Eddy Covariance. Proceeding of the EWRI World Water and Environmental Resources Congress 2005: Impacts of Global Change. May 15-19 2005, Anchorage, Alaska. 17 pp.
- Allen, R.G., Tasumi, M., Morse, A., Trezza, R., Wright, J.L., Bastiaanssen, W., Kramber, W., Lorite, I., Robison, C.W., 2007a. Satellite-Based Energy Balance for Mapping Evapotranspiration with Internalized Calibration (METRIC) – Applications. *J. Irrig. Drain. Engr.*, 133(4), 395-406.
- Allen, R.G., Tasumi, M., Trezza, R., 2007b. Satellite-Based Energy Balance for Mapping Evapotranspiration with Internalized Calibration (METRIC) – Model. *J. Irrig. Drain. Engr.*, 133(4), 380-394.
- Allen, R.G., Tasumi, M., Trezza, R., Kjaersgaard, J.H., 2008. METRIC. Mapping Evapotranspiration at High Resolution. Applications Manual, V 2.0.4. University of Idaho. 166 pp.
- ASCE-EWRI, 2005. The ASCE Standardized Reference Evapotranspiration Equation. ASCE, Reston, Virginia.
- Burnett, B., 2007. A Procedure for Estimating Total Evapotranspiration using Satellite-Based Vegetation Indices with Separate Estimates from Bare Soil. M.Sc. Thesis, University of Idaho. 175 pp.
- Kjaersgaard, J., Allen, R.G., 2009. Loading the Landsat thermal band preprocessed using the EROS LPGS system. Kimberly R&E Center, University of Idaho. Report. 9 pp.
- Tasumi, M., Allen, R.G., Trezza, R., Wright, J.L., 2005. Satellite-Based Energy Balance to assess Within-Population Variance of Crop Coefficient Curves. *J. Irrig. Drain. Engr.*, 131(1), 94-109.
- Trezza, R., Allen, R.G., 2008. Analysis of vertical shift in Band 6 of Landsat 5 images in the EROS L1T product. University of Idaho, Kimberly, Idaho. 25 pp. Accessed online on June 17 2009 at <http://www.idwr.idaho.gov/GeographicInfo/PDFs/trezza-allen-thermal-band-shift.pdf>
- Wright, J.L., 1982. New evapotranspiration crop coefficients. *J. Irrig. Drain. Engr.*, 108(1), 57-74.

Appendices



Appendix A

Quality Control of the Weather Data from the Weather Stations used during the Processing of the 1997, 2002 and 2005 Images.

By J. Kjaersgaard and R. Allen, University of Idaho. December 2007. *Revised August 2010*

Processing of Landsat imagery using METRIC to produce monthly and seasonal ET estimates requires the use of hourly meteorological data for calibration of METRIC and requires the creation of a 'surface' of daily reference ET for the image domain for use during interpolation of ET_r between images. For the applications to year 1997, hourly and daily meteorological information from 11 High Plains Regional Climate Center (HPRCC) weather stations, 3 Colorado Agricultural Meteorological Network (CoAgMet) and 55 National Weather Service Cooperative Observer Program (COOP) were assembled and analyzed. The names and locations of the stations are listed in Tables 1 and 2.

For 2002 and 2005, where only three "snapshots" of daily ET was estimated each year, hourly and daily meteorological information from 5 HPRCC weather stations were analyzed and used, viz. Alliance North, Alliance West, Scottsbluff, Sidney and Torrington, WY.

The HPRCC and CoAgMet weather stations are of interest because they measure and report meteorological information relevant to the estimation of alfalfa reference evapotranspiration (ET_r) calculated using the ASCE standardized Penman-Monteith equation (ASCE-EWRI, 2005), which in turn is required input for the satellite image processing using METRIC. The meteorological parameters needed are hourly values of solar radiation (R_s), air temperature (T_a), air humidity (expressed as relative humidity (RH); dew point temperature (T_{dew}); or vapor pressure (e_a)) and wind speed (WS). In addition daily values of precipitation are required to establish a water balance for the upper soil layers

During the processing of the satellite images, the METRIC model was calibrated using hourly data from the Scottsbluff, Sidney and the Alliance North HPRCC weather stations. ET_r and precipitation from these three stations were used to establish daily estimates of bare soil evaporation used during METRIC calibrations. In addition, ET_r and precipitation from these three stations and all other stations listed in Tables 1 and 2 were used to establish distributed estimates of bare soil evaporation using a gridded daily process model to adjust the monthly and seasonal ET estimates for background evaporation from antecedent rainfall. Distributed ET_r estimated from the stations listed in Table 1 were additionally used during the estimation of daily ET, in mm, between the satellite image dates.

Several of the weather stations are located outside the geographical domain of the Landsat scenes processed. These stations were included to improve the accuracy of ET_r and precipitation along the image edges, when interpolating between the point locations of the weather stations to fully distributed estimates.

Table 1. Names, station IDs, weather station network, locations and elevation of the weather stations used to estimate distributed maps of reference ET.

| Station | StationID | Network | State | Latitude* | Longitude* | Elevation, m* |
|------------------|-----------|---------|-------|-----------|------------|---------------|
| Alliance_North | 1 | HPRCC | NE | 42 18 | -102 92 | 1213 |
| Alliance_West | 2 | HPRCC | NE | 42 02 | -103 13 | 1213 |
| Arapahoe_Prairie | 3 | HPRCC | NE | 41 48 | -101 85 | 1097 |
| Arthur | 4 | HPRCC | NE | 41 65 | -101 52 | 1097 |
| Gudmundsen_Ranch | 5 | HPRCC | NE | 42 07 | -101 43 | 1049 |
| Mitchell_Farms | 6 | HPRCC | NE | 41 93 | -103 7 | 1098 |
| Scottsbluff | 7 | HPRCC | NE | 41 88 | -103 67 | 1208 |
| Sidney | 8 | HPRCC | NE | 41 22 | -103 02 | 1397 |
| Sterling | 9 | HPRCC | CO | 40 47 | -103 02 | 2000 |
| Torrington | 10 | HPRCC | WY | 42 03 | -104 18 | 1216 |
| Gordon | 11 | HPRCC | NE | 42 73 | -102 17 | 1109 |
| CSU_ARDEC | 12 | CoAgMet | CO | 40 65 | -105 | 1558 |
| FortCollins_AERC | 13 | CoAgMet | CO | 40 59 | -105.137 | 1561 |
| Haxtun | 14 | CoAgMet | CO | 40 67 | -102 65 | 1231 |

Latitude, longitude and elevation obtained from <http://www.hprcc.unl.edu/index.php> and <http://climate.colostate.edu/~coagmet/>; last accessed August 1 2010

Table 2. Names, station IDs, state and county, locations and elevation of the weather stations used to estimate distributed maps of precipitation (in addition to the HPRCC and CoAgMet stations in Table 1).

| Station_Name | Station_ID | STATE | COUNTY | Latitude | Longitude | Elevation, m |
|-------------------|------------|-------|-----------|----------|-----------|--------------|
| AGATE 3 E | 250030 | NE | SIoux | 42 42 | -103.73 | 1423 |
| AGATE 5N | 250035 | NE | SIoux | 42 50 | -103.80 | 1447 |
| ALLIANCE 1WNW | 250130 | NE | BOX BUTTE | 42 10 | -102.88 | 1217 |
| BIG SPRINGS | 250865 | NE | DEUEL | 41 03 | -102 13 | 1121 |
| BRIDGEPORT | 251145 | NE | MORRILL | 41 67 | -103 10 | 1117 |
| CHADRON MUNI AP | 251575 | NE | DAWES | 42 83 | -103.08 | 1011 |
| CHADRON 3SW | 251575 | NE | DAWES | 42 80 | -103 05 | 1031 |
| CRAWFORD | 251973 | NE | DAWES | 42 70 | -103 42 | 1119 |
| CRESCENT LAKE NWR | 252000 | NE | GARDEN | 41 75 | -102 43 | 1164 |
| DALTON | 252145 | NE | CHEYENNE | 41 40 | -102 95 | 1304 |
| ELLSWORTH | 252645 | NE | SHERIDAN | 42 05 | -102 27 | 1190 |
| ELLSWORTH 15 NNE | 252647 | NE | SHERIDAN | 42 25 | -102 20 | 1210 |
| FT ROBINSON | 253015 | NE | DAWES | 42 65 | -103 45 | 1162 |
| HARRISBURG 12WNW | 253605 | NE | BANNER | 41 62 | -103 95 | 1387 |
| HARRISON | 253615 | NE | SIoux | 42 68 | -103 88 | 1478 |
| HAY SPRINGS | 253710 | NE | SHERIDAN | 42 67 | -102 68 | 1175 |
| HAY SPRINGS 12 S | 253715 | NE | SHERIDAN | 42 50 | -102.68 | 1160 |
| HEMINGFORD | 253755 | NE | BOX BUTTE | 42 32 | -103.07 | 1301 |
| KIMBALL 2NE | 254440 | NE | KIMBALL | 41 23 | -103.63 | 1435 |

| | | | | | | |
|-----------------------|--------|----|--------------|-------|---------|------|
| LISCO | 254865 | NE | GARDEN | 41 48 | -102 62 | 1071 |
| LODGEPOLE | 254900 | NE | CHEYENNE | 41 13 | -102 63 | 1168 |
| LYMAN | 255020 | NE | SCOTTS BLUFF | 41 92 | -104 03 | 1234 |
| MITCHELL 5E | 255590 | NE | SCOTTS BLUFF | 41 93 | -103 70 | 1244 |
| OSHKOSH | 256385 | NE | GARDEN | 41 40 | -102 33 | 1033 |
| OSHKOSH 8 SW | 256390 | NE | GARDEN | 41 30 | -102 43 | 1167 |
| POTTER | 256880 | NE | CHEYENNE | 41 22 | -103 32 | 1350 |
| RUSHVILLE | 257415 | NE | SHERIDAN | 42 72 | -102 45 | 1146 |
| SCOTTSBLUFF HEILIG AP | 257665 | NE | SCOTTS BLUFF | 41 87 | -103 58 | 1202 |
| SIDNEY 6 NNW | 257830 | NE | CHEYENNE | 41 22 | -103 02 | 1317 |
| ALBIN | 480080 | WY | LARAMIE | 41 40 | -104 10 | 1629 |
| ARCHER | 480270 | WY | LARAMIE | 41 15 | -104 65 | 1832 |
| CARPENTER 3N | 481547 | WY | LARAMIE | 41 08 | -104 37 | 1657 |
| CHEYENNE MUNI AP | 481675 | WY | LARAMIE | 41 15 | -104 82 | 1868 |
| CHUGWATER | 481730 | WY | PLATTE | 41 75 | -104 82 | 1617 |
| DOUBLE FOUR RCH | 482680 | WY | ALBANY | 42 17 | -105 40 | 1865 |
| DOUGLAS 1 SE | 482685 | WY | CONVERSE | 42 73 | -105 35 | 1484 |
| HECLA 1E | 484442 | WY | LARAMIE | 41 15 | -105 17 | 2039 |
| LA GRANGE | 485260 | WY | GOSHEN | 41 63 | -104 17 | 1399 |
| LINGLE 2WSW | 485612 | WY | GOSHEN | 42 12 | -104 38 | 1267 |
| OLD FT LARAMIE | 486852 | WY | GOSHEN | 42 20 | -104 55 | 1295 |
| PHILLIPS | 487200 | WY | GOSHEN | 41 62 | -104 48 | 1519 |
| PINE BLUFFS 5W | 487240 | WY | LARAMIE | 41 17 | -104 15 | 1579 |
| PINE BLUFFS 10 NW | 487248 | WY | LARAMIE | 41 30 | -104 18 | 1625 |
| SYBILLE RSCH UNIT | 488808 | WY | ALBANY | 41 75 | -105 37 | 1859 |
| TORRINGTON EXP FARM | 488995 | WY | GOSHEN | 42 07 | -104 22 | 1249 |
| TORRINGTON 29N | 488997 | WY | GOSHEN | 42 48 | -104 15 | 1481 |
| WHEATLAND 4 N | 489615 | WY | PLATTE | 42 10 | -104 93 | 1414 |
| YODER 5 W | 489925 | WY | GOSHEN | 41 90 | -104 38 | 1320 |
| CHEYENNE | 999999 | WY | LARAMIE | 41 15 | -104 80 | 1868 |
| BRIGGSDALE | 50945 | CO | WELD | 40 63 | -104 32 | 1473 |
| NEW RAYMER | 55922 | CO | WELD | 40 60 | -103 83 | 1458 |
| NEW RAYMER 21 N | 55934 | CO | WELD | 40 92 | -103 87 | 1579 |
| NUNN | 56023 | CO | WELD | 40 70 | -104 78 | 1584 |
| STERLING | 57950 | CO | LOGAN | 40 62 | -103 20 | 1199 |
| VIRGINIA DALE 7 ENE | 58690 | CO | LARIMER | 40 95 | -105 22 | 2138 |
| WELLINGTON 5 WNW | 58907 | CO | LARIMER | 40 72 | -105 10 | 1603 |

Calculation of ET_r

For the purpose of calculating ET_r using the Standardized Penman-Monteith equation, hourly values of T_a , T_d , R_s and WS along with information of year, month, date and time-of-day for each time step were assembled from HPRCC and CoAgMet archives and exported to comma separated text files.

ET_r was calculated using the RefET V3.1 software, developed by Dr. Rick Allen, University of Idaho. RefET computes ET_r following the recommendations of ASCE-EWRI (2005). RefET is very flexible regarding the units of the individual weather parameters in the input file, and units for the output file is selected by the user; metric units are preferred to be congruent with the units used in METRIC (no pun intended).

The software and additional information, including a user manual, are available from <http://www.kimberly.uidaho.edu/ref-et/index.html>

Daily ET_r was calculated by summing hourly ET_r estimates to 24-h values. It should be noted, that it is recommended (Allen et al., 2006; ASCE-EWRI, 2005, Irmak et al., 2005) to calculate daily ET_r as the sum of hourly values rather than summing or averaging hourly input parameters (T_a , T_d , R_s and WS) to daily values before calculating ET_r .

Weather data quality control

A description of procedures and thresholds for quality control of weather data is in appendix D of ASCE-EWRI (2005). This publication further provides insight and methods for calculating a theoretical clear sky solar radiation curve, which is a powerful parameter to use for indicating not only possible errors in R_s (e.g. calibration errors, sensor misalignment, damaged sensor etc), **but also errors in datalogger time stamps and internal clock.**

Daily R_s is compared to calculated clear sky solar radiation, R_{s0} . R_{s0} is calculated based on atmospheric pressure, sun angle and precipitable water in the atmosphere. On clear sky days the measured R_s should approach the value of R_{s0} . The R_{s0} curve may be obtained as one of the outputs from the RefET software.

Figure 1 shows daily solar radiation from the Alliance West HPRCC weather station for year 1997. From the beginning of the year until about day of year (DOY) 135 the recorded values for R_s were about 17 % lower than the R_{s0} curve. The errors in R_s were rectifiable by applying an appropriate multiplication factor. The solar radiation after applying a correction factor of 1.17 is also shown in Figure 1.

In general, as summarized in Table 3, the solar radiation data for the HPRCC required a substantially amount of adjustment, especially during the first third of 1997. Low calibrations of sensors may have occurred as an artifact of the calibration procedures practiced by HPRCC at that time.

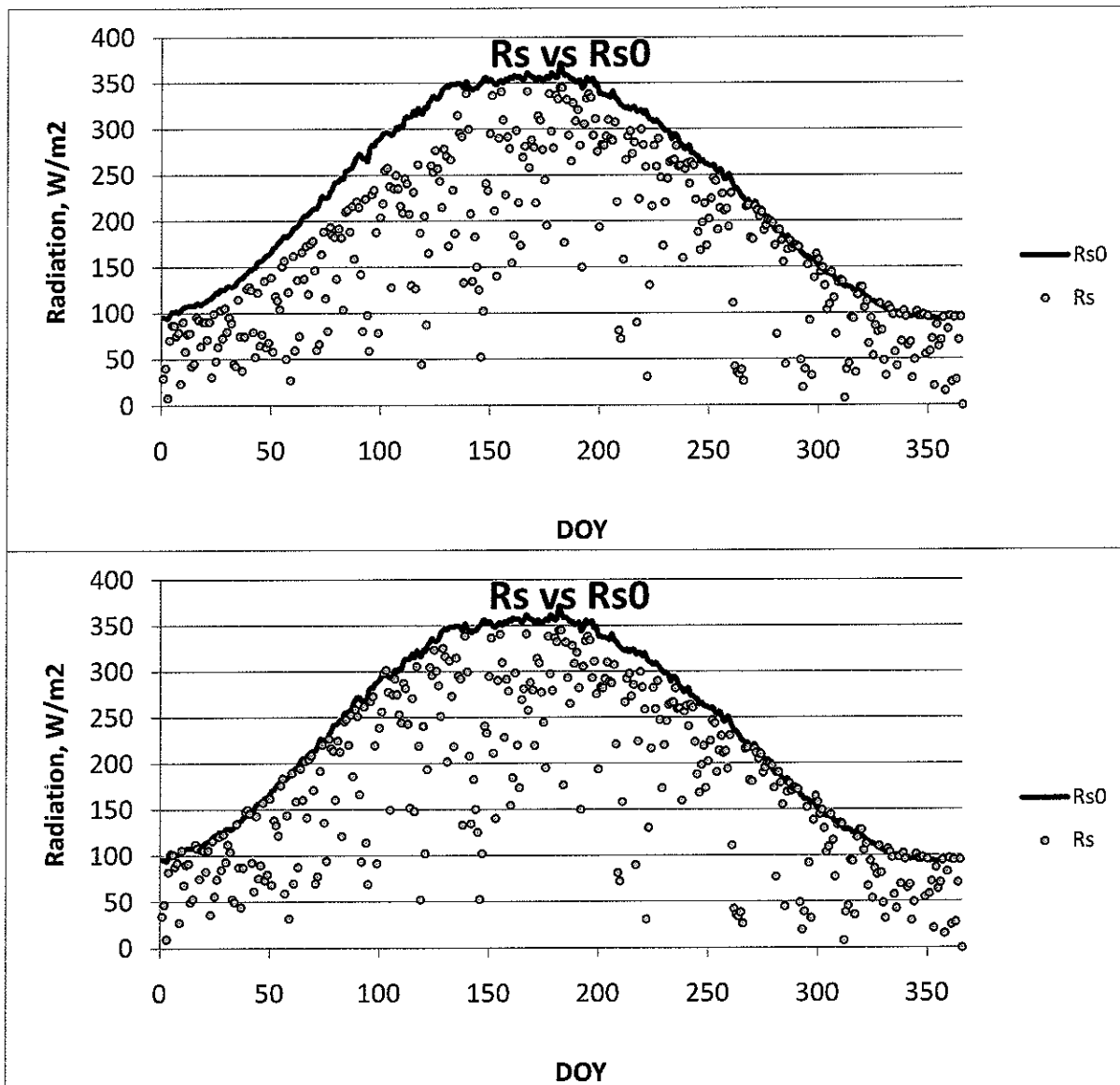


Figure 1 Daily recorded solar radiation (R_s) and the theoretical clear sky solar radiation curve (R_{s0}) for the Alliance West HPRCC weather station for 1997 before (top) and after (bottom) correction (multiplying by 1.17 prior to DOY 135).

Daily 24-h air temperature data were screened to check the dataset for outliers and the expected annual occurrence of maximum and minimum temperatures. Air temperature data were analyzed by subtracting the average of 24 hourly T_a from the difference between daily temperature extremes (minimum and maximum T_a). Systematic differences greater than 2-3 °C may indicate erroneous extremes in air temperature or impacts of missing hourly data.

Air humidity is shown in Figure 2 as minimum and maximum daily RH. In relatively arid regions such as the Nebraskan Panhandle, daily minimum RH may run as low as 15 – 20 % during the dry part of the year. Daily maximum RH is generally in the range of 90 - 100 % for irrigated areas having sufficient fetch and adequate water supply, especially during “wet”

portions of the year. An example using humidity and precipitation from the Scottsbluff HPRCC weather station is shown in Figure 2. These data appear to be of good quality, although the very low values of RH_{\min} less than 10% during March and April are somewhat unexpected. If real, these data represent the advection of extremely dry air into the region.

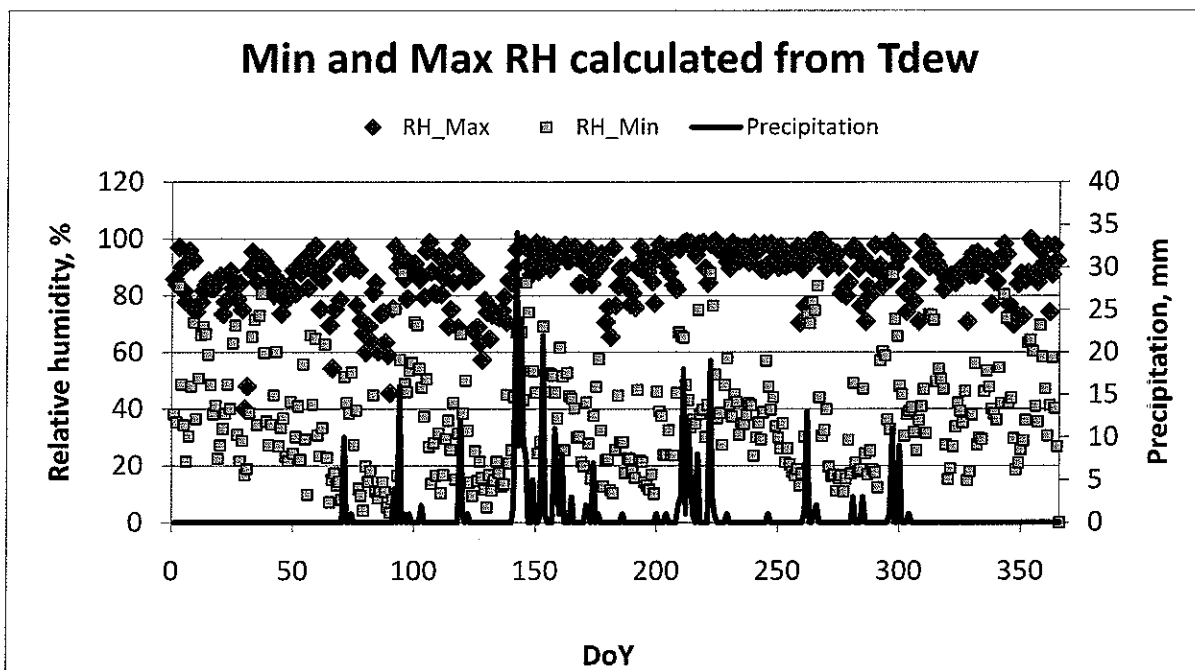


Figure 2 Daily maximum and minimum relative humidity (%) calculated from T_d and T_a , and precipitation recorded at the Scottsbluff HPRCC weather station during 1997

Daily average wind speed data were plotted as a function of day of year (DOY) to check for outliers. Continuous periods with wind speeds less than 1 m/s may indicate problems with the anemometer. Also, daily wind speed data were compared among the three calibration stations to identify spuriously high values and systematically higher wind speeds as compared to the other stations. The gust factor, calculated as the ratio of maximum daily wind speed to mean daily wind speed, is plotted to evaluate the functioning of the anemometer. If the gust factor over time shows a period of large values the anemometer may be malfunctioning. Also, if the gust factor drops to a value of 1 the sensor may be failing completely. An example using wind speed from the Scottsbluff HPRCC weather station is shown in Figure 3.

Daily values of precipitation were compared for all stations to evaluate the temporal occurrence of precipitation and the amount received. Generally precipitation is very heterogeneous, however if one of the stations systematically recorded substantially less precipitation this may indicate a dirty or malfunctioning rain gauge. Precipitation is not measured during the winter period at the HPRCC stations. The cumulative precipitation for the period March 15 – October 31 1997 from six HPRCC weather stations are shown in Figure 4.

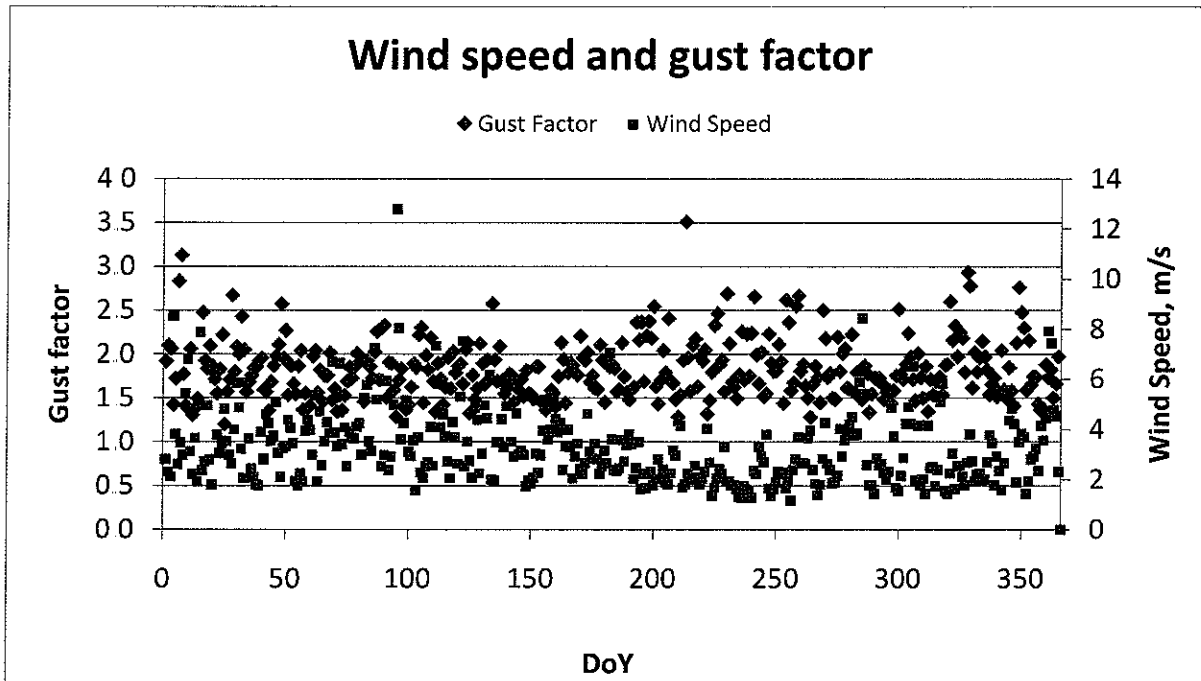


Figure 3 Daily gust factor and average wind speed (m/s) recorded at the Scottsbluff HPRCC weather station

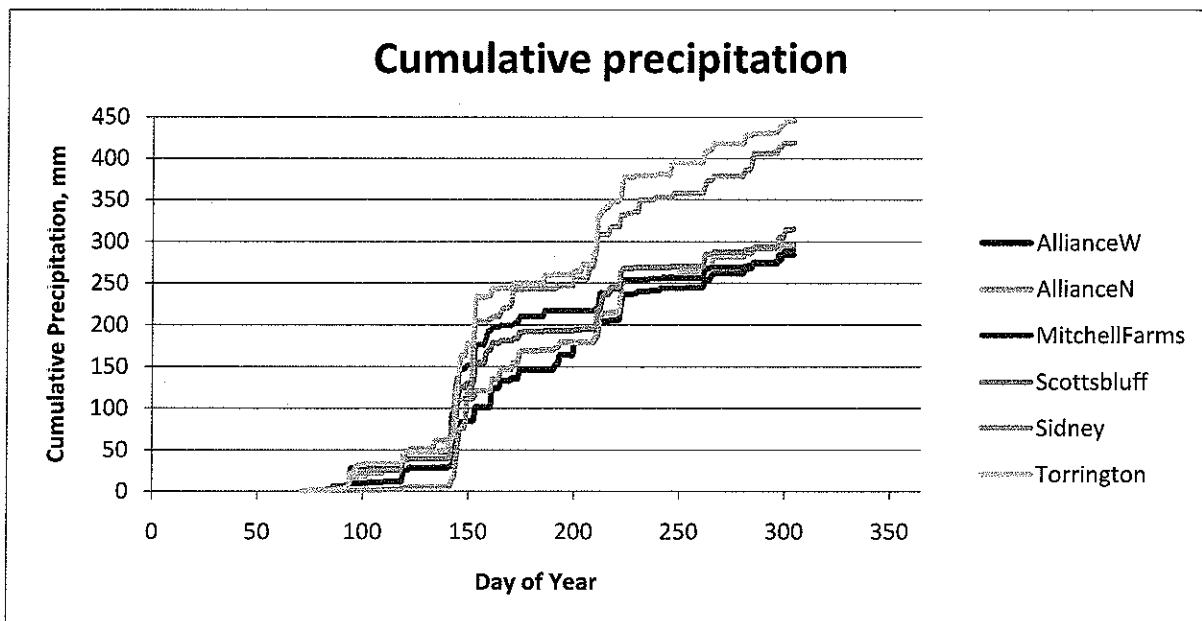


Figure 4. Daily cumulative precipitation from March 15 – October 31 1997 from the Alliance W, Alliance N, Mitchell Farms, Scottsbluff, Sidney, and Torrington HPRCC weather stations

Precipitation data from 111 COOP station were downloaded from the COOP data access website at <http://www.ncdc.noaa.gov/oa/climate/stationlocator.html>. The precipitation data were screened for location relative to the study area, completeness of data, missing data values and

relative precipitation amounts. 56 COOP stations were filtered from the dataset. At the COOP stations, precipitation is recorded year round. Snow depths are converted to depth of water.

A summary of the weather data quality control is shown in Table 3.

Table 3. Summary of the weather data quality control of the weather data from the HPRCC and CoAgMet weather stations. Meteorological parameters are within expected ranges unless otherwise noted. DOY is day of year.

| Station | Year | Status | Comment or remedy |
|----------------------|------|---|--|
| AllianceN | 1997 | R _s calibration drifting | R _s adjusted up 5% between DOY 1-138, adjusted down 4 % DOY 268-365 |
| AllianceN | 2005 | OK | |
| AllianceW | 1997 | R _s calibration error | R _s adjusted up 17% between DOY 1-135 |
| Arapahoe | 1997 | R _s calibration error | R _s adjusted up 11% between DOY 1-123, adjusted down 9 % DOY 124-365 |
| Arthur | 1997 | R _s calibration error | R _s adjusted up 19% between DOY 1-123, adjusted up 6 % DOY 124-139 |
| Gordon | 1997 | OK | |
| Gudmundsen | 1997 | R _s calibration error | R _s adjusted up 18% between DOY 204-252, adjusted up 10 % DOY 252-365 |
| Mitchell Farms | | OK | |
| Scottsbluff | 1997 | R _s offset, probably caused by sensor being tilted East T _a DOY 5-7 out of phase with normal diurnal pattern | Radiation data adjusted hour-by-hour using linear and polynomial functions to correct sensor misalignment Data from AllianceW and AllianceN used to fill in |
| Scottsbluff | 2002 | OK | |
| Scottsbluff | 2005 | R _s calibration error | R _s adjusted down 5 % between DOY 1-123 |
| Sidney | 1997 | R _s calibration error | R _s adjusted down 7 % between DOY 1-46 |
| Sidney | 2002 | R _s calibration error | R _s adjusted up 10 % between DOY 1-130 |
| Sidney | 2005 | R _s calibration error | R _s adjusted down 5 % between DOY 1-124 |
| Sterling | 1997 | R _s calibration error | R _s adjusted down 30% between DOY 1-106, adjusted down 26 % DOY 107-281, adjusted down 49 % DOY 282-365 |
| Torrington | 1997 | R _s calibration error | R _s adjusted down 5 % between DOY 76-139 |
| CSU_ARDEC | 1997 | OK | |
| Fort Collins AERC | 1997 | Missing R _s | Some missing days from DOY 290 onwards, filled in using CSU_ARDEC |
| Haxtun | 1997 | R _s calibration error | Measurements available from DOY 86; R _s adjusted up 75% between DOY 86-107, adjusted down 6 % DOY 108-365 |

Calculated reference evapotranspiration

Reference evapotranspiration, ET_r, is calculated using the ASCE-EWRI (2005) standardized Penman-Monteith equation and is applied for both the alfalfa reference and the grass reference. Alfalfa based ET_r is used in METRIC in the calculation of sensible heat flux, and data are presented below. The ET_r values shown in this section were calculated following correction of R_s for all HPRCC and CoAgMet stations.

Figure 5 shows the cumulative ET_r calculated for the six HPRCC weather stations located within Landsat path 32/33 row 31. ET_r runs slightly higher at Sidney compared to the other stations. The Mitchell Farms station, which is located about 10 miles north east of Scottsbluff runs lower

than the other stations. The Mitchell Farms weather station is located in an agricultural equipment yard, and nearby machinery and building may slow the wind speed and thus decrease the ET_r .

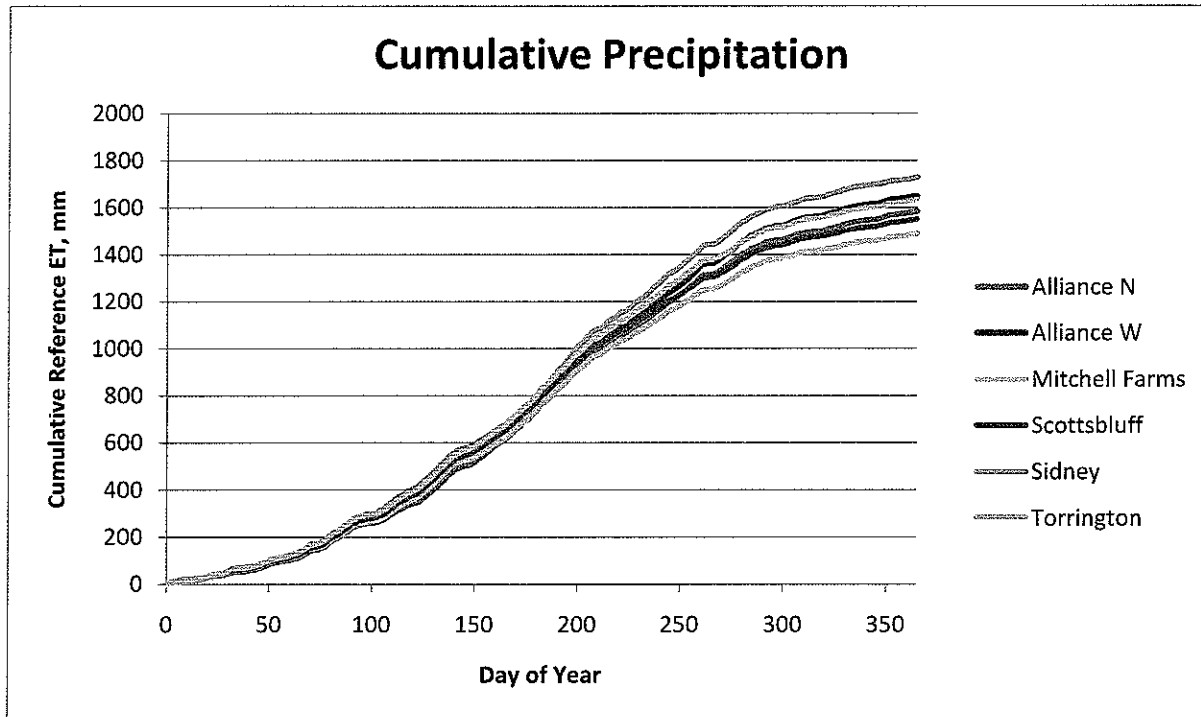


Figure 5 Daily cumulative reference ET (ET_r) from 1997 calculated from hourly weather data from the Alliance W, Alliance N, Mitchell Farms, Scottsbluff, Sidney, and Torrington HPRCC weather stations following QA/QC of weather data.

References

- Allen, R.G., 1996. Assessing Integrity of Weather Data for Reference Evapotranspiration Estimation. *J. Irrig. Drain. Engr.*, 122, 97-106.
- Allen, R.G., et al., 2006. A Recommendation on the Standardized Surface Resistance for Hourly Calculation of Reference ET by the FAO56 Penman-Monteith Method. *Agric Water Manag.*, 81, 1-22.
- Allen, R.G., Tasumi, M., Morse, A., Trezza, R., Wright, J.L., Bastiaanssen, W., Kramber, W., Lorite, I., Robison, C.W., 2007a. Satellite-Based Energy Balance for Mapping Evapotranspiration with Internalized Calibration (METRIC) – Applications. *J. Irrig. Drain Engr.*, 133(4), 395-406.
- Allen, R.G., Tasumi, M., Trezza, R., 2007b. Satellite-Based Energy Balance for Mapping Evapotranspiration with Internalized Calibration (METRIC) – Model. *J. Irrig. Drain Engr.*, 133(4), 380-394.
- ASCE-EWRI, 2005. The ASCE Standardized Reference Evapotranspiration Equation. ASCE, Reston, Virginia.

Irmak, S., T. A. Howell, R. G. Allen, J. O. Payero, D. L. Martin. 2005. Standardized ASCE Penman-Monteith: impact of sum-of-hourly vs. 24-hour timestep computations at reference weather station sites. *Trans ASABE*. Vol. 48(3): 1063-1077.

Appendix B

Selection of images for METRIC processing for the Nebraska Panhandle

By J. Kjaersgaard and R. Allen, University of Idaho. August 2007. Revised August 2010.

Introduction and image selection criteria

This note describes the procedure for selecting Landsat satellite images from 1997, 2002 and 2005 to be processed using the METRIC ET procedure for the Nebraska Panhandle. For this application, images from the Landsat 5 and Landsat 7 satellites were utilized due to their band combinations and high resolution. The image archive for Landsat 5 dates back to 1984 and the satellite is still in operation. Landsat 7 was launched in 1999, but the scan line corrector failed in May 2003 resulting in subsequent images having wedge shaped stripes of missing data across the scenes. There is no information contained in the stripes.

The North Platte and the South Platte Natural Resource Districts (NRDs) are located in two Landsat scene path/rows, i.e. path 32 and 33, row 31.

As part of the project, three years of particular interest were identified. Because water legislation in Nebraska operates with year 1997 as a 'base' year, this year has high priority to be processed. In order to identify the two remaining years, which preferably should be a relatively wet year and a relatively dry year, each year 1997 – 2006 was assessed for the annual precipitation relative to normal precipitation values. Table 1 shows the annual precipitation at the Scottsbluff HPRCC weather station and an assessment of whether each year 1997 – 2006 is dry, average or wet.

Table 1. Precipitation at the Scottsbluff HPRCC weather station and an assessment of whether each year is dry, average or wet relative to the normal of 15-16 inches annually.

| Year | Precipitation (inches) | Relative to Normal | Comments |
|------|------------------------|--------------------|--------------------------|
| 1997 | 20 | Wet | High rain in April-July |
| 1998 | 17 | Ave | |
| 1999 | 17 | Ave | |
| 2000 | 15 | Ave | Rain in April, September |
| 2001 | 13 | Ave | Rain in April-July |
| 2002 | 8 | Dry | |
| 2003 | 10 | Dry | |
| 2004 | 12 | Ave | |
| 2005 | 20 | Wet | Wet April-June |
| 2006 | 12 | Ave | |

The most important criteria for the image selection is an assessment of cloud conditions at the time of the satellite overpass. The occurrence of conditions impeding the clearness of the atmosphere, such as clouds (including thin cirrus clouds and jet contrails), smoke, haze and similar over the study area may render parts of an image unusable for processing in METRIC. Even very thin cirrus clouds have a much lower

surface temperature than the ground surface and because METRIC needs surface temperature estimates to solve the energy balance, areas with cloud cover cannot be used in the surface energy balance estimations. In addition, in cases of partial cloud cover, land areas recently shaded by clouds may be cooler as they have not yet reached a thermal equilibrium corresponding to the clear sky energy loading, and will also have to be masked out.

To aid the selection of images an image rating system was employed, where the usability of an image in terms of cloudiness and smoke was ranked as a fraction on a scale between "0" and "1", where "0" is an unusable image (e.g. complete cloud cover) and "1" is a nice, usable image. If an image has partial cloud cover over the study area it was rated accordingly, e.g. if an estimated 70% of the study area or area of interest is judged to be free of clouds and cloud shadows, it may be rated 0.7.

A graphical representation of the ratings for path 32/33, row 31 for the years 1997, 2002 and 2005 is shown in Figures 1 – 3. Images are assessed using the USGS on-line image preview tool glovis at <http://glovis.usgs.gov/>

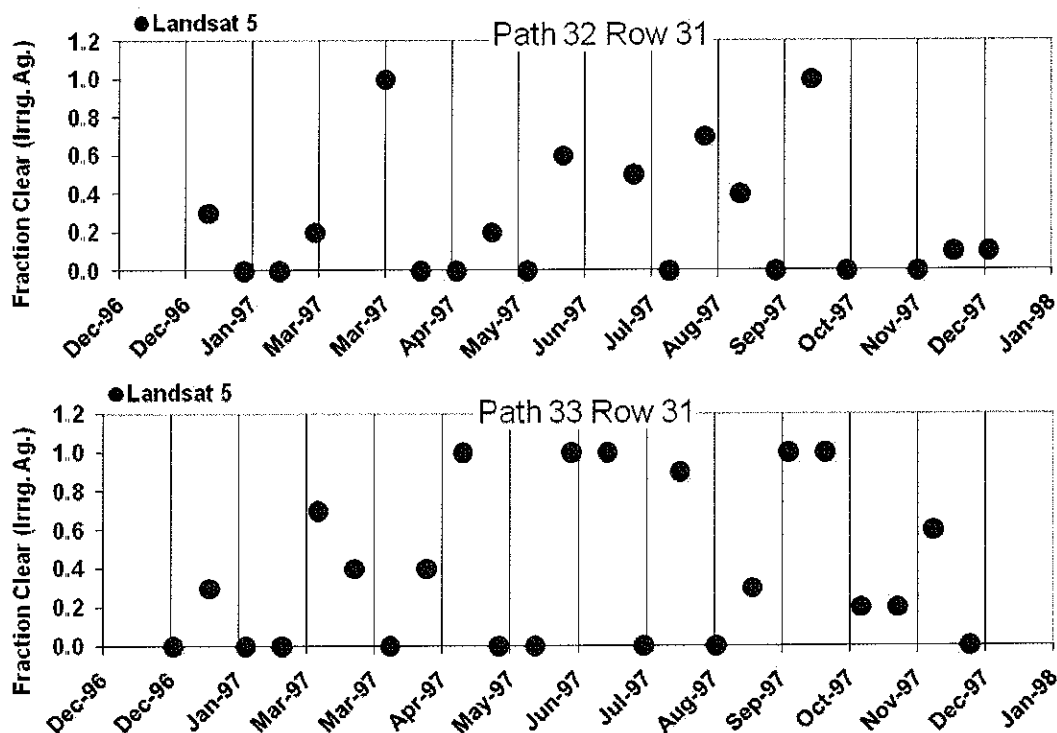


Figure 1. Usability rating of Landsat images in terms of cloudiness for path 32 row 31 (top) and path 33 row 31 (bottom) for 1997, primarily over areas of interest (irrigated areas).

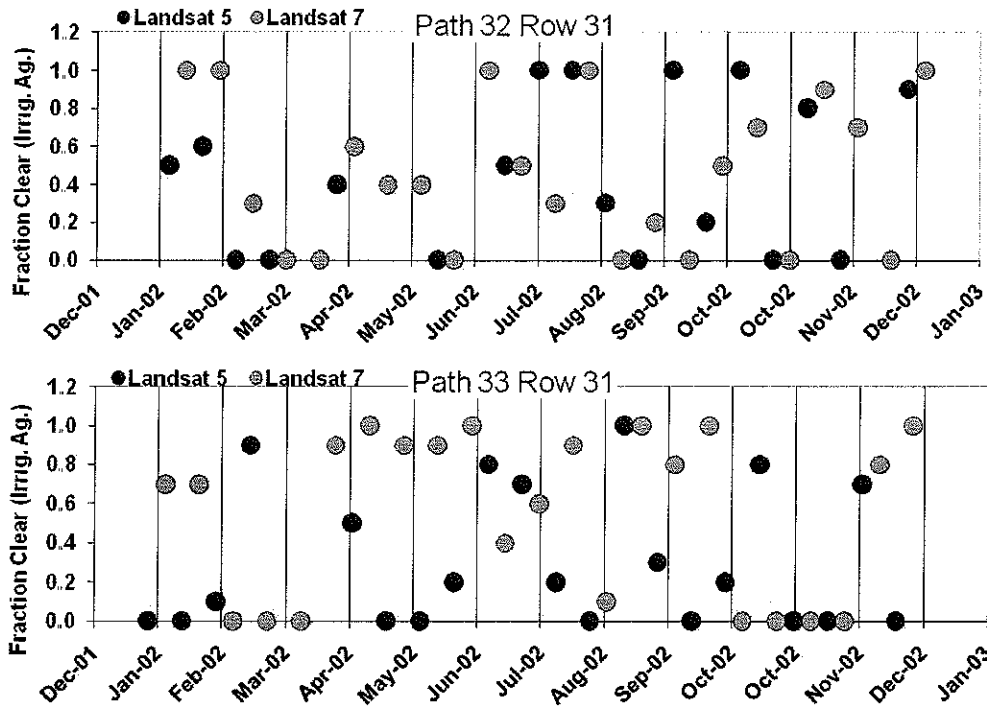


Figure 2. Usability rating of Landsat images in terms of cloudiness for path 32 row 31 (top) and path 33 row 31 (bottom) for 2002.

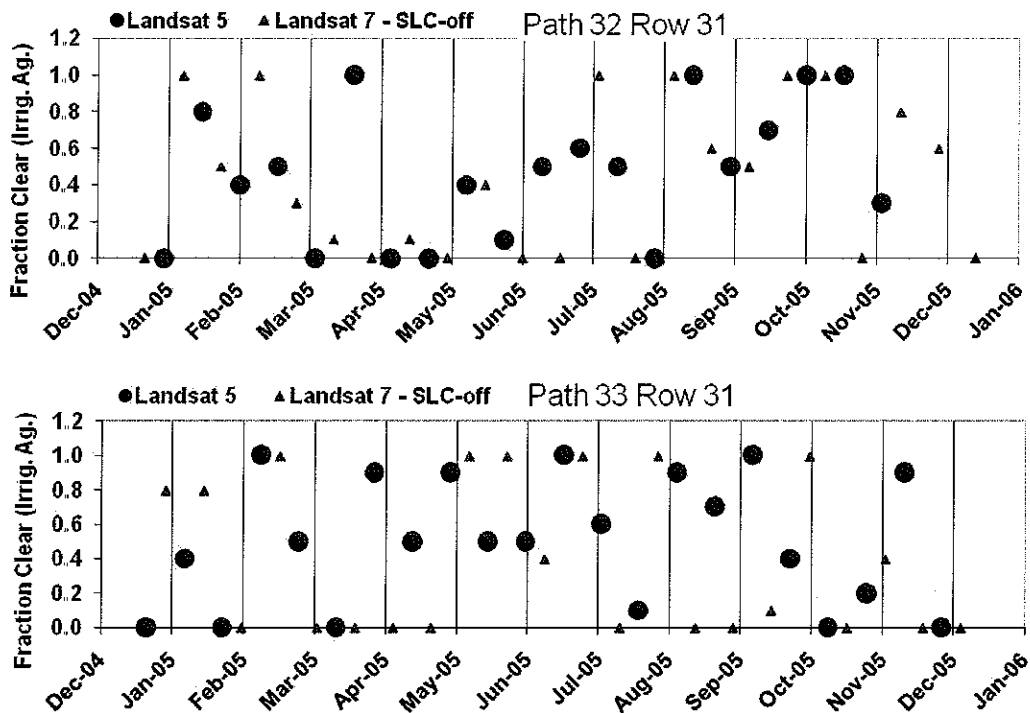


Figure 3. Usability rating of Landsat images in terms of cloudiness for path 32 row 31 (top) and path 33 row 31 (bottom) for 2005

Images from Landsat 7 (SLC-off) are generally less suited for the METRIC processing, as portions of the image contain no data. Even though the study area is located towards the center of the image, some parts were still covered by blank areas. Due to the temporal spacing between images, it is difficult to fill these gaps, resulting in “holes” when ET calculated from each image is aggregated to monthly and seasonal ET. Information must therefore be interpolated from adjacent image dates, which causes some loss in developmental information on ET.

The image assessment in terms of cloudiness and image sequence distribution for the years 1997 – 2007 are summarized in Table 2

Table 2. Image assessment in terms of cloudiness and sequence distribution for the years 1997 – 2007.

| Year | Image Sequence Summary |
|------|--|
| 1997 | Path 33 has 7 good images, but nothing earlier than April 23 and 6-week gap in mid-May through June and mid August through September Path 32 has a 2 month gap during April - mid June and a 6 week gap during Sept.-early Oct. |
| 1998 | Path 33 has only 5 good images with 2 month gaps in April-May, July - Aug., and Oct.-Nov. |
| 1999 | Path 33 has only a few good images |
| 2000 | Path 33 is not a bad sequence, but is weak in April-May (no LS5 and partly cloudy LS7 before June 1) Good after that Path 32 has a two-month gap during Mar.-April., otherwise, good combo. with LS5 and LS7 |
| 2001 | Path 33 has no LS5 before late May, weak (partly cloudy with LS7) until May 7 Good year after that Path 32 is weak in Mar.-April, otherwise, OK |
| 2002 | Path 33, LS5 has 2 month gaps during April-May, June-Aug and Aug-Sept., LS7 fills in well for the most part. Path 32 is acceptable |
| 2003 | Path 33 has 6-week gap from mid Feb-Mar., 2 month gap in April-June (LS5) and too many cloudy LS7 dates to use. |
| 2004 | Path 33 has good LS5 except for a 2 month gap during May-June Can use SLC-off LS7 to fill in partly Path 32 is weak, with 3 month gap mid-June – early September |
| 2005 | Path 33 has some gaps in the Landsat sequence, but Landsat 7 can be used to fill in Path 32 has mostly cloudy images between mid-March through early July |
| 2006 | Nearly average year for precipitation, so not of interest. |
| 2007 | Project year start midway through this year, so it was not considered. |

Image selection

Based on the wet/dry year assessments and the image usability assessments, the years 1997, 2002 and 2005 were selected by UNL and UI to be processed. Path 32 generally has more clouded images compared to path 33. As a result, only one image from path 32 is available to process for the year 1997, while there are sufficient images to estimate monthly and seasonal ET estimates from path 33 in 1997.

A total of nine images from 1997, three from 2002 and three from 2005 were selected for processing by UI, Table 3, as part of the contractual partnership with UNL. The images were selected so that they were distributed as evenly as possible throughout the

1997 growing season with preferably no more than 32 days between images so as to adequately follow the evolution of vegetation development. The images from 2002 and 2005 were selected to represent early, middle and late growing season conditions, both Landsat paths and both Landsat 5 and Landsat 7 to be used for training and for comparisons to parallel processing by the University of Nebraska.

Table 3. Dates, satellite platform and path/row processed using METRIC by the University of Idaho.

| Date | Satellite | Path | Row |
|-------------------|-----------|------|-----|
| 04/23/1997 | Landsat 5 | 33 | 31 |
| 05/09/1997 | Landsat 5 | 33 | 31 |
| 06/26/1997 | Landsat 5 | 33 | 31 |
| 07/12/1997 | Landsat 5 | 33 | 31 |
| 08/13/1997 | Landsat 5 | 33 | 31 |
| 08/22/1997 | Landsat 5 | 32 | 31 |
| 09/30/1997 | Landsat 5 | 33 | 31 |
| 10/16/1997 | Landsat 5 | 33 | 31 |
| 12/03/1997 | Landsat 5 | 33 | 31 |
| 03/28/2002 | Landsat 7 | 33 | 31 |
| 06/08/2002 | Landsat 5 | 33 | 31 |
| 07/03/2002 | Landsat 5 | 32 | 31 |
| 05/15/2005 | Landsat 5 | 33 | 31 |
| 08/19/2005 | Landsat 5 | 33 | 31 |
| 10/14/2005 | Landsat 7 | 33 | 31 |

Attachment 2

Appendix C

Vertical shift in the thermal band in the Landsat 5 images

J. Kjaersgaard and R. G. Allen, September 2008. *Revised August 2010*

It was previously noted (Trezza and Allen, 2008) that the thermal band (band 6) of L1T terrain-corrected Landsat 5 images processed by EROS using the NLAPS preprocessing system during the 2007 to 2009 period was typically shifted by up to 120 m (and generally 60 m) in the southerly direction relative to the visible and near-infrared bands. The shift was found to be consistent throughout the image. It is important that the pixels of all bands in the Landsat image 'line up' in order to perform a correct solution to the surface energy balance during the METRIC process. Therefore, prior to METRIC processing, images were screened and the shift corrected. The shift and its remedy are described in this Appendix C. The shifting procedure is no longer needed with post Jan. 2010 images obtained from EROS due to their use of an updated process. No shift between the thermal band and the short wave bands has been found for Landsat 7 images.

The source of the shift is not clear, but it arises during the terrain correction preprocessing of the raw Landsat images performed by EROS using the NLAPS preprocessing system and where the 120 m pixels for the thermal band are resampled to 30 m pixel size. When the terrain correction is undertaken by other image preparation providers, this shift does not occur. The shift may or may not occur in increments divisible of 30 m.

It is important that the pixels of all seven bands in the Landsat image "line up" in order to perform a correct calibration when using the METRIC model to estimate the energy balance components.

The images used in the energy balance estimations were prepared (including terrain correction) by EROS. The images were screened and corrected for this thermal shift.

Screening

The screenings was done by displaying bands 2, 3, 4 (false color) and the thermal band side-by-side in ERDAS Imagine Viewers and identifying locations with sudden changes in land surface cover, such as a water-land interface, edges between irrigated fields and surrounding dry rangeland or desert. Normalized Difference Vegetation Index, NDVI and lapse corrected surface temperature, T_{s_dem} for approximately 20 pixels north and south of the land cover change were resampled at a number of these break points throughout the Landsat image for each image date. Great care was taken during the selection of break points to identify points that were representative for the area. The data were imported into a spreadsheet and the covariance was calculated while shifting the thermal pixel values incrementally 30 m north, i.e. 0, 30, 60, 90 and 120 m north. The covariances were used to indicate the magnitude of the shift. This magnitude was controlled by comparing break points throughout images visually.

An example of the shift is shown in Figure 1. On the left side of the figure is a portion of a river shown in false color (shortwave bands 2,3 and 4), while the T_{s_dem} for the same portion of the river is shown on the right. In the false color image, green vegetation shows up as red, bare soil is tan to brown while water is dark blue. In the T_{s_dem} image temperatures are shown in grey scale with bright hues indicating warmer temperatures and darker hues indicating colder temperatures. The water in the river is colder than the predominantly bare soil along the river. The pixel sizes of the shortwave bands are 30 m and the original pixel size of the thermal band is 120 m, causing the T_{s_dem} to have a coarser resolution and a more 'jagged' appearance. The crosshair in the images is placed at the same location in accordance to the projection. While the crosshair is in the middle of the river on the false color image, it is north of the river on the T_{s_dem} image indicating the shortwave and long-wave bands do not overlap.

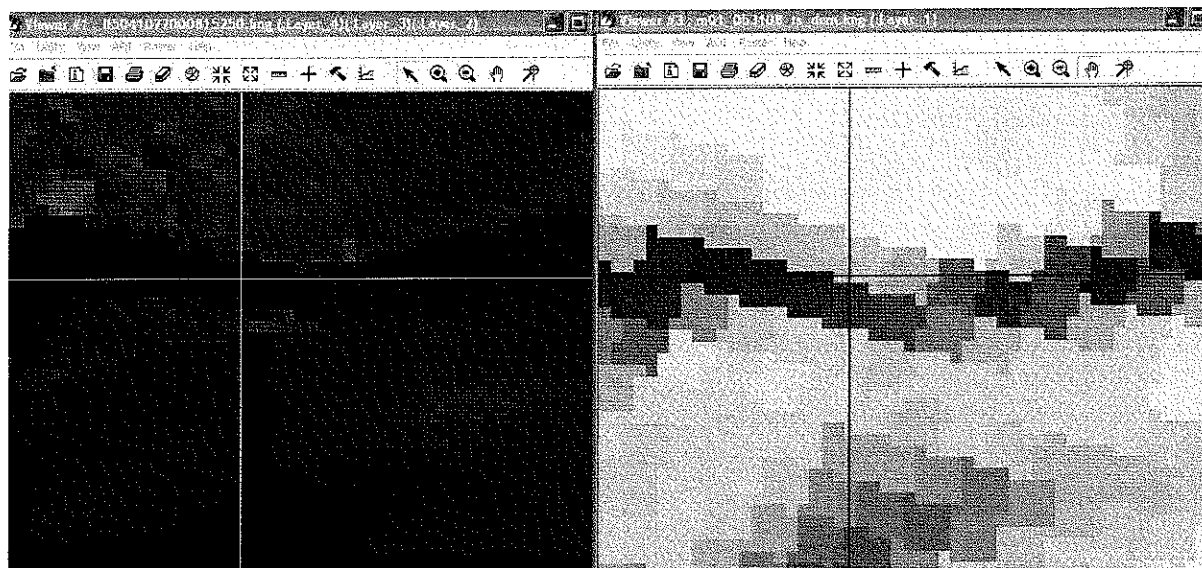


Figure 1 Incongruent depiction of the location of a river between a false color image (left) and elevation adjusted surface temperature map. The cross hair is at the geographical same location.

Correction of the shift

As a result of the screening, incongruencies were found between the shortwave and longwave band for all Landsat 5 images. The vertical shift was 60 m for all images. No shift was found in the east-west direction.

To correct the misalignment, the thermal bands were shifted upward relative to the shortwave bands by the distance shown in Table 1 prior processing. The shifting was done prior to layer stacking by displaying band 6 in an ERDAS Imagine Viewer, opening the Layer Info dialog, selecting Edit – Change Map Model, and adding the shift (30 or 60 m) to the coordinate in the Upper Left Y box. The 7 bands (including the shifted band 6) were subsequently stacked the normal way.

Creating a common area among Landsat band for processing

It is noted, that the north and south edges of the shortwave bands and the thermal band no longer had the same geographical extent after the shift. This may cause problems with 'undefined numbers' along the north and south edges of the image (2 pixel layers thick) in some of the products from the METRIC processing. This can be avoided by e.g. defining an Area of Interest, AOI, limiting the METRIC calculations to be carried out for the largest common area i.e. only on pixels that have valid numbers for both the shortwave and the longwave bands.

A model to create a mask for the largest common area is shown in Figure 2. Inputs are the 7-band Landsat image, the DEM and the LU map. The background value must be specified in the two scalar boxes for the DEM and the LU (normally 0, if no background value is present in the image, the background value should be set to a value lower than the smallest pixel value occurring in the image). The output is a binary map, where pixels that are common across all

Model to create the largest common area between a Landsat image, a DEM and a Land Use Map
J. Kjaersgaard, R. Allen, University of Idaho

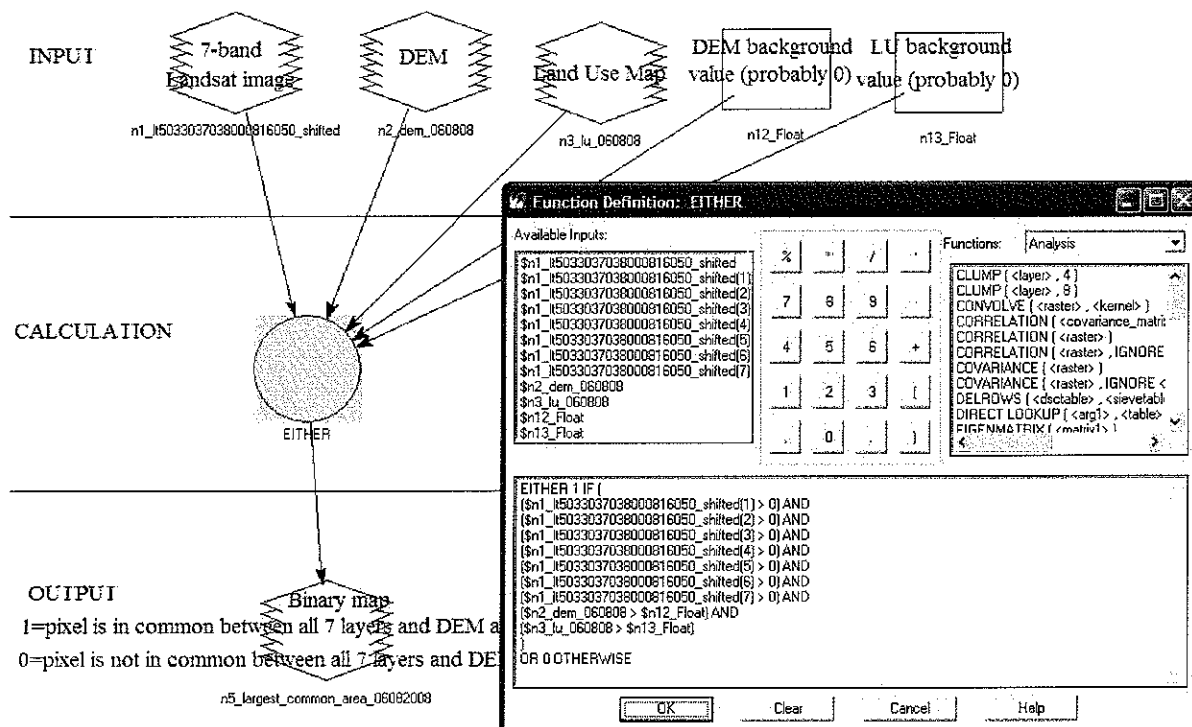


Figure 2. Model to calculate the largest common area between the 7-band Landsat image, the DEM and the Land Use map. In the model above the background value for the DEM and the LU must be specified (they are normally 0). The function is shown in the dialog on the right

seven bands and the DEM and the LU have the value 1 and all pixels that are not present in all seven bands and the DEM and the LU have the value 0. This binary map can be used as the input file when creating the AOI as outlined by e.g. Kjaersgaard (2009)

References

- Kjaersgaard, J., 2009. Defining an AOI in ERDAS Imagine to the exact outline of an existing image. Technical Report, University of Idaho, Kimberly, Idaho. 4 pp.
- Trezza, R., Allen, R.G., 2008. Analysis of vertical shift in Band 6 of Landsat 5 images in the EROS L1T product. University of Idaho, Kimberly, Idaho. 25 pp. Accessed online on June 17 2009 at <http://www.idwr.idaho.gov/GeographicInfo/PDFs/trezza-allen-thermal-band-shift.pdf>

Appendix D Maps of Land Use and Elevation for the Nebraskan panhandle

By J. Kjaersgaard and R. Allen, University of Idaho. January 2008, *revised August 2010*

The land use maps and elevation maps considered for the METRIC processing of the Landsat images from path 32/33 row 31 for the North Platte and South Platte NRDs application are described below. The area covered by Landsat scenes includes the southern portion of the Nebraskan Panhandle, and a portion of south-east Wyoming and north-east Colorado, as shown in Figure 1

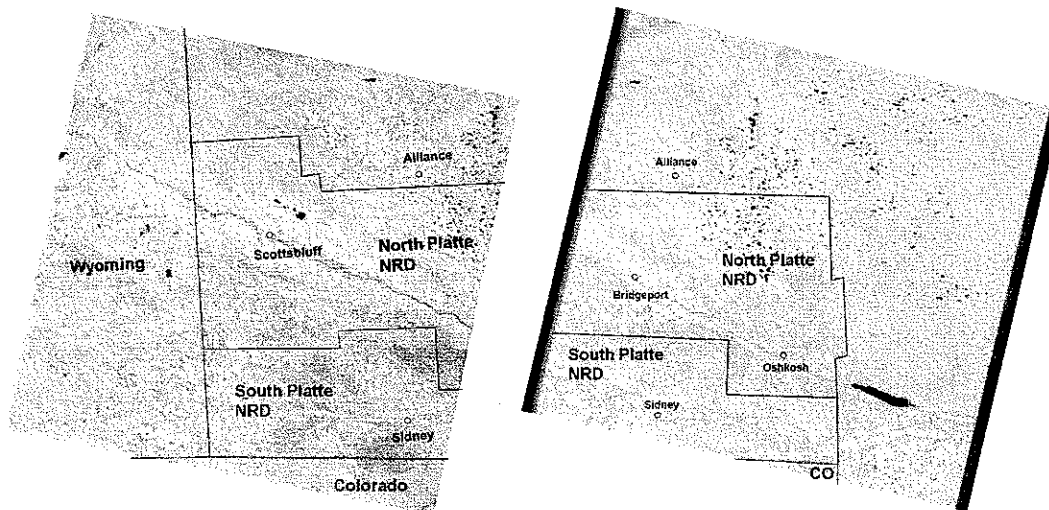


Figure 1 The Landsat image for Landsat path 33 row 31 from June 26 1997 and path 32 row 31 from June 8 2002 showing the state boundaries (red lines) and the approximate boundaries of the North Platte and the South Platte Natural Resource Districts (NRDs) (black lines)

Digital Elevation Map

A digital elevation map, DEM, at 30 m resolution was downloaded in GeoTiff format from the national elevation dataset, NED at <http://seamless.usgs.gov/>. The map was converted into an Imagine file using the ERDAS Imagine import function and reprojected into the same projection as the Landsat images using cubic convolution. The DEM was downloaded as several overlapping sub-maps, which were “stitched” together in one operation using the “StackLayers” followed by the “Stack Max” procedures in ERDAS Imagine Modelmaker, thereby creating a seamless DEM for an area slightly larger than the p32 r31 and the p33 r31 Landsat scenes. The boundaries of the DEM were tailored to fit the geographic extent of each Landsat scene.

Land use map

Three options of land use maps at 30 m resolution were considered. The three maps have been produced for different applications and purposes.

1. COHYST land use maps

The Cooperative Hydrology Study (COHYST) was established to gain understanding of the hydrological and geological conditions in the Platte Basin in Nebraska upstream of Columbus, Nebraska and to address endangered species issues along the Platte river basin. Parts of these efforts included building databases and provide tools to support scientific analysis and modeling of the hydrological cycle in the Platte Basin. The COHYST study area for 1997 and 2001 is shown in Fig 2.

One of the outcomes from COHYST was the generation of land use maps for the study area. The land use maps were based on Landsat 5 satellite imagery and a classification was done for the years 1997, 2001 and 2005. The Landsat coverage of the study area is outlined in Fig 3. For 2005, a complete land use classification for the entire state of Nebraska was carried out.

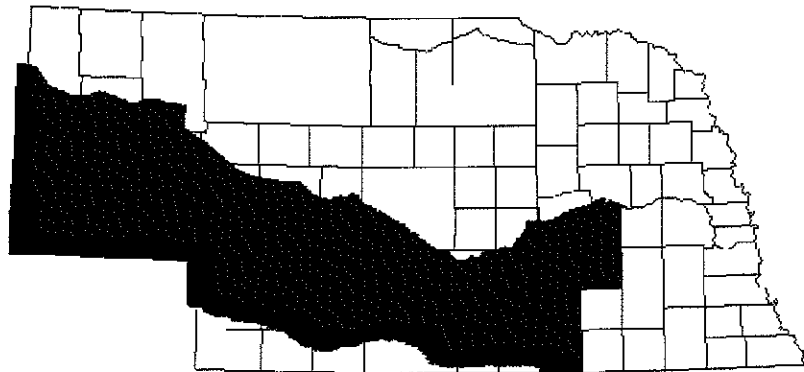


Fig 2 The COHYST 1997 study area (in blue) superimposed onto a map of Nebraska counties

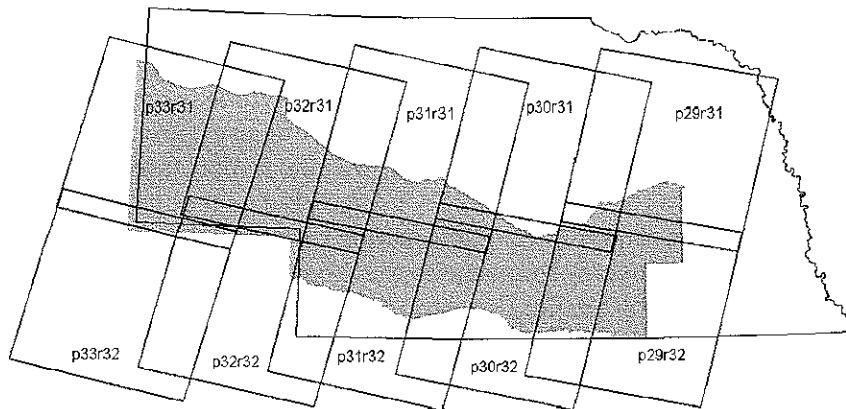


Fig 3. Landsat coverage of the 1997 COHYST study area by path/row superimposed onto a map of Nebraska

The area being studied in this project is Kimball, Cheyenne and Deuel Counties (South Platte NRD) and Banner, Morrill, Scotts Bluff, Garden and the south portion of Sioux Counties (North Platte NRD). The counties and the spatial coverage of the COHYST land

use maps are shown in Fig 4. The SP-NRD and NP-NRD study area is almost entirely covered by the COHYST land use maps except the far NE corner of Garden County.

This map was produced by Center for Advanced Land Management Information Technologies (CALMIT) at UNL followed by ground truthing to minimize misclassifications

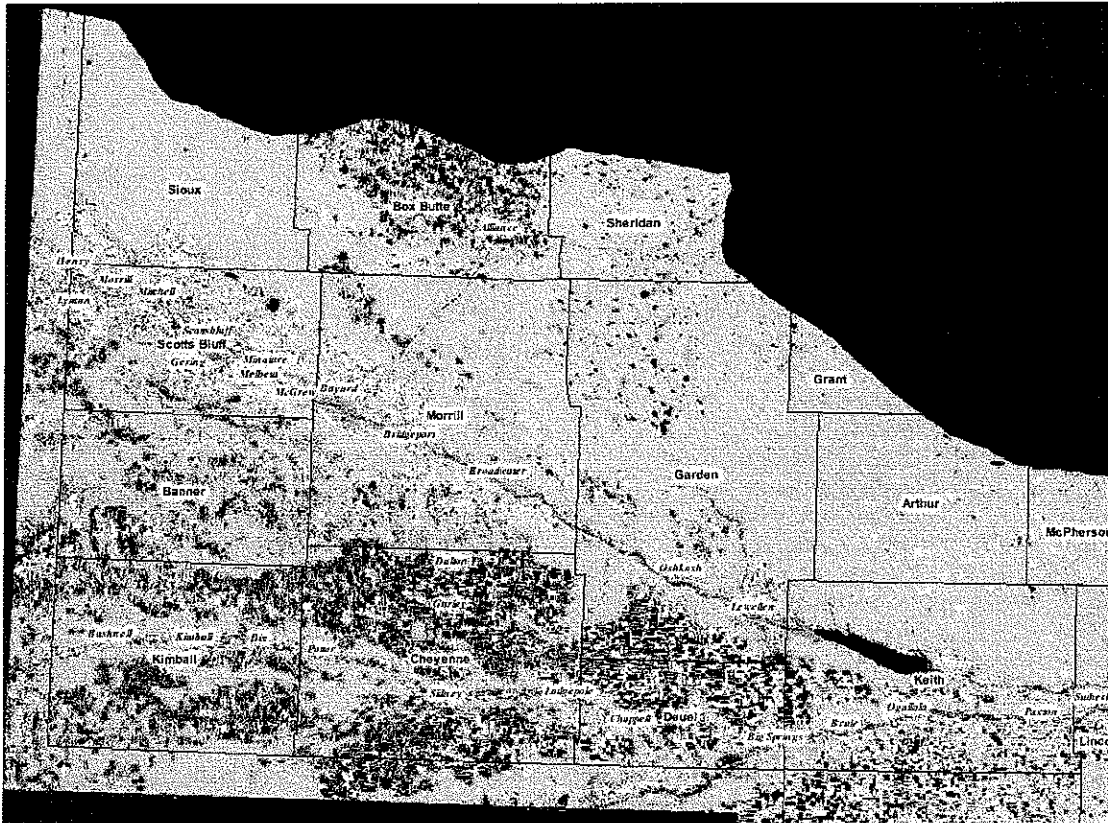


Figure 4 Coverage of the COHYST land use maps on the Nebraskan panhandle.

The classification system employed in the COHYST land use maps are shown in Table 1. There are a few small differences in the classification systems between 1997 and 2001/2005. The primary objective when creating the land use map was to identify individual crop types. The classification accuracy is reported to be between 80 and 82 %. More information about COHYST, the land use maps and the classification system can be found on <http://www.calmit.unl.edu/cohyst/index.shtml>

Table 1 COHYST classification system (source:
<http://www.calmit.unl.edu/2005landuse/index.shtml>)

| Class | Category (1997) | Category (2001, 2005) |
|-------|--|--|
| 1 | Irrigated corn | Irrigated corn |
| 2 | Irrigated sugar beets | Irrigated sugar beets |
| 3 | Irrigated soybeans | Irrigated soybeans |
| 4 | Irrigated sorghum (Milo, Sudan) | Irrigated sorghum (Milo, Sudan) |
| 5 | Irrigated dry edible beans | Irrigated dry edible beans |
| 6 | Irrigated potatoes | Irrigated potatoes |
| 7 | Irrigated alfalfa | Irrigated alfalfa |
| 8 | Irrigated small grains | Irrigated small grains |
| 9 | Range, pasture, grass | Range, pasture, grass |
| 10 | Urban land | Urban land |
| 11 | Open water | Open water |
| 12 | Riparian forest and woodlands | Riparian forest and woodlands |
| 13 | Wetlands | Wetlands |
| 14 | Other agric land (farmstead, feedlots) | Other agric land (farmstead, feedlots) |
| 15 | Irrigated sunflower | Irrigated sunflower |
| 16 | Summer fallow | Summer fallow |
| 17 | Roads | Roads |
| 18 | Dryland corn | Dryland corn |
| 19 | Dryland soybeans | Dryland soybeans |
| 20 | Dryland sorghum | Dryland sorghum |
| 21 | Dryland dry edible beans | Dryland dry edible beans |
| 22 | Dryland alfalfa | Dryland alfalfa |
| 23 | Dryland small grains | Dryland small grains |
| 24 | Dryland sunflower | Dryland sunflower |
| 25 | Dryland sugar beets | Barren |
| 26 | Dryland potatoes | |

A land use map covering the entire state for the year 2005 was prepared by CALMIT in 2007. The classification followed the principles and classification system as employed during the 2001 COHYST land use mapping. For more information see <http://www.calmit.unl.edu/2005landuse/index.shtml>

2. NE GAP land use map

The Nebraska Gap Analysis Program (NE GAP) land use classification is part of a nationwide effort seeking to “identify the degree to which all native plant and animal species and natural communities are or are not represented in our present-day mix of conservation lands”. GAP maps are produced by each state based on guide lines provided by USGS Biological Resources Division.

This NE GAP land use map was produced by CALMIT at UNL in 2005. The map was developed using Landsat TM images acquired during 1991 – 1993 followed by ground truthing to minimize misclassifications. More information about land cover classification may be found at <http://www.calmit.unl.edu/gap/index.shtml>. The classes of the classification system are shown in Table 2. One of the primary objectives during the NE GAP was to identify and distinguish between natural vegetation.

Table 2. NE GAP land cover classification (source: <http://www.calmit.unl.edu/gap/index.shtml>)

| Class | Category |
|-------|---|
| 1 | Ponderosa pine forest (sparse) |
| 2 | Deciduous forests |
| 3 | Juniper woodlands (sparse) |
| 4 | Sandsage shrubland |
| 5 | Sandhill upland prairie |
| 6 | Lowland tallgrass prairie |
| 7 | Upland tallgrass prairie |
| 8 | Little bluestem-gramma mixedgrass prairie |
| 9 | Western wheatgrass mixedgrass prairie |
| 10 | Shortgrass prairie |
| 11 | Barren/sand/outcrop |
| 12 | Agricultural field |
| 13 | Open water |
| 14 | Fallow agric. field |
| 15 | Aquatic bed wetland (temporarily flooded) |
| 16 | Emergent wetland – e.g. sedge, cattail |
| 17 | Riparian shrubland |
| 18 | Riparian woodland - e.g. poplar, willow, oak, maple |
| 19 | Low density residential |
| 20 | High density residential |

3. NLCD land use map

The USGS has produced national land use maps since the 1960s. The maps are from the National Land Cover Dataset from 2001 (NLCD 2001). The classification system as it applies to the Nebraskan panhandle are shown in Table 3. The NLCD land cover classification is identical for the United States and the classification lacks detail about e.g. vegetation type for agricultural land use or areas with natural vegetation. More information about the land use system can be found at <http://landcover.usgs.gov/usgslandcover.php>

Table 3. NLCD 2001 land cover classification (source: <http://landcover.usgs.gov/usgslandcover.php>)

| Class | Category |
|-------|-----------------------------|
| 0 | Background |
| 11 | Water |
| 21 | Developed, open space |
| 22 | Developed, low density |
| 23 | Developed, medium density |
| 24 | Developed, high density |
| 31 | Barren land |
| 41 | Deciduous forest |
| 42 | Evergreen forest |
| 43 | Mixed forest |
| 52 | Shrub |
| 71 | Grassland |
| 81 | Pasture/hay |
| 82 | Cultivated crops |
| 90 | Woody wetlands |
| 95 | Emergent herbaceous wetland |

4. Generation of a composite land use map

In general, the NLCD map offers the least detail about agricultural land and natural vegetation. When visually comparing the NLCD map to the NE GAP map they appear to have similar accuracy (e.g. both maps classify the same pixels as agricultural, range land etc). However, where the NLCD map describes the land use of e.g. range land as “Grassland”, the NE GAP indexes this land cover type in six different categories. Hence, one loses detail when using the NLCD map compared to the COHYST and NE GAP maps.

Greatest detail for natural vegetation and riparian zones are found in the NE GAP map, while the greatest detail in agricultural crop diversity is found in the COHYST maps. Land use generally only changes slightly from year to year, except for agricultural lands where crops are rotated every year. Using a land use map that includes detail about crop type could potentially increase the accuracy of the ET estimates from agricultural crops (especially corn).

Examples of NE GAP and COHYST 1997 land use maps are shown in Figs 4 and 5 for the primarily agricultural area along a section of the North Platte River northwest of Scottsbluff.

To maintain the greatest amount of detail, a composite land use map was created and used, where the NE GAP land use map was used as the ‘base’ map. For areas within the Nebraska state boundary, the Nebraska GAP map was used for non-agricultural classes and a COHYST map was used for agricultural classes. The COHYST data extends across the Nebraska border by 2 miles. For areas not covered by the COHYST and NE GAP maps (SE Wyoming and NE Colorado) the NLCD map was used.

Because some of the land use categories are not the same (Tables 1 – 3), new classification values were assigned to the NE GAP and COHYST classes. The resulting land use categories are shown in Table 4. The map was converted into an Imagine file using the ERDAS Imagine import function and reprojected into the same projection as the Landsat images using nearest neighbor

A land use map for agricultural areas for year 2002 was created using supervised classification based on the 1997 and 2005 COHYST maps.

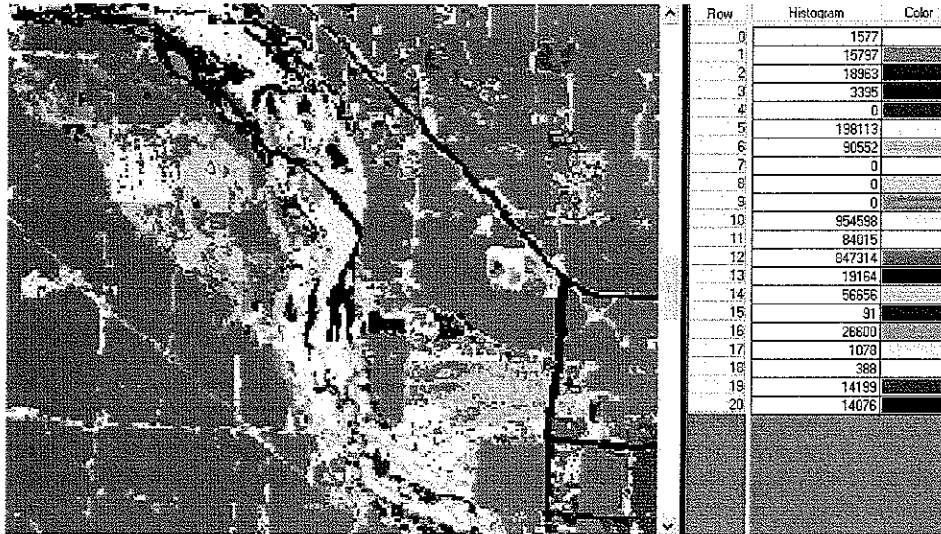


Fig 4. Subset of the NE GAP land use map along the North Platte River. A small section of Scottsbluff appears in the SE corner. See Table 2 for classification (“Row” in Fig 4 legend = “Class” in Table 2)

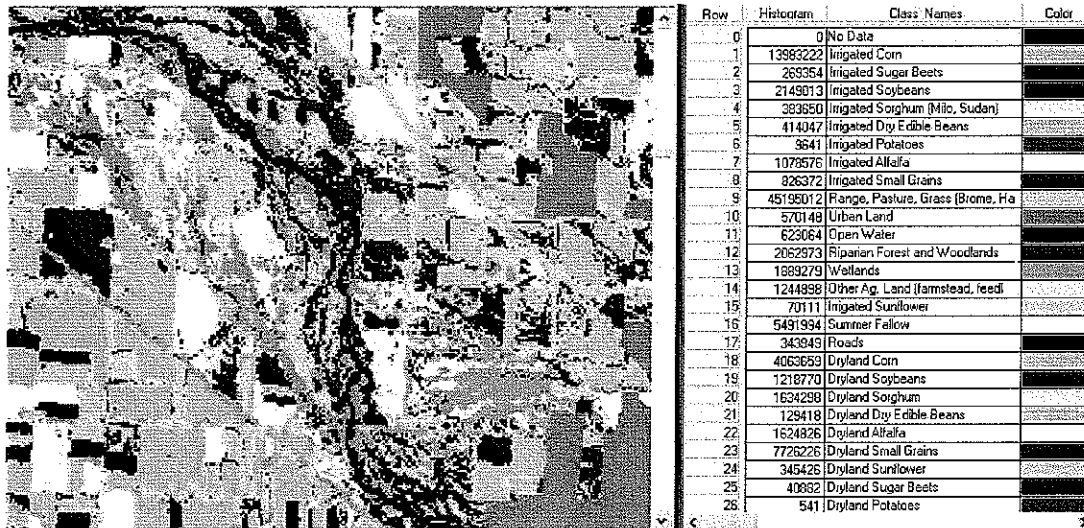


Fig 5. Subset of the COHYST land use map along the North Platte River. A small section of Scottsbluff appears in the SE corner.

Table 4 Land use classes of the composite land use map, the original classification value and dataset (Tables 1-3), class name and the year the input data is based on. After Ratcliffe, 2008.

| Class Value | Original Value | Class Name | Dataset | Year |
|-------------|----------------|---------------------------------------|---------|-----------|
| 0 | 0 | Background | NLCD | 2001 |
| 11 | 11 | Water | NLCD | 2001 |
| 21 | 21 | Developed, open space | NLCD | 2001 |
| 22 | 22 | Developed, low density | NLCD | 2001 |
| 23 | 23 | Developed, medium density | NLCD | 2001 |
| 24 | 24 | Developed, high density | NLCD | 2001 |
| 31 | 31 | Barren land | NLCD | 2001 |
| 41 | 41 | Deciduous forest | NLCD | 2001 |
| 42 | 42 | Evergreen forest | NLCD | 2001 |
| 43 | 43 | Tall trees | NLCD | 2001 |
| 52 | 52 | Shrub | NLCD | 2001 |
| 71 | 71 | Grassland | NLCD | 2001 |
| 81 | 81 | Pasture/hay | NLCD | 2001 |
| 82 | 82 | Cultivated crops | NLCD | 2001 |
| 90 | 90 | Woody wetlands | NLCD | 2001 |
| 95 | 95 | Emergent herbaceous wetland | NLCD | 2001 |
| 101 | 1 | Ponderosa Pine Forests and Woodlands | NE GAP | 1991-1993 |
| 102 | 2 | Deciduous Forest/Woodlands | NE GAP | 1991-1993 |
| 103 | 3 | Juniper Woodlands | NE GAP | 1991-1993 |
| 104 | 4 | Sandsage Shrubland | NE GAP | 1991-1993 |
| 105 | 5 | Sandhills Upland Prairie | NE GAP | 1991-1993 |
| 106 | 6 | Lowland Tallgrass Prairie | NE GAP | 1991-1993 |
| 107 | 7 | Upland Tallgrass Prairie | NE GAP | 1991-1993 |
| 108 | 8 | Little Bluestem-Gramma Mixedgrass | NE GAP | 1991-1993 |
| 109 | 9 | Western Wheatgrass Mixedgrass | NE GAP | 1991-1993 |
| 110 | 10 | Western Shortgrass Prairie | NE GAP | 1991-1993 |
| 111 | 11 | Barren/Sand/Outcrop | NE GAP | 1991-1993 |
| 112 | 12 | Agricultural Fields | NE GAP | 1991-1993 |
| 113 | 13 | Open Water | NE GAP | 1991-1993 |
| 114 | 14 | Fallow Agricultural Fields | NE GAP | 1991-1993 |
| 115 | 15 | Aquatic Bed Wetland | NE GAP | 1991-1993 |
| 116 | 16 | Emergent Wetland | NE GAP | 1991-1993 |
| 117 | 17 | Riparian Shrubland | NE GAP | 1991-1993 |
| 118 | 18 | Riparian Woodland | NE GAP | 1991-1993 |
| 119 | 19 | Low Intensity Residential | NE GAP | 1991-1993 |
| 120 | 20 | Commercial/Industrial/Transportation) | NE GAP | 1991-1993 |
| 121 | 1 | Irrigated Corn | COHYST | 2005 |
| 122 | 2 | Irrigated Sugar Beets | COHYST | 2005 |
| 123 | 3 | Irrigated Soybeans | COHYST | 2005 |
| 124 | 4 | Irrigated Sorghum (Milo, Sudan) | COHYST | 2005 |
| 125 | 5 | Irrigated Dry Edible Beans | COHYST | 2005 |
| 126 | 6 | Irrigated Potatoes | COHYST | 2005 |
| 127 | 7 | Irrigated Alfalfa | COHYST | 2005 |

| | | | | |
|-----|----|-------------------------------------|--------|------|
| 128 | 8 | Irrigated Small Grains | COHYST | 2005 |
| 129 | 9 | Range, Pasture, Grass | COHYST | 2005 |
| 130 | 10 | Urban Land | COHYST | 2005 |
| 131 | 11 | Open Water | COHYST | 2005 |
| 132 | 12 | Riparian Forest and Woodlands | COHYST | 2005 |
| 133 | 13 | Wetlands | COHYST | 2005 |
| 134 | 14 | Other Ag. Land (farmstead, feedlot) | COHYST | 2005 |
| 135 | 15 | Irrigated Sunflower | COHYST | 2005 |
| 136 | 16 | Summer Fallow | COHYST | 2005 |
| 137 | 17 | Roads | COHYST | 2005 |
| 138 | 18 | Dryland Corn | COHYST | 2005 |
| 139 | 19 | Dryland Soybeans | COHYST | 2005 |
| 140 | 20 | Dryland Sorghum | COHYST | 2005 |
| 141 | 21 | Dryland Dry Edible Beans | COHYST | 2005 |
| 142 | 22 | Dryland Alfalfa | COHYST | 2005 |
| 143 | 23 | Dryland Small Grains | COHYST | 2005 |
| 144 | 24 | Dryland Sunflower | COHYST | 2005 |

References

Ratcliffe, I. 2008 Land Use Description. Excel spreadsheet. University of Nebraska, Lincoln, 2008

Appendix E

Cloud Masking and Extrapolating ET Values from Instantaneous to Daily, Monthly and Seasonal Estimates

J Kjaersgaard and R. Allen, University of Idaho. July 2010. *Revised August 2010*

Because usable Landsat images are available only once or twice per month, on average, the $ET_{r,F}$ (fraction of alfalfa based reference evapotranspiration) images were generated by METRIC on a relatively infrequent basis (eight times during 1997). Consequently, to determine monthly and seasonal ET, the $ET_{r,F}$ products have to be interpolated over days between Landsat images and multiplied by daily reference ET to produce monthly average crop coefficients and total monthly evapotranspiration, as described below. $ET_{r,F}$ is similar to the well-known crop coefficient (K_c) and represents the ratio of actual ET to the reference ET. In METRIC, the alfalfa reference ET_r is used for calibration and determination of $ET_{r,F}$.

Cloud masking and Cloud Gap Filling

Because of the lower temperature of the surface of clouds and their opaque nature, areas covered by clouds (including thin cirrus clouds), jet contrails, smoke and other major atmospheric disturbances cannot be processed with METRIC for ET. The $ET_{r,F}$ estimates for such areas within an image are not representative of the $ET_{r,F}$ at the ground surface. In addition, the shadows cast by clouds on the ground surface are generally cooler than sunlit portions that may lead to an overestimation of $ET_{r,F}$ by METRIC. Areas with cloud cover and other major atmospheric disturbances and their shadows must therefore be identified and masked (removed areas with cloud cover within the images) out.

The cloud recognition was based on visual identification of clouds within each image and the cloud masking was done manually. When masking for clouds, areas of up to a kilometer around both the clouds and the cloud shadows were masked. This ensures that thin, almost transparent edges of the clouds as well as portions of the ground, just upwind of the current shadow, that do not yet have the same surface temperature as they would have had if there had been no shadow cast on them, are masked out.

Because there was some degree of cloud cover in four of the eight images processed for path 33 row 31 for 1997, the areas with cloud cover were masked out. It was previously agreed that the University of Idaho would be responsible for processing the 1997 images using METRIC and to extrapolate the results to produce maps of monthly and seasonal ET.

The cloud masked images are shown in Figure 1. The black portions within each image are the areas masked for clouds. There were no clouds on 05/09-1997, 06/26-1997, and 10/30-1997.

$ET_{r,F}$ for cloud masked areas is filled in for individual Landsat dates prior to splining $ET_{r,F}$ between images. The $ET_{r,F}$ data inserted into masked areas are 'borrowed' from adjacent images in time. The cloud mask gap filling and interpolation of ET between image dates entails interpolating the $ET_{r,F}$ for the missing area from the previous and following images. Because of

the sometimes relatively rapid change in the temporal development of vegetation and because of the substantial spatial and temporal heterogeneity in the precipitation (such as local summer showers) within the Panhandle a new method for cloud gap filling and adjustment for background evaporation from soil was developed

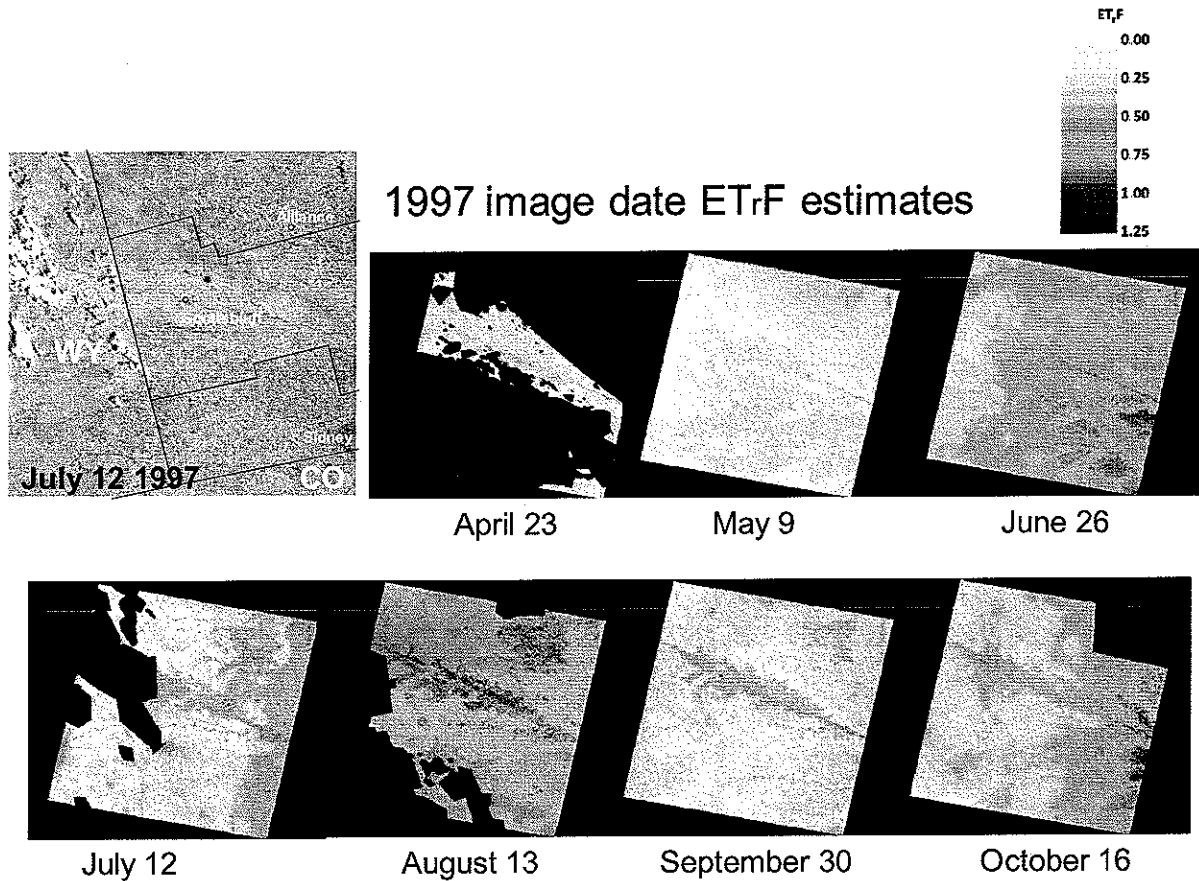


Figure 1. Maps of cloud masked ET_rF from seven 1997 images dates. The geographical extent of the NP and SP NRD boundaries is shown on the image in the top left corner.

Cloud gap filling

The gaps in the ET_rF maps occurring as a result of the cloud masking are filled in using linear time-weighted interpolation of ET_rF values from the previous image and the nearest following satellite image date having a valid ET_rF estimate, adjusted for vegetation development. The Normalized Difference Vegetation Index, NDVI, which is derived from Landsat satellite bands 3 and 4, is used to indicate change in vegetation amount. The principle is sketched in Figure 2 where a location in the two nearest images (i-1 and i+1) happen to be clouded. During the gap filling, the interpolated values for the areas having mostly bare soil are adjusted for differences in residual soil moisture between the image dates occurring as a result of heterogeneities in precipitation (such as by local summer showers) based on NDVI and ET_rF for the previous and following satellite image dates. This procedure is needed to remove artifacts of this

precipitation-derived evapotranspiration that are unique to specific image dates but that may not be representative of the image date that is to be represented by the ET,F from the previous and the following images. A comparison between cloud gap filling without and with adjustment for background evaporation is shown in Figure 3.

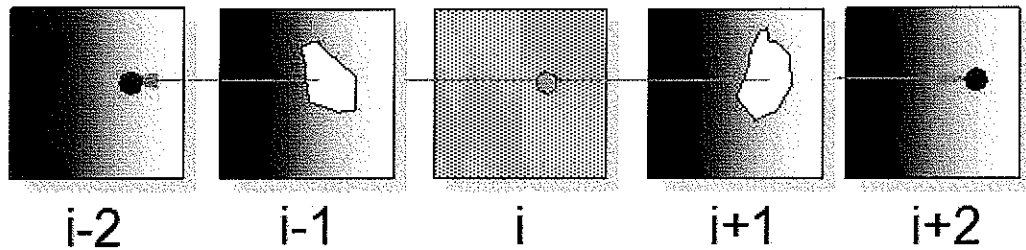


Figure 2 Principle of cloud gap filling. “i” is the image having cloud masked areas to be filled; “i-1” and “i-2” are the two earlier images than image i; “i+1” and “i+2” are the two following images.

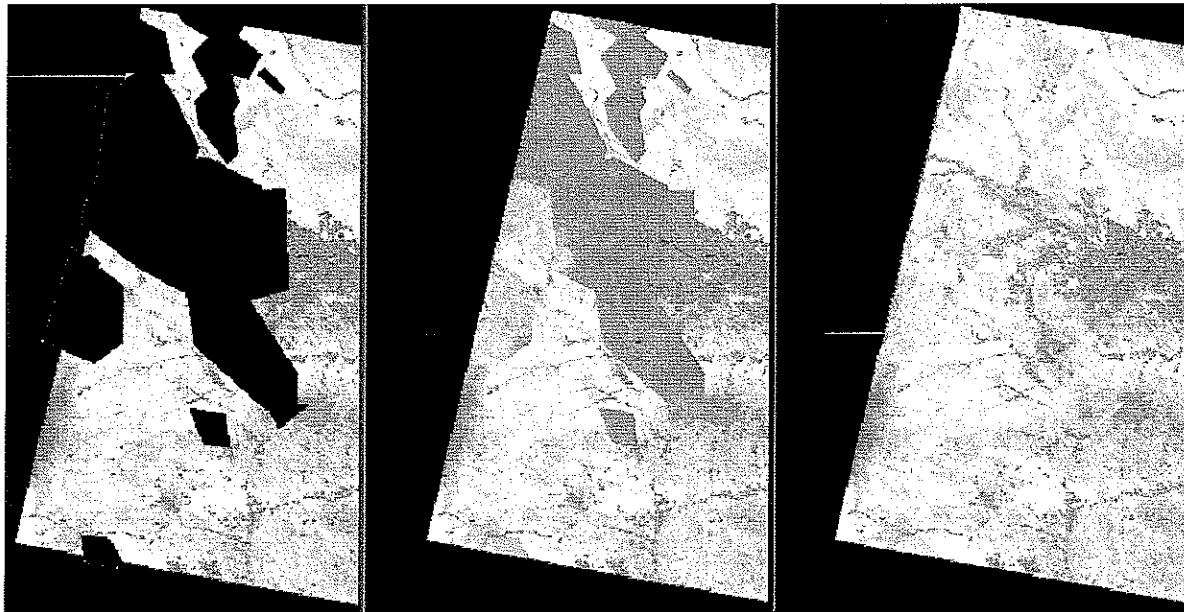


Figure 3 Maps of ETrF from July 12 1997 after cloud masking (left) (black indicate areas removed during cloud masking or background); and after cloud gap filling without (center) and with (right) adjustment for vegetation amount and background evaporation from antecedent rainfall.

The procedure for cloud gap filling uses linear interpolation to fill in ET,F information for cloud-impacted pixels. The METRIC models that create monthly and seasonal ET,F and ET images that use the products from the cloud gap filling, however, use a cubic spline procedure for more accurate interpolation for each day between images. The result is a small incongruity between the cloud gap filled value and the splined value, Figure 4. However, the need to search for cloud free pixels across multiple images, coupled with the need to utilize at least four images in a spline application, make that procedure and ERDAS model quite complicated. In

addition, interpolation across large time intervals is less speculative when using linear interpolation.

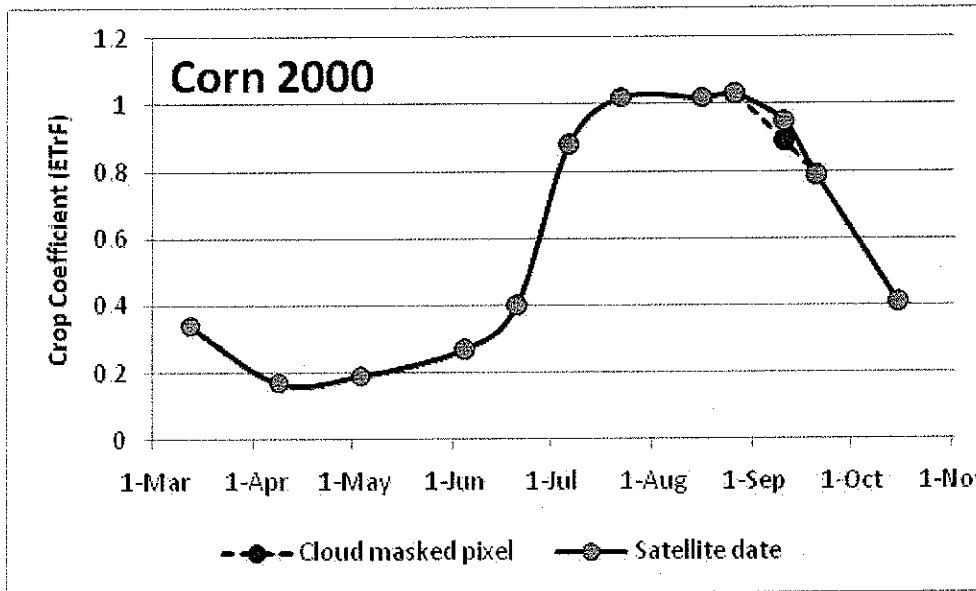


Figure 4 Schematic representation of the linear cloud gap filling and the cubic spline used to interpolate between image dates for a corn. The green points represent image dates and the black line is the splined interpolation between points; the red point represents the value of ET_{rF} that is interpolated linearly from the two adjacent image dates had the field had cloud cover on September 10.

The procedure for adjusting ET_{rF} for background evaporation is described in Appendix F.

Estimation of daily ET_{rF} using a cubic spline model

The daily estimates of ET_{rF} for the satellite overpass dates were extrapolated between image dates using a cubic spline model. The cubic spline model used for the extrapolation has been described by Allen et al. (2010) and Trezza et al. (2008). The spline creates a smooth curve for ET_{rF} between images to simulate the day-to-day development of vegetation.

The spline estimates the ET_{rF} value for each day of a month (such as e.g. the month of June) based on the ET_{rF} values estimated for the image date(s) for that month plus two image dates earlier than the month and two image dates later than the month.

There were not two independent ET_{rF} images available prior the months of April and May to be used for the splining of the ET_{rF} . At this early period of the growing season, crop development is stagnant or very slow, and changes in vegetation cover are small.

Because the first satellite image date was at the end of April, producing an estimate of the monthly ET_{rF} for April is somewhat challenging since no information was available for the beginning of the month. Because of the cold temperatures experienced in this area, very little

crop development is expected to occur until May. The ET_rF and ET estimates for April were scaled from bare soil evaporation as estimated using the daily gridded evaporation model, which in most cases gives a reasonable estimate of the ET during the non-growing season portion of the year. The evaporation from bare soil represents 'average' bare soil conditions regarding drainage, soil type and texture for the particular soil type. As a consequence, additional uncertainty in the ET_rF and ET estimates for April may exist for fields with soil and drainage properties different from those for the soil type simulated, and for fields covered by a layer of senesced plant material, mulch or having a relatively dense cover of green plant cover. Users are cautioned to consider these factors on a field-to-field basis before using the estimates of ET_rF and ET for the month of April. A similar approach was employed when estimating the ET for the month of October 1997.

Estimation of monthly ET and ET_rF

Daily values of ET for each pixel within the images was estimated using

$$ET_{daily} = ET_{r,daily} \times ET_rF_{daily} \quad (6)$$

where ET_{daily} is the daily evapotranspiration (mm/day), $ET_{r,daily}$ are daily values of alfalfa based reference evapotranspiration (mm/day) and ET_rF_{daily} are the daily ET_rF values. Gridded ET_r , estimated using daily input weather data from nine HPRCC and three CoAgMet weather weather stations using the University of Idaho RefET software, were used. The development of a gridded surface of ET_r is described in Appendix F.

In the case of rangeland vegetation, where, by definition, any mid-afternoon advection of energy and increased ET as represented in the ET_r estimated by the Penman-Monteith method does not exist, the evaporative fraction (EF) was used to transfer relative ET from the satellite overpass time (~1100 hours) to the 24-hour period and to establish the ET_rF_{daily} . Details of the EF application are given in Appendix G.

Daily values of ET were summed to monthly totals (mm/month) as

$$ET_{month} = \sum_{i=m}^n ET_{daily} \quad (7)$$

where ET_{month} is the cumulative monthly ET (mm/month), and m and n are the first and last day of the month.

The monthly average fractions of ET_rF_{month} were estimated using

$$ET_rF_{month} = \frac{ET_{month}}{ET_{r,month}} \quad (8)$$

where ET_{month} is the monthly ET (mm/month) and $ET_{r,month}$ is the monthly ET_r obtained by summing the gridded ET_r estimates from each day of that month. As a sample, the monthly and seasonal ET_r from Scottsbluff for 1997 is shown in Table 2.

Table 2 Monthly, seasonal (April through October) and annual ET_r (mm) estimated from the Scottsbluff weather data set

| Month | ET _r , mm |
|-----------------|----------------------|
| January | 51 |
| February | 55 |
| March | 144 |
| April | 122 |
| May | 195 |
| June | 213 |
| July | 239 |
| August | 173 |
| September | 143 |
| October | 117 |
| November | 55 |
| December | 43 |
| April-Oct Total | 1202 |
| Year Total | 1549 |

Treatment of negative ET_rF

In some cases, due to statistical uncertainty and insufficient model calibration, some land use types may take on slightly negative values in the final ET_rF map generated at each satellite image date. During the calibration process, very dry desert areas are normally considered to have an ET_rF close to zero. Due to the heterogeneity of the desert areas (slight differences in soil characteristics, vegetation and similar) the ET_rF values will hover around zero, with some ET_rF values slightly above zero while others are slightly below zero. When spatially averaged over a medium to large area, variations will tend to cancel out.

In the ET_{month} products generated from METRIC, a floor was applied so that negative values were set to zero. When generating the seasonal ET estimates from the monthly ET estimates, a possible negative estimate of ET in one month may somewhat counteract a positive ET estimate the following month which may lead to an overall underestimation in seasonal ET. Because for some land use types, such as desert where the negative ET values are countered by positive ET values when viewed over a larger area (e.g. several km²), this may lead to a slight positive bias in the estimates.

No floor was used when generating the ET_rF_{month} product, hence the negative values are included in the ET_rF_{month} maps. This will allow the user to avoid creating a bias from dry desert or similar areas when summarizing the values over a larger area.

Estimation of Seasonal (April Through October) ET and ET_rF

Seasonal estimates (April through October) of total ET, ET_s (mm/season) and seasonal ET_rF, ET_rF_{season} were calculated as

$$ET_{season} = \sum_{i=m}^n ET_{month} \quad (9)$$

where ET_{season} is the cumulative seasonal ET (mm/season), and m and n are the first (m=4) and last (m=10) month of the season, and

$$ET_r F_{season} = \frac{ET_{season}}{ET_{r,season}} \quad (10)$$

where $ET_{r,season}$ is the seasonal ET_r obtained by summing gridded ET_r estimates from each day of the season.

The primary focus in the application of METRIC in the south-west portion of the Nebraskan Panhandle was to estimate the ET from irrigated and non-irrigated agricultural land (including range land). The ET_{month} and ET_{season} estimates from other land cover types such as for asphalt roads (including rural roads) have a high degree of uncertainty compared to other urban structures. The ET from a road is normally very low as the surface is almost impermeable so there is very little residual ET once the surface is dry. Excess water during precipitation events will either run off the road (often through storm drains) or removed by traffic, reducing the annual evaporation from the road surface to as little as 10 % of the precipitation.

References

- Allen, R.G. (2009) "Methodology for adjusting METRIC-derived ETrF Images for Background Evaporation from Precipitation Events prior to Cloudfilling and Interpretation of ET between Image Dates." Note. University of Idaho, Kimberly R&E Center, Kimberly, Idaho. 11 pp. revised 2010.
- Allen, R.G., Tasumi, M., Trezza, R., Kjaersgaard, J.H. (2010). "METRIC Applications Manual." Version 2.0.6. University of Idaho, Kimberly, Idaho. 164 pp.
- Trezza, R., Allen, R.G., Garcia, M. (2007). "Methodology for Cloud Gap Filling in METRIC." University of Idaho, Kimberly, Idaho. 7 pp.
- Trezza, R., Allen, R.G., Garcia, M., Kjaersgaard, J.H. (2008). "Using a Cubic Spline to Interpolate between Images." University of Idaho, Kimberly, Idaho. 9 pp.

Appendix F

Setting up a Daily, Spatially Distributed Version of the FAO-56 Soil Water Balance on Landsat Image Scale and Adjusting Image Date ET_F Estimates for Background Evaporation

By J. Kjaersgaard and R. Allen, University of Idaho, April 2010. *Revised August 2010*

Introduction

When setting up the METRIC satellite-based surface energy balance model the evaporation from bare soil is normally estimated for the area immediately around a single weather station located within the image. These estimates of residual evaporation from antecedent rainfall are used during the calibration of the estimates of sensible heat flux from the surface.

The FAO56 bare soil water balance (Allen et al., 1998) are commonly used with METRIC and are parameterized in a spreadsheet for a single location based on soil hydrological properties, daily point measurements of precipitation and on alfalfa-based reference evapotranspiration, ET_r, calculated from air temperature, air humidity, wind speed and solar radiation.

Because the evaporation from bare soil and sparsely vegetated areas at the satellite overpass dates may not be representative for a longer period, such as one month, an adjustment for the average ET_F for that period must be made. The primary approach is to remove impacts of wetting events that are immediately prior to the image date, and then add back in the background evaporation from soil that is similar to the average evaporation expected for the averaging period. The averaging period is the period midway, in time, between the previous image date and the current image date, and extending forward in time to midway between the current and the following image date.

Spatially distributed estimates of daily soil evaporation are needed to make this adjustment. The parameterization of a spatially distributed soil water balance using the FAO56 method is described in this report

The FAO56 soil water balance model

The FAO56 soil water evaporation model assumes that the evaporation of water from a slab of the the upper 0.1 – 0.15 m of bare soil can be described using a two-stage linear function. The model is described by Allen et al. (1998).

During stage 1, the energy limiting drying stage, the soil water content is at or near field capacity and the soil surface remains wet. The depth of water being evaporated is limited by the amount of energy that is available. In the model, the depth of water being evaporated during stage 1 drying is termed readily evaporable water, REW (mm).

Stage 2, the falling rate drying stage, starts when the hydraulic properties of the upper soil are such that it no longer can supply water to the surface at the rate the amount of energy can evaporate it. During stage 2 drying the evaporation is assumed to decrease in proportion to the amount of water remaining in the soil. The total depth of water being evaporated during stage 1 and stage 2 drying, i.e. the total amount of water that can be depleted by evaporation during a complete drying cycle, is termed total evaporable water, TEW (mm)

TEW is estimated as

$$TEW = 1000(\theta_{FC} - 0.5\theta_{WP})Z_e \quad (1)$$

where θ_{FC} is the water content at field capacity (m^3/m^3), θ_{WP} is the water content at the wilting point (m^3/m^3) and Z_e is the depth of the slab of soil (0.1-0.15 m) that is subject to drying by evaporation. Information about the soil bulk properties are typically found in soil databases, from local soil surveys or from analysis of field soil samples. Typical values of θ_{FC} , θ_{WP} and REW published by Allen et al (1998) are reproduced in Table 1

Table 1. Typical soil water characteristics for different soil types (after Allen et al., 1998)

| Soil type (USA Soil Texture Classification) | Soil water characteristics | | | Evaporation parameters | |
|--|----------------------------|---------------|-----------------------------|---|--|
| | θ_{FC} | θ_{WP} | $(\theta_{FC}-\theta_{WP})$ | Amount of water that can be depleted by evaporation | |
| | | | | stage 1 REW | stages 1 and 2 TEW ($Z_e = 0.10$ m) |
| | M^3/m^3 | m^3/m^3 | m^3/m^3 | mm | Mm |
| Sand | 0.07 - 0.17 | 0.02 - 0.07 | 0.05 - 0.11 | 2 - 7 | 6 - 12 |
| Loamy sand | 0.11 - 0.19 | 0.03 - 0.10 | 0.06 - 0.12 | 4 - 8 | 9 - 14 |
| Sandy loam | 0.18 - 0.28 | 0.06 - 0.16 | 0.11 - 0.15 | 6 - 10 | 15 - 20 |
| Loam | 0.20 - 0.30 | 0.07 - 0.17 | 0.13 - 0.18 | 8 - 10 | 16 - 22 |
| Silt loam | 0.22 - 0.36 | 0.09 - 0.21 | 0.13 - 0.19 | 8 - 11 | 18 - 25 |
| Silt | 0.28 - 0.36 | 0.12 - 0.22 | 0.16 - 0.20 | 8 - 11 | 22 - 26 |
| Silt clay loam | 0.30 - 0.37 | 0.17 - 0.24 | 0.13 - 0.18 | 8 - 11 | 22 - 27 |
| Silty clay | 0.30 - 0.42 | 0.17 - 0.29 | 0.13 - 0.19 | 8 - 12 | 22 - 28 |
| Clay | 0.32 - 0.40 | 0.20 - 0.24 | 0.12 - 0.20 | 8 - 12 | 22 - 29 |

The soil water balance model as it has been implemented in a spreadsheet (Tasumi, 2003) used to support satellite image processing using MEIRIC is described below

The value of ET_rF (ET_rF is the fraction of alfalfa-based reference ET) for bare soil at a point is estimated as

$$ET_rF = ET_rF_{max} \times K_r \quad (2)$$

where ET_rF_{max} is the maximum ET_rF following rain or irrigation. ET_rF_{max} is assumed to be 1.0. K_r is a dimensionless evaporation reduction coefficient. During stage 1 drying the cumulative depth of evaporation from the soil slab at the end of the previous day, $D_{e,i-1}$ (mm) is smaller than or equal to REW and K_r is

$$K_r = 1 \quad (\text{Stage 1 drying}) \quad (3)$$

The test used to determine whether the soil evaporation is in stage 1 is:

$$IF (TEW - D_{e,i-1} + P_i) > (TEW - REW) THEN Stage 1 \quad (4)$$

where P_i is the precipitation (mm) on day i

During stage 2 drying evaporation decreases in proportion to the amount of water remaining in the slab and K_r is estimated from

$$K_r = \frac{TEW - D_{e,i-1}}{TEW - REW} \quad (\text{Stage 2 drying}) \quad (5)$$

The cumulative depth of evaporation for day i , $D_{e,i}$ (mm) is calculated for a sequence of time steps, such as for every day during a year. It is assumed that no ponding of water occurs on the soil surface and that if precipitation minus evaporation exceeds TEW, the excess water percolates through the slab and the water content at the end of the time step is at field capacity. $D_{e,i}$ is calculated as

$$D_{e,i} = (TEW - D_{e,i-1}) + P_i - E_i \quad (6)$$

$D_{e,i}$ should be restricted to $0 \leq D_{e,i} \leq TEW$. E_i is the evaporation (mm) on time step i estimated using

$$E_i = ET_{r,i} \times K_{r,i} \quad (7)$$

where $ET_{r,i}$ is the alfalfa-based ET estimated for time step i . The soil water balance was adjusted to account for skin evaporation as described in Appendix F.

It is noted, that in the version of the excel spreadsheet that has been distributed for use with METRIC up till March 2010, the lower boundary of the $D_{e,i}$ ($0 \leq D_{e,i}$) was not invoked. As a consequence, the soil evaporation model gets numerically unstable in conditions where the amount of water available for evaporation during stage 2 drying (i.e. TEW-REW) is relatively small such as is the case for sandy soils.

An example of a simulation of a daily soil water balance for a loamy soil is shown in Figure 1 and for a sandy soil is shown in Figure 2. The model becomes unstable when the residual water content is slightly less than the amount of water to be evaporated during stage 2 drying (TEW-REW), causing K_r estimated from Eq. 5 to be close to 1 in combination with the depth of evaporation is greater than $D_{e,i}$.

In most cases, the soil properties in agricultural areas have sufficient water holding capacities to avoid errors caused by the lower boundary not being invoked. However, when estimating the residual evaporation in the Nebraskan Sandhills or areas where finer soil particles have been washed away, such as bluffs or along water ways or reservoirs, the evaporation model can become unstable.

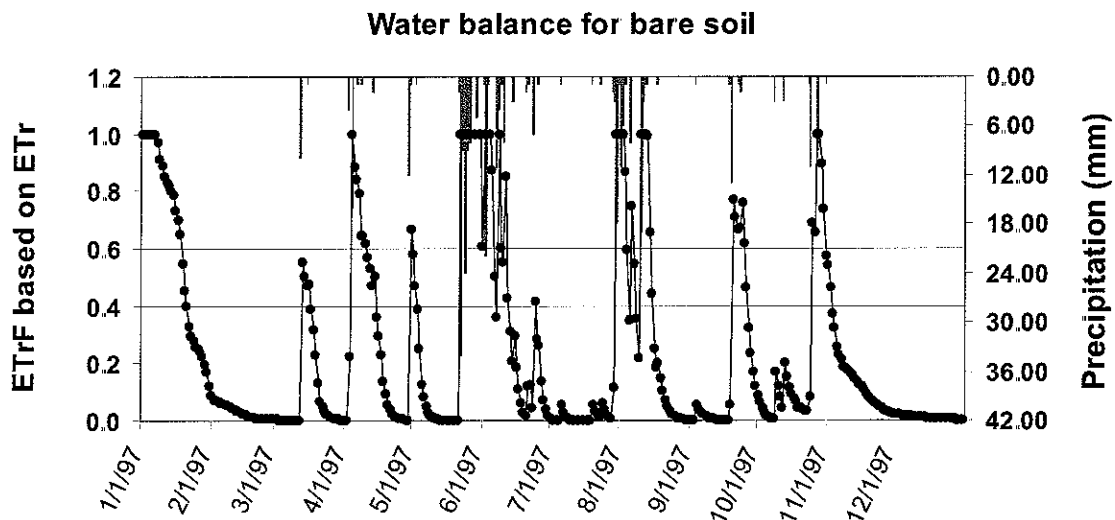


Figure 1. Simulation of the soil water balance for bare soil calculated using meteorological information from the Scottsbluff HPRCC AWS during 1997 assuming the soil type is loam with TEW=28 mm; REW= 10 mm and TEW-REW=18 mm

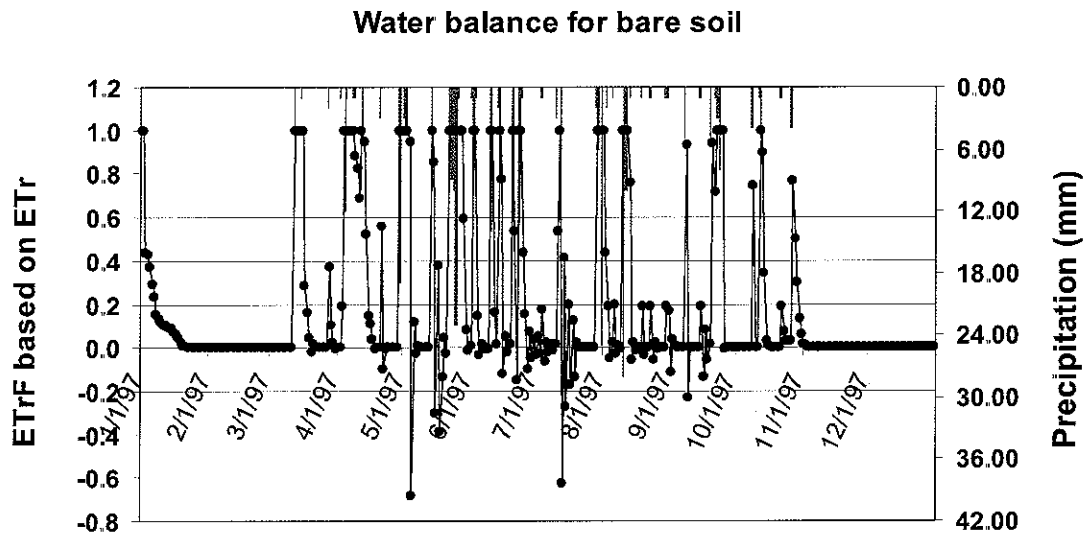


Figure 2 Simulation of the soil water balance for bare soil calculated using meteorological information from the Alliance North HPRCC AWS during 1997 assuming the soil type is sand with TEW=9.5 mm; REW= 4 mm and TEW-REW=5.5 mm. The error in the METRIC spreadsheet leading to the negative values of ETr,F for bare soil has been corrected by March 2010

Spatially distributed estimates of soil evaporation using the FAO56 method

An ERDAS Imagine ModelMaker model was developed during this study to apply the daily soil water balance on a 900 m grid for the study area (Landsat path 33 row 31). Maps of soil properties, precipitation and ETr, covering the study area, such as one Landsat scene, are needed to calculate

spatially distributed estimates of the soil evaporation. In this application, soil water holding properties were derived from the STATSGO data base and included soil water content at one-third bar, soil water content at 15 bar and soil type classification. Because the daily evaporation model is a slab model, only soils data representing the upper 125 mm of soil water utilized. The ERDAS ModelMaker produced daily grids of evaporation estimates from bare soil that were similar to those produced by an Arc-GIS model created by Ranade (2010) that were also based on the FAO56 slab model.

Daily meteorological information values from the High Plains Regional Climate Center (HPRCC) automated weather stations (AWS), the Colorado Agricultural Meteorological Weather Network (CoAgMet) and from the National Weather Service Cooperative Observer Program (NWS COOP) networks is used to populate the map of precipitation. Because the Landsat scene processed for 1997 covers a portion of NE Colorado and SE Wyoming, COOP stations from these areas were also included when generating the map of gridded precipitation. Precipitation information from 31 COOP locations in Nebraska, 23 stations in Wyoming and 11 stations in Colorado is used to supplement precipitation information from the six HPRCC stations located within the scene. The locations of the stations are shown in Figure 3. The daily precipitation amounts recorded at each measurement location were interpolated to a spatial coverage using inverse distance weighting using ArcGIS software. This relatively simple interpolation method was selected compared to more advanced methods such as a spline with or without tension model because of the proximity, in distance, between several weather stations waving uneven readings (such a following a local rain event) can cause the spline to ‘whack the tail’ and predict too high of values.

Reference ET is calculated using weather data from 11 HPRCC and 3 CoAgMet AWS and interpolated to cover the Landsat scenes. The station locations are listed in Table 2. Reference evapotranspiration

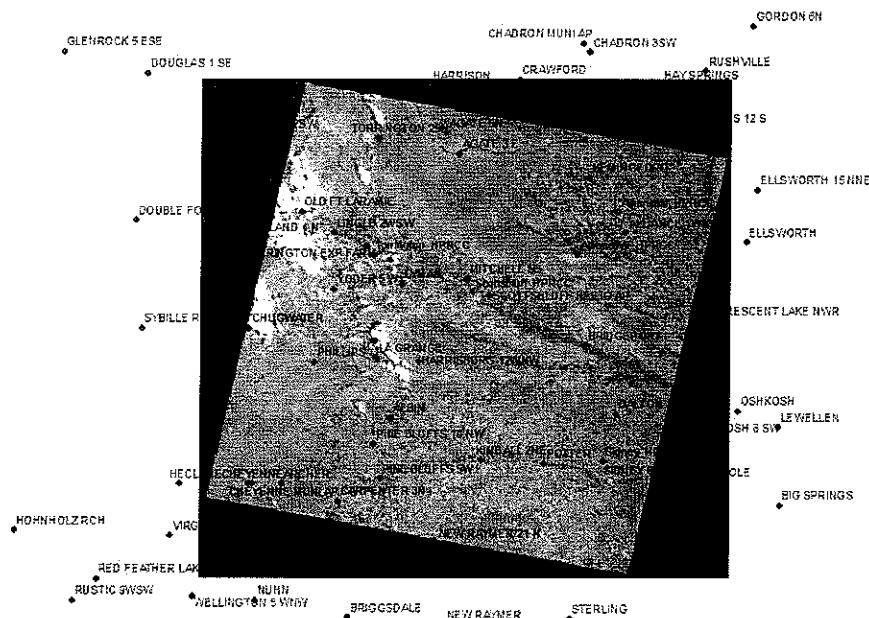


Figure 3. Location of the COOP stations, the HPRCC and CoAgMet weather stations within the Landsat scene processed for 1997.

Table 2. Names, station IDs, locations and elevation of the weather stations used to estimate distributed maps of reference ET.

| Station | StationID | Latitude | Longitude | Elevation |
|---------------------|-----------|----------|-----------|-----------|
| AllianceN_AWS | 1 | 42 18 | -102 92 | 1213 |
| AllianceW_AWS | 2 | 42 02 | -103 13 | 1213 |
| ArapahoePrairie_AWS | 3 | 41 48 | -101 85 | 1097 |
| Arthur_AWS | 4 | 41 65 | -101 52 | 1097 |
| Gudmundsen_AWS | 5 | 42 07 | -101 43 | 1049 |
| MitchellFarms_AWS | 6 | 41 93 | -103 7 | 1098 |
| Scottsbluff_AWS | 7 | 41 88 | -103 67 | 1208 |
| Sidney_AWS | 8 | 41 22 | -103 02 | 1397 |
| Sterling_AWS | 9 | 40 47 | -103 02 | 2000 |
| Torrington_AWS | 10 | 42 03 | -104 18 | 1216 |
| Gordon_AWS | 11 | 42 73 | -102 17 | 1109 |
| CSU_ARDEC_AWS | 12 | 40 65 | -105 | 1558 |
| FortCollinsAERC_AWS | 13 | 40 59 | -105 137 | 1561 |
| Haxtun_AWS | 14 | 40 67 | -102 65 | 1231 |

Major soil types and their soil water characteristics, including soil water content at field capacity and at wilting point were obtained from the from the NRCS SSURGO soil database, as described by Ranade (2010).

The FAO56 daily bare soil evaporation model was coded into ERDAS Modelmaker and run on a grid size of 900 m.

Table 3. Summary of the setup of the spatially distributed FAO56 soil evaporation model

| | Description |
|------------------------------------|----------------------------|
| Code environment | ERDAS Imagine |
| Precipitation data source | HPRCC, CoAgMet, COOP |
| Meteorological data source | HPRCC, CoAgMet |
| Soil information | NRCS SSURGO soil data base |
| Precipitation interpolation method | Inverse distance weighted |
| ET, interpolation method | Spline |
| Grid size | 900 m |
| Time step | Daily |
| Unit for Evaporation Estimates | mm |

Adjusting for background evaporation

Often a Landsat or other image is processed on a date where antecedent rainfall has caused the evaporation from bare soil to exceed that for the surrounding monthly period. Often, for input to water balance applications, it is desirable that the final ET image represent the average evaporation conditions for the month. In that case, the 'background' evaporation of the processed image can be adjusted to better reflect that for the month or other period that it is to represent. This period may be the time period that is half way between other adjacent images.

An example of a sequence of Landsat images processed using the METRIC surface energy balance model for the south-western portion of the Nebraskan Panhandle is shown in Figure 4 along with daily precipitation from the Scottsbluff High Plains Regional Climate Center weather station. The August 13 image date was preceded by a wet period and followed by a very dry period, thus the evaporation from non-irrigated areas at the satellite image date is not representative for the month.

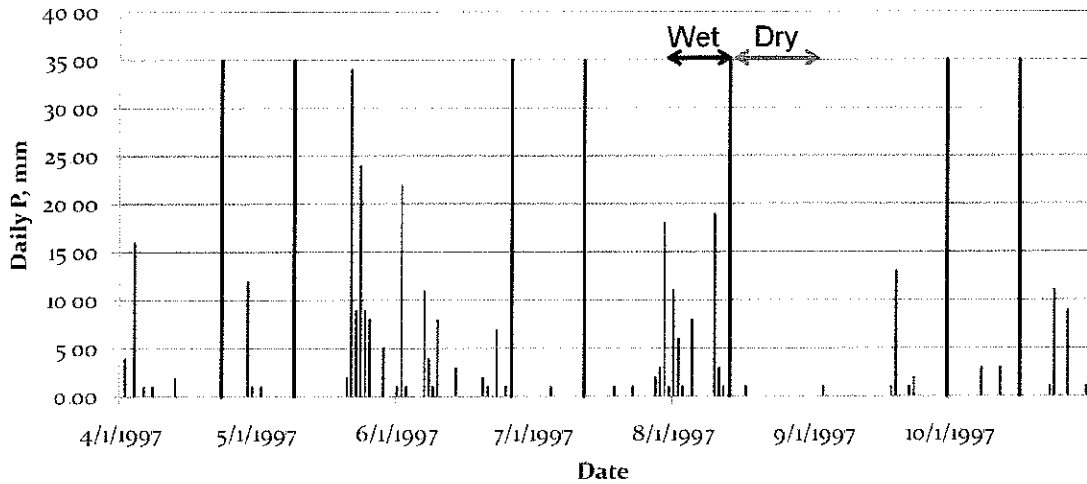


Figure 4. Image dates of nearly cloud free Landsat 5 path 33 row 31 images from the Nebraskan Panhandle in 1997 (black vertical bars) and precipitation recorded at the Scottsbluff HPRCC weather station (red bars). When interpolating between image dates each image roughly represents the ET halfway, in time, between the previous and the following image date. The August 13 1997 image fell immediately after a relatively wet period resulting in a high ET estimate from non-irrigated areas including dryland agriculture and rangeland. Because the period following the image was dry, the ET estimates for that image are too high for the period it is representing

In making the adjustment for background evaporation, one can assume that full adjustment is made for areas of completely bare soil, represented by $NDVI = NDVI_{bare\ soil}$, that no adjustment is needed for areas having full ground covered by vegetation, represented by $NDVI = NDVI_{full\ cover}$, and with linear adjustment in between. The following methodology is taken from a white paper developed by the University of Idaho during 2008 and 2009 (Allen 2008, rev. 2010). The ET, F of the Landsat image can first be adjusted to a 'basal' condition, where the evaporation estimate is free of rainfall induced evaporation, but still may contain any irrigation induced evaporation:

$$(ET, F_i)_b = ET, F_i - (ET, F_{background})_i \left(\frac{NDVI_{full\ cover} - NDVI_i}{NDVI_{full\ cover} - NDVI_{bare\ soil}} \right) \quad (8)$$

where $(ET, F_{background})_i$ is the background evaporation on the image date (i) for bare soil, computed using the FAO-56 two-stage evaporation model.

The $(ET, F_{background})_i$ was spatially distributed evaporation for a bare soil condition across the image for a specific image date, and was developed by applying the output from the FAO-56 soil evaporation model running under the ERDAS Imagine modelmaker code with spatially distributed precipitation, reference ET, and soil properties as input.

Riparian vegetation

For riparian vegetation, where soil water stress is not likely to occur, an adjusted ET_rF is computed for the image date that reflects background evaporation averaged over the surrounding period in proportion to the amount of ground cover represented by NDVI:

$$(ET_rF_i)_{adjusted} = (ET_rF_i)_b + \overline{(ET_rF_{background})} \left(\frac{NDVI_{full\ cover} - NDVI_i}{NDVI_{full\ cover} - NDVI_{bare\ soil}} \right) \quad (9)$$

where $\overline{(ET_rF_{background})}$ is the average evaporation from bare soil due to precipitation over the averaging period (e.g., one month), calculated as:

$$\overline{(ET_rF_{background})} = \frac{\sum_i^n (ET_rF_{background})_i}{n} \quad (10)$$

Equations 8 and 9 can be combined as:

$$(ET_rF_i)_{adjusted} = ET_rF_i + \left(\overline{(ET_rF_{background})} - (ET_rF_{background})_i \right) \left(\frac{NDVI_{full\ cover} - NDVI_i}{NDVI_{full\ cover} - NDVI_{bare\ soil}} \right) \quad (11)$$

with limits $NDVI_{bare\ soil} \leq NDVI_i \leq NDVI_{full\ cover}$

The outcome of this adjustment will be to preserve any significant evaporation stemming from irrigation or ground-water and any transpiration stemming from vegetation, and only adjusting for evaporation stemming from precipitation to account for differences between the image date and that of the surrounding time period. In other words, if the initial ET_rF_i , prior to adjustment, was high due to evaporation from irrigation or from high ground-water condition, much of that evaporation would remain in the adjusted ET_rF_i estimate

Non-riparian vegetation

The following refinement to Eq. 8-11 was made for application to non-riparian vegetation, to account for those situations where, during long periods (i.e., month), soil moisture may have become limited enough that even transpiration of vegetation has been reduced due to moisture stress. If the Landsat image is processed during that period of moisture stress, then the ET_rF value for vegetated or partially vegetated areas will be lower than the potential (nonstressed) value. This can happen, for example, during early spring when winter wheat may go through stress prior to irrigation or a rainy period.

This causes a problem in that the above method of Eq. 9-11 attempts to 'preserve' the ET_rF of the vegetated portion of a pixel that was computed by METRIC on the image date. However, when a rain event occurs following the image date, not only will the ET_rF of exposed soil increase, but the vegetation will equally 'recover' from moisture stress and the ET_rF of the vegetation fraction of the surface will increase. This situation may occur for rangeland and dryland agricultural systems. It therefore assumed that the ET_rF of nonstressed vegetation will be at least as high as the ET_rF of

bare soil over the same time period, since it should have equal access to shallow water. An exception would be if the vegetation were sufficiently stressed to not recover transpiration potential. However, this amount of stress should be evidenced by a reduced NDVI. A minimum limit is therefore placed, using the background $ET_rF_{background}$ for the period.

To show how to derive the modified Eq. 11, it is useful to first isolate the ‘transpiration’ portion of the ET_rF . On the satellite image date, the bulk ET_rF computed by METRIC for a pixel, is decomposed to:

$$ET_rF_i = (1 - f_c)(ET_rF_{background})_i + f_c(ET_rF_{transpiration})_i \quad (12)$$

where $ET_rF_{transpiration}$ is the apparent transpiration from the fraction of ground covered by vegetation, f_c . The f_c is estimated as $1 - f_s$, where f_s is the fraction of bare soil, and for consistency with equations 9-11, f_s is estimated as:

$$f_s = \left(\frac{NDVI_{full\ cover} - NDVI_i}{NDVI_{full\ cover} - NDVI_{bare\ soil}} \right) \quad (13a)$$

so that:

$$f_c = 1 - \left(\frac{NDVI_{full\ cover} - NDVI_i}{NDVI_{full\ cover} - NDVI_{bare\ soil}} \right) \quad (13b)$$

Eq. 12 is not used as is, since ET_rF_i comes from METRIC. However, one can rearrange Eq. 12 to solve for $ET_rF_{transpiration}$:

$$f_c(ET_rF_{transpiration})_i = ET_rF_i - (1 - f_c)(ET_rF_{background})_i \quad (14)$$

Now, if $ET_rF_{transpiration}$ is limited to the maximum of the $ET_rF_{transpiration}$ on the day of the image, or the $(ET_rF_{background})$ for the period, then:

$$(ET_rF_{transpiration})_{adjusted} = \max\left[(ET_rF_{transpiration})_i, (ET_rF_{background})\right] \quad (15)$$

Then the new ET_rF adjusted value becomes:

$$\begin{aligned} (ET_rF_i)_{adjusted} &= (1 - f_c)(ET_rF_{background}) + f_c(ET_rF_{transpiration})_{adjusted} \\ \text{or} & \\ (ET_rF_i)_{adjusted} &= (1 - f_c)(ET_rF_{background}) + f_c \max\left[(ET_rF_{transpiration})_i, (ET_rF_{background})\right] \end{aligned} \quad (16)$$

where $(ET_rF_{background})$ is the average evaporation from bare soil due to precipitation over the averaging period (e.g., one month) and $ET_rF_{transpiration}$ is the original transpiration computed from Eq. 14. Eq. 14 and 16 can be combined so that:

$$(ET, F_i)_{adjusted} = (1 - f_c) \overline{(ET, F_{background})} + \max \left[\left((ET, F_i - (1 - f_c) \overline{(ET, F_{background})}) \right)_i, f_c \overline{(ET, F_{background})} \right] \quad (17)$$

Only areas with bare soil or partial vegetation cover are adjusted. Pixels having full vegetation cover, defined as when NDVI > 0.75, are not adjusted. An example of an image date where the adjustment increased the ET_rF for bare soil and partially vegetated areas is shown in Figure 5. Figure 6 shows an example of an image date where the ET_rF from bare soil and partially vegetation cover was decreased by the adjustment

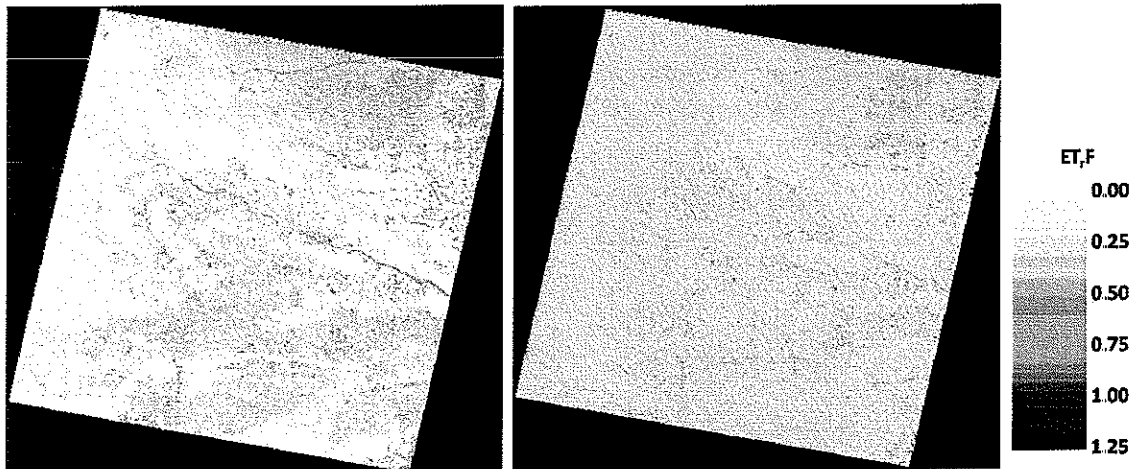


Figure 5. ET_rF from May 9 1997 before (left) and after (right) adjustment for background evaporation representing the time period (~month) represented by that image

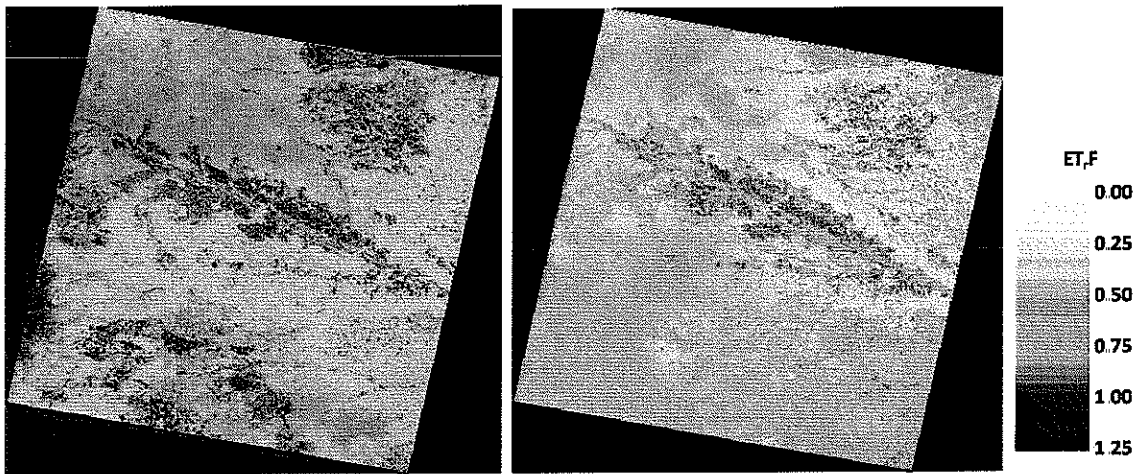


Figure 6. ET_rF on August 13 1997 before (left) and after (right) adjustment to reflect soil evaporation occurring over the time period (~ 1 month) represented by that image. Note that irrigated fields with full vegetation cover having a substantial transpiration component were not affected by the adjustment.

Average ET_rF on image dates before and after adjustment from ten rangeland locations are shown in Figure 8. For some image dates, such as early and late in the season, the ET_rF values were “wetter” so to be representative for the wetter periods surrounding the images than that represented

by the original image. Similarly, for other images dates, such as in the middle of the growing season, the images were “dried” some

Daily Precipitation and Rangeland ETrF Before and After Adjustment for Background Evaporation (n=10)

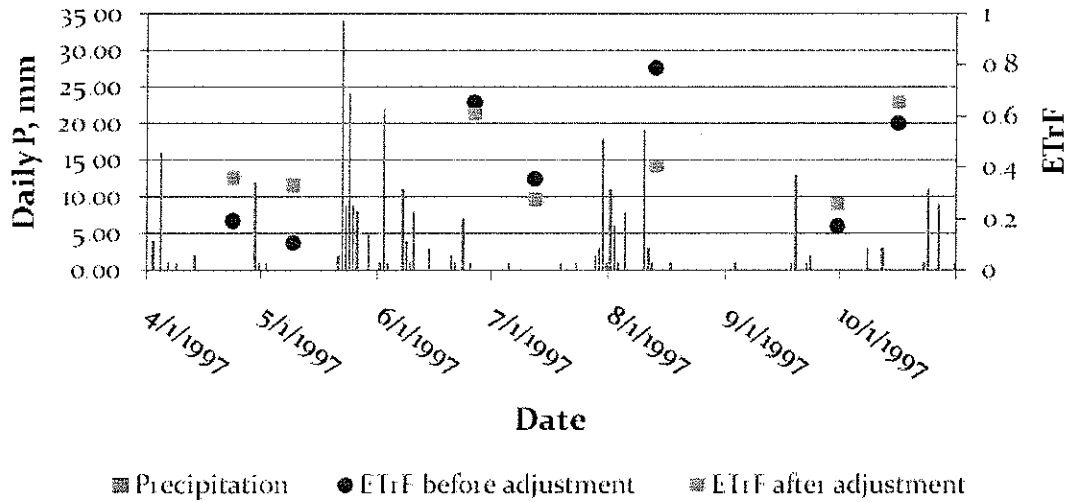


Figure 8. Average ETrF from ten rangeland locations before and after adjustment. Also shown is the precipitation from the Scottsbluff HPRCC weather station

References

- Allen, R.G. 2008, rev. 2009, 2010. Procedures for adjusting METRIC-derived ETrF Images for Background Evaporation from Precipitation Events prior to Cloudfilling and Interpretation of ET between Image Dates. Internal memo., University of Idaho. 11 pages. Version 7, last revised April 2010.
- Ranade, P. (2010). Spatial Water Balance for Bare Soil. University of Nebraska Report, 10 pp.

Appendix G

Extrapolating ET Estimates from instantaneous to daily Time Steps

By R.Allen and J. Kjaersgaard, University of Idaho, August 2010.

Challenges in estimating ET for daily and longer periods using 'snapshots' of ET from essentially instantaneous satellite images, such as from Landsat, are uncertainties in the behavior of ET of vegetation relative to the potential ET demand, especially in cases where the vegetation is water stressed or is wild vegetation where survival is often more important than growth and therefore substantial degrees of stomatal regulation may be employed. In the case of agricultural vegetation where modern cultivars have been selected where limiting stomatal regulation and thus photosynthesis and bio-yield has been discouraged, the relative ET rate during late morning (i.e., Landsat overpass time) and as represented by $ET_{r,F}$ has been consistently shown to stay consistent through the day (Allen et al 2007b, 2008). Therefore, the 24-hour $ET_{r,F}$ for agricultural crops, especially nonstress crops, is generally equal to the late morning value. Because the reference ET estimate (ET_r) on which the $ET_{r,F}$ is based tends to capture the impact of afternoon advection on increasing potential ET demand, the use of $ET_{r,F}$ tends to assume that the vegetation (surface) being modeled has similar behavior and response to advection.

On the other hand, rangeland vegetation, when water stressed, is likely to exercise increased stomatal regulation during afternoon periods on hot, dry days. Under these conditions, the rangeland vegetation is likely fluxing the same amount of sensible heat to the atmosphere as the surrounding region, so that, by definition, there is no net advection of energy for increasing evaporation to the surface. Because of this, the use of $ET_{r,F}$ for rangeland, where $ET_{r,F}$ does suggest the response of vegetation to the presence of advection, may overstate daily ET. In contrast, the evaporative fraction, EF, representing the ratio of ET to the difference of net radiation and soil heat flux, tends to not account for influences of advection occurring during afternoon. In consideration of these phenomena, in the METRIC applications in the Nebraska panhandle, the evaporative fraction, EF, was used to extrapolate from instantaneous to daily values of ET, rather than $ET_{r,F}$, since, by definition, no net transfer of advective energy exists with rangeland systems. Daily ET in mm/day was calculated by multiplying the $ET_{r,F}$ by daily ET_r , or by multiplying the EF by daily net radiation. In both cases, a daily $ET_{r,F}$ was computed by dividing daily ET by daily ET_r . The procedures for obtaining daily estimates of ET and $ET_{r,F}$ are further explained in appendix E.

For land covers other than rangeland, the estimate of daily $ET_{r,F}$ was set equal to the instantaneous at the satellite overpass time, based on extensive ET measurements made using precision weighing lysimeters at Kimberly, Idaho (Allen et al. 2007b, 2008).

Using $ET_{r,F}$ as the vehicle to estimate 24-hour ET from instantaneous ET (at satellite overpass time) may therefore overestimate the 24-hour (or longer) period ET for natural vegetation systems. An alternative, and relatively simple, method using the evaporative fraction, EF, to extrapolate from instantaneous to 24-hour has been set up in ERDAS Imagine.

Because the EF is the ratio of ET to the amount of energy from net radiation (R_n) less ground heat flux (G), viz

$$EF = \frac{LE}{R_n - G} \quad (1)$$

and impacts of advection beyond those that occur at satellite overpass time, are not considered. For natural vegetation with a limited supply of soil water 24-hour ET is estimated via EF as:

$$ET_{24} = EF_{inst} (R_n - G)_{24} = \frac{ET_{METRIC}}{(R_n - G)_{inst}} (R_n - G)_{24} \quad (2)$$

Instantaneous R_n and G are output by METRIC. G can be assumed to be zero for 24-h periods (Allen et al., 1998). The EF transfer method expressed in Eq. 2 has long been used by Bastiaanssen and others (1998, 2005; Brutsaert, 19xx) to estimate 24-hour ET during remote sensing. In Eq. 2, 24-hour R_n , R_{n24} , can be estimated using e.g. the Slob method for net longwave radiation (unpublished, c.f. de Bruin and Stricker, 1982).

$$R_{nl24slob} = (c_s \frac{R_s}{R_a}) \quad (3)$$

where R_s is solar radiation, R_a is the extraterrestrial radiation and c_s is the Slob calibration coefficient. Because the albedo, α , varies with changing sun angle, the albedo integrated over the day may be slightly higher than the instantaneous value at the satellite overpass time.

Because net longwave radiation, R_{nl} , is a function of surface temperature, the Slob function is calibrated to the reference conditions (the hot and the cold pixel) of METRIC, and scaled to the 24-hour R_{nl} for any pixel within the image between the two R_{nl} estimates using instantaneous surface temperature:

$$R_{nl24pixel} = \frac{T_s - T_{scold}}{T_{shot} - T_{scold}} (R_{nlhot24} - R_{nlcold24}) + R_{nlcold24} \quad (4)$$

where T_s is the instantaneous surface temperature, T_{scold} and T_{shot} are the surface temperatures of the cold and the hot pixels. $R_{nlhot24}$ and $R_{nlcold24}$ are net longwave radiation estimated for the hot and the cold pixel using Eq. 3 using $c_s = 110 \text{ W/m}^2$ (Kjaersgaard and Allen, 2010) for the hot pixel and $c_s = 140 \text{ W/m}^2$ (Allen and Bruin, 2008) for the cold pixel.

24-hour R_n is then calculated as

$$R_{n24} = (1 - \alpha)R_s - R_{nl24pixel} \quad (5)$$

An alternative is to use the Brunt (1932) method, parameterized as described in e.g. ASCE-EWRI (2005).

Eqs. 1 – 5 (i.e. EF) should only be used for land use classes and areas that are predominantly rainfed, i.e. not irrigated, phreatophytic vegetation, riparian zones or areas having a shallow ground water table. For the composite Land use maps used in the Nebraskan Panhandle, EF was used with the following Landuse classes: 21, 52, 71, 105, 106, 108, 109, 110, 111, 114, 136, 138, 139, 140, 141, 142, 143 and 144.

Implementation in ERDAS Imagine Modelmaker

The calculation of spatially distributed 24-hour R_n using the Slob method is calculated using the model shown in Figure 5, developed by Kjaersgaard (2010 pers. commun). The model is named using the prefix 'f09' to indicate that it should be run in the step immediately following model 'f08', and before cloud gap filling.

The input required for the model is summarized in Table 1.

Table 1. Input for model F09 where instantaneous ET estimates from METRIC is extrapolated to 24-hour values using either EF or ET_rF .

| Input parameter | Comments |
|--|---|
| Net Radiation | Instantaneous net radiation as generated by METRIC in model f05 |
| Ground heat flux | G_adj from METRIC model f08 (NB: The model needs to be modified to output this file) |
| Land use map | Land use map |
| ET24 | ET24 generated in model f08 |
| ETrF_inst | Instantaneous ETrF from model f08 |
| Set LU classes | For the composit Landuse maps used in the Nebraskan Panhandle, EF was used with the following Landuse classes: 21, 52, 71, 105, 106, 108, 109, 110, 111, 114, 136, 138, 139, 140, 141, 142, 143 and 144. |
| Ts | Surface temperature from model f04 |
| Albedo | Surface albedo from model f02 |
| Ts cold pixel | Surface temperature of the cold pixel (from the METRIC spreadsheet) |
| Ts hot pixel | Surface temperature of the hot pixel (from the METRIC spreadsheet) |
| ETr inst mm/hour | Instantaneous reference ET (from the METRIC spreadsheet) |
| ETr24 mm/day | 24-h reference ET (from the METRIC spreadsheet) |
| Daily Rs W/m² | Measured daily shortwave radiation at the weather station used for calibration of METRIC |
| Daily R_a W/m² | Daily extraterrestrial radiation. This value can be calculated using the equations in e.g. ASCE-EWRI, 2005 or Allen et al , 1998 (FAO56). R _a is also calculated by RefET and output in the .in2 file. |
| Slob coeff. Cold | Slob coefficient used at the cold pixel; 140 W/m ² is used |
| Slob coeff. hot | Slob coefficient used at the hot pixel; 110 W/m ² is used |

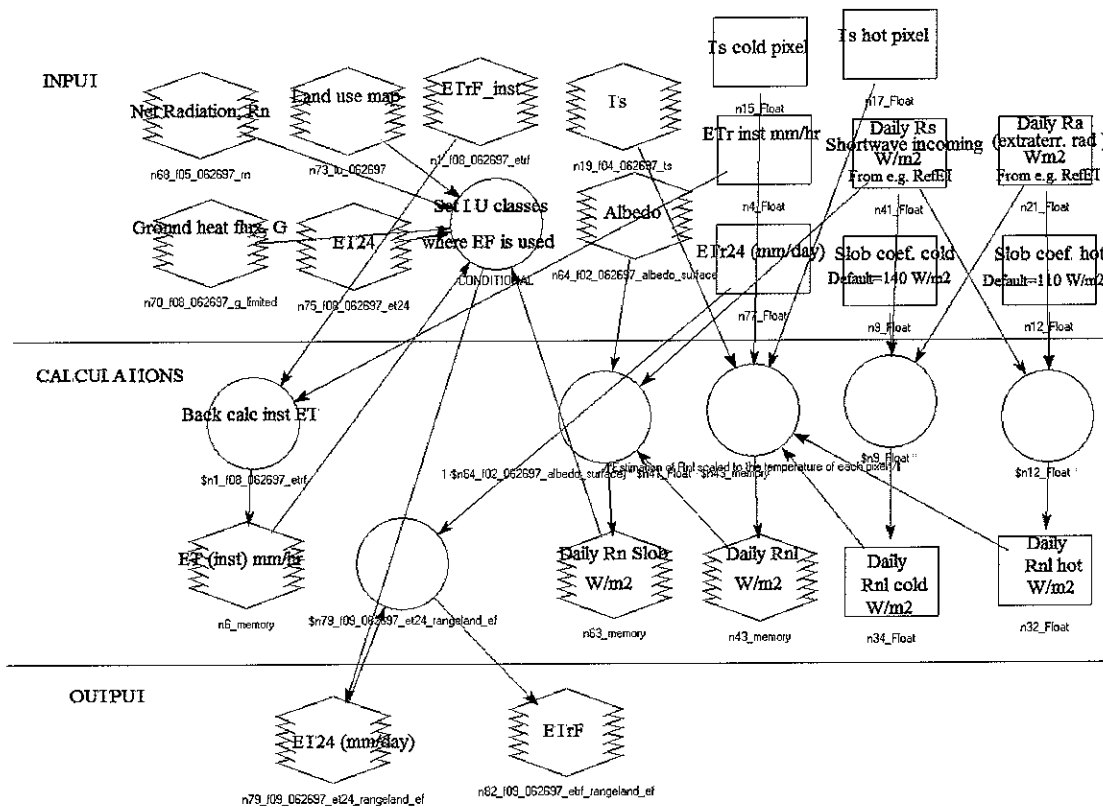


Figure 5. ERDAS Imagine model to estimate spatially distributed net radiation using the Slob method (by Kjaersgaard, 2010, pers. commun.).

References

- Allen, R.G. (2009). "Methodology for adjusting METRIC-derived ETrF Images for Background Evaporation from Precipitation Events prior to Cloudfilling and Interpretation of ET between Image Dates" Note University of Idaho, Kimberly R&E Center, Kimberly, Idaho. 11 pp., revised 2010
- Allen, R. (2010). "Algorithm to adjust spline interpolated ETrF between Satellite Image to Dampen inter-image periods of ETrF exceeding approximately 1.00." Note University of Idaho, Kimberly R&E Center, Kimberly, Idaho. 2 pp.
- Allen, R.G. and H. deBruin (2008). Calibration of the Slob net long wave radiation equation for reference ET conditions. draft paper, still in progress
- Allen, R.G., Tasumi, M., Trezza, R., Kjaersgaard, J.H. (2010). "METRIC Applications Manual." Version 2.0.6. University of Idaho, Kimberly, Idaho. 164 pp.
- Kjaersgaard, J. and R.G. Allen. 2010. Calibration of the Slob net long wave radiation equation using surface temperature from dry surfaces. draft report/paper, still in progress.

Trezza, R , Allen, R.G., Garcia, M. (2007). "Methodology for Cloud Gap Filling in METRIC." University of Idaho, Kimberly, Idaho. 7 pp.

Trezza, R., Allen, R.G , Garcia, M., Kjaersgaard, J.H. (2008). "Using a Cubic Spline to Interpolate between Images." University of Idaho, Kimberly, Idaho. 9 pp

Attachment 2

'Value-added' products from METRIC Evapotranspiration and Crop Coefficient Maps

R.Allen¹, G. Hergert², A.Irmak³, J.Kjaersgaard¹, I.Ratcliffe³
22 October, 2010, revised 24 October, 2010.

The North Platte and South Platte Natural Resources District (NRD) and USDA-NRCS funded work by the Univ. Nebraska and Univ. Idaho has produced monthly and growing season evapotranspiration (ET) over major areas of the North Platte and South Platte NRDs for years 1997, 2002 and 2005. These ET maps show water consumption at 30 m detail that can provide useful information on field to field variability, crop to crop variability, within crop variability and spatial variation regionally in regard to water consumption. Current Geographical Information System (GIS) capabilities of the two NRD's is sufficient to produce water consumption products, based on the METRIC products, that may be useful for managing overall water consumption within the NRD's, water consumption by water source, water consumption by user group, water consumption by location, and for preparing hydrologic and conformance reports. It is these value added products, made in GIS, that may prove to be most useful to the NRD water managers and boards and can provide for improved visualization of water consumption. In addition they can provide the ability to contrast differences among various locations, sources of water, relative wetness of years, and impacts of types of agriculture and irrigation systems, type of land use, etc.

The following points are a list of GIS based products that can be created within the NRD's by GIS specialists. The two Universities can provide guidance on the creation of these products:

- 1 **Crop water use (CWU) from irrigated land**
 - CWU can be defined in terms of
 - total ET from a land parcel or
 - ET of irrigation water (that ET that is above the ET component of natural precipitation)
 - The CWU can be in the form of spatial maps and as means and variances over aggregated areas
 - CWU from GW vs. SW sources
 - CWU by crop type
 - CWU by land use
 - CWU by Year (1997, 2002, 2005)

- 2 **CWU from nonirrigated land** and other natural vegetation such as riparian systems.
 - CWU from riparian systems as a function of

¹ University of Idaho, Kimberly, Idaho

² University of Nebraska, Scottsbluff

³ University of Nebraska, Lincoln

- vegetation density
- vegetation type
- understory
- depth to ground water
- invasive species control
- CWU by type of rangeland
- CWU (and ground-water recharge) by type of fallow farming (continuous vs. every other year)

3. Annual and peak season **Crop Coefficients**

- by crop
 - by Year (1997, 2002, 2005)
 - Spatially across the NRD's
 - Spatially by Water Source or by Stream Basin
- by NRD or sub-NRD or water source
 - to provide spatial contrast in relative water use
 - to indicate differences among relative water use (i.e., Kc) among years
 - due to relative water supply
 - due to implementation of any curtailment programs or policies

4. Crop coefficient (Kc) curves can be created by averaging among many fields having the same crop type and then splining between Landsat image dates. For example, the following figure 1 shows a crop coefficient curve developed for dry beans in the Twin Falls, Idaho vicinity using METRIC produced ET from year 2000. Several hundred bean fields were sampled and averaged (grey symbols and curve). Also shown are Kc from a standard Kc curve produced by the US Bureau of Reclamation Agrimet⁴ system (based on Kc data by Wright 1981⁵, originally) and Kc by Allen and Robison (2007)⁶ that is based on the 'dual Kc' method where evaporation from wet soil is considered and where estimates were made all twelve months of the year, including nongrowing season. The agreement among the three systems of Kc's is relatively good, indicating that the Agrimet and Allen-Robison curves are appropriate for the area. If the curves were substantially different, due to differences in assumed planting dates, etc., they could be adjusted using the METRIC-based curves.

⁴ <http://www.usbr.gov/pn/agrimet/>

⁵ Wright, J.L. (1981). Crop coefficients for estimates of daily crop evapotranspiration *Irrig. Sched. for Water and Energy Conserv. in the 80's*, Am. Soc. of Agr. Engrs., Dec. 18-26.

⁶ Allen, Richard G. and Clarence W. Robison, 2007. *Evapotranspiration and Consumptive Irrigation Water Requirements for Idaho*, Research Technical Completion Report, Kimberly Research and Extension Center, University of Idaho, Moscow, ID <http://www.kimberlyuidaho.edu/ETIdaho/>

**Dry Beans
Twin Falls, Idaho 2000**

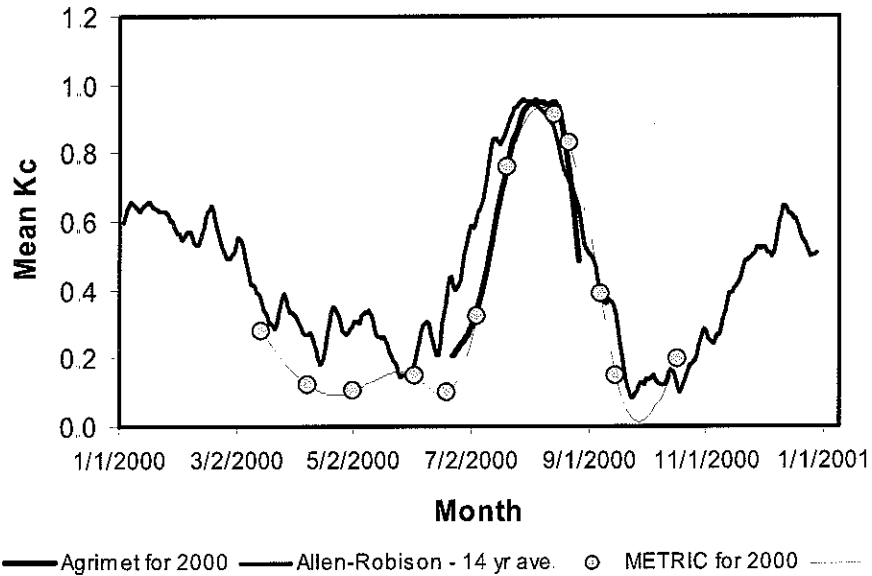


Figure 1. An average crop coefficient curve (grey symbols) developed for dry beans in the Twin Falls, Idaho vicinity using METRIC produced ET from year 2000. Also shown are Kc from a standard Kc curve published by the US Bureau of Reclamation Agrimet⁷ system and a Kc curve simulated from Kc tables by Allen and Robison (2007)⁸

The following figure 2 shows a sampling of Kc from about 700 corn fields via METRIC ET in southcentral Idaho where each vertical line represents a satellite image date and each small blue point represents the Kc of one field. The large black circles represent the average Kc on each satellite image date over all fields. Large variation in Kc early in the year is caused by wetness of individual fields.

⁷ <http://www.usbr.gov/pn/agrimet/>

⁸ Allen, Richard G. and Clarence W. Robison, 2007. *Evapotranspiration and Consumptive Irrigation Water Requirements for Idaho*, Research Technical Completion Report, Kimberly Research and Extension Center, University of Idaho, Moscow, ID <http://www.kimberlyuidaho.edu/ETIdaho/>

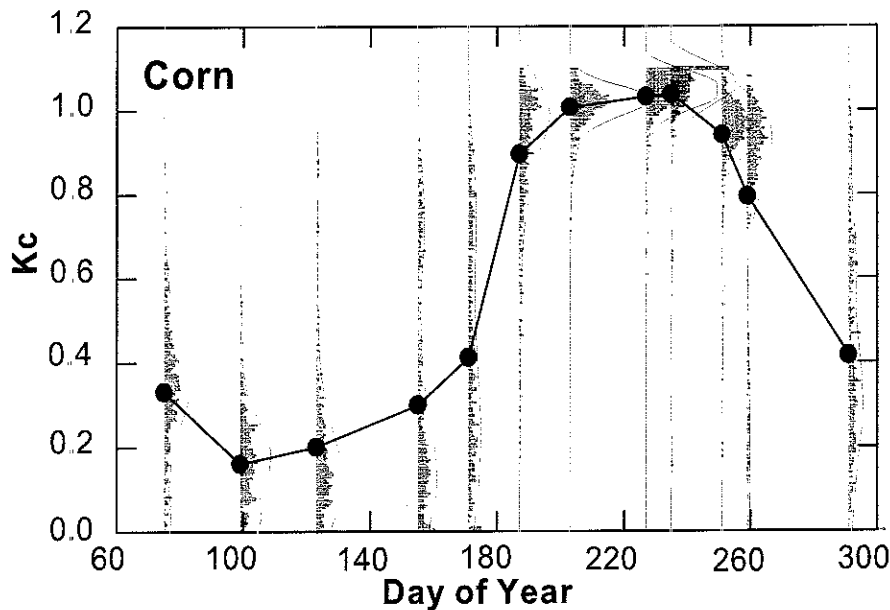


Figure 2. Kc on individual satellite image dates (vertical lines) and averaged Kc curve for the year (solid black symbols and curve) for southcentral Idaho as determined from METRIC ET.

5 Estimated **Ground water Recharge**

- Recharge can be estimated as Precipitation (P) less ET, or $P - ET$, for time periods long enough that soil water storage can be neglected.
- The recharge estimate can be expressed on a growing season or annual basis (the annual basis is preferred to account for evaporation of wintertime P. However, METRIC based ET is generally not available for wintertime due to clouds.) Wintertime ET can be estimated from daily water balance models using precipitation and reference ET as inputs. These types of models were prepared for the study area during the METRIC applications and can be made available. The following graphic in Figure 3 shows an image of April – October $P - ET$ from a presentation made at a remote sensing conference in Jackson, Wyo. in September 2010 (slide 19). The ppt is at: <http://www.kimberly.uidaho.edu/~rallen/Nebraska/>

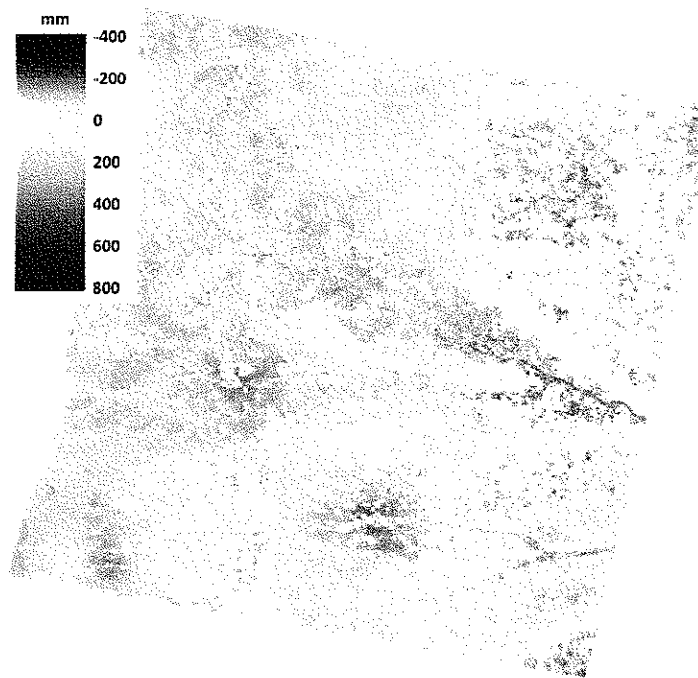


Figure 3. Growing Season (April 1 – October 31) evapotranspiration minus precipitation for 1997 for the south-west corner of the Nebraskan Panhandle. Positive values for $ET - P$ generally occur for irrigated areas where ET is supplied by irrigation in addition to P. Areas of negative $ET - P$ indicate areas of potential ground-water recharge.

One cautionary point in any analysis of $ET - P$ (or $P - ET$) where ET is taken from METRIC, is that the maps used for P need to be 'congruent' with the maps for P used in creating the METRIC product. A gridded soil water balance / evaporation model was operated on a daily basis using maps of P for all three years and the estimated evaporation was used during the METRIC ET process for interpolation among satellite image dates to incorporate evaporation from rainfall events. Therefore, the ET maps from METRIC are 'biased' toward the particular precipitation maps utilized in the process model.

- 6 Impacts of cultural practices on ET:
 - no-tillage cultivation vs. tillage cultivation
 - pre irrigation vs. no pre-irrigation
 - high plant population or narrow rows vs. low plant population
 These comparisons will require field by field information that is not available via remote sensing.

7. Variation in CWU by soil type.

8. Variation in CWU by basin: for example, Pumpkin Creek Basin vs. North Platte Valley (where annual allocations are currently 12 and 18 inches, respectively)
9. Comparison of CWU from METRIC with estimates by COHYST, etc.

Additional examples of spatial aggregation and expression of ET-based information are provided by the following illustrations. A number of other types of graphics are possible.

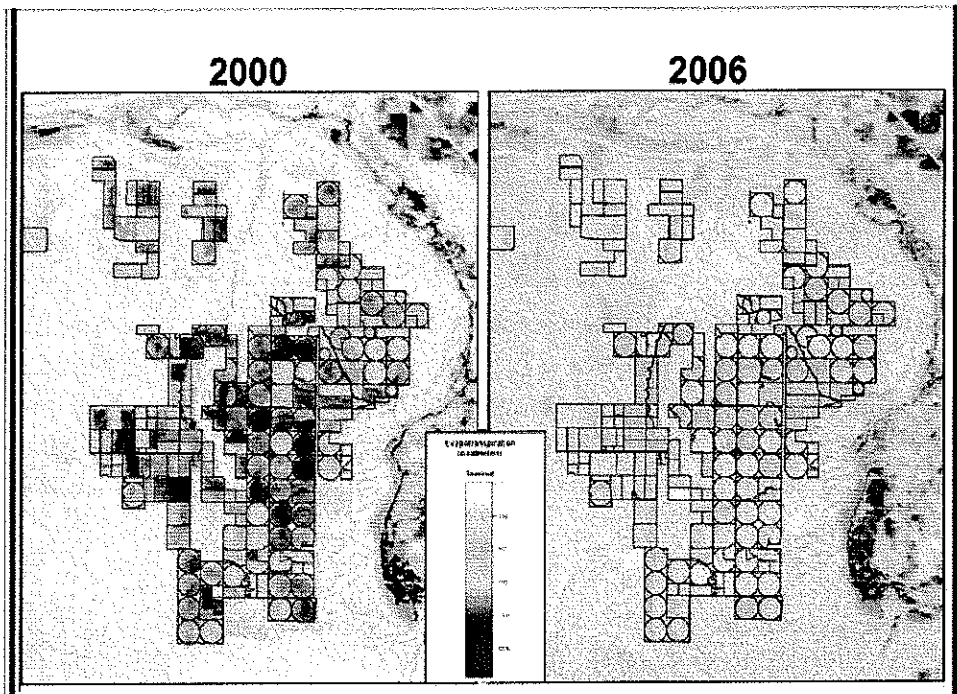
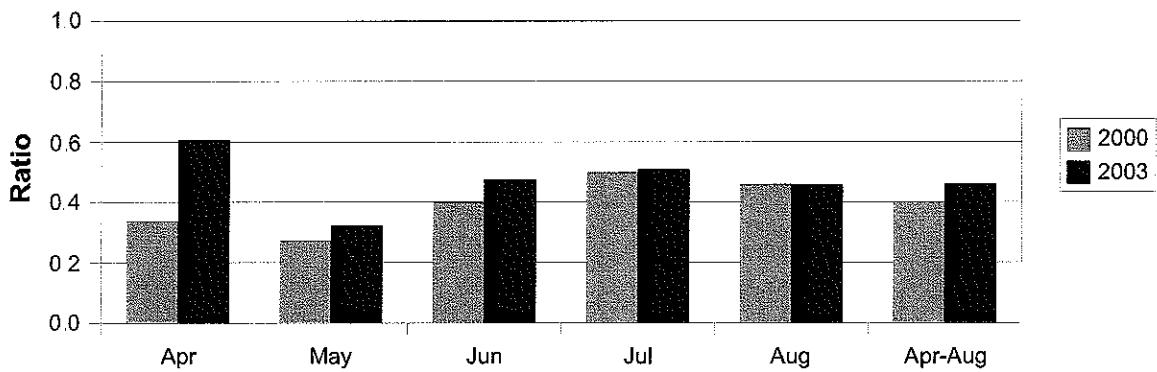


Figure 4. Growing Season (April – October) Evapotranspiration from the “Bell Rapids Mutual Irrigation Company” lands (~25,000 acres) during year 2000 and in year 2006, one year after selling rights to their water to the State of Idaho for Salmon Recovery. The ET in 2006 is from residual soil water storage. Water rights polygons are overlaid onto the ET map. Graphic from W. Kramber, IDWR 2009, pers. commun., ET data from Allen et al., UI, 2009.

Evapotranspiration as a Ratio of Diversion plus Precipitation



Project wide Crop Coefficient -- METRIC Twin Falls Tract -- 220,000 acres -- Alfalfa Reference Basis

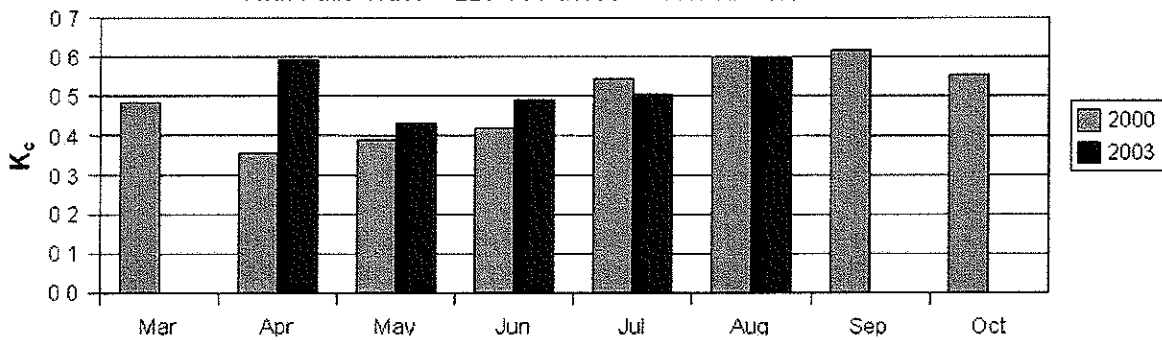


Figure 5. "Performance" of the 202,000 acre Twin Falls Canal Company tract of southcentral Idaho (top) expressed as the ratio of ET to the sum of canal diversions plus precipitation. Sept-Oct. 2003 ET data were not available due to clouded images. The bottom image shows a tract-averaged crop coefficient by month (alfalfa reference basis) (Allen and Robison, UI internal report, 2005). Diversions plus diversions less ET are anticipated to return to the fresh water system as surface return flow and as ground-water recharge.

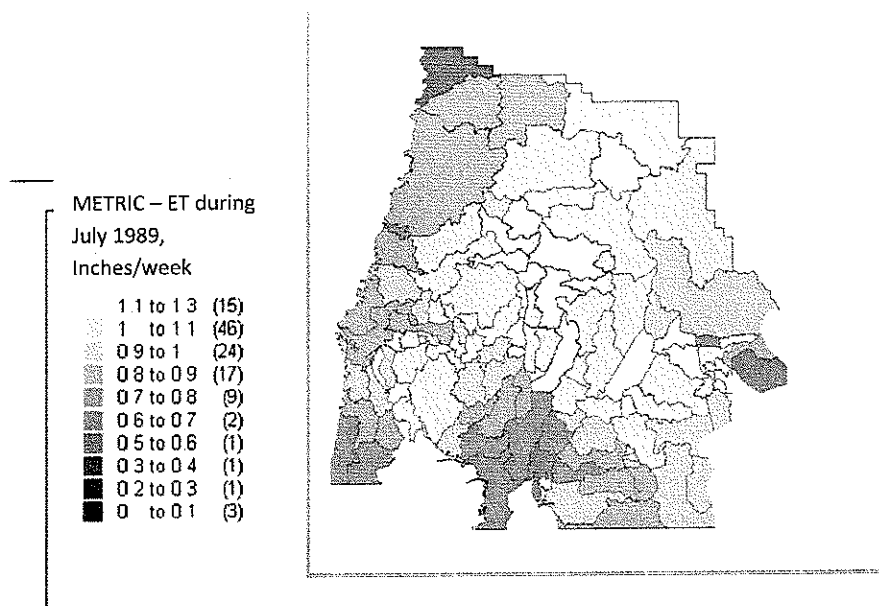


Figure 6. ET derived from METRIC and Landsat for the watershed source area of the city of Tampa Bay, Florida, aggregated by hydrologic unit. Data by R.Allen for Tampa Bay Water.

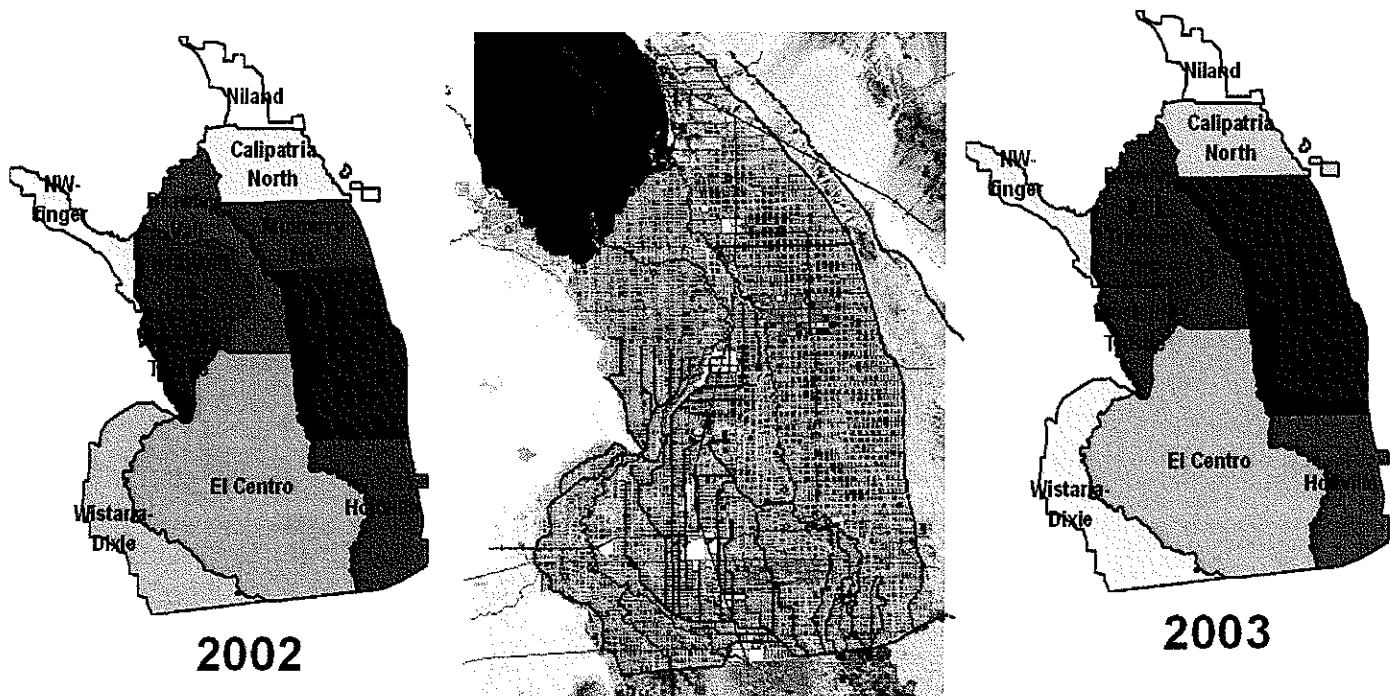


Figure 7. Relative depths of winter ET for vegetables, aggregated by Irrigation Management Area, within the Imperial Irrigation District of California. Data via METRIC by Allen et al., 2003.

Attachment 3

Evapotranspiration Mapping Using Landsat Visible and Thermal Data with METRIC™ for the Nebraska Panhandle for Years 2002 and 2005

Final Report Submitted to

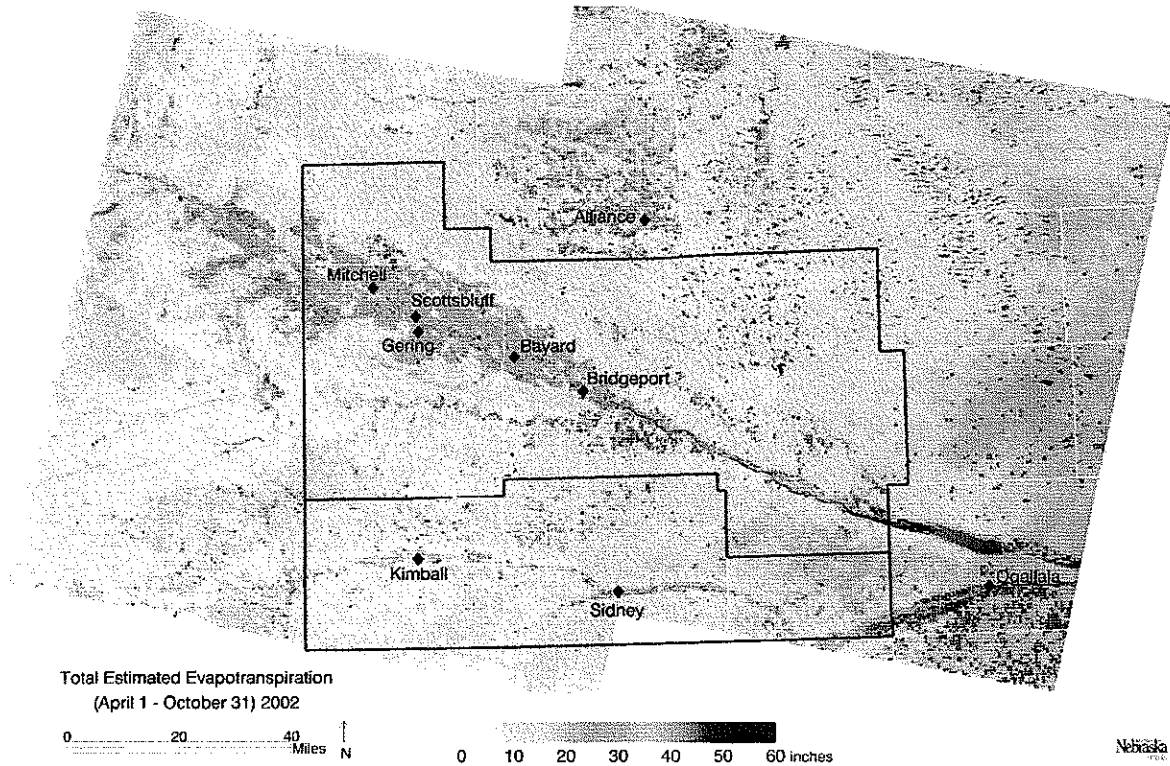
North and South Platte Natural Resource Districts

March 2011

Ayşe Irmak¹, Ian Ratcliffe², Parikshit Ranade²

¹School of Natural Resources and Department of Civil Engineering, University of Nebraska-Lincoln, Lincoln, NE

²School of Natural Resources, University of Nebraska-Lincoln, Lincoln, NE



UNIVERSITY OF
Nebraska
Lincoln



ACKNOWLEDGEMENTS

The authors wish to express their sincere appreciation to the USDA Natural Resources Conservation Service, the North Platte Natural Resources District, and the South Platte Natural Resources District, for providing financial and other support for this project. We wish to acknowledge the collaboration in this study with the University of Idaho, most notably with Drs. Richard Allen and Jeppe Kjaersgaard of the Kimberly Research and Extension Center who provided initial training on the METRIC model, provided initial computer code, and provided advice and review during the study. Drs. Allen and Kjaersgaard also worked with UNL faculty to advance the development of methods to integrate ET between satellite image dates that better account for impacts of episodic precipitation events between image dates and to advice on the implementation of spatial ET products in NRD operational processes. Portions of this report were derived from report sections by Kjaersgaard and Allen (2010) as part of the UNL-UI collaboration.

The authors also would like to thank to Dr. Suat Irmak at Biological System Engineering of University of Nebraska for his review and valuable insights during the research. Dr. Sami Akasheh was helpful with for providing technical support since 2011. His time and help is greatly appreciated. We also would like to thank Bryan C. Leavitt of Center for Advanced Land Management Information Technologies (CALMIT) at the University of Nebraska-Lincoln for providing IT support for during project.

INTRODUCTION

The goal of this project was to produce spatial crop evapotranspiration (ET) information for agricultural and rangeland areas of the North and South Platte Natural Resources Districts (NPNRD, SPNRD) of western Nebraska, and to improve the understanding of relevant processes that control ET in these settings. A specific objective was to produce spatial ET information for monthly periods and over growing seasons (April through October) for multiple years spanning relatively wet and dry periods. This report describes the setup and processing of Landsat satellite imagery encompassing the Nebraska Panhandle area for years 2002 and 2005 by University of Nebraska using the METRICTM procedure (Mapping Evapotranspiration at high Resolution using Internalized Calibration) developed by the University of Idaho (Allen et al., 2007a, 2010) and further developed during this study.

Evapotranspiration (ET) is calculated within the METRIC platform using a surface energy balance that calculates actual ET rates at the approximately 11:00 am satellite overpass time and then transforms these instantaneous estimates into daily values for ET and ultimately into monthly and growing season totals. Two growing seasons were processed during this study, representing years 2002 and 2005. These years were relatively dry and wet years, respectively and compliment the year 1997 that was processed by the University of Idaho (Kjaersgaard and Allen 2010). Landsat path 33/row 31 was processed for 2005 while two paths, path 33/row 31 and path 32/row 31, were processed for 2002. Path 33 is the western path shown in Figure 9 and in the graphic on this report's cover. Path 32 lies to the east of path 33 and covers the eastern portions of the two NRD's. The two paths share a common overlapped area of about 50 km (30 miles) width. Only path 33 was processed for 2005 due to too many images occluded by clouds. A total of 8 and 17 Landsat satellite images were processed for 2005 and 2002, respectively, to produce estimates of monthly and growing season ET. The dates of the satellite images processed using METRIC are listed in Table 2 of Appendix B. Each Landsat scene covers approximately a 150 x 150 km area and has a spatial resolution of 30 meters for shortwave bands and 60/120 meters (Landsat 7/Landsat 5) spatial resolution in the thermal band. A combination of Landsat 7 and Landsat 5 images were utilized, where each of the two satellites revisit a particular path each 16 days and each satellite follows the other by 8 days. Many potential images could not be processed, however, due to cloudiness.

The METRIC procedure utilizes the visible, near-infrared, and thermal infrared energy spectrum bands from the Landsat sensor and hourly weather data to calculate ET on a pixel by pixel basis. Energy is partitioned into net incoming radiation (both solar and thermal), ground heat flux (G), sensible heat flux to the air (H) and latent heat flux (LE). The latent heat flux, which represents the energy consumed by the evaporation process, is calculated as the residual of the energy balance. In general, large amounts of energy are required to evaporate water vapor so that the energy balance represents a relatively stable, consistent and accurate means to estimate water consumption. The strong advantage of using a surface energy balance is that actual rates of ET are determined, where actual ET rates can be constrained to rates below potential rates due to

water shortage, disease, poor irrigation water management and other factors based ET estimates are a better representation of actual ET than are products of other approaches such as tying crop coefficients to vegetation indices to estimate actual ET.

The topography of the region was incorporated into METRIC via a digital elevation model (DEM), and used to account for impacts lapse rate on near surface air temperature gradients used in aerodynamic components of the energy balance. The model was run with the appropriate inputs (weather, soil properties, water balance, etc.) for each individual Landsat path and row. Individual daily ET maps for 2002 and 2005 were produced for the area encompassing the Nebraska Panhandle from Landsat 5 and Landsat 7 satellite imagery. The model was calibrated for each image utilizing ground based meteorological information and identified anchor conditions (cold and hot pixels) present in each satellite image. A detailed description of METRIC can be found in Allen et al. (2007a,b; 2010).

This report is organized to describe the processes involved to produce daily, monthly, and seasonal ET maps from instantaneous Landsat satellite imagery. A detailed description of quality control of weather data; selection of Landsat images for METRIC model; pre-processing of digital elevation map and a land use map; the procedures for cloud masking, and estimating monthly and seasonal fraction of reference evapotranspiration (ET_0 , equivalent to crop coefficients) and ET from daily values; and estimation of distributed soil evaporation and adjustment for background evaporation are given in Appendix A through F. Appendix G describes extrapolation of ET estimates from instantaneous (snapshot) images to produce daily, monthly, and seasonal time steps.

The project results presented here can be used to develop the capacity to use ET maps in hydrologic water balances and to develop crop coefficient curves for specific crops. This information is critical in improving irrigation scheduling, in water-use monitoring and in ground-water modeling work. The following is a list of “value added” products that can be used by NPNRD and SPNRD staff and managers. The ET products provide the ability to contrast differences in ET among various locations and types of agriculture in addition to supporting efforts in applying the COHYST model:

1. Support ground-water model calibration (i.e. MODFLOW) and operation.
2. Quantify water use by irrigated agriculture within NPNRD and SPNRD
3. Quantify net differences in ET from irrigated agriculture and rainfed (dryland) agriculture
4. Quantify historical water use for any water rights buyouts, curtailments, leasing, or fallowing programs
5. Water budgets for hydrologic modeling
6. Calibration of crop models including DSSAT, CROPSIM, Hybrid-Maize, and SWAP (i.e. Irmak and Kamble, 2009)
7. Estimate aquifer depletion with groundwater (i.e. MODFLOW) models
8. Monitor compliance with water rights and permits, and support water resources systems planning

Table 1. List of Appendices for METRIC™ ET processing.

| Appendix | Title |
|----------|---|
| A | Quality control of weather data |
| B | Selection of Landsat images for METRIC processing |
| C | Preparation of digital elevation model and land use map |
| D | Treatment of cloud cover in satellite imagery |
| E | FAO 56 modified water balance using ArcGIS |
| F | Adjustment of ET _r F for background evaporation |
| G | Estimation of Monthly and Seasonal Evapotranspiration |
| H | 'Value-added' products from METRIC Evapotranspiration and Crop Coefficient Maps |

The METRIC Model: Algorithms

In the absence of horizontal advective flux, METRIC computes latent heat flux (LE) as a residual of the energy balance as:

$$LE = R_n - G - H \quad (1)$$

where R_n is the net radiation, G is the soil heat flux, H is the sensible heat flux, and LE is the latent heat flux. The units for all the fluxes are in $W m^{-2}$. The minor energy components are ignored in the model.

METRIC calculates net radiation (R_n) as the difference between incoming radiation at all wavelengths and reflected short-wavelength ($\sim 0.3 - 3 \mu m$) and both reflected and emitted long-wavelength ($3 \sim 60 - \mu m$) radiation (Allen et al., 2007a). The model uses a simple empirical equation developed by Tasumi (2003) to compute soil heat flux (G) as a function of R_n and T_s .

$$\frac{G}{R_n} = 0.05 + 0.18 e^{-0.521LAI} \quad (\text{if } LAI \geq 0.5) \quad (2)$$

$$\frac{G}{R_n} = (1.80(T_s - 272.15)/R_n + 0.084) \quad (\text{if } LAI < 0.5)$$

where T_s (K) is the radiometric surface temperature from satellite. Equation 2 suggests that the G/R_n ratio increases with higher rates of T_s and decreases with increasing Leaf area index (LAI).

Using the aerodynamic function, sensible heat flux (H) is expressed as:

$$H = \frac{\rho * C_p * dT}{r_{ah}} \quad (3)$$

where ρ is the air density (kg m^{-3}), C_p is the specific heat of air ($1004 \text{ J kg}^{-1} \text{ K}^{-1}$), dT is the near surface and air temperature difference (K), and r_{ah} is the aerodynamic resistance to heat transfer (s m^{-1}) over the vertical distance. The dT parameter is used because of the difficulties in estimating radiometric surface temperature accurately from the satellite due to uncertainties in air temperature (T_{air}), atmospheric attenuation, contamination, and radiometric calibration of the sensor (Bastiaanssen et al., 1998; Allen et al., 2007a).

The transfer of the heat from the evaporating surface into the air above the canopy was determined by the r_{ah} as suggested by Brutsaert (1982).

$$r_{ah} = \frac{1}{k u_*} \ln\left(\frac{z_2}{z_1}\right) \quad (4)$$

where z_1 and z_2 are heights (m) above zero plane displacement (d) of the vegetation. The values of 0.1 m for z_1 and 2.0 m for z_2 are used in METRIC. The $z_1=0.1$ m is assumed to be greater than the aerodynamic roughness length for H for dense vegetation and $z_2=2$ m is low enough that it can be assumed to be situated in the equilibrium boundary layer above most surfaces. u_* is the friction velocity (m s^{-1}) which quantifies the turbulent velocity fluctuations in the air, and k is the Von Karman's constant (0.41)

Equations (3) and (4) are arranged to use a temperature gradient (dT) between two heights above the surface to free up calculation of r_{ah} from having to estimate a second aerodynamic roughness for sensible heat transfer. METRIC does not require the actual absolute values of air temperatures (T_{air}) above each pixel, but only near surface temperature difference (dT) is required to solve for H . Thus, the dT for each pixel is calculated as:

$$dT = T_{z1} - T_{z2} \quad (5)$$

where T_{z1} and T_{z2} are the air temperatures at height z_1 and z_2 for any particular pixel, and are generally unknown. The dT is estimated assuming a linear relationship between dT and T_s that is calibrated to each satellite image to compensate for uncertainties in surface radiometric temperature T_s and air temperature (T_{air}):

$$dT = b + aT_s \quad (6)$$

where a and b are correlation coefficients determined with a linear function between dT and T_s derived using known pairs of dT and T_s at two anchor points (hot and cold pixels). This has been

done in a spreadsheet by plotting dT_{cold} vs. T_{s_cold} and dT_{hot} vs. T_{s_hot} and correlation coefficients a and b are derived from regression. More details are described under “Hot and Cold Pixel Selection for Estimation of Sensible Heat Flux” below. The linearity assumption is based on the field research demonstrated by Wang et al. (1995), Bastiaanssen (1995), Franks and Beven (1997a), Franks and Beven (1997b), METRIC uses two anchor pixels (hot and cold) where a value of H can be estimated. The G and H are then subtracted from R_n to calculate the “residual” energy available for evapotranspiration (LE).

The LE time integration was split into two steps. The first step was to convert the instantaneous value of LE into daily values of actual ET (ET_{24}) values by holding the reference ET fraction constant over the 24-hour period (Allen et al., 2007a). An instantaneous value of ET (ET_{inst}) in equivalent evaporation depth is the ratio of LE to the latent heat of vaporization. The reference ET fraction (ET_rF) usually range from 0 to 1.05 and is defined as the ratio of instantaneous ET (ET_{inst}) for each pixel to the alfalfa-reference ET calculated using the standardized ASCE Penman-Monteith equation for alfalfa (ET_r) following the procedures given in ASCE-EWRI (2005):

$$ET_rF = \frac{ET_{inst}}{ET_r} \quad (7)$$

The procedures outlined in ASCE-EWRI (2005) were used to calculate parameters in the hourly ET_r equation. The daily ET at each pixel was estimated by considering ET_rF and 24-hour ET_r as:

$$ET_{24} = ET_rF \times ET_{r-24} \quad (8)$$

where ET_{24} is the daily values of actual ET (mm day^{-1}), ET_{r-24} is 24 hour ET_r for the day of image and calculated by summing hourly ET_r values over the day of image.

The daily ET at each pixel was estimated by considering ET_rF and 24-hour ET_r as:

$$ET_{24} = ET_rF \times ET_{r-24} \quad (9)$$

where ET_{24} is the daily values of actual ET (mm day^{-1}), ET_{r-24} is 24 hour ET_r for the day of image and calculated by summing hourly ET_r values over the day of image

DATA PROCESSING

Weather data

METRIC utilizes alfalfa reference ET (i.e., ET_r) as calculated by the ASCE standardized Penman-Monteith equation (ASCE-EWRI 2005) for calibration of the energy balance process and to establish a daily soil water balance to estimate residual soil evaporation from bare soil following precipitation events (Allen et al., 2007a).

ET_r is used in METRIC as a means to 'anchor' the surface energy balance by representing the ET from locations having high levels of vegetation at full ground cover and full water supply. These locations tend to have cooler surface temperatures due to the effect of evaporative cooling. Since METRIC ties-down the energy balance components to ET_r , high quality estimates of ET_r are needed, which in turn, require high quality weather data. Therefore, before processing of satellite imagery, the quality and accuracy of the meteorological data were assessed

Weather data at a single weather station from each Landsat Path/Row were used for the internal calibration of METRIC for the area of interest. High Plains Regional Climate Center (HPRCC) Automated Weather Data Network (AWDN) weather stations were used from the Scottsbluff (Landsat path 33, row 31) and Sidney (Landsat path 32, row 31) stations.

The AWDN stations record hourly data for air temperature, humidity, soil temperature, wind speed and direction, solar radiation, and precipitation. The reference ET (ET_r) values were calculated using the ASCE-EWRI (2005) standardized Penman-Monteith equation for alfalfa reference generated from the Ref-ET software developed by the University of Idaho. Hourly precipitation and ET_r values were summed together to compute daily, 24-hour, ET_r values. Instantaneous and daily ET_r values from the station in each path were used for calibration of METRIC model, with data from the Scottsbluff used for path 33 and data from Sidney AWDN station used for path 32. The generation of final METRIC products for monthly periods was produced from the individual images using daily reference ET maps derived from reference ET data from all AWDN stations in and surrounding the two Landsat paths. The daily reference ET maps were developed via interpolated maps of reference ET for the project area and were used to develop the monthly and seasonal ET maps. The weather data quality control is described in Appendix A.

A daily soil water balance model was used to determine whether any residual evaporation existed from exposed soil at the time of each satellite image due to recent rainfall events. The

residual evaporation was considered when assigning a value for ET from the 'hot' anchor pixel during the METRIC calibration process, where the hot anchor pixel was generally a bare soil condition located within about 20 km of the weather station. The FAO-56 (Allen et al., 1998) soil evaporation model was used to estimate residual evaporation from the upper 0.125 m soil layer. Soil properties of the area were obtained from Soil Survey Geographic (SSURGO) Database from Natural Resources Conservation Services (NRCS).

Satellite Imagery

Individual satellite images were selected by the project PIs from the University of Idaho and the University of Nebraska based on a list of available Landsat 5 and Landsat 7 preview images for the years 1997-2007 prepared by the University of Idaho. Representatives from the North Platte and South Platte NRDs approved the list. Generally, one Landsat image per month is desired to document progression of vegetation and ET over time and to establish monthly and seasonal ET estimates. The principles of the image selection are described in Appendix B. Landsat images were ordered from the USGS Earth Resources Observation Systems (EROS) in Sioux Falls, S.D by the CALMIT, University of Nebraska (prior to the free-data policy of EROS). The images were ordered as an L1T product, which includes both radiometric, geographic, and terrain correction. Based on advice from the NRDs, the geographic projection of the images was specified as GRS 1980, NAD83, UTM zone 13, and resampling of the thermal band to 30 m pixel size was done by EROS using nearest neighbor resampling. The imagery used for this project was from the Landsat 5 and Landsat 7 satellites. Since Landsat 7 was operational in 1999, the imagery processed by University of Idaho included only Landsat 5 images.

The Landsat program is a series of earth-observing satellites managed by NASA and the U.S. Geological Survey. Since 1972, Landsat satellites have been collecting data over the Earth's surface. Landsat 5 and Landsat 7 are the only Landsat satellites currently operating. Landsat 5 employs the Thematic Mapper (TM) sensor that collects spectral data across seven separate wavelengths. The TM sensor has a spatial resolution of 30 meters (~98.5 ft) for bands 1-5 and 7 and 120 meters (~394 ft) for band 6 (Thermal). Landsat 7 employs the Enhanced Thematic Mapper Plus (ETM+) and collects spectral data across the same wavelengths as the TM sensor, and has an added panchromatic band with a spatial resolution of 15 meters. Also, the thermal band (band 6) on the ETM+ sensor has a spatial resolution of 60 meters (~197 ft). Both sensors provide an approximate image size of 115 by 105 miles (185 by 170 km).

METRIC can only estimate ET in satellite imagery free of major atmospheric disturbances such as clouds, jet contrails and smoke and cloud shadows. The major image selection criteria were therefore based on whether 1) the irrigated agricultural areas along the South Platte River and

along Pumpkin Creek were relatively cloud free, and, of secondary importance, that 2) rangeland areas within the NRDs were free from clouds. Most imagery had some degree of cloud cover.

It was previously noted by Trezza and Allen (2008) that the thermal band (band 6) of L1T terrain-corrected Landsat 5 images processed by EROS using the NLAPS preprocessing system during the 2007 to 2009 period was typically shifted 60 m in the southerly direction relative to the visible and near-infrared bands. The shift was found to be consistent throughout the image. It is important that the pixels of all bands in the Landsat image 'line up' in order to perform a correct solution to the surface energy balance during the METRIC process. Therefore, prior to METRIC processing, images were screened and the shift corrected. The shift and its remedy are described in Appendix C. The shifting procedure is no longer needed with post Jan. 2010 images obtained from EROS due to their use of an updated process.

Gap-filling of Landsat 7 ETM+ due to the failure of the Scan Line Corrector (SLC)

On May 31, 2003, image data from the ETM+ sensor onboard the Landsat 7 satellite began exhibiting "striping" artifacts (USGS, 2008). It was determined that the problem was a result of the failure of the Scan Line Corrector (SLC) which compensates for the forward motion of the satellite. The post-SLC failure images of Landsat 7 are termed as SLC-off images. Due to the SLC failure, about 22% of the scene area is missing in SLC-off images. Processing of SLC-off images for 2005 required replacing the missing data. Various approaches are used for filling the missing data. Some of these approaches use data from the previously acquired images to replace the missing pixels. However, this approach is not very useful for agricultural applications due to temporal dynamics. Because Landsat 7 was still able to acquire imagery, the USGS developed new image products to fix the striping problem by combining two separate dates or by interpolation to fill in the data gaps.

We carried out our own correction to the scan line correction for Landsat7 datasets by using convolution filtering (nearest neighborhood method) with a 5X5 pixels majority function (Singh et al , 2008; Sing and Irmak, 2009). In our application, we have used the approach of gap filling utilizing same time images with spectral information from the neighboring pixels. For this, the convolution filtering algorithm with majority function has been used to replace the missing data. The majority function is preferred due to our overall objective of estimating ET from the agricultural fields. This technique works well for the inner missing lines. However, the missing pixels at the edges of the image scene are not well represented due to large gaps.

Digital Elevation Model

A digital elevation model (DEM), a map of the surface topography, is required input for METRIC. A DEM is used for the calculation of DEM-corrected surface temperature, determination of hot and cold pixel elevations, and the calculation of air density for use in sensible heat estimation. A DEM of the study area was obtained from the EROS Data Center Seamless Data Distribution System (<http://seamless.usgs.gov>). The DEM data has a spatial resolution of 30 meters and was reprojected to UTM13, NAD 83. The data distribution system has a limit on the areal extent. Generally, more than one DEM image is required to cover a study area. Because of this, the DEM files were mosaicked, or stitched, together in order to provide a single, seamless dataset that encompassed the entire Nebraska Panhandle study area.

Land Use Data

A land use map was used for the parameterization and estimation of the aerodynamic roughness parameter and soil heat flux in the METRIC model. A composite land use map was generated by combining (1) the 1991-1993 Nebraska Gap Analysis Program (GAP), (2) the 1997, 2001, or 2005 Nebraska Cooperative Hydrology Study (COHYST), and (3) the 2001 National Land Cover Dataset (NLCD). Three land use maps were created for the Nebraska Panhandle by University of Nebraska: 1997, 2001, and 2005. These maps correspond to the years the COHYST land use maps were generated. The land use maps were reprojected into NAD 83 GRS 1980 UTM 13 using nearest neighbor resampling.

For areas within the Nebraska state boundary, the Nebraska GAP map was used for non-agricultural classes and a COHYST map was used for agricultural classes. For areas outside of Nebraska, the 2001 NLCD map was used. The COHYST data extends across the Nebraska border by 2 miles.

Due to the different land use systems having the same values for different classes, NE GAP and NE COHYST values were reclassified. For the GAP data, a value of 100 was added to each class. For the COHYST data, a value of 120 was added to each class. Values for non-agricultural classes in the COHYST data were then reclassified to zero. The 2001 land use data, used for input to ET estimation for 2002, was considered acceptable because for agricultural areas, the surface roughness parameter is a function of LAI not specific crop type.

By combining the classification strengths of both maps, the surface roughness estimation was improved. The focus of the land cover classes differs between the two maps. The classification classes of the Nebraska Land Use Map describe in detail crop types within agricultural areas,

whereas, the classification classes of the Nebraska GAP map describe in more detail forested/woodland, prairie/rangeland, and riparian areas

Due to the different land cover systems having the same values for different classes, the Nebraska GAP and Nebraska Land Use values were reclassified. A value of 100 was added to the GAP data and a value of 120 was added to the Nebraska Land Use data. Pixels of non-agricultural classes were removed from the Nebraska Land Use Map and replaced with the geographically corresponding pixels from the Nebraska GAP map. A value of 100 was used in order to account for class values (1-99) from National Land Cover Dataset (NLCD) data.

Calibration of METRIC Model

METRIC version 2.0.4 was applied for UNL processing. This version was released by the University of Idaho in June 2008 (Allen et al., 2008). The primary focus for this project was to generate estimates of ET from agricultural areas. Because of this, METRIC was calibrated with a focus on accurate estimation of ET from agricultural areas. However, because the entire Landsat scenes were processed, efforts were made to minimize uncertainty in ET estimates from other land cover types present within the imagery, including forests, riparian vegetation, and rangeland.

Refinements to METRIC during this work

To better account for impacts of local precipitation events and image cloudiness in the study area on the final ET estimates, new methods were developed and implemented, especially during integration of ET between satellite images, to account for conditions that deviate from the description of the standard Level 1 METRIC model application. Some of these adjustments are referred to as Level 2 processing (Allen et al., 2010).

Improvements to METRIC that were advanced during this study include a new cloud gap filling procedure for the ET_F estimates that automatically adjusts for background evaporation from recent precipitation, gap filling of NDVI, the generation of grids of precipitation and ET_r used to estimate distributed bare soil evaporation that is, in turn, used to adjust the satellite date ET estimates for background evaporation. In addition, UNL collaborated with UI to explore the use of evaporative fraction, EF , rather than ET_F , as the vehicle to extrapolate from the instantaneous, at-satellite overpass time ET estimates to daily values for rangeland portions of scenes. These new developments and their applications are described in Appendix E

Calibration Philosophy

The METRIC model calculates actual ET by utilizing satellite images containing both short wave and thermal bands. The model ignores minor energy components and considers only vertical fluxes (horizontal advective flux is not explicitly included, but regional advection is considered via negative values for H) to estimate LE as a residual in the EB equation (Fig.9). The sensible heat (H) for each pixel of an image is estimated at each pixel and equation (1) is used to find LE. Values for H are calculated across an image according to the surface temperature (T_s). This is done using a “dT vs. T_s ” function. The dT can be estimated as a linear function of surface temperature (Bastiaanssen et al., 1998). dT is the difference between the air temperature very near the surface, at 0.1 m above the zero plane displacement height, d, and the air temperature at 2 m above the zero plane displacement height.

The linear equation for dT vs. T_s in METRIC is developed by using the dT values for the cold and hot pixels which provide internal and automatic calibration. In addition, internal calibration of the EB utilizes ground-based reference ET (ET_r) to tie-down the derived EB (Allen et al., 2007a, b). Therefore, use of quality controlled hourly- ET_r is important to improve accuracy of daily and longer period ET estimates.

In METRIC, cold and hot pixels should be located near the weather station (~within 50 km). The cold pixel is used to define the amount of ET occurring from the well-watered and fully vegetated areas of the image which represent instances where the maximum (or near maximum) amount of available energy is being consumed by evaporation. For this study, we selected a number of cold pixel candidates for each image representing an agricultural area under center pivot irrigation system that has vegetation at full cover (LAI is usually greater than $4.0 \text{ m}^2 \text{ m}^{-2}$) to estimate ET at the cold pixel. We assumed that $ET = 1.05 ET_r$ at the cold pixel. The ET_r is the rate of ET from the alfalfa reference calculated using the ASCE Standardized Penman-Monteith equation for alfalfa. H for the cold pixel was then calculated as $H = R_n - G - 1.05 ET_r$.

The selection of the hot pixel follows the same procedure as for the cold pixel. The hot pixel should be located in a dry and bare agricultural field where one can assume evaporative flux is 0. We selected the hot pixel candidates with a surface albedo similar to dry and bare fields (0.175-0.2) with very low LAI (usually less than 0.1). In western Nebraska, we found that the hot pixels could not be assumed to have zero evaporation because of high variability of rain in the region that tended to supply some residual evaporation over extended periods. Therefore, H was estimated as $R_n - G - ET_{\text{bare soil}}$, where $ET_{\text{bare soil}}$ was obtained by running a daily soil water balance model of the surface soil using ground-based weather measurements (Allen et al., 1998). The METRIC model was then run for each of the cold and hot pixel candidates. The best suitable anchor pixels were determined based on the distribution of ET_r/F over the image. For

instance, ET_r/F of well-irrigated and fully vegetated agricultural crops should have an ET_r/F of 1.0, on average. The $ET_r/F = 1.0$ represents a crop coefficient $K_c = 1.0$ when the alfalfa reference ET is used.

Special Calibration Cases

For the April 6, 2002 and the April 13, 2005 images, we were unable to locate fields with full vegetation cover for the cold pixel due to immature development of vegetation. Because of this, the ET_r/F value assigned to the cold pixel was expected to be lower than that for the alfalfa reference ET_r/F value of 1.05. ET_r/F for the cold pixel on these two dates was calculated using the relationship between ET_r/F and the normalized difference vegetation index (NDVI) as: $ET_{r/cold} = 1.25 * NDVI$ (Tasumi et al., 2005; Burnett, 2007). NDVI generally ranges from 0.1-0.2 for bare soil to 0.75-0.85 for full vegetation cover.

The hot pixel is generally considered to be a dry, bare soil having no residual evaporation (i.e. $ET_r/F=0$). This is generally true if there have been no precipitation events for several weeks prior to the image overpass date. In the case where there have been recent precipitation events, the soil may not be dry and there will likely be some residual evaporation from the soil that must be accounted for during calibration of energy balance parameters and processing of ET for satellite images. In addition, there can often be residual evaporation from tilled agricultural soils that have substantial water storage at depth, in these situations, an $ET_r/F=0.05$ to 0.10 may be appropriate.

Daily Soil Water Balance Model to check METRIC calibration

A daily soil water balance model was applied for 2002 and 2005 using precipitation and ET_r from the Sidney and Scottsbluff AWDN stations. The model is based on the two-stage daily soil evaporation model of the United Nations Food and Agriculture Organization's Irrigation and Drainage Paper 56 (Allen et al., 1998). The soil water balance is a 'slab' model, where the soil is assumed to dry uniformly. The results from the soil water balance were used to determine ET_r/F for hot pixel selection, an internal calibration step for running METRIC. An example of soil water balance simulations for the top 0.125 meter of soil based on soil properties and meteorological data from Scottsbluff is shown in Figure 1.

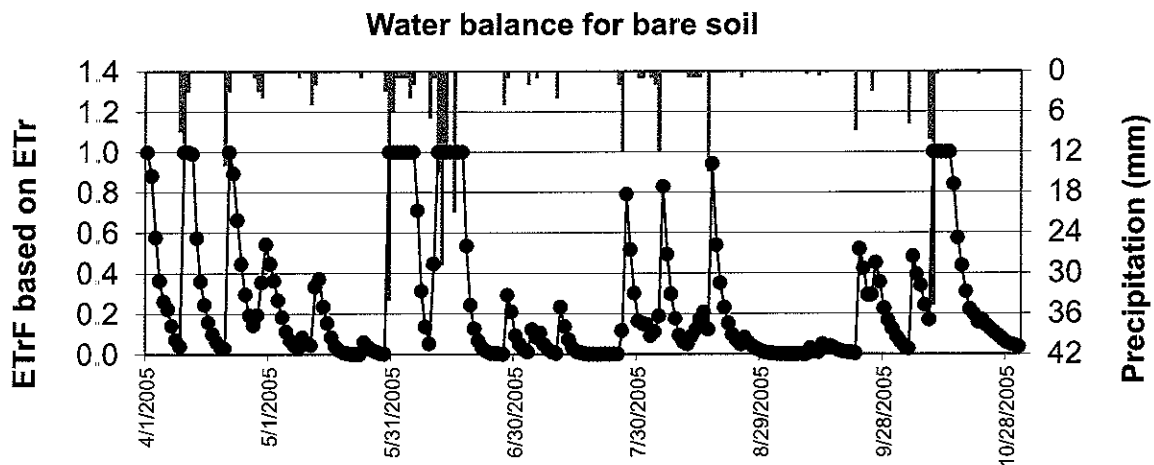


Figure 1. Daily ET_r/F determined from a daily soil water balance for the upper 0-125 m of soil as calculated from meteorological data from Scottsbluff, NE for 2005

The October 14 2005 image and the May 31 2005 image fell immediately after substantial rainfall was recorded at the Scottsbluff weather station. As a consequence, the soil water content for all bare fields around Scottsbluff were near to or exceeding field capacity, and the ET_r/F value predicted by the soil water balance, for the hot pixel, was near 1 leaving a narrow span in ET_r/F values for the calibration.

As a means to verify the calibration of the hot pixel in METRIC, based on the Scottsbluff soil water balance, the soil water balance model was also set up using meteorological information from the Alliance North weather station, which is about 50 km NE of Scottsbluff, and where the water holding capacity of the soil is lower (due to sandy soils) compared to Scottsbluff. When rainfall timing and magnitudes are different between the two locations, similarity between estimated ET_r/F by METRIC at Alliance, using a calibration based on Scottsbluff, and the evaporation model estimate for Alliance provides good indication of appropriate calibration and estimation over the image.

During the drying cycle after a wetting event, a typical bare agricultural soil can be expected to continue to evaporate at a small rate beyond the first several weeks due to diffusion of liquid water and vapor from beneath the upper soil layer. This evaporation can continue at very low rates for several additional weeks, provided no new wetting events occur, especially from tilled soils that have a moderate amount of water stored within the soil profile. This is typical of agriculture. Because wetting events greater than a few millimeters generally occurred every 3-4 weeks in the study area, a minimum ET_r/F value of 0.05 was generally used to estimate the minimum rate of evaporation from bare soil conditions, representing agricultural fields, and selected as the hot calibration pixels for all image dates (desert and range soils having low water profiles are expected to go lower than the $ET_r/F=0.05$ residual). If the soil water balance

suggested a higher ET_{rF} value for bare soil than the residual evaporation rate of 0.05, the higher value was used as shown in Equation 10:

$$ET_{rF_{\text{bare soil for the hot pixel}}} = \text{Maximum}(\text{Soil water balance model estimate}, 0.05) \quad (10)$$

Exceptions from Eq. 10 were for the April 13 2002, May 8 2002, May 15 2002, May 31 2002, June 8 2002, July 27 2002, July 2 2005, and July 10 2005 image dates, where only trace amounts of precipitation had been recorded in the prior weeks. As a consequence, the ET_{rF} value was set to below 0.05 (Allen et al. 2010). Table 2 lists the ET_{rF} assigned to and location of the hot and cold pixels for the image dates

Model calibration exceptions

Desert and range soils typically run ‘hotter’ in terms of surface temperature than bare agricultural soils. Reasons for this include effects of organic mulches, shielding of the soil surface by sparse live or dead vegetation, delamination of soil crusts, and increased soil porosity caused by animals and roots that is common to these land uses, but not to bare agricultural soils. To prevent the higher temperatures in desert and range from overestimating the near surface air temperature gradient (dT) and thus H, thereby causing ET from the energy balance to even go negative at times, adjustments were made to the dT estimation and estimation of soil heat flux when surface temperature exceeded a threshold temperature. On all image dates the soil heat flux and the slope of the dT function were reduced for those pixels where the surface temperature exceeded the surface temperature of a dry agricultural pixel as described by Allen et al. (2008). Usually the slope of the dT function was reduced to ¼ of the primary slope when surface temperature exceeded the surface temperature of the hot pixel by 2 K.

Table 2. ET_{rF} values assigned to and locations (UTM 13 coordinates) for the hot and cold pixels for each image date for both paths 33 and 32.

| | | | | | | |
|-----------|------|------|--------|---------|--------|---------|
| 4/6/2002 | 0.05 | 0.81 | 644879 | 4570781 | 599268 | 4647657 |
| 4/13/2002 | 0.04 | 1.05 | 600780 | 4635632 | 599268 | 4647657 |
| 5/8/2002 | 0.03 | 1.05 | 638669 | 4582681 | 599268 | 4647657 |
| 5/15/2002 | 0.01 | 1.05 | 587376 | 4652422 | 599268 | 4647657 |
| 5/31/2002 | 0.0 | 1.05 | 591948 | 4652193 | 599268 | 4647657 |
| 6/8/2002 | 0.02 | 1.05 | 649253 | 4605553 | 604714 | 4651698 |
| 6/9/2002 | 0.05 | 1.05 | 656608 | 4571126 | 599268 | 4647657 |
| 7/3/2002 | 0.05 | 1.05 | 701598 | 4588119 | 669269 | 4603659 |
| 7/18/2002 | 0.05 | 1.05 | 597383 | 4647432 | 599268 | 4647657 |
| 7/27/2002 | 0.03 | 1.05 | 666893 | 4571221 | 599268 | 4647657 |
| 8/11/2002 | 0.05 | 1.05 | 639973 | 4653580 | 599117 | 4657378 |

| | | | | | | |
|-------------------|------|------|--------|---------|--------|---------|
| 8/19/2002 | 0.05 | 1.05 | 630700 | 4615428 | 599268 | 4647657 |
| 9/4/2002 | 0.2 | 1.05 | 586919 | 4629000 | 599268 | 4647657 |
| 9/5/2002 | 0.07 | 1.05 | 679618 | 4577906 | 599268 | 4647657 |
| 9/20/2002 | 0.1 | 1.05 | 617630 | 4621601 | 599268 | 4647657 |
| 10/7/2002 | 0.27 | 1.05 | 669682 | 4661235 | 646871 | 4623297 |
| 10/14/2002 | 0.05 | 1.05 | 664983 | 4653061 | 599268 | 4647657 |
| 4/13/2005 | 0.56 | 0.9 | 630025 | 4634084 | 604162 | 4650847 |
| 5/15/2005 | 0.16 | 1.05 | 592026 | 4644543 | 599626 | 4639209 |
| 5/31/2005 | 0.8 | 1.05 | 590465 | 4611526 | 603468 | 4650962 |
| 7/2/2005 | 0.02 | 1.05 | 563725 | 4636852 | 645988 | 4624826 |
| 7/10/2005 | 0.02 | 1.05 | 646826 | 4644988 | 671345 | 4658844 |
| 8/19/2005 | 0.13 | 1.05 | 592962 | 4611389 | 671585 | 4665450 |
| 8/28/2005 | 0.05 | 1.05 | 669747 | 4693056 | 649524 | 4629756 |
| 9/20/2005 | 0.05 | 1.05 | 588149 | 4621849 | 615956 | 4629056 |
| 10/14/2005 | 0.8 | 1.05 | 597298 | 4643009 | 643232 | 4683576 |

A surface temperature lapse rate is used during the METRIC process to normalize the surface temperature image for changes in temperature caused by normal lapse effects associated with elevation changes within the image. This normalization is needed in any energy balance process before estimating near surface air temperature gradients and the associated sensible heat flux (Allen et al., 2007a). A lapse rate of 6.5 K/km elevation change was used for all images. However, this lapse rate can be custom fitted to an image when the range in surface temperatures across an image varies for the same evaporative conditions (wet or dry).

RESULTS

Reference Evapotranspiration

Traditionally, reference evapotranspiration used for estimating ET_c has been based either on grass (ET_o) or alfalfa (ET_r) reference surfaces (ASCE-EWRI 2005). Since ET_r or ET_o represents the evaporative demand of the atmosphere, it is highly dependent upon the spatial variability of the climatic parameters. The ET_r values for each of the weather station under the study area were estimated using the standardized American Society of Civil Engineers Penman-Monteith (ASCE-PM) equation (ASCE-EWRI 2005) on an hourly time step. Hourly time steps are needed to produce ET_r for calibration of the METRIC energy balance estimation process at the time of the Landsat overpasses. The hourly ET_r values are summed to daily totals to provide a basis for producing daily and monthly ET.

We used the RefET software (version 3) of the University of Idaho (Allen, 2008). Automatic weather station (AWS) data, obtained from the High Plain Regional Climate Center (HPRCC), were used for ET_r calculations. The datasets measured at the stations included daily maximum and minimum temperature (T_{max} and T_{min}), relative humidity (RH), wind speed (u), and solar radiation (R_s). Since estimates of ET_{ref} can only be as good as the weather data quality, a rigorous data quality check was carried out on the climatic data. The details of data quality check are described in Appendix A.

Daily (24-h) ET_r totals for the processed Landsat 5 and Landsat 7 image dates are listed in Table 3. When the $ET_{r,F}$ images were interpolated over time to create monthly ET images, daily $ET_{r,F}$ was determined by spline and multiplied by daily ET_r . During the interpolation process, daily ET_r 'surfaces' were created over the image area, as described in Appendix A, using HPRCC and NWS COOP weather stations from within and outside the image footprint.

Daily Fraction of Reference Evapotranspiration(Relative ET or Crop Coefficient)

$ET_{r,F}$ maps were generated from Landsat 5 and Landsat 7 satellite imagery. Each satellite image for 2002 and 2005 was processed on a pixel by pixel basis using METRIC to estimate land surface energy balance fluxes. Meteorological data used for the model inputs came from the respective AWDN weather stations. Maps of reflectance of short wave radiation, vegetation indices (NDVI and LAI), surface temperature, net radiation, and soil heat flux were generated as intermediate products during the METRIC processing.

Table 3. Day of year and calculated alfalfa based ET, ET_r (mm/day) for the satellite image dates.

| Image Date | Day of year | Path | Row | ET _r (mm/day) |
|------------|-------------|------|-----|--------------------------|
| 4/6/2002 | 96 | 32 | 31 | 6.78 ² |
| 5/8/2002 | 128 | 32 | 31 | 8.68 ² |
| 6/9/2002 | 160 | 32 | 31 | 12.99 ² |
| 7/3/2002 | 184 | 32 | 31 | 11.56 ² |
| 7/27/2002 | 208 | 32 | 31 | 12.67 ² |
| 9/5/2002 | 248 | 32 | 31 | 9.67 ² |
| 10/7/2002 | 280 | 32 | 31 | 6.35 ² |
| 8/28/2005 | 240 | 32 | 31 | 6.94 ² |
| 4/13/2002 | 103 | 33 | 31 | 8.51 ¹ |
| 5/15/2002 | 135 | 33 | 31 | 6.97 ¹ |
| 5/31/2002 | 151 | 33 | 31 | 10.05 ¹ |
| 6/8/2002 | 159 | 33 | 31 | 11.29 ¹ |
| 7/18/2002 | 199 | 33 | 31 | 11.31 ¹ |
| 8/11/2002 | 223 | 33 | 31 | 8.73 ¹ |
| 8/19/2002 | 231 | 33 | 31 | 8.59 ¹ |
| 9/4/2002 | 247 | 33 | 31 | 5.80 ¹ |
| 9/20/2002 | 263 | 33 | 31 | 5.60 ¹ |
| 10/14/2002 | 287 | 33 | 31 | 4.78 ¹ |
| 4/13/2005 | 103 | 33 | 31 | 6.06 ¹ |
| 5/15/2005 | 135 | 33 | 31 | 7.53 ¹ |
| 5/31/2005 | 151 | 33 | 31 | 5.20 ¹ |
| 7/2/2005 | 183 | 33 | 31 | 8.88 ¹ |
| 7/10/2005 | 191 | 33 | 31 | 7.45 ¹ |
| 8/19/2005 | 231 | 33 | 31 | 5.75 ¹ |
| 9/20/2005 | 263 | 33 | 31 | 6.44 ¹ |
| 10/14/2005 | 287 | 33 | 31 | 3.50 ¹ |

¹Calculated from Scottsbluff AWDN weather station data; ²Calculated from Sidney AWDN weather station data.

The final output from the METRIC model were images showing instantaneous ET_{r,F} (fraction of alfalfa based reference ET, ET_r) at the satellite overpass time. The ET_{r,F} is defined as the ratio of instantaneous ET (ET_{inst}) for each pixel to the alfalfa-reference ET calculated using the standardized ASCE Penman-Monteith equation for alfalfa (ET_r) following the procedures given in ASCE-EWRI (2005). The ET_{r,F} serves as a surrogate for K_c (basal crop coefficient) and has been used with 24-hour ET_r in order to estimate the daily ET at each Landsat pixel. The ET_{r,F} values range from 0 to about 1.05. The ET_{r,F} of well-irrigated and fully vegetated agricultural crops usually have an ET_{r,F} of 1.0 on average, while the dry and bare agricultural fields have little

evaporative flux and range from 0 to 0.15 unless there is a recent precipitation event prior to satellite overpass. Daily ET in mm/day was calculated by multiplying ET_rF by daily ET_r values. Procedures for obtaining daily estimates of ET and ET_rF are further explained in Appendix E.

A map sequence of daily ET_rF for an area along the North Platte River between Scottsbluff and Bridgeport (subset of path 33, row 31) for the 4/13/2002, 5/15/2002, 6/8/2002, 7/18/2002, 8/19/2002, 9/4/2002, 9/20/2002 and 10/14/2002 image dates are shown in Figure 2 and 3. Differences in spatial ET_rF and changes over time are apparent. The ET_rF is highly variable in space and time due to variability in land use, soil properties, and management practices. Spatial variation in soil properties affects surface soil evaporation and surface energy balances. This caused within-field and across field variability in ET.

In the April 13 image, most of the area had an ET_rF value of around 0.4-0.5. This is typical in the beginning of the growing season due to cool temperatures and high soil moisture from the previous winter. Higher ET_rF values (0.8-1.0) are apparent along the North Platte River and for some agricultural fields. In the May 15 image, lack of precipitation and warmer temperatures show that most of the fields have a lower ET_rF value than the April 13 image. Peak ET_rF values are evident in the July 18 image. The difference between agricultural fields in the northern part of the image, and rangeland grasses in the southern portion of the image are distinct. The August 19 and September 4 images show agricultural fields mostly covered by crops having apparently good vigor. Many fields were evapotranspiring near the reference level ($ET_rF \sim 1.0$). In the September 20 and October 14 images, senescence and harvesting caused lower ET rates for most of the area.

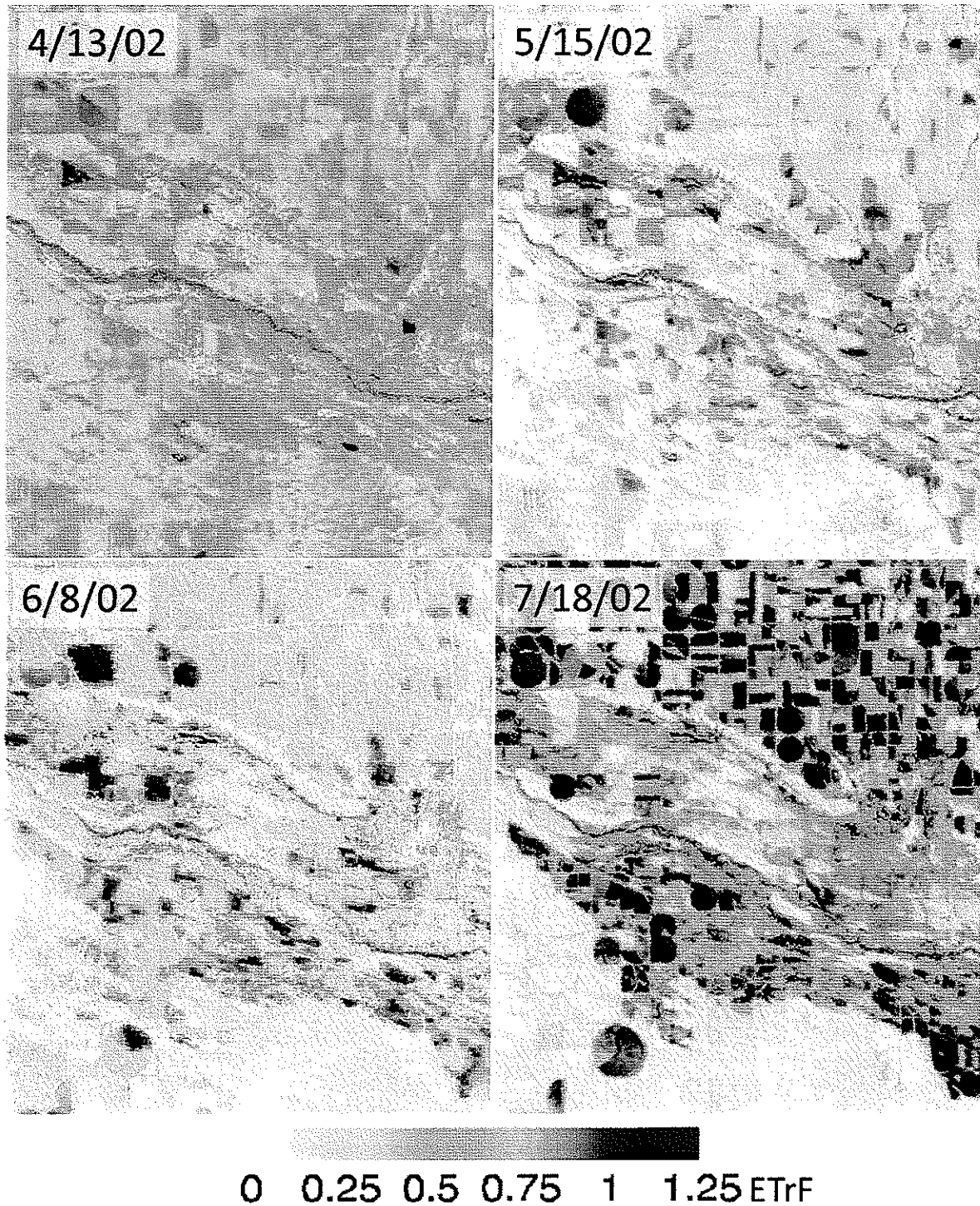


Figure 2. Image series showing the spatial distribution of daily METRIC ET,F for an area along the North Platte River between Scottsbluff and Bridgeport during the 2002 growing season

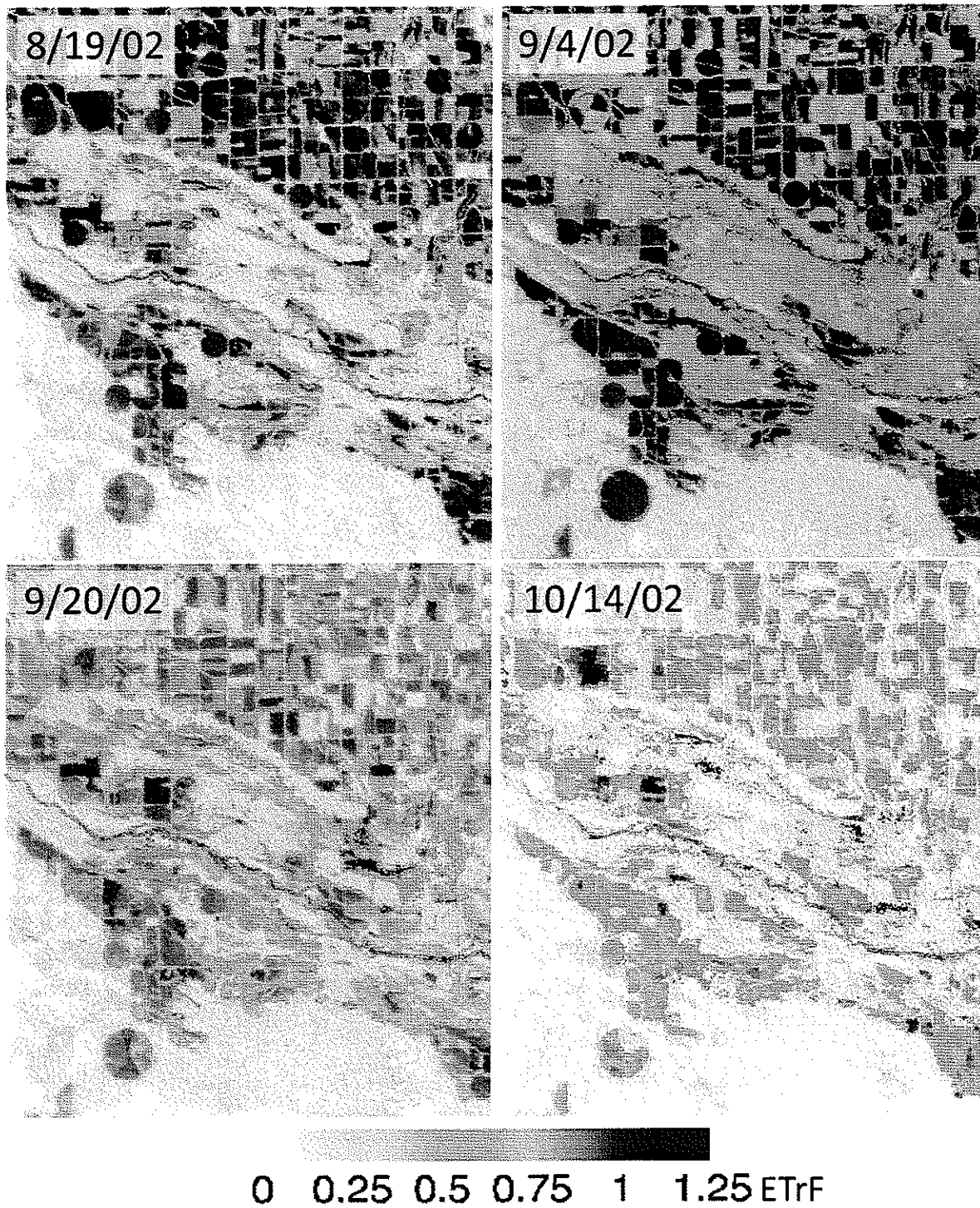


Figure 3 Image series showing the spatial distribution of daily METRIC ET_rF for an area along the North Platte River between Scottsbluff and Bridgeport during the 2002 growing season

Treatment of Cloud Cover

Evapotranspiration cannot be directly estimated for cloud covered land surfaces. Before ET_{rF} images could be used in the generation of monthly and seasonal ET maps for 2002 and 2005, the clouded areas were manually identified, masked out, and then filled in by interpolating ET_{rF} information from adjacent images in time as described in Appendix E. It is essential that all satellite imagery be checked for cloud cover and shadows, and be masked out for further processing. Masked out areas must be filled in so that further image processing can be uniformly applied to the study area. Figure 4 shows the before, masked out, and after cloud filling results for July 10, 2005 from path 33 row 31.

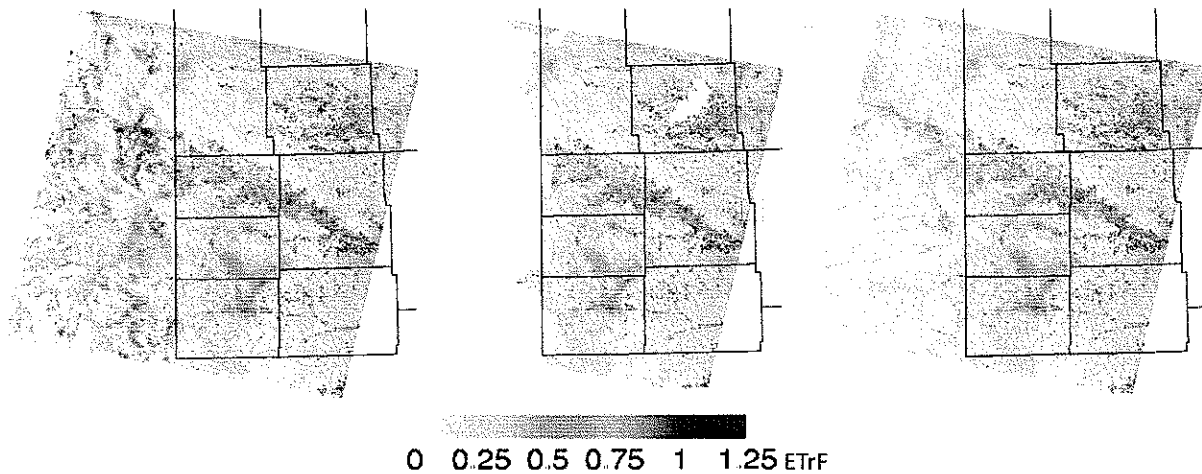


Figure 4 Sequence showing cloud filling process for July 10, 2005. The left image shows the cloud contamination (high ET_{rF} values and white areas) near the left edge of the image. The center image shows the area that was masked out in white (left part of image and area near top right corner). The right image shows the filled-in cloud area carried out using the cloud filling method.

Adjustment of ET_{rF} for Background Evaporation

Frequently, a Landsat image is processed on a date where previous rainfall has caused the evaporation from bare soil to exceed that for the surrounding monthly period. For our purposes, it is the goal that the final ET image represents the average evaporation conditions for the month. In order to achieve this, the 'background' evaporation of the processed image can be adjusted to better reflect that for the month or other period that it is to represent. This adjustment removes impacts of wetting events that occurred immediately prior to the image date and then adds back in background evaporation that is similar to the average evaporation expected for the averaging period. This period is identified as the time period that is halfway between other adjacent images. The outcome of this adjustment will be to preserve any significant evaporation stemming from irrigation and any transpiration stemming from vegetation, but with adjustment to evaporation stemming from precipitation from that on the

image date to that of the surrounding time period. This adjustment process is further discussed in Appendix E.

Monthly and Seasonal ET_r F and ET

In order to produce monthly and seasonal ET maps, individual ET_r F maps generated from METRIC were interpolated using a cubic spline model. Values of ET_r F for each day were multiplied by the corresponding ET_r data for that day and then integrated over the target month. The spline model is a deterministic interpolation method which fits a mathematical function through data points to create a surface (Hartkamp, 1999). The spline surface was achieved through weights (λ_i) and number of points (N). A regularized spline was used because this method results in a smoother surface. Using the spline interpolation of daily ET maps, monthly ET maps were generated for Landsat path 33, row 31 for 2005 and Landsat paths 32-33, row 31 for 2002.

Figures 5 through 8 show the progression of ET from April through October for 2002. Figure 9 shows the seasonal ET (Sum of April 1 through October 31) for 2002. Figures 10 through 13 show the progression of ET from April through October for 2005. Figure 14 shows the seasonal ET (Sum of April 1 through October 31) for 2005. The monthly ET maps generated by the METRIC model showed the progression of ET during the growing season as surface conditions continuously changed. Evapotranspiration in agricultural fields increases gradually from April and May, after crop emergence and growth, through July and August as vegetation starts to transpire at a potential rate for most vegetation surfaces. July is usually the peak ET month with high incoming solar radiation, high temperatures, and large vapor pressure deficit that increase ET. The ET shows variation throughout the North Platte and South Platte NRDs as a function of different ET rates of various land covers. With physiological maturity, leaf aging and senescence, ET starts to decrease gradually in September. With harvest in October, most of the ET in this month represents the soil evaporation component of ET. As shown in monthly ET maps, mapping ET on large scales can provide vital information on the progression of ET for various vegetation surfaces over time. Information gained enables the prediction of the timing and the spatial extent of potential depletions or gains in both the short-term and in the long-term management of surface and ground water used for irrigated systems.

Contrasting ET for 2002 and 2005

Comparison of Figures 9 and 14 for growing season ET for 2002 and 2005 show substantial differences in ET for rangeland and non-irrigated (rainfed) agricultural areas. Rainfed regions around Scottsbluff averaged about 12 inches of ET during April-October 2002, whereas these same areas averaged about 18 inches of ET for 2005. These differences in ET are consistent with precipitation recorded at the Scottsbluff station, as summarized in Table 2, where

recorded rainfall was only 8 inches during 2002 and was 20 inches during 2005. It is recognized that these rainfall totals are for point locations and can contain some error. However, 2002 is known as a dry year and 2005 as a wet year, which is exhibited by the ET images produced during this study.

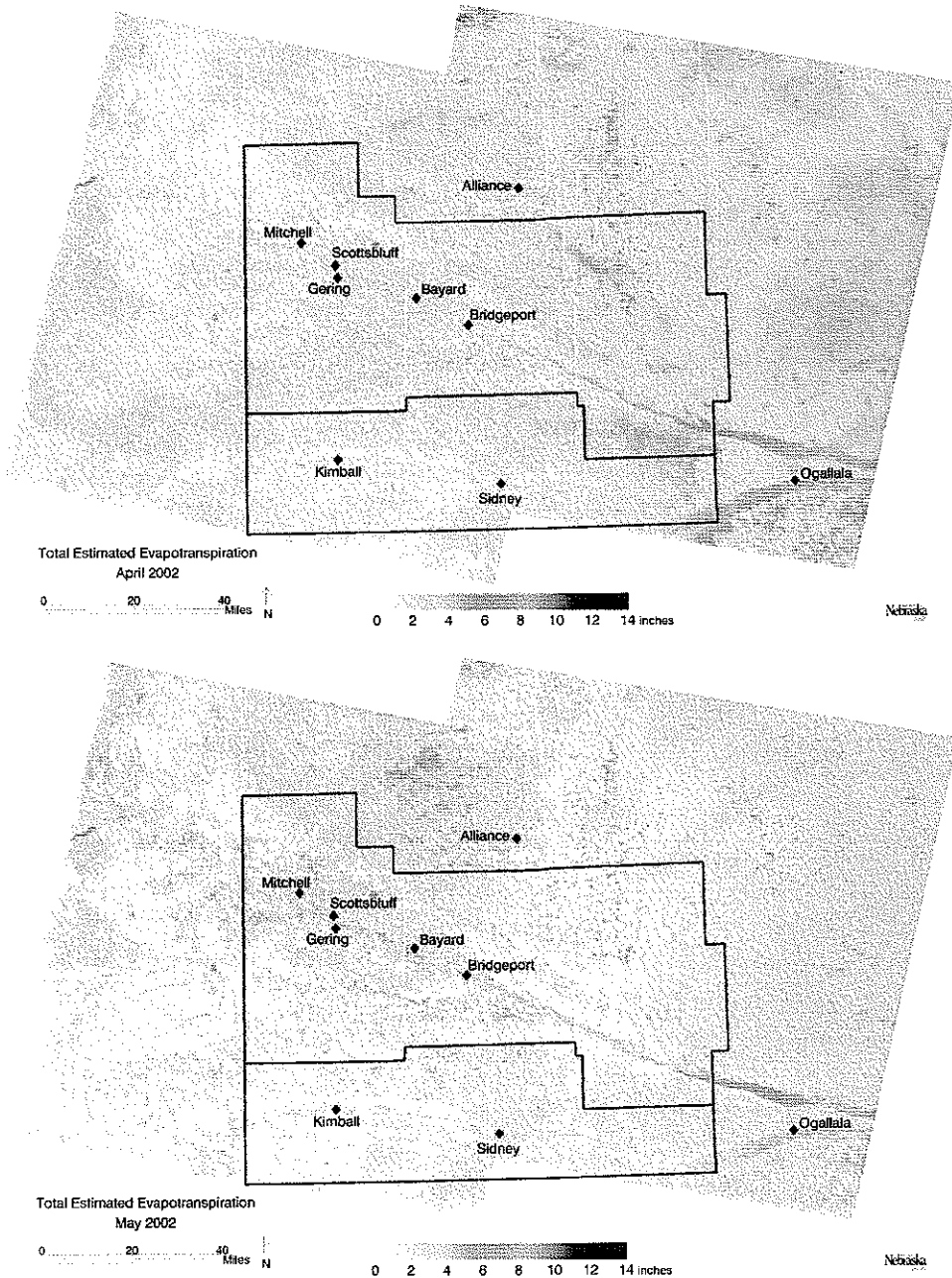


Figure 5. Monthly ET generated from METRIC for Landsat path 32-33, row 31 for 2002. Blue lines indicate North Platte and South Platte boundaries.

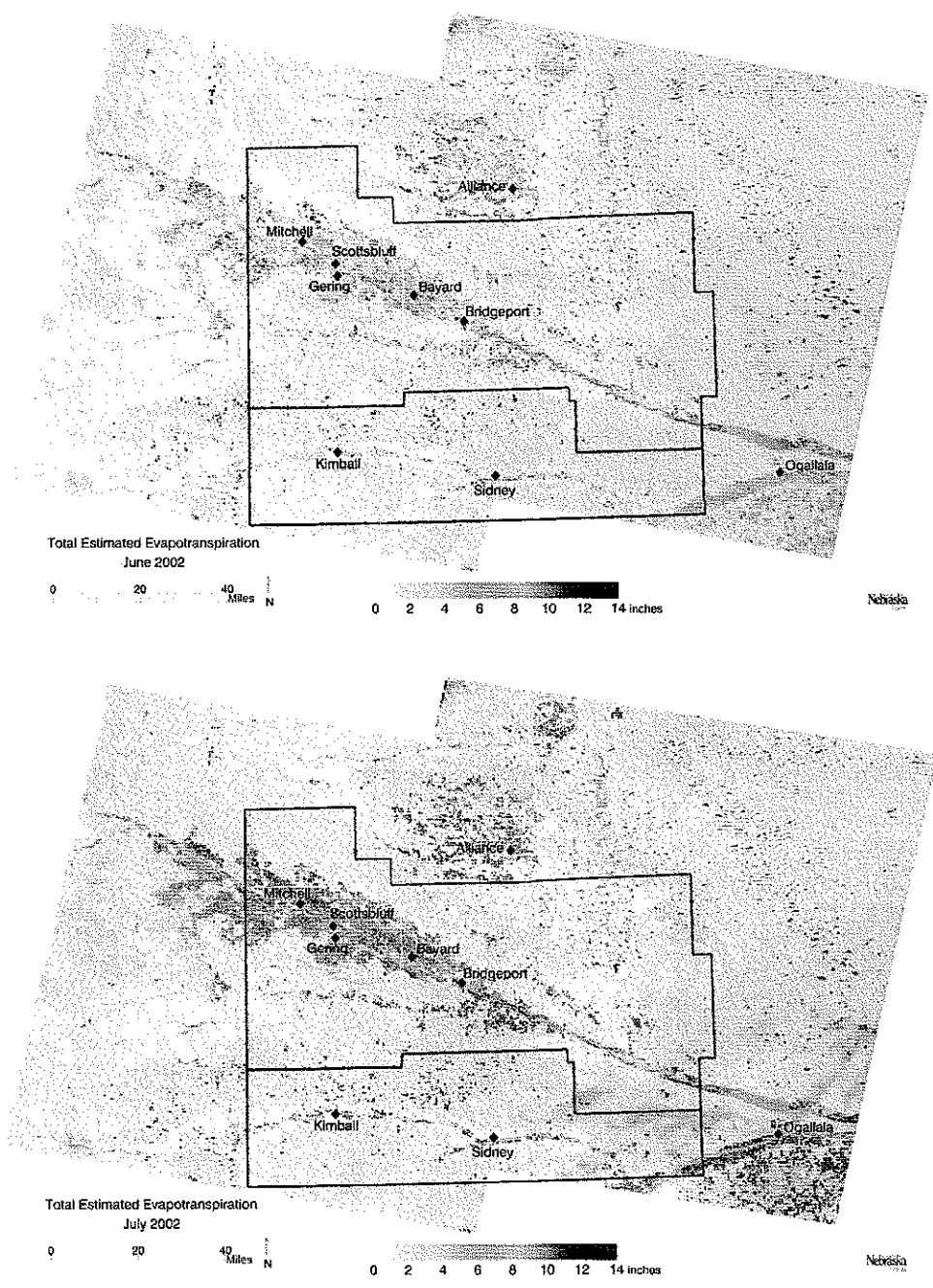


Figure 6. Monthly ET generated from METRIC for Landsat path 32-33, row 31 for 2002. Blue lines indicate North Platte and South Platte boundaries

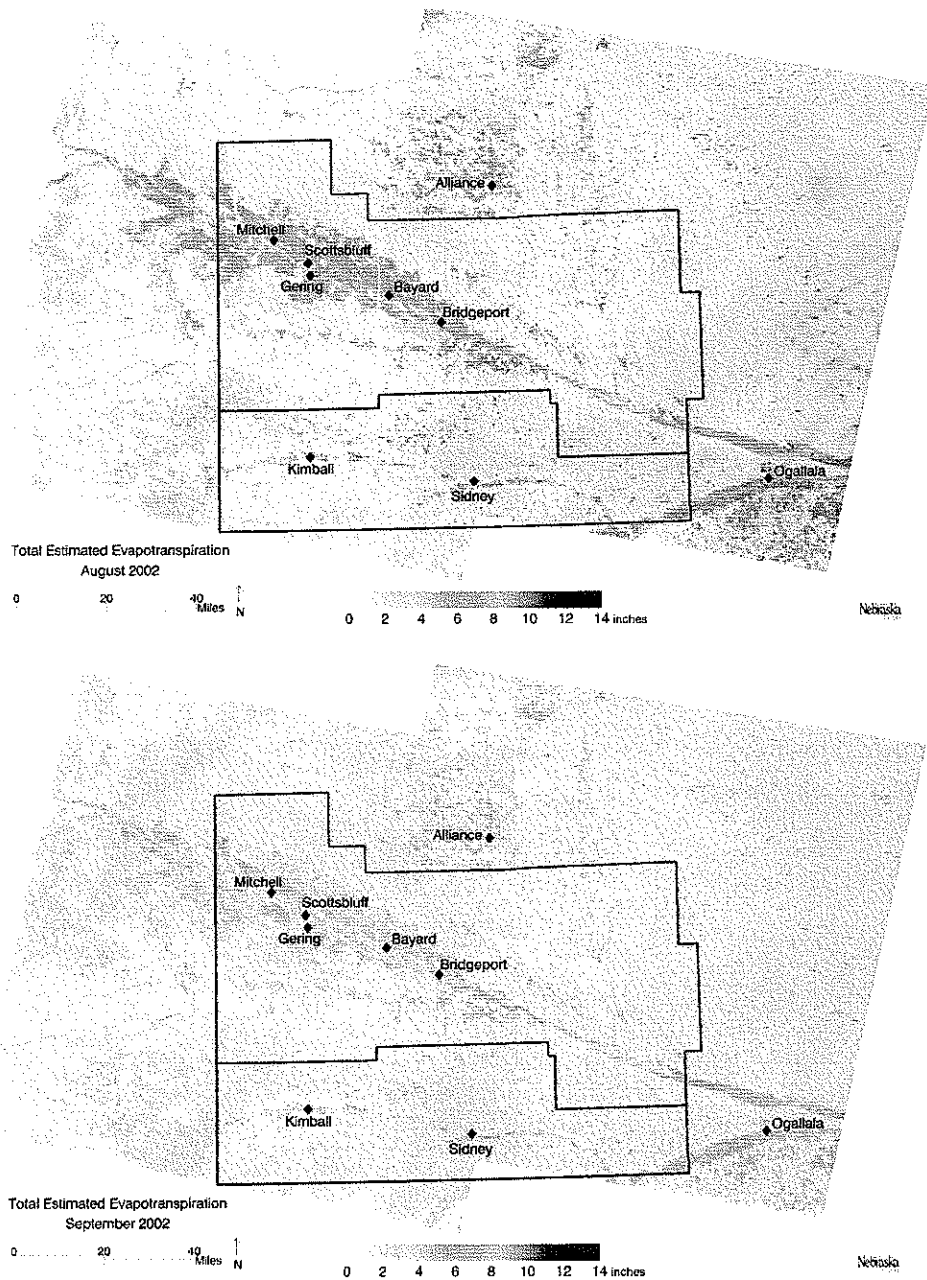


Figure 7. Monthly ET generated from METRIC for Landsat path 32-33, row 31 for 2002. Blue lines indicate North Platte and South Platte boundaries

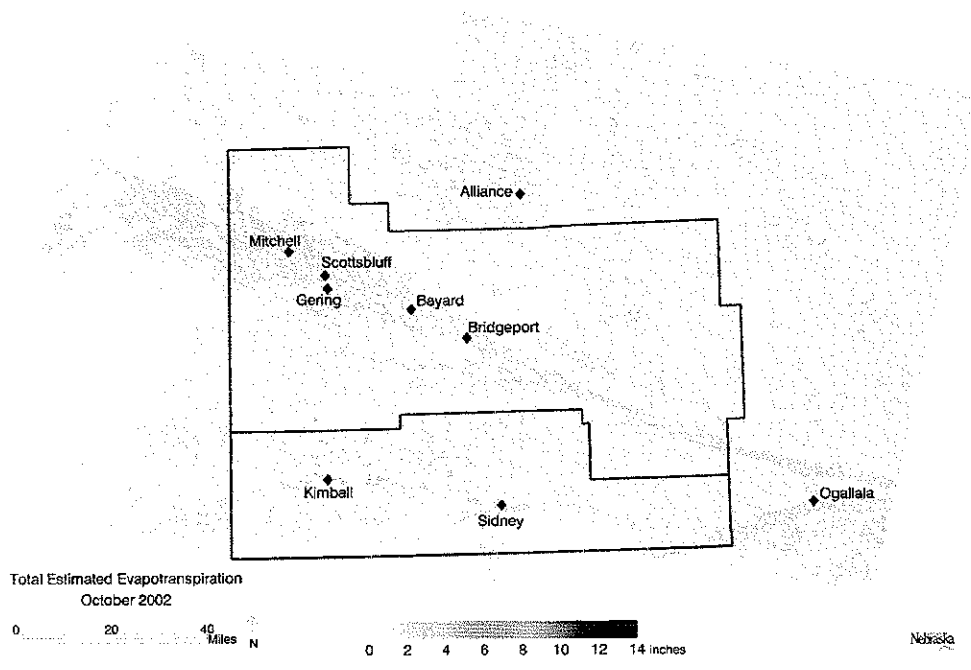


Figure 8. Monthly ET generated from METRIC for Landsat path 32-33, row 31 for 2002. Blue lines indicate North Platte and South Platte boundaries

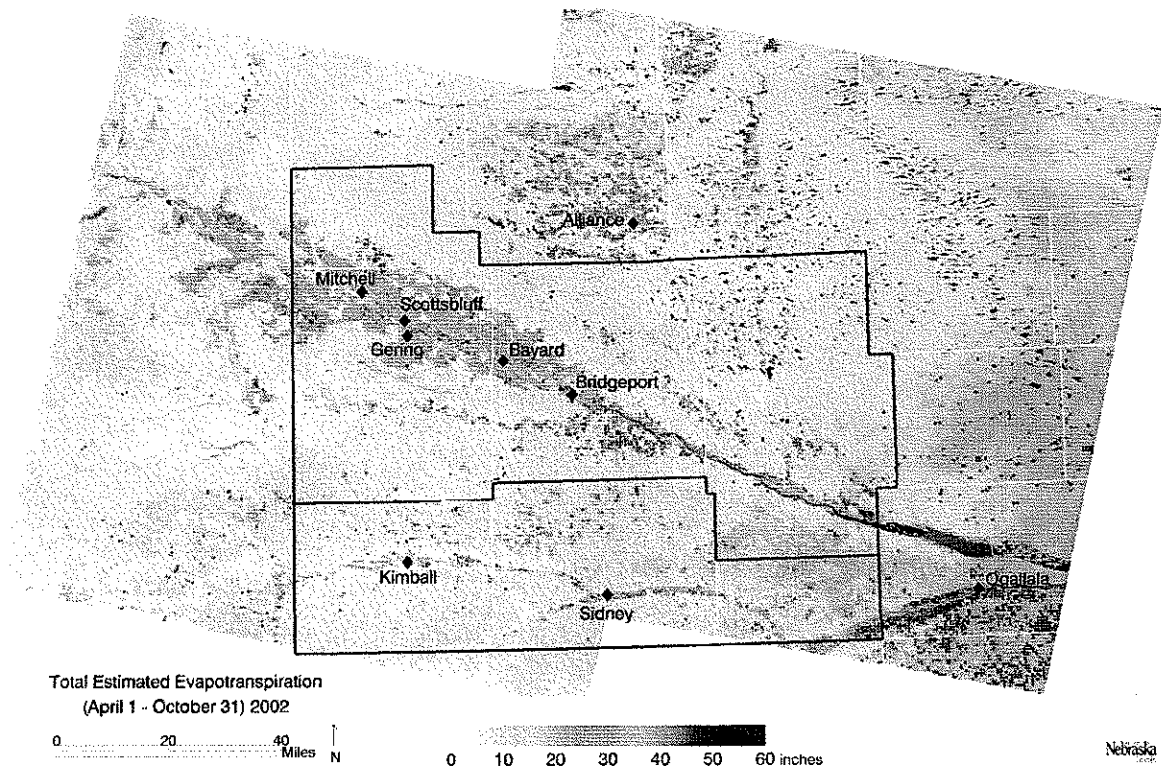


Figure 9. Year 2002 Seasonal ET generated from METRIC for the North Platte and South Platte NRDs. Seasonal ET is the sum of the monthly ET maps (April-October). Blue lines indicate North Platte and South Platte boundaries.

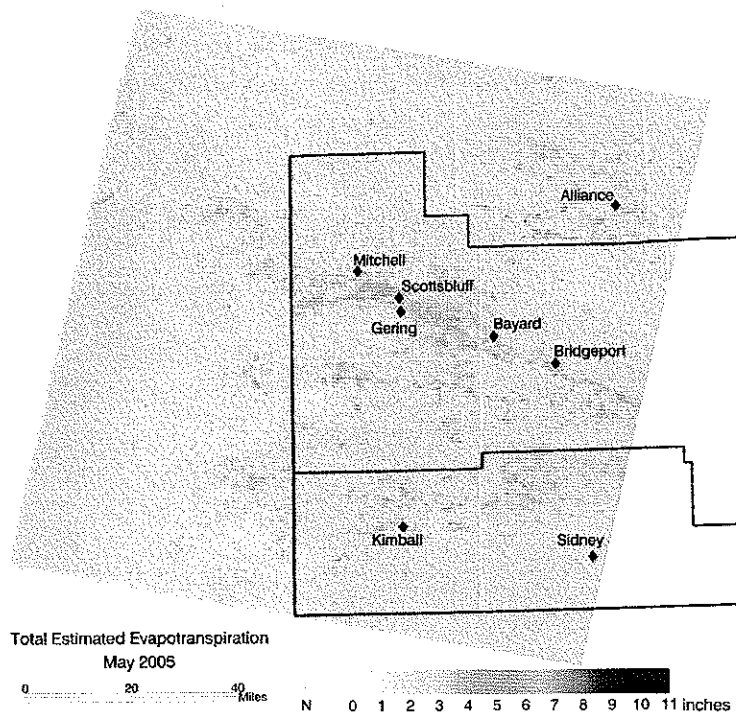
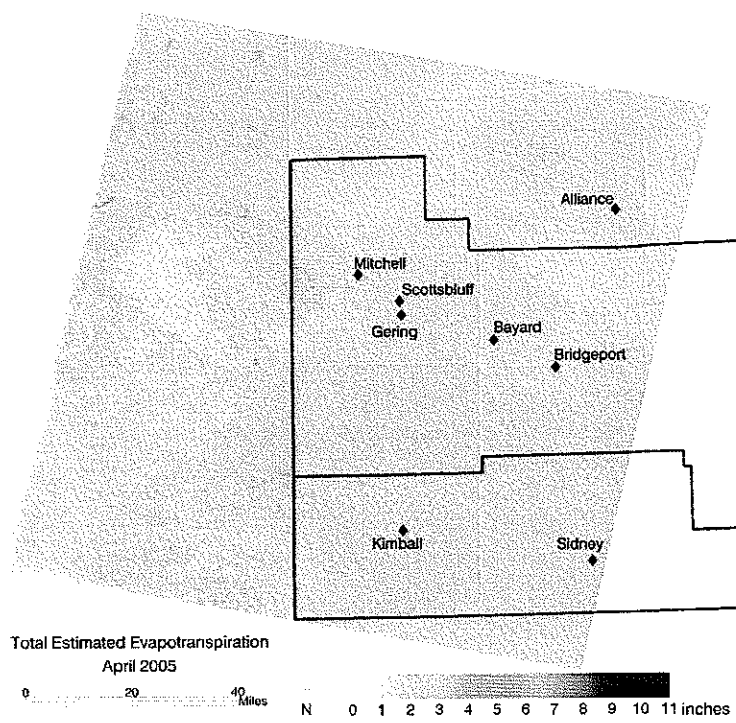


Figure 10 Monthly ET generated from METRIC for Landsat path 33, row 31 for 2005. Blue lines indicate North Platte and South Platte boundaries.

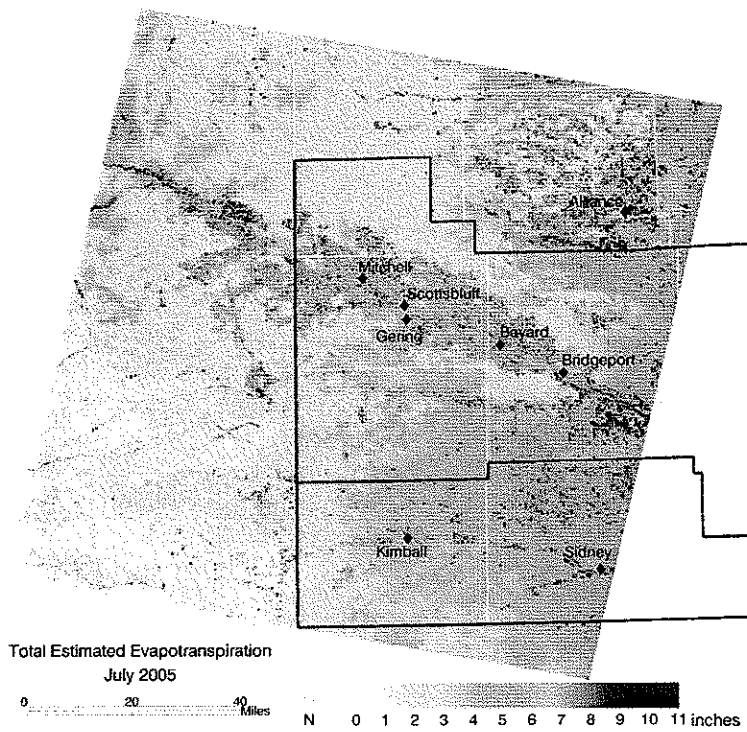
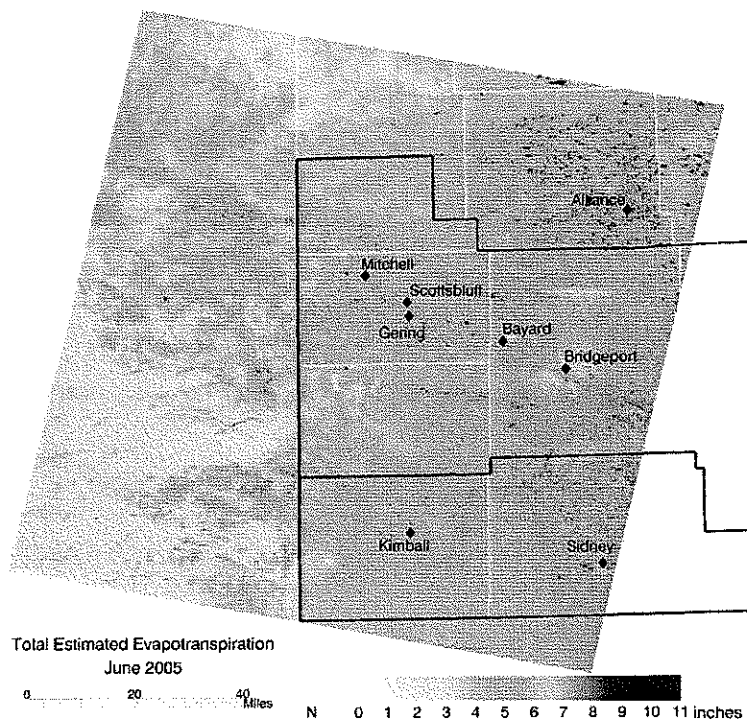


Figure 11 Monthly ET generated from METRIC for Landsat path 33, row 31 for 2005. Blue lines indicate North Platte and South Platte boundaries.

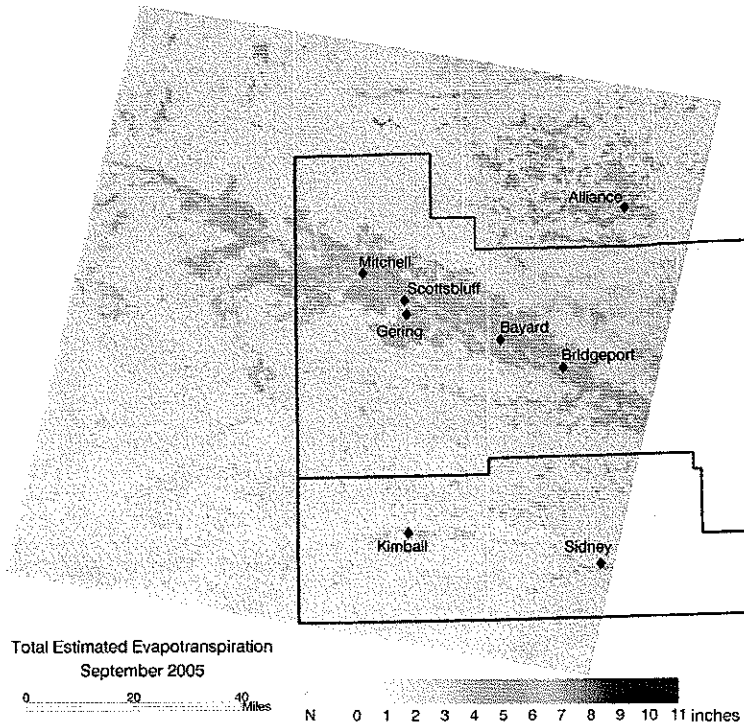
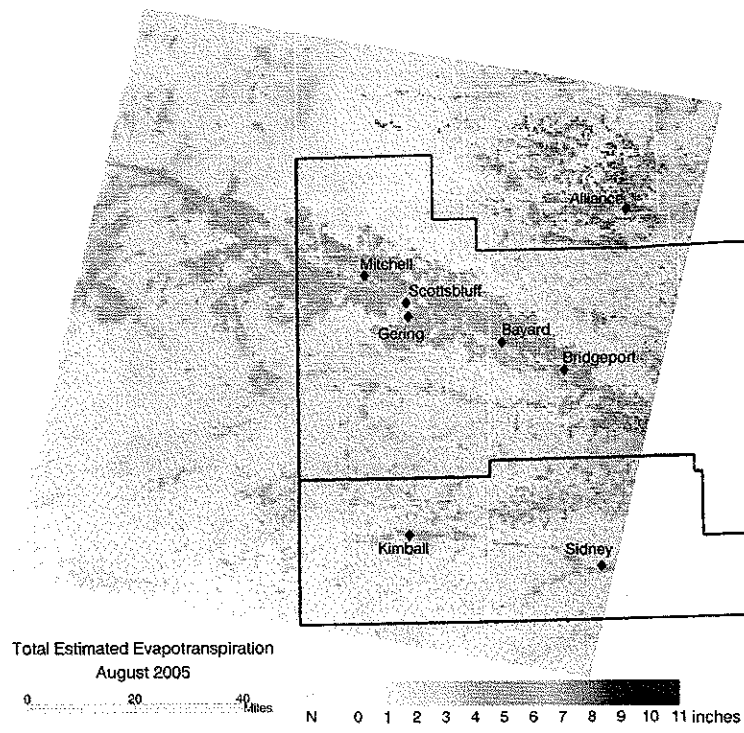


Figure 12 Monthly ET generated from METRIC for Landsat path 33, row 31 for 2005. Blue lines indicate North Platte and South Platte boundaries.

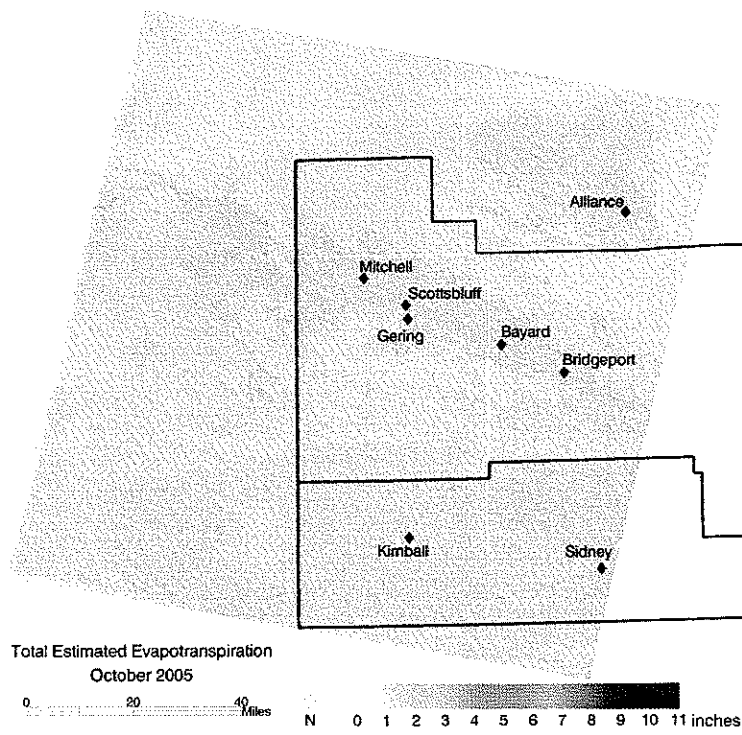


Figure 13. Monthly ET generated from METRIC for Landsat path 33, row 31 for 2005. Blue lines indicate North Platte and South Platte boundaries.

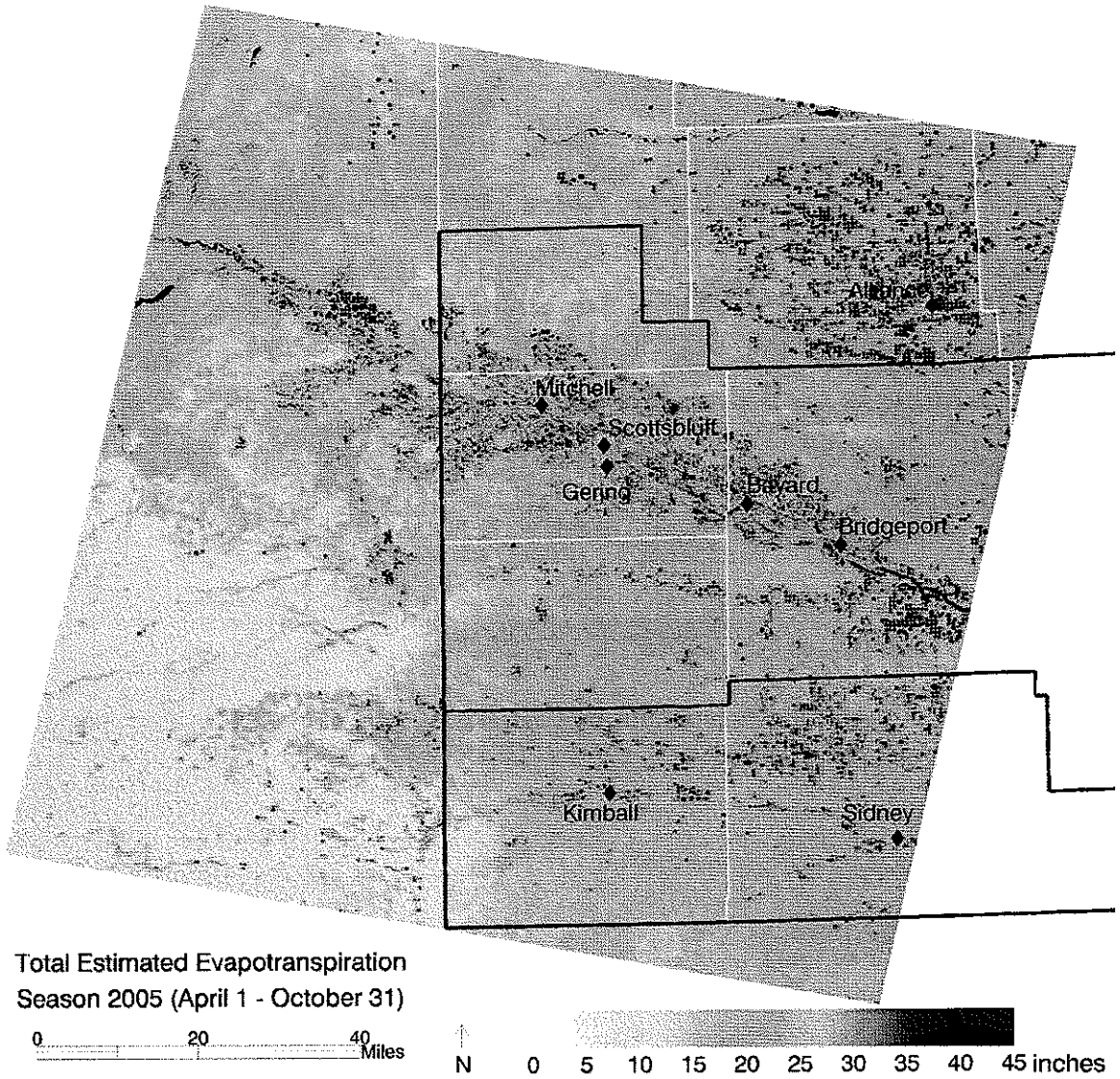


Figure 14 Year 2005 seasonal ET generated from METRIC for the North Platte and South Platte NRDs
 Seasonal ET is the sum of the monthly ET maps (April-October) Blue lines indicate North Platte and South Platte boundaries

Table 5 Annual precipitation at the Scottsbluff HPRCC weather station and an assessment of whether each year is dry, average, or wet relative to the normal annual rainfall of 15-16 inches.

| Year | Annual Precipitation (inches) | Assessment | Notes |
|------|-------------------------------|------------|-----------------------------|
| 1997 | 20 | Wet | High rainfall in April-July |
| 1998 | 17 | Avg. | Rain in April, September |
| 1999 | 17 | Avg. | Rain in April-July |
| 2000 | 15 | Avg. | |
| 2001 | 13 | Avg. | |
| 2002 | 8 | Dry | |
| 2003 | 10 | Dry | |
| 2004 | 12 | Avg. | |
| 2005 | 20 | Wet | Wet April-June |
| 2006 | 12 | Avg. | |

Generation of Synthetic ET Images for Endpoints in the Spline Interpolation for Monthly and Seasonal ET

Estimates of ET produced using METRIC normally use a cubic spline model when interpolating to monthly or seasonal estimates (Allen et al. 2010). Interpolation of ET_rF requires two images before and after the period being interpolated. Typically during the beginning and end of the growing season, two prior or following images may not be available. In general, there are fewer clear sky images available during the months of October to April. Also, differences in surface temperature due to evaporative cooling are very small or the land surface may have snow cover making it very difficult to calibrate METRIC. Because of this, synthetic images of ET_rF were generated for use as endpoints for early April and late October dates in the spline model.

During the early and late periods of the growing season, agricultural fields are typically bare from tillage and seed bed preparation or due to senescence and harvesting. A large portion of ET is therefore evaporation while the transpiration component is small. Therefore, ET during these periods can be approximated using estimations of evaporation from a soil evaporation model (Allen et al. 2010).

For calculation of monthly ET using the spline interpolation, each image date is used to represent ET_rF part way during a period. The effective period represented by a date in essence extends to the halfway point between image dates. Therefore, the synthetic image needs to be representative of the soil evaporation conditions prior to or following the first or last month to be splined. ET_rF from the soil water balance model was therefore averaged over the range

between the date of the first (last) image and the first (last) day of the month. During the spline calculation, the synthetic image was given a date of immediately prior to the first month or immediately after the last month to be splined. A spatial resolution of 90 meters was used for the bare soil water balance model

Evaporation from Water

The METRIC model applied in this study attempts to account for variations among open water bodies, provided the water bodies are classified and partitioning algorithms between water heat storage and net radiation are adjusted accordingly (Allen et al., 2010). The partitioning can change with time of year. Because such classification and description of partitioning were not available for water bodies in the study area, and because the primary project goal was to estimate ET from agricultural crops and not evaporation from open water, the evaporation from open water bodies (lakes, rivers, canals, reservoirs, farm ponds, etc.) was estimated using a single algorithm that is calibrated to southern Idaho lakes (Allen et al., 2010), which tend to be moderately deep and clear. This algorithm was applied in this study regardless of water body size, depth and turbidity. Since the surface energy balance of water bodies varies depends on their properties, especially depth, temperature profiles and turbidity, use of a locally calibrated single algorithm might have caused some bias in estimates for open water evaporation.

The algorithms used in METRIC to estimate open water ET represent “implicit “large” water body properties. This will likely increase the uncertainty of ET from the water within the Landsat image (Allen and Tasumi, 2005). This algorithm may underestimate the ET from small water bodies such as cattle ponds, shallow lakes etc. Therefore, end users are cautioned if extracting estimates of open water evaporation from the maps of ET or ETrF. Research is underway with METRIC to test the use of an aerodynamic function for evaporation from water. We believe that use of an aerodynamic function may have better accuracy to calculate evaporation from water in future applications with METRIC.

The seasonal (April 1 –October 31) precipitation subtracted from the seasonal (April 1 –October 31) ET, in mm, estimated from METRIC is shown in Figures 15 and 16. Negative values in the figures indicate that precipitation exceeded the ET. ET from desert areas surrounding the agricultural areas in the project area is typically similar to or slightly higher than reported rainfall amounts. If real, the additional ET from these areas may have been derived from the change in stored soil moisture between April 1 and October 31. On April 1 there was still residual moisture in the soil from winter precipitation, and the soil profile dried as the summer progressed.

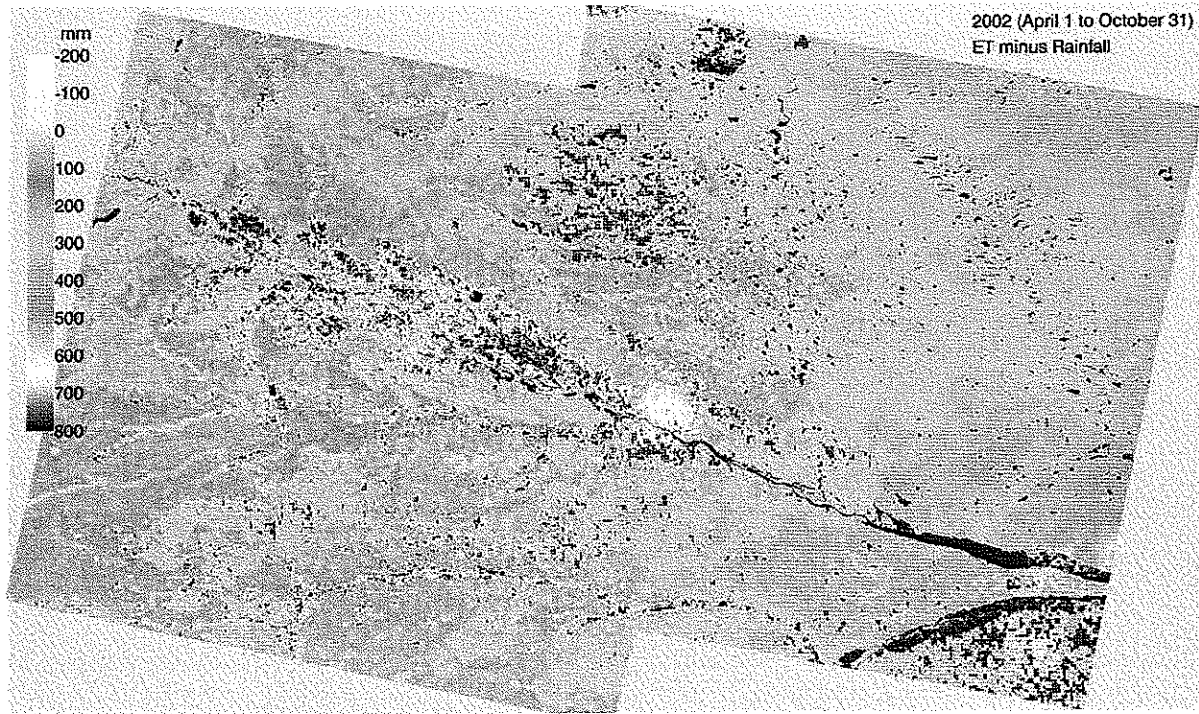


Figure 15 Seasonal (April 1 – October 31 2002), distributed precipitation subtracted from seasonal (April – October 31 2002) ET estimated from METRIC for both entire Landsat scenes, path 32 row 31 and path 33 row 31. Negative values indicate where precipitation exceeded the ET

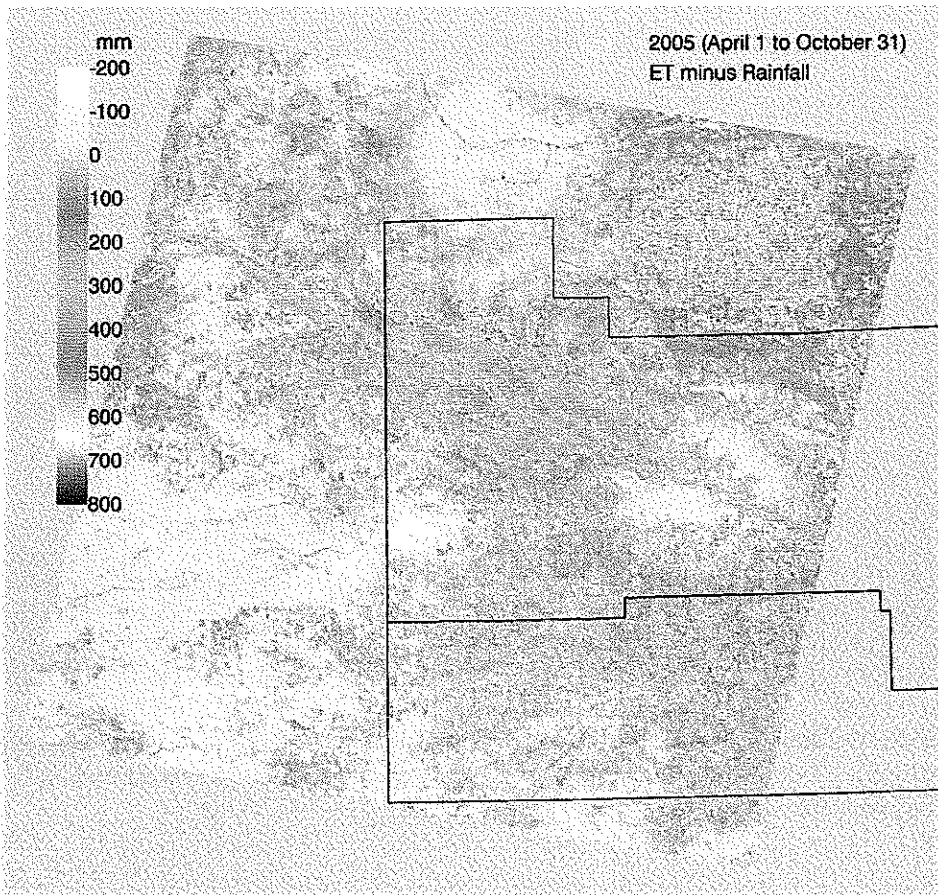


Figure 16 Seasonal (April 1 – October 31 2005), distributed precipitation subtracted from seasonal (April – October 31 2005) ET estimated from METRIC for the entire Landsat scene, path 33 row 31. Negative values indicate where precipitation exceeded the ET

Contrasting “Crop Coefficients” derived from METRIC with the Classical Crop Coefficient

Ayse Irmak and Rick Allen

Crop coefficients (K_c) are used with reference evapotranspiration (ET_{ref}) to estimate specific crop evapotranspiration (ET_c). The crop coefficient is a dimensionless number and usually between 0 and 1.2. The effects of characteristics that distinguish field crops from grass are integrated into K_c . The ET_c can be used to help an irrigation manager schedule when irrigation should occur and how much water should be applied back into the soil. The equation to estimate K_c and ET_c is as following:

$$K_c = K_e + K_{cb\ pot}$$

$$ET_c = K_c ET_{ref}$$

Where K_c : Total K_c including evaporation from soil and stress ($K_c = 0$ to 1.0)

K_e : Evaporation from soil (from both irrigation and rainfall) ($K_e = 0$ to 1.0)

K_s : Stress coefficient ($K_s = 0$ to 1.0). $K_s=1.0$ means no stress.

$K_{cb\ pot}$: Potential ‘basal’ K_c including essentially only ‘transpiration’ (no direct evaporation from soil (only low level diffusive evaporation)) and no stress

Most of the effects of the various weather conditions are incorporated into the ET_{ref} estimate. Therefore, as ET_{ref} represents an index of climatic demand, K_c varies predominately with the specific crop characteristics and only to a limited extent with climate. This enables the transfer of standard values for K_c between locations and between climates. This has been a primary reason for the global acceptance and usefulness of the crop coefficient approach and the K_c factors developed in past studies (FAO-56).

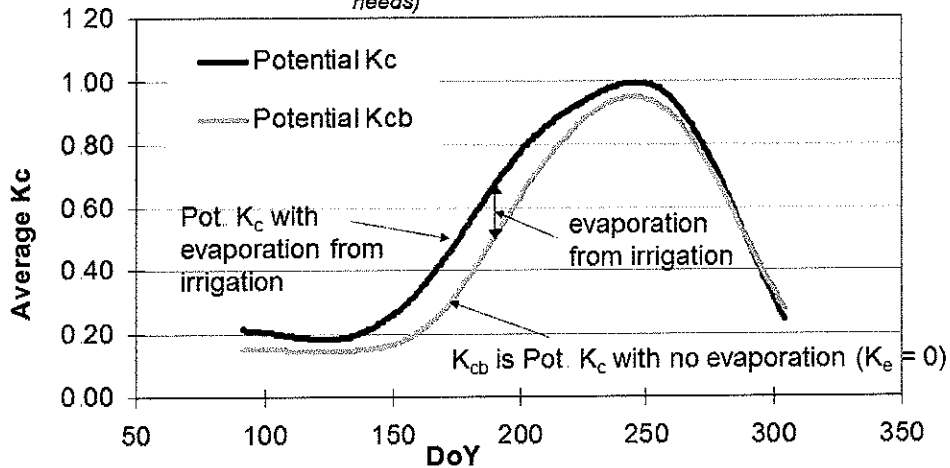
Figure 17 show the differences between potential K_c and Potential K_{cb} . Figure 18 shows the differences between K_c from METRIC model and potential K_c . Explanation of differences between Actual K_c from METRIC and Potential K_c where potential K_c is computed to represent K_c with all ET from irrigation only, in the absence of any rain are demonstrated in figure 19.

Explanation of differences between Potential K_c and Potential K_{cb}

$$K_{c \text{ pot}} = K_{cb \text{ pot}} + K_e \text{ irrigation}$$

Corn

(this is the definition for $K_{c \text{ pot}}$ used when scheduling irrigation, etc because K_e from rainfall is neglected for purposes of fulfilling plant water needs)



$$K_{cb \text{ pot}} = K_c \text{ with no stress } (K_s = 1) \text{ and no evaporation } (K_e = 0)$$

Figure 17

in this graph, K_s (stress coefficient) = 1.0 (no stress)

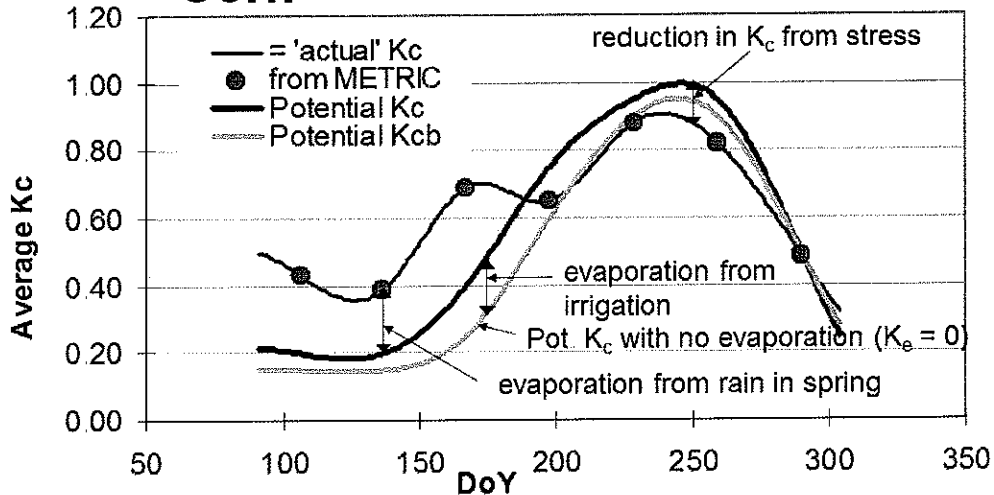
Explanation of differences between K_c from METRIC and Potential K_c

$$K_{c \text{ actual}} = K_s K_{cb \text{ pot}} + K_e \text{ total}$$

$$K_{c \text{ pot}} = K_{cb \text{ pot}} + K_e \text{ irrigation}$$

Corn

(K_c from METRIC is $K_{c \text{ actual}}$)

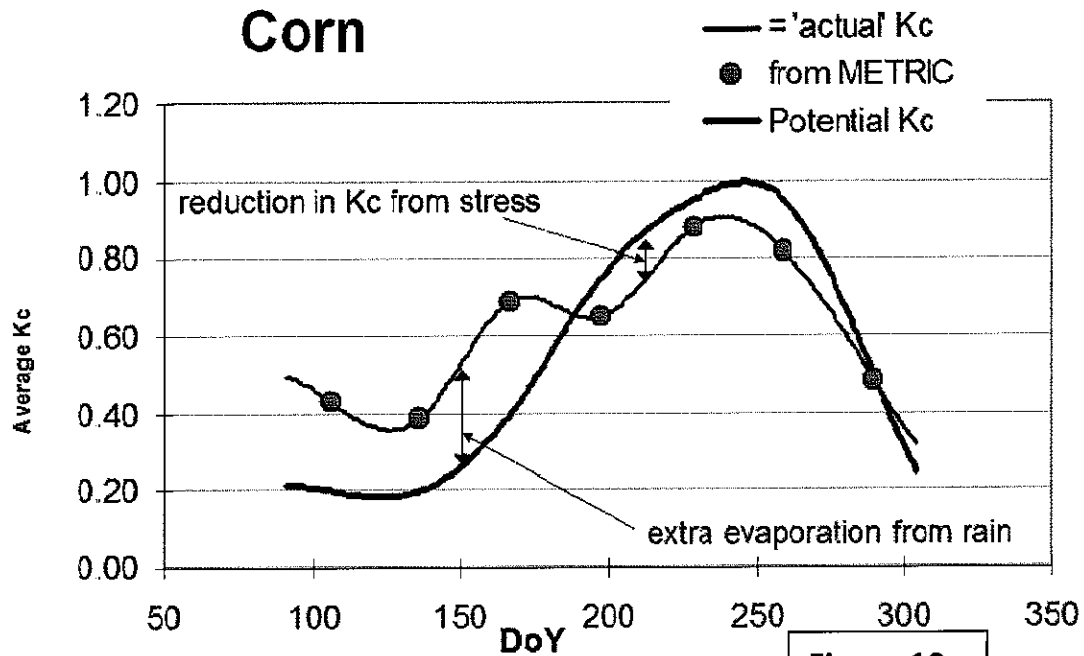


$$K_{cb \text{ pot}} = K_c \text{ with no stress } (K_s = 1) \text{ and no evaporation } (K_e = 0)$$

Figure 18

$$K_e \text{ total} = K_e \text{ rainfall} + K_e \text{ irrigation}$$

Explanation of differences between Actual K_c from METRIC and Potential K_c where potential K_c is computed to represent K_c with all ET from irrigation only, in the absence of any rain.



$$K_{c, \text{actual}} = K_s K_{cb} + K_{e, \text{total}}$$

Reader should note that all potential K_c curves shown on these slides are made up for illustration only. They do not represent any literature values. The METRIC derived curve on However, K_c curves on figure 19 is real and is obtained from Landsat path 33, row 31 for 2005 by UNL team members (Ayse Irmak and Ian Ratcliffe).

Potential use of K_c for irrigation scheduling

- Reduce irrigation amounts when there is rain that supplies part of the K_{cb} requirement (but not the part that becomes K_e).
- The objective is to normally prevent stress and maximize crop yields
- Potential K_c can often be developed from vegetation indices from satellite (NDVI): ($K_c \sim 1.2 \times \text{NDVI}$)

Potential use K_c from METRIC for hydrologic applications

- Calculate water balances
- Estimate recharge
- Estimate actual depletion to the water resource
- Estimate evaporation even during the nongrowing season
- Construct historical time series
- Use different actual K_c curves for wet and dry years

The K_c derived from METRIC can 'contain' the following components:

- The basal K_{cb}
- A K_s stress multiplier (whose value is unknown, but which reduces the K_{cb} amount)
- An evaporation component, K_e , that contains evaporation from both irrigation and rainfall

The three components can not be easily separated nor identified and are 'mixed' together

- It may be possible to estimate K_{cb} based on NDVI: ($K_c \sim 1.1$ to $1.2 \times$ NDVI) to separate it out.
- It may be possible to estimate K_e from rain using a daily water balance model and rain inputs
- It is usually not possible to identify or estimate K_e from irrigation from satellite
- Therefore, it is difficult to separate out K_s unless there is no recent evaporation from irrigation, in which case,
$$K_s = K_c / K_{cb} - K_e / K_{cb}$$

where K_{cb} is estimated from vegetation amount. This approach was recently used in a manuscript by Cristina Santos and Ignacio Lorite of Andalusia, Spain for olives.

Generation of Crop Coefficients from METRIC

Ayse Irmak, Ian Ratcliffe and Sami Akasheh

Crop coefficients (K_c) produced from METRIC are defined as total K_c including evaporation from soil and crop stress with values typically ranging from 0.0 to 1.0. METRIC derived K_c values differ from potential K_c values. METRIC K_c values are generated in METRIC as fraction of reference ET (ET_r) for each image. Application of METRIC K_c values include calculation of water balances, estimation of recharge, estimation of actual depletion to the water source, estimation of evaporation during non-growing season, and to construct historical time series.

Approximately 20-30 fields were sampled for each crop type (corn, sugar beets, alfalfa, and wheat) from Landsat path 33, row 31 for 2005. The results are presented on Figure 20. We were careful to not sample from the center of irrigation pivots. Approximately 30-50 pixels were sampled from each field. Figure 5 shows **Kc on individual satellite image dates and averaged Kc curve** for the 2005 year (symbols and curve) for Corn, Sugar Beets, Alfalfa, and Small Grains for Nebraska Panhandle (Landsat path33, row31) as determined from METRIC ET.

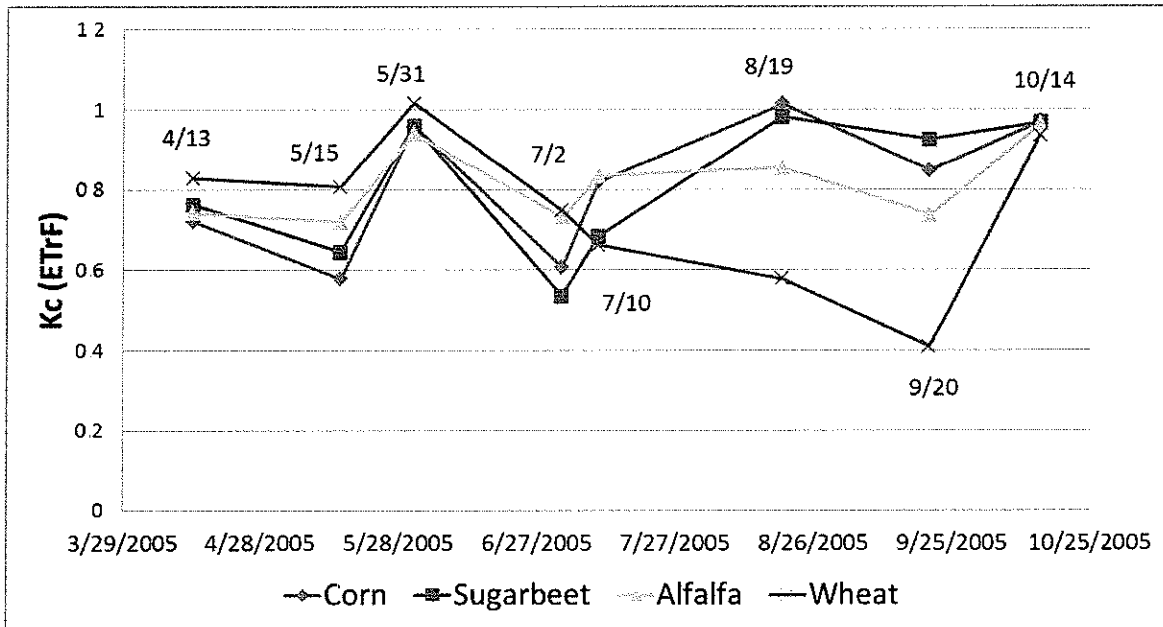


Figure 20. Crop coefficients (K_c) for irrigated corn, sugar beets, alfalfa, and wheat for 2005. High values on 5/31 and 10/14 were a result of heavy rainfall the previous days

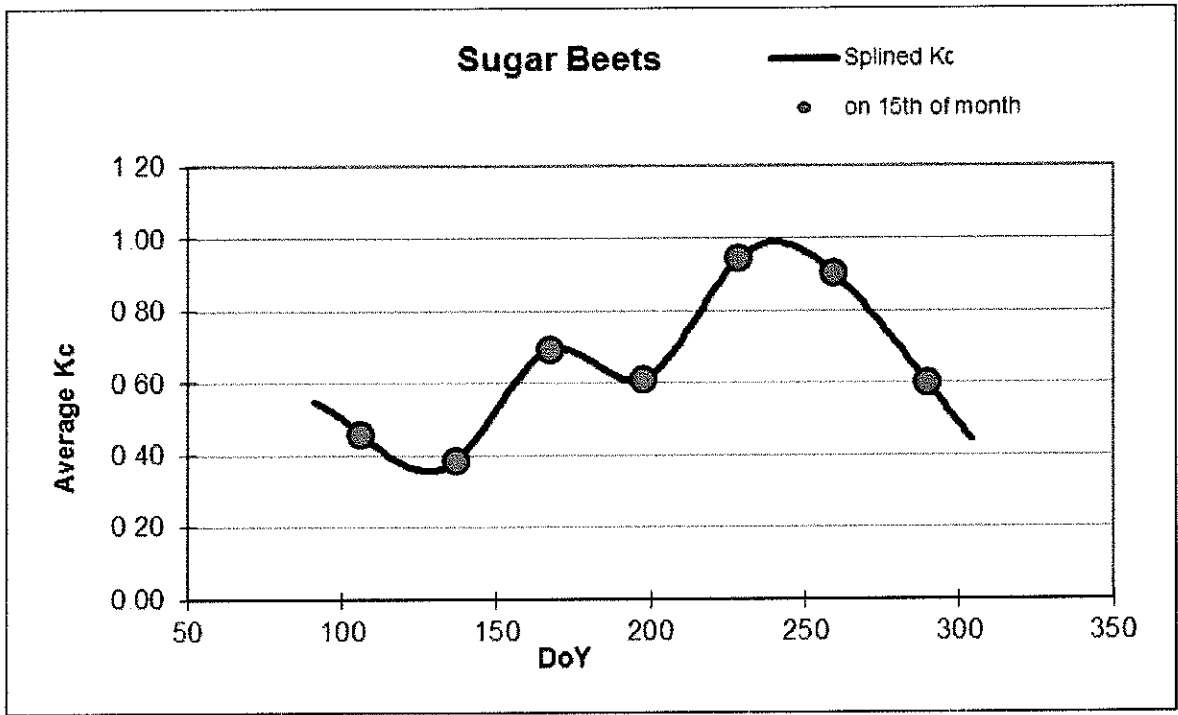
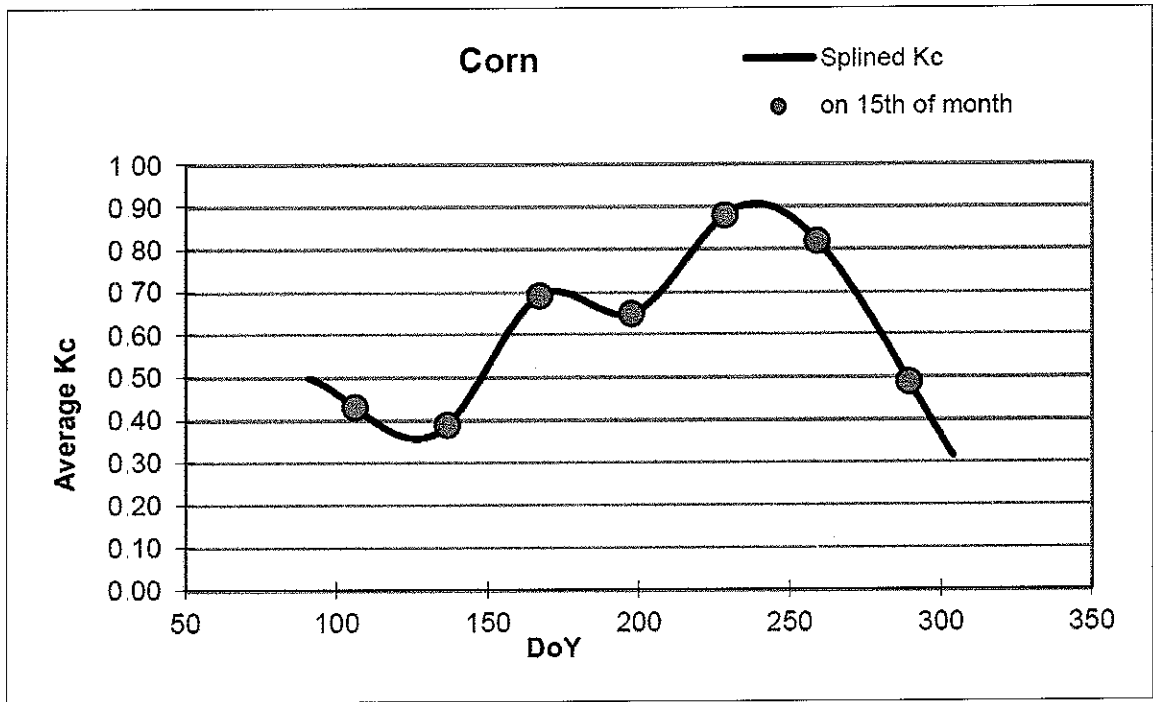


Figure 21. The Kc on individual satellite image dates and averaged Kc curve for the 2005 year (symbols and curve) for Corn, Sugar Beets, Alalfa, and Small Grains for Nebraska Panhandle (Landsat path33, row31) as determined from METRIC ET.

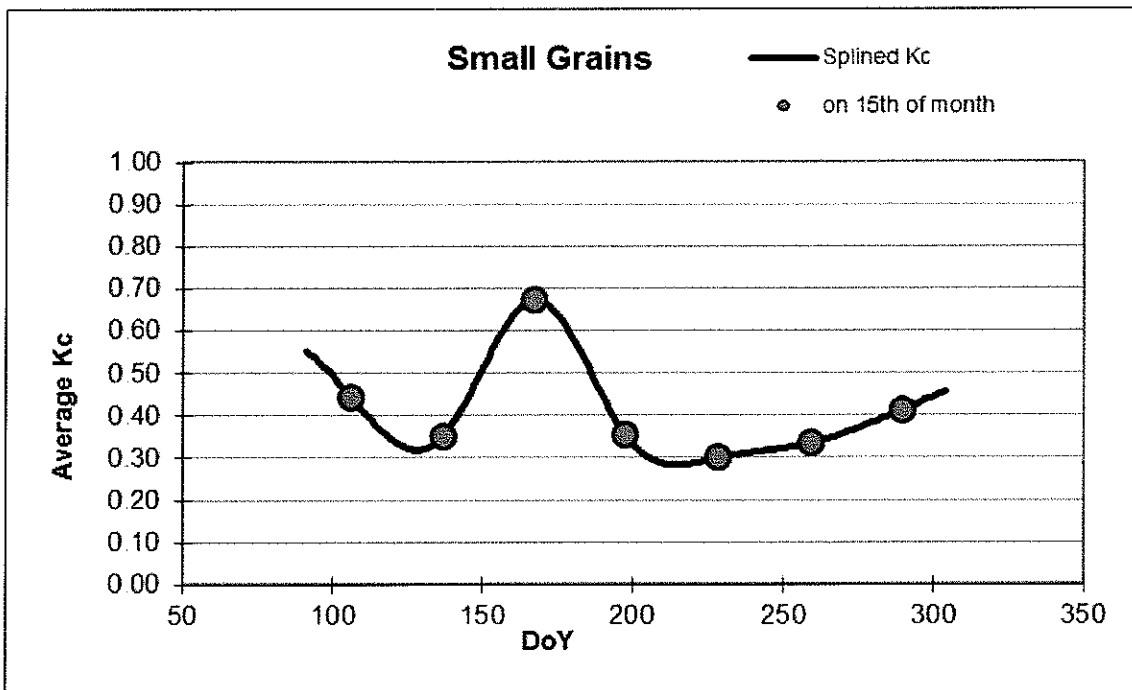
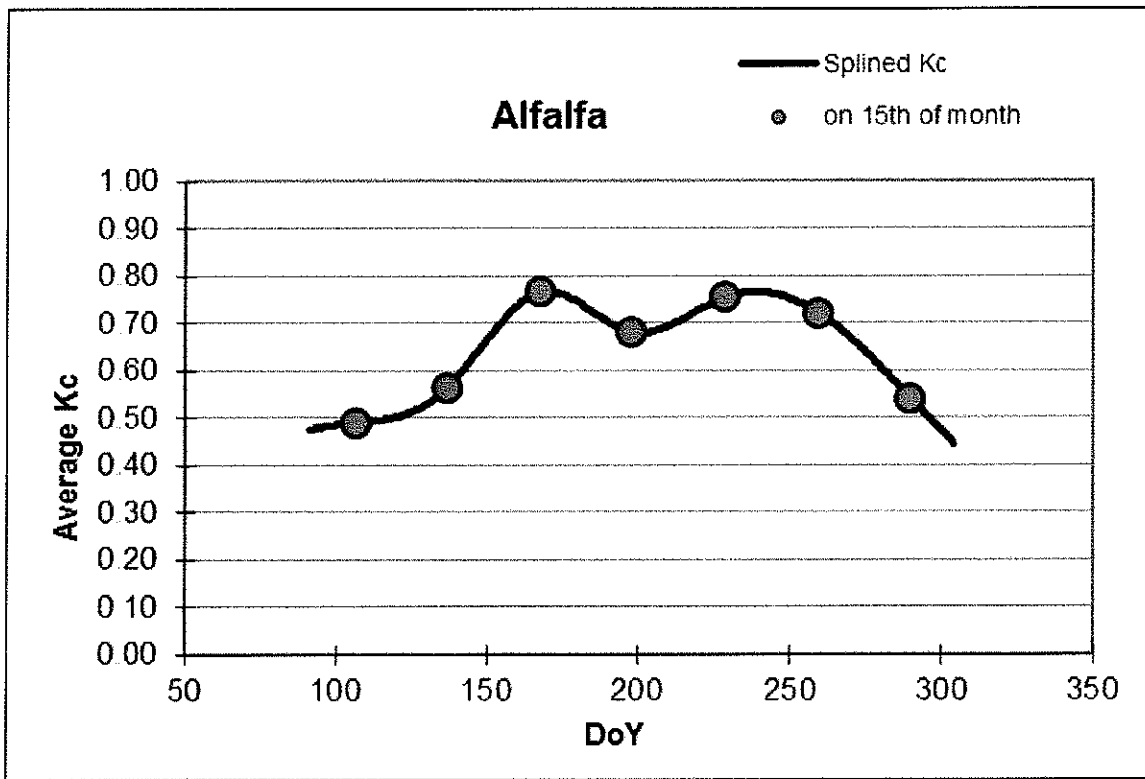


Figure 21. Kc on individual satellite image dates and averaged Kc curve for the 2005 year (symbols and curve) for Corn, Sugar Beets, Alfalfa, and Small Grains for Nebraska Panhandle (Landsat path33, row31) as determined from METRIC ET.

Summary and Discussion

The METRIC model has been introduced to estimate surface energy fluxes at the same scale as the input imagery, which is 30x30 m pixel size in the case of Landsat 5 and/or 7 satellite images (Allen et al., 2010). The METRIC algorithms to Landsat 5/7 TM images have been applied over a crop growing season (April to October) for 2002 and 2005 for the North Platte and South Platte NRDs. The project area consists of Landsat path 32-33, row 31 for 2002 and path 33, row 31 for 2005. Meteorological information from automated weather stations (AWS) was used during the calibrations of METRICTM. AWS data from Scottsbluff were used in for path 33 row 31 and the Sidney AWS was used for path 32, row 31. Extensive data quality analyses were conducted on climate data. A distributed daily water balance model was used to estimate residual moisture from the bare soil for 2002 and 2005.

Images were acquired as systematic terrain-corrected (Level 1T) with a 30m spatial resolution and the thermal band was re-sampled to 30m pixels. The satellite overpass times were acquired from the image meta data files to estimate zenith angle of the sun, instantaneous values of wind speed at 200m, air humidity, and reference evapotranspiration (ET_r).

Creating maps of ET that are useful in management and in quantifying and managing water resources requires the computation of ET over monthly and longer periods such as growing seasons or annual periods. Interpolation between images involves treatment of clouded areas of images, accounting for evaporation from wetting events occurring prior to satellite overpass. Daily ET maps of the Nebraska Panhandle are shown in Appendix B. The images shown there have not had cloud masks applied. Innovative cloud filling methods developed to reconstruct clouded areas of images to acceptable ranges, and monthly and seasonal ET map were generated for each path and row. The monthly and seasonal ET for 2002 was completed by combining (mosaicking) Landsat paths 32-33.

Our results show that ET is highly variable in space and time due to variability in landuse, climatic conditions, soil properties, and management practices. Spatial variation in soil properties affect surface soil evaporation and surface energy balances, and cause within-field and across field variability in ET. Satellite remote sensing provides an opportunity for representing spatial and temporal variation of ET.

REFERENCES

- Allen, R G , 1996. Assessing Integrity of Weather Data for Reference Evapotranspiration Estimation *J. Irrig Drain. Engr.*, 122, 97-106.
- Allen, R. G., Pereira, L. S., Raes, D., and Smith, M. 1998. Crop evapotranspiration: Guidelines for computing crop water requirements. *United Nations FAO, Irrigation and Drainage*, N.Y., Paper No. 56. (<http://www.fao.org/docrep/X0490E/X0490E00.htm>) February 5, 2007.
- Allen, R.G., et al., 2006. A Recommendation on the Standardized Surface Resistance for Hourly Calculation of Reference ET by the FAO56 Penman-Monteith Method *Agric. Water Manag.*, 81, 1-22.
- Allen, R.G., Tasumi, M., Trezza, R., 2007a. Satellite-Based Energy Balance for Mapping Evapotranspiration with Internalized Calibration (METRIC) – Model *J. Irrig. Drain. Engr.*, 133(4), 380-394.
- Allen, R.G., Tasumi, M., Morse, A., Trezza, R., Wright, J.L., Bastiaanssen, W., Kramber, W., Lorite, I., Robison, C.W., 2007b. Satellite-Based Energy Balance for Mapping Evapotranspiration with Internalized Calibration (METRIC) – Applications *J. Irrig. Drain. Engr.*, 133(4), 395-406.
- Allen, R.G. 2010. Procedures for adjusting METRIC-derived ETrF Images for Background Evaporation from Precipitation Events prior to Cloudfilling and Interpretation of ET between Image Dates. Report., University of Idaho. 11 pages. Version 7, last revised April 2010.
- ASCE-EWRI, 2005. The ASCE Standardized Reference Evapotranspiration Equation. R.G. Allen, I.A. Walter, R.L. Elliot, T.A. Howell, D. Itenfisu, M.E. Jensen, and R.L. Snyder (eds.). Environmental and Water Resources Institute (EWRI) of the Am. Soc. of Civil. Engrs., ASCE, Standardization of Reference Evapotranspiration Task Committee Final Report. ASCE, Reston, Virginia.
- Bastiaanssen, W. G. M. 1995. Regionalization of surface flux densities and moisture indicators in composite terrain: A remote sensing approach under clear skies in Mediterranean climates. Ph.D. Dissertation, CIP Data Koninklijke Bibliotheek, Den Haag, The Netherlands.
- Bastiaanssen, W. G. M., Menenti, M., Feddes, R. A. and Holtslag, A. A. M. 1998. "A remote sensing surface energy balance algorithm for land (SEBAL): 1. Formulation" *J. Hydrol.*, 212-213, 198-212.
- Brutsaert, W. 1982. *Evaporation into the atmosphere*, Reidel, Dordrecht, The Netherlands.
- Franks, S. W., and K. J. Beven. 1997a. Estimation of evapotranspiration at the landscape scale: A fuzzy disaggregation approach. *Water Resour. Res.*, 33(12), 2929–2938.

- Franks, S. W., and K. J. Beven. 1997b. Bayesian estimation of uncertainty in land surface-atmosphere flux predictions, *J. Geophys. Res.* 102(D20), 23,991-999.
- Franks, S. W., and K. J. Beven. 1999. Conditioning a multiple-patch SVAT Model using uncertain time-space estimates of latent heat fluxes as inferred from remotely sensed data *Water Resour. Res.*, 35(9), 2751–2761
- Irmak, S., T. A. Howell, R. G. Allen, J. O. Payero, D. L. Martin. 2005. Standardized ASCE Penman-Monteith: impact of sum-of-hourly vs. 24-hour timestep computations at reference weather station sites. *Trans. ASABE*. Vol. 48(3): 1063-1077.
- Irmak, A., and B. Kamble. 2009. Evapotranspiration Data Assimilation with Genetic Algorithms and SWAP Model for On-demand Irrigation. *Irrigation Science*. 28:101-112.
- Ranade, P. 2010. Spatial Water Balance for Bare Soil. University of Nebraska. Report, 10 pp.
- Singh, R. K., A. Irmak, S. Irmak and D. L. Martin. 2008. Application of SEBAL for mapping evapotranspiration and estimating surface energy fluxes in south central Nebraska. *J. Irrig. and Drain. Eng.*, ASCE 134(3):273-285
- Singh R., and A. Irmak. 2009. Estimation of Crop Coefficients Using Satellite Remote Sensing. *J. Irrig. and Drain. Eng.*, ASCE 135(5): 597-608
- Tasumi, M. 2003. Progress in operational estimation of regional evapotranspiration using satellite imagery. Ph.D. dissertation, Univ. of Idaho, Moscow, Idaho.

APPENDIX A

Quality Control of Weather Data

Processing of Landsat imagery using METRIC to produce monthly and seasonal ET estimates requires the use of hourly meteorological data for calibration of METRIC and requires the creation of a 'surface' of daily reference ET for the image domain for use during interpolation of ET_r between images. For the applications to year 2002 and 2005, hourly and daily meteorological information from 23 High Plains Regional Climate Center (HPRCC) weather stations, 2 Colorado Agricultural Meteorological Network (CoAgMet) and 62 National Weather Service Cooperative Observer Program (COOP) were assembled and analyzed (figure 1). The names and locations of the stations are listed in Tables 1 and 2.

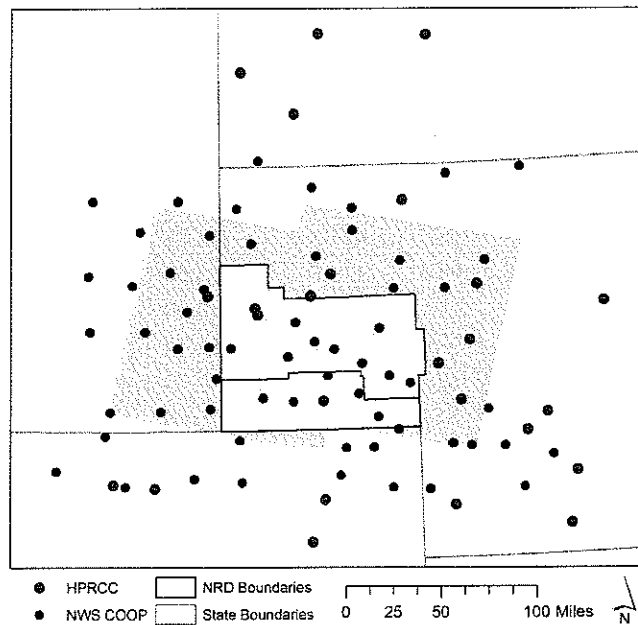


Figure 1 The locations of weather stations used for METRIC ET processing.

The HPRCC and CoAgMet weather stations are of interest because they measure and report meteorological information relevant to the estimation of alfalfa reference evapotranspiration (ET_r) calculated using the ASCE standardized Penman-Monteith equation (ASCE-EWRI, 2005), which in turn is required input for the satellite image processing using METRIC. The meteorological parameters needed are hourly values of: solar radiation (R_s); air temperature (T_a); air humidity, expressed as relative humidity (RH); dew point temperature (T_{dew}) or vapor pressure (e_a); and wind speed (WS). In addition, daily values of precipitation are required to establish a water balance for the upper soil layers.

During processing of the satellite images, the METRIC model was calibrated using hourly data from the Scottsbluff and Sidney HPRCC weather stations. ET_r and precipitation from these stations were used to establish daily estimates of bare soil evaporation used during METRIC calibrations. In addition, ET_r and precipitation from these stations and all other stations listed in Tables 1 and 2 were used to establish distributed estimates of bare soil evaporation using a gridded daily process model to adjust the monthly and seasonal ET estimates for background evaporation from rainfall.

Several of the weather stations are located outside the geographical domain of the Landsat scenes processed. These stations were included to improve the accuracy of ET_r and precipitation along the image edges, when interpolating between the point locations of the weather stations to fully distributed estimates.

Table 1. The station names, weather station network, and locations of the weather stations used to estimate distributed maps of reference ET.

| Station Name | Network | State | Latitude | Longitude |
|-------------------|---------|-------|----------|-----------|
| Akron | HPRCC | CO | 40.15 | -103.15 |
| Alliance North | HPRCC | NE | 42.18 | -102.92 |
| Alliance West | HPRCC | NE | 42.02 | -103.13 |
| Arapahoe Prairie | HPRCC | NE | 41.48 | -101.85 |
| Arthur | HPRCC | NE | 41.65 | -101.52 |
| Caputa | HPRCC | SD | 44.00 | -103.00 |
| Champion | HPRCC | NE | 40.40 | -101.72 |
| Gordon | HPRCC | NE | 42.73 | -102.17 |
| Gudmundsen Ranch | HPRCC | NE | 42.07 | -101.43 |
| Halsey | HPRCC | NE | 41.90 | -100.15 |
| Jewel Cave | HPRCC | SD | 43.72 | -103.82 |
| McCook | HPRCC | NE | 40.23 | -100.58 |
| Mitchell Farms | HPRCC | NE | 41.93 | -103.70 |
| North Platte | HPRCC | NE | 41.08 | -100.77 |
| Oral | HPRCC | SD | 43.40 | -103.27 |
| Scottsbluff | HPRCC | NE | 41.88 | -103.67 |
| Sidney | HPRCC | NE | 41.22 | -103.02 |
| Sterling | HPRCC | CO | 40.47 | -103.02 |
| Torrington | HPRCC | WY | 42.03 | -104.18 |
| Cedar Point | HPRCC | NE | 41.20 | -101.63 |
| Cottonwood | HPRCC | SD | 43.97 | -101.87 |
| Curtisunsta | HPRCC | NE | 40.63 | -100.50 |
| Dickens | HPRCC | NE | 40.95 | -100.98 |
| Fort Collins AERC | CoAgMet | CO | 40.59 | -105.13 |
| Ault | CoAgMet | CO | 40.56 | -104.72 |

Table 2. The station names, weather station network, and locations of the weather stations used to estimate distributed maps of precipitation (in addition to the HPRCC and CoAgMet station in Table 1).

| STATION NAME | NETWORK | LONGITUDE | LATITUDE |
|------------------|----------|-----------|----------|
| AGATE 3 E | NWS COOP | 42.42 | -103.73 |
| ALBIN | NWS COOP | 41.40 | -104.10 |
| ARCHER | NWS COOP | 41.15 | -104.66 |
| ARDMORE 2 N | NWS COOP | 43.05 | -103.65 |
| BAYARD 4 NNE | NWS COOP | 41.82 | -103.29 |
| BRIDGEPORT | NWS COOP | 41.67 | -103.10 |
| BRIDGEPORT 18WSW | NWS COOP | 41.56 | -103.37 |
| BRIGGSDALE | NWS COOP | 40.64 | -104.33 |
| BROADWATER 3WNW | NWS COOP | 41.61 | -102.90 |
| CHADRON MUNI AP | NWS COOP | 42.84 | -103.10 |
| CHAPPELL | NWS COOP | 41.09 | -102.47 |
| CHUGWATER | NWS COOP | 41.76 | -104.82 |
| CRESCENT LAKE | NWS COOP | 41.76 | -102.44 |
| CROOK | NWS COOP | 40.86 | -102.80 |
| DALTON | NWS COOP | 41.41 | -102.97 |
| DOUBLE FOUR RCH | NWS COOP | 42.18 | -105.40 |
| DOUGLAS 1 SE | NWS COOP | 42.75 | -105.36 |
| ELLSWORTH | NWS COOP | 42.06 | -102.28 |
| ELLSWORTH 15 NNE | NWS COOP | 42.27 | -102.21 |
| FLEMING 3 SW | NWS COOP | 40.65 | -102.86 |
| FT COLLINS 4 E | NWS COOP | 40.58 | -105.02 |
| GRANT 2 N | NWS COOP | 40.87 | -101.73 |
| HARRISBURG 12WNW | NWS COOP | 41.63 | -103.95 |
| HARRISON | NWS COOP | 42.69 | -103.88 |
| HAY SPRINGS | NWS COOP | 42.68 | -102.69 |
| HAY SPRINGS 12 S | NWS COOP | 42.51 | -102.69 |
| HAYES CENTER | NWS COOP | 40.52 | -101.03 |
| HECLA 1E | NWS COOP | 41.15 | -105.17 |
| HEMINGFORD | NWS COOP | 42.32 | -103.07 |
| HOLYOKE | NWS COOP | 40.55 | -102.34 |
| HYANNIS 5N | NWS COOP | 42.05 | -101.76 |
| JULESBURG | NWS COOP | 40.99 | -102.27 |
| KEELINE 7 SW | NWS COOP | 42.52 | -104.87 |
| KILGORE 1 NE | NWS COOP | 42.95 | -100.95 |
| KIMBALL 2NE | NWS COOP | 41.25 | -103.63 |
| LA GRANGE | NWS COOP | 41.64 | -104.17 |
| LAMAR | NWS COOP | 40.53 | -101.97 |
| LEWELLEN | NWS COOP | 41.34 | -102.14 |
| LISCO | NWS COOP | 41.50 | -102.62 |
| LODGEPOLE 8N | NWS COOP | 41.27 | -102.66 |
| LUSK 2 SW | NWS COOP | 42.75 | -104.48 |
| MADRID | NWS COOP | 40.85 | -101.54 |
| MERRIMAN | NWS COOP | 42.92 | -101.71 |
| MULLEN 21 NW | NWS COOP | 42.25 | -101.34 |

Table 2 continued.

| STATION | NETWORK | ELEVATION (m) | LONGITUDE |
|---------------------|----------|---------------|-----------|
| NEW RAYMER | NWS COOP | 40.61 | -103.85 |
| NEW RAYMER 21 N | NWS COOP | 40.93 | -103.87 |
| OLD FT LARAMIE | NWS COOP | 42.21 | -104.56 |
| OSHKOSH | NWS COOP | 41.40 | -102.35 |
| PAXTON | NWS COOP | 41.12 | -101.36 |
| PHILLIPS | NWS COOP | 41.63 | -104.49 |
| PINE BLUFFS 5 W | NWS COOP | 41.17 | -104.16 |
| POTTER | NWS COOP | 41.22 | -103.32 |
| RUSTIC 9 WSW | NWS COOP | 40.70 | -105.71 |
| SEDGWICK 5 S | NWS COOP | 40.86 | -102.52 |
| SYBILLE RSCH UNIT | NWS COOP | 41.76 | -105.38 |
| TORRINGTON 29 N | NWS COOP | 42.49 | -104.16 |
| TORRINGTON EXP FARM | NWS COOP | 42.08 | -104.22 |
| VIRGINIA DALE 7 ENE | NWS COOP | 40.97 | -105.22 |
| WALLACE 2 W | NWS COOP | 40.84 | -101.21 |
| WELLFLEET | NWS COOP | 40.76 | -100.73 |
| WHEATLAND 4 N | NWS COOP | 42.11 | -104.95 |
| YODER 2 WSW | NWS COOP | 41.91 | -104.39 |

Calculation of ET_r

For the purpose of calculating ET_r using the Standardized Penman-Monteith equation, hourly values of T_a , T_{dew} , R_s and WS along with information of year, month, date, and time-of-day for each time step were assembled from HPRCC and CoAgMet archives and exported to comma separated text files.

ET_r was calculated using the RefET V3.1 software, developed by Dr. Rick Allen, University of Idaho. RefET computes ET_r following the recommendations of ASCE-EWRI (2005). RefET is very flexible regarding the units of the individual weather parameters in the input file, and units for the output file is selected by the user; scientific units are preferred, in order to be congruent with the units used in the METRIC model.

The software and additional information, including a user manual, are available from <http://www.kimberly.uidaho.edu/ref-et/index.html>.

Daily ET_r was calculated by summing hourly ET_r estimates to 24-h values. It should be noted, that it is recommended (Allen et al., 2006; ASCE-EWRI, 2005; Irmak et al., 2005) to calculate daily ET_r as the sum of hourly values rather than summing or averaging hourly input parameters (T_a , T_{dew} , R_s and WS) to daily values before calculating ET_r .

Weather data quality control

A description of procedures and thresholds for quality control of weather data is in appendix D of ASCE-EWRI (2005). This publication further provides insight and methods for calculating a

theoretical clear sky solar radiation curve, which is a powerful parameter to use for indicating not only possible errors in R_s (e.g. calibration errors, sensor misalignment, damaged sensor, etc.), **but also errors in datalogger time stamps and internal clock.**

Daily R_s is compared to calculated clear sky solar radiation, R_{s0} . R_{s0} is calculated based on atmospheric pressure, sun angle and precipitable water in the atmosphere. On clear sky days the measured R_s should approach the value of R_{s0} . The R_{s0} curve may be obtained as one of the outputs from the RefET software

Figure 2-3 shows daily solar radiation from the Scottsbluff HPRCC weather station for 2002. From day of year (DOY) 78 until the end of the year, the recorded values for R_s were about 6% lower than the R_{s0} curve. The errors in R_s were corrected by applying an appropriate multiplication factor. The solar radiation after applying a correction factor of 1.06 is also shown in Figures 2-3.

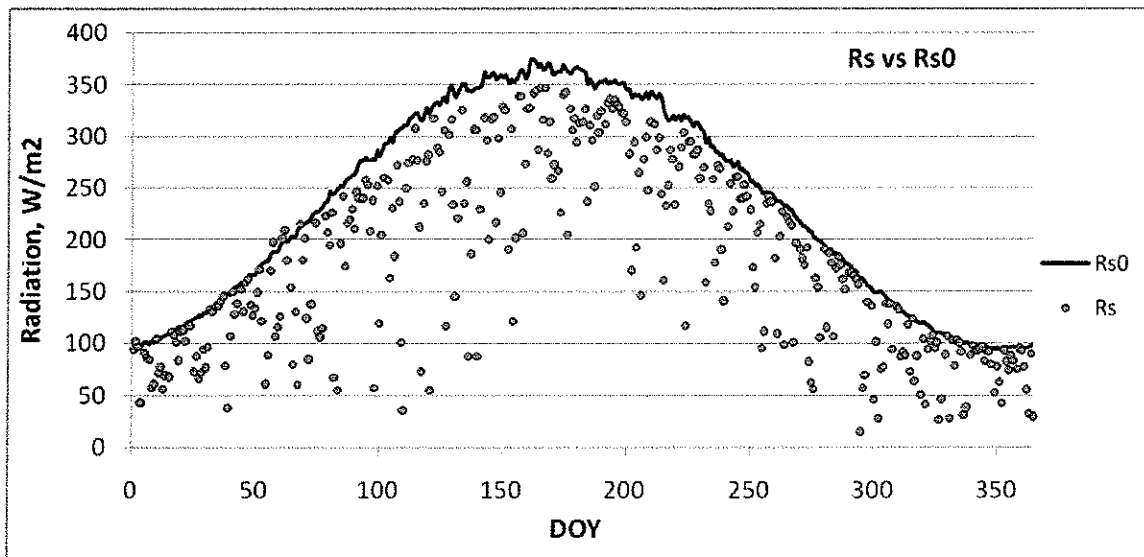


Figure 2 Daily recorded solar radiation (R_s) and the theoretical clear sky solar radiation curve (R_{s0}) for the Scottsbluff HPRCC weather station for 2002 before correction.

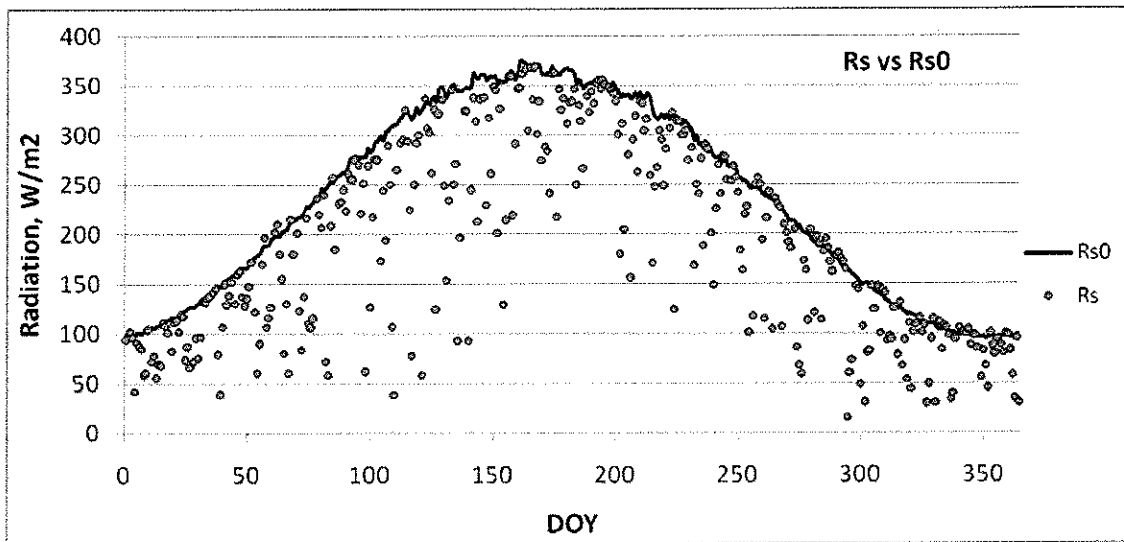


Figure 3. Daily recorded solar radiation (R_s) and the theoretical clear sky solar radiation curve (R_{s0}) for the Scottsbluff HPRCC weather station for 2002 after correction (R_s was increased by 6% after DOY 78)

Daily 24-h air temperature data were screened to check the dataset for outliers and the expected annual occurrence of maximum and minimum temperatures. Air temperature data were analyzed by subtracting the average of 24 hourly T_a from the difference between daily temperature extremes (minimum and maximum T_a). Systematic differences greater than 2-3 °C may indicate erroneous extremes in air temperature or impacts of missing hourly data.

Air humidity is shown in Figure 4 as minimum and maximum daily RH. In relatively arid regions such as the Nebraskan Panhandle, daily minimum RH may run as low as 15 – 20 % during the dry part of the year. Daily maximum RH is generally in the range of 90 - 100 % for irrigated areas having sufficient fetch and adequate water supply, especially during “wet” portions of the year. An example using humidity and precipitation from the Scottsbluff HPRCC weather station is shown in Figure 4.

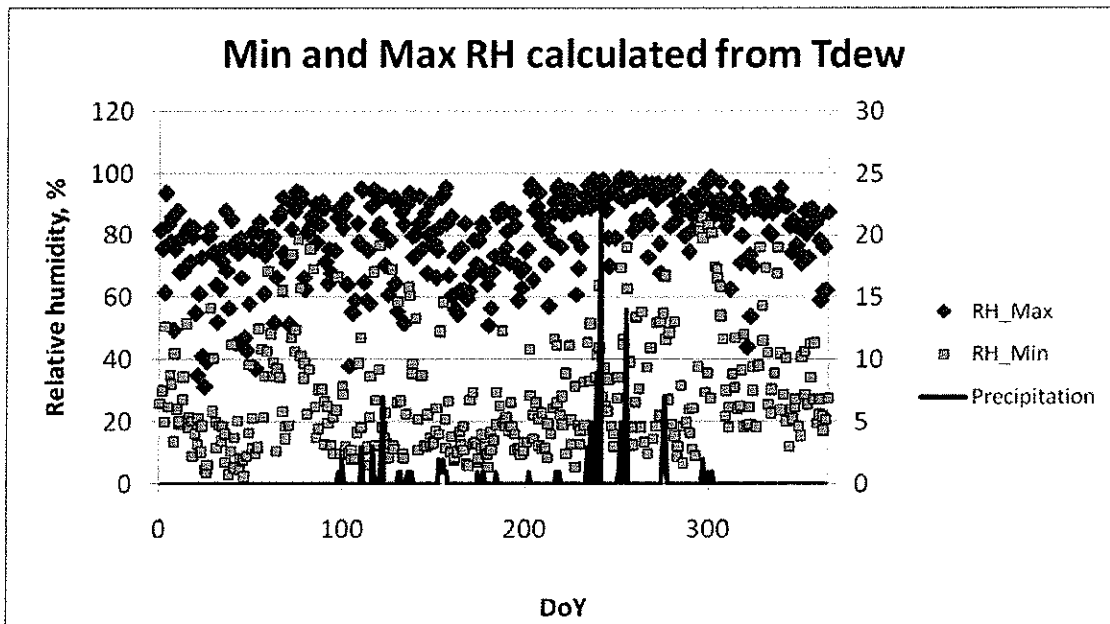


Figure 4 Daily maximum and minimum relative humidity (%) calculated from Td and Ta, and precipitation recorded at the Scottsbluff HPRCC weather station during 2002.

Daily average wind speed data were plotted as a function of day of year to check for outliers. Continuous periods with wind speeds less than 1 m/s may indicate problems with the anemometer. Also, daily wind speed data were compared among the three calibration stations to identify spuriously high values and systematically higher wind speeds as compared to the other stations. The gust factor, calculated as the ratio of maximum daily wind speed to mean daily wind speed, is plotted to evaluate the functioning of the anemometer. If the gust factor over time shows a period of large values the anemometer may be malfunctioning. Also, if the gust factor drops to a value of 1 the sensor may be failing completely. An example using wind speed from the Scottsbluff HPRCC weather station is shown in Figure 5.

Daily values of precipitation were compared for all stations to evaluate the temporal occurrence of precipitation and the amount received. Generally precipitation is very heterogeneous, however if one of the stations systematically recorded substantially less precipitation this may indicate a dirty or malfunctioning rain gauge. Precipitation is not measured during the winter period at the HPRCC stations. The cumulative precipitation for the period March 15 – October 31 2005 from seven HPRCC weather stations are shown in Figure 6.

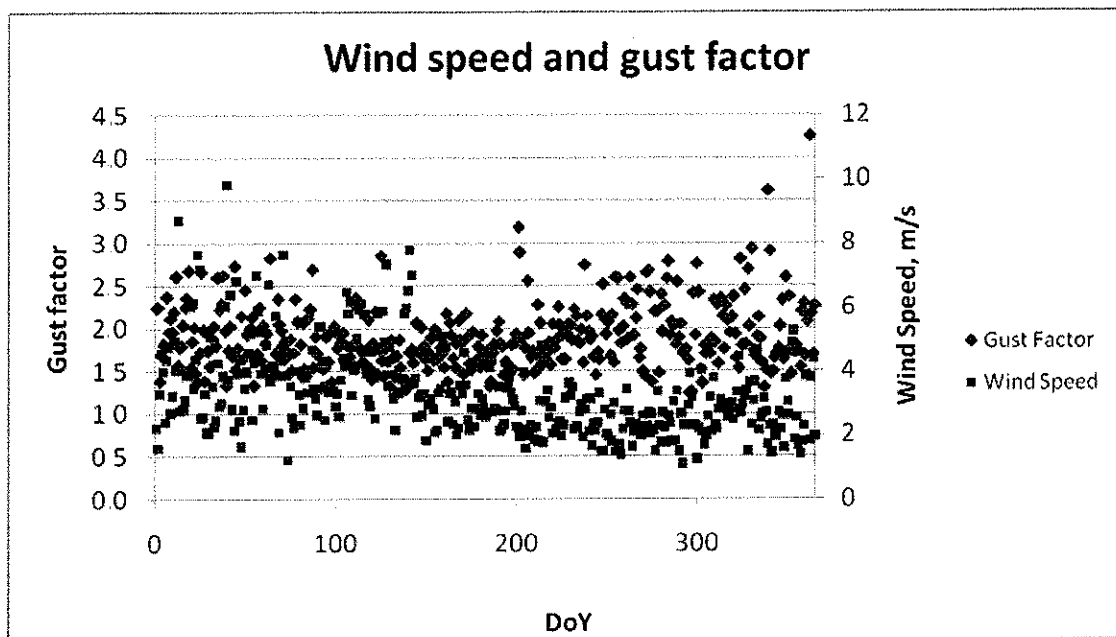


Figure 5. Daily gust factor and average wind speed (m/s) recorded at the Scottsbluff HPRCC weather station for 2002.

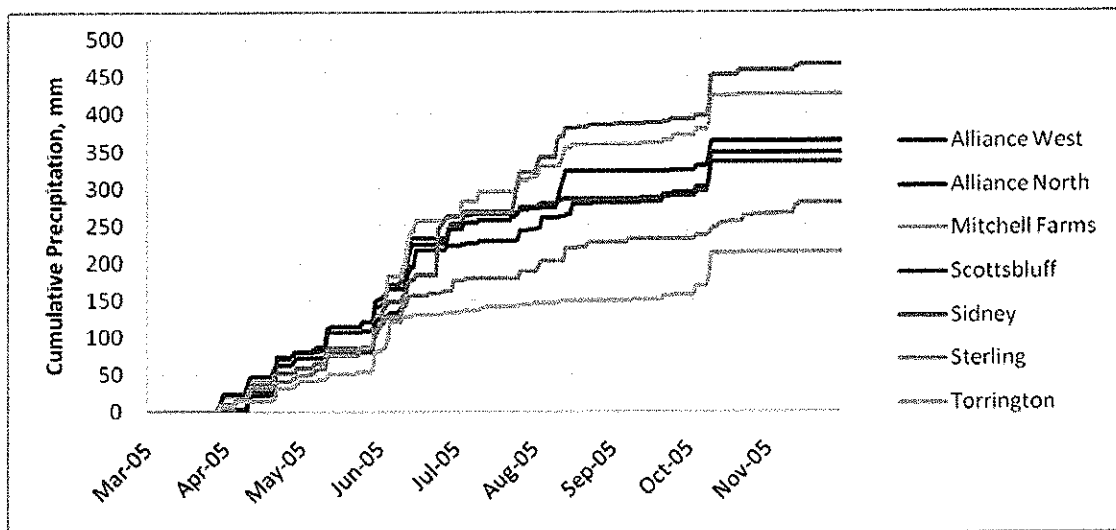


Figure 6. Daily cumulative precipitation from March 15 – November 31 2005 from the Alliance West, Alliance North, Mitchell Farms, Scottsbluff, Sidney, Sterling, and Torrington HPRCC weather stations.

Precipitation data from 62 COOP station were downloaded from the COOP data access website at <http://www.ncdc.noaa.gov/oa/climate/stationlocator.html>. The precipitation data were screened for location relative to the study area, completeness of data, missing data values and relative precipitation amounts. At the COOP stations, precipitation is recorded year round. Snow depths are converted to depth of water

Calculated reference evapotranspiration

Reference evapotranspiration is calculated using the ASCE-EWRI (2005) standardized Penman-Monteith equation and is applied for both the alfalfa reference and the grass reference. Alfalfa based ET_r is used in METRIC in the calculation of sensible heat flux, and data are presented below. The ET_r values shown in this section were calculated following correction of R_s for all HPRCC stations. Figure 7 show the cumulative ET_r calculated for the seven HPRCC weather stations located within Landsat path 33, row 31.

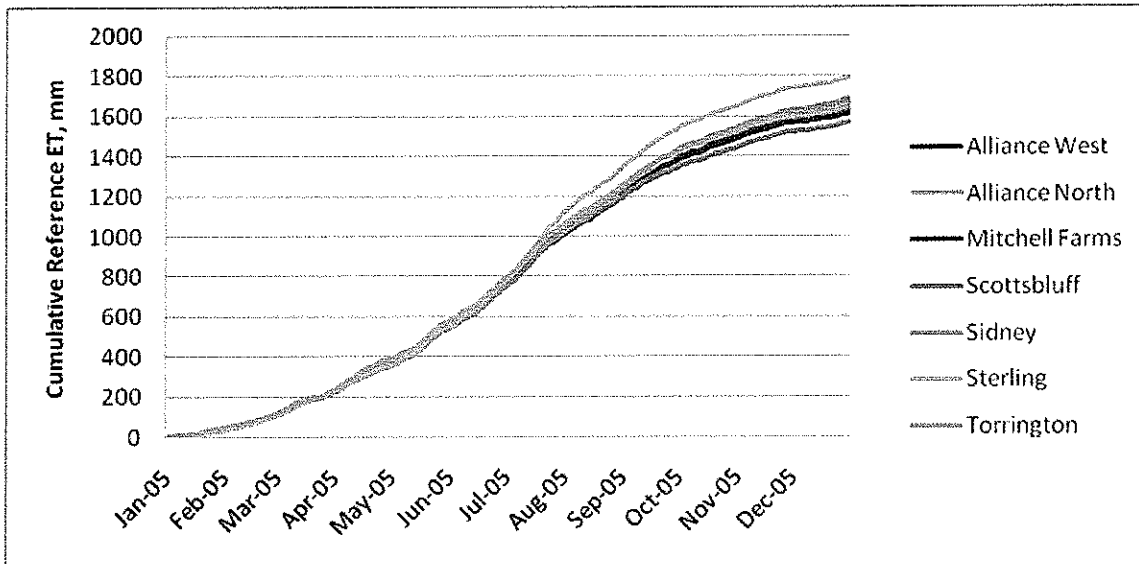


Figure 7 Daily cumulative reference ET (ET_r) from 2005 calculated from hourly weather data from the Alliance W, Alliance N, Mitchell Farms, Scottsbluff, Sidney, and Torrington HPRCC weather stations following QA/QC of weather data

References

- Allen, R.G., 1996. Assessing Integrity of Weather Data for Reference Evapotranspiration Estimation. *J. Irrig. Drain. Engr.*, 122, 97-106.
- Allen, R.G., et al., 2006. A Recommendation on the Standardized Surface Resistance for Hourly Calculation of Reference ET by the FAO56 Penman-Monteith Method *Agric. Water Manag.*, 81, 1-22.
- Allen, R.G., Tasumi, M., Morse, A., Trezza, R., Wright, J.L., Bastiaanssen, W., Kramber, W., Lorite, I., Robison, C.W., 2007a. Satellite-Based Energy Balance for Mapping Evapotranspiration with Internalized Calibration (METRIC) – Applications *J. Irrig. Drain. Engr.*, 133(4), 395-406.
- Allen, R.G., Tasumi, M., Trezza, R., 2007b. Satellite-Based Energy Balance for Mapping Evapotranspiration with Internalized Calibration (METRIC) – Model *J. Irrig. Drain. Engr.*, 133(4), 380-394.
- ASCE-EWRI, 2005. The ASCE Standardized Reference Evapotranspiration Equation. ASCE, Reston, Virginia.

APPENDIX B

Selection of Landsat Satellite Imagery for METRIC Processing

This note describes the procedure for selecting Landsat satellite images from 1997, 2002 and 2005 to be processed using the METRIC ET procedure for the Nebraska Panhandle. For this application, images from the Landsat 5 and Landsat 7 satellites were utilized due to their band combinations and high resolution. The image archive for Landsat 5 dates back to 1984 and the satellite is still in operation. Landsat 7 was launched in 1999, but the scan line corrector failed in May 2003 resulting in subsequent images having wedge shaped stripes of missing data across the scenes. There is no information contained in the stripes. The North Platte and the South Platte Natural Resource Districts (NRDs) are located in two Landsat scene path/rows, i.e. path 32 and 33, row 31.

As part of the project, three years of particular interest were identified. Because water legislation in Nebraska operates with year 1997 as a 'base' year, this year has high priority to be processed. In order to identify the two remaining years, which preferably should be a relatively wet year and a relatively dry year, each year 1997 – 2006 was assessed for the annual precipitation relative to normal precipitation values. Table 1 shows the annual precipitation at the Scottsbluff HPRCC weather station and an assessment of whether each year 1997 – 2006 is dry, average or wet.

Table 1. Precipitation at the Scottsbluff HPRCC weather station and an assessment of whether each year is dry, average, or wet relative to the normal annual rainfall of 15-16 inches.

| Year | Rainfall (inches) | Rating | Comments |
|------|-------------------|--------|-----------------------------|
| 1997 | 20 | Wet | High rainfall in April-July |
| 1998 | 17 | Avg. | Rain in April, September |
| 1999 | 17 | Avg. | Rain in April-July |
| 2000 | 15 | Avg. | |
| 2001 | 13 | Avg. | |
| 2002 | 8 | Dry | |
| 2003 | 10 | Dry | |
| 2004 | 12 | Avg. | |
| 2005 | 20 | Wet | Wet April-June |
| 2006 | 12 | Avg. | |

The most important criteria for the image selection is an assessment of cloud conditions at the time of the satellite overpass. The occurrence of conditions impeding the clearness of the

atmosphere, such as clouds (including thin cirrus clouds and jet contrails), smoke, haze and similar over the study area may render parts of an image unusable for processing in METRIC. Even very thin cirrus clouds have a much lower surface temperature than the ground surface and because METRIC needs surface temperature estimates to solve the energy balance, areas with cloud cover cannot be used in the surface energy balance estimations. In addition, in cases of partial cloud cover, land areas recently shaded by clouds may be cooler as they have not yet reached a thermal equilibrium corresponding to the clear sky energy loading, and will also have to be masked out.

To aid the selection of images an image rating system was employed, where the usability of an image in terms of cloudiness and smoke was ranked as a fraction on a scale between “0” and “1”, where “0” is an unusable image (e.g. complete cloud cover) and “1” is a nice, usable image. If an image has partial cloud cover over the study area it was rated accordingly, e.g. if an estimated 70 % of the study area or area of interest is judged to be free of clouds and cloud shadows, it may be rated 0.7.

A graphical representation of the percentage of cloud cover for each image for path 32-33, row 31 for 2002 and path 33, row 31 for 2005 is shown in Figures 1 – 3. Images were assessed using the USGS on-line image preview tool GloVis at <http://glovis.usgs.gov/>.

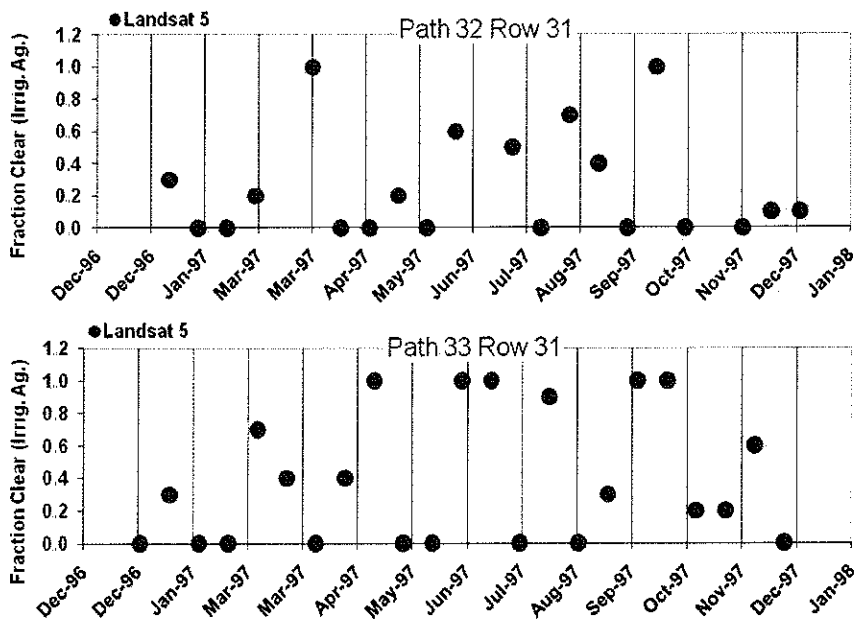


Figure 1. Usability rating of Landsat images in terms of cloudiness for path 32, row 31 (top), and path 33 row 31 (bottom) for 1997, primarily over areas of interest (irrigated areas).

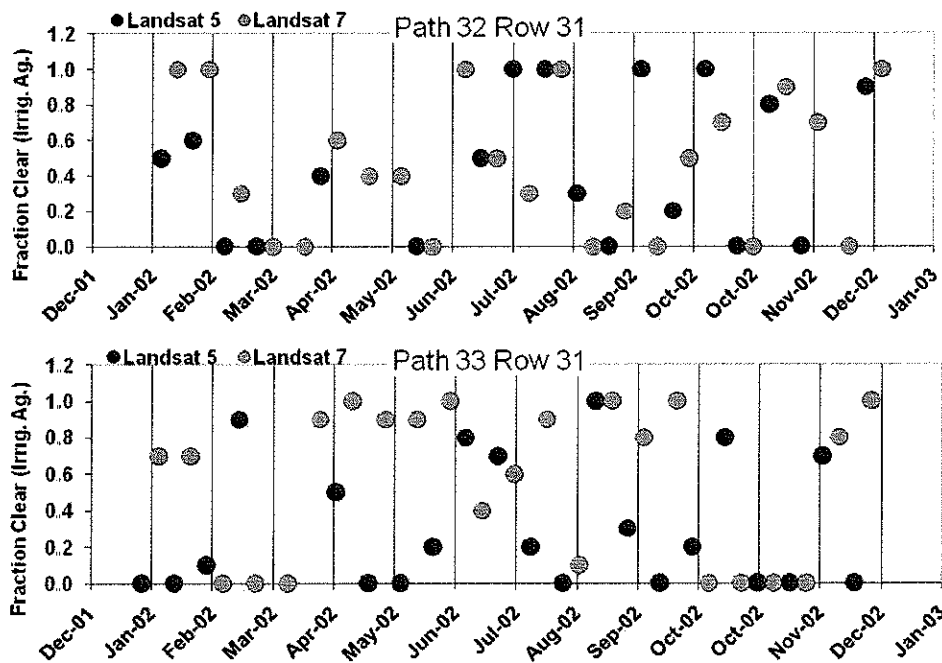


Figure 2 Usability rating of Landsat images in terms of cloudiness for path 32 row 31 (top) and path 33 row 31 (bottom) for 2002.

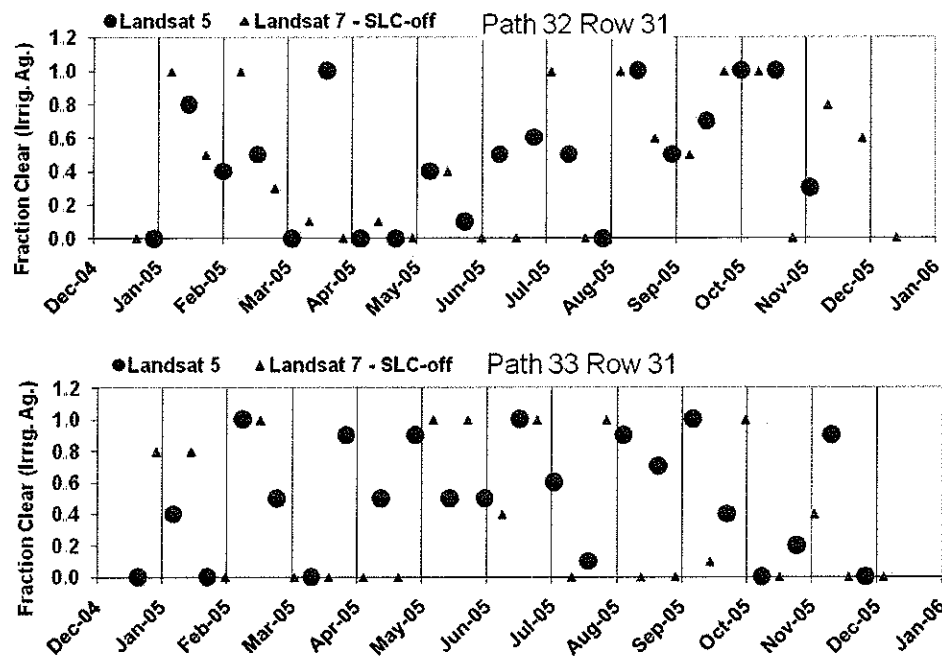


Figure 3. Usability rating of Landsat images in terms of cloudiness for path 32 row 31 (top) and path 33 row 31 (bottom) for 2005.

Images from Landsat 7 (SLC-off) are generally less suited for the METRIC processing, as portions of the image contain no data. Even though the study area is located towards the center of the image, some parts were still covered by blank areas. Due to the temporal spacing between images, it is difficult to fill these gaps, resulting in “holes” when ET calculated from each image is aggregated to monthly and seasonal ET. Information must therefore be interpolated from adjacent image dates, which causes some loss in developmental information on ET.

The image assessment in terms of cloudiness and image sequence distribution for the years 1997 – 2007 are summarized in Table 2.

Table 2. Image assessment in terms of cloudiness and sequence distribution for the years 1997 – 2007.

| Year | Image Assessment |
|------|--|
| 1997 | Path 33 has 7 good images, but nothing earlier than April 23 and 6-week gap in mid-May through June and mid-August through September. Path 32 has a 2 month gap during April - mid June and a 6 week gap during Sept.-early Oct. |
| 1998 | Path 33 has only 5 good images with 2 month gaps in April-May, July - Aug., and Oct -Nov. |
| 1999 | Path 33 has only a few good images. |
| 2000 | Path 33 is not a bad sequence, but is weak in April-May (no LS5 and partly cloudy LS7 before June 1). Good after that. Path 32 has a two-month gap during Mar -April, otherwise, good combo with LS5 and LS7. |
| 2001 | Path 33 has no LS5 before late May, weak (partly cloudy with LS7) until May 7. Good year after that path 32 is weak in Mar.-April, otherwise OK. |
| 2002 | Path 33 LS5 has 2 month gaps during April-May, June-Aug., and Aug-Sept. LS7 fills in well for the most part. Path 32 is acceptable. |
| 2003 | Path 33 has 6-week gap from mid Feb-Mar, 2 month gap in April-June (LS5) and too many cloudy LS7 dates to use. |
| 2004 | Path 33 has good LS5 except for a 2 month gap during May-June. Can use SLC-off LS7 to fill in partly. Path 32 is weak with 3 month gap mid-June – early September. |
| 2005 | Path 33 has some gaps in the Landsat sequence, but Landsat 7 can be used to fill in path 32 has mostly cloudy images between mid-March through early July. |
| 2006 | Nearly average year for precipitation, so not of interest. |
| 2007 | Project year start midway through this year, so it was not considered. |

Image selection

Based on the wet/dry year assessments and the image usability assessments, the years 1997, 2002 and 2005 were selected by UNL and UI to be processed. Path 32 generally has more clouded images compared to path 33. As a result, only one image from path 32 is available to process for the year 1997, while there are sufficient images to estimate monthly and seasonal ET estimates from path 33 in 1997.

A total of nine images from 1997, three from 2002 and three from 2005 were selected for processing by UI, Table 3, as part of the contractual partnership with UNL. The images were selected so that they were distributed as evenly as possible throughout the 1997 growing season with preferably no more than 32 days between images so as to adequately follow the evolution of vegetation development. The images from 2002 and 2005 were selected to represent early, middle and late growing season conditions, both Landsat paths and both Landsat 5 and Landsat 7 to be used for training and for comparisons to parallel processing by the University of Nebraska.

Table 3. Dates, satellite platform and path/row processed using METRIC by the University of Nebraska.

| | | | |
|-------------------|-----------|----|----|
| 4/6/2002 | Landsat 7 | 32 | 31 |
| 4/13/2002 | Landsat 7 | 33 | 31 |
| 5/8/2002 | Landsat 7 | 32 | 31 |
| 5/15/2002 | Landsat 7 | 33 | 31 |
| 5/31/2002 | Landsat 7 | 33 | 31 |
| 6/8/2002 | Landsat 5 | 33 | 31 |
| 6/9/2002 | Landsat 7 | 32 | 31 |
| 7/3/2002 | Landsat 5 | 32 | 31 |
| 7/18/2002 | Landsat 7 | 33 | 31 |
| 7/27/2002 | Landsat 7 | 32 | 31 |
| 8/11/2002 | Landsat 5 | 33 | 31 |
| 8/19/2002 | Landsat 7 | 33 | 31 |
| 9/4/2002 | Landsat 7 | 33 | 31 |
| 9/5/2002 | Landsat 5 | 32 | 31 |
| 9/20/2002 | Landsat 7 | 33 | 31 |
| 10/7/2002 | Landsat 5 | 32 | 31 |
| 10/14/2002 | Landsat 5 | 33 | 31 |
| 4/13/2005 | Landsat 5 | 33 | 31 |
| 5/15/2005 | Landsat 5 | 33 | 31 |
| 5/31/2005 | Landsat 5 | 33 | 31 |
| 7/2/2005 | Landsat 5 | 33 | 31 |
| 7/10/2005 | Landsat 7 | 33 | 31 |
| 8/19/2005 | Landsat 5 | 33 | 31 |
| 8/28/2005 | Landsat 5 | 33 | 31 |
| 9/20/2005 | Landsat 5 | 33 | 31 |
| 10/14/2005 | Landsat 7 | 33 | 31 |

APPENDIX C

Preparation of Digital Elevation Model and Land Use Map

The land use maps and elevation maps considered for the METRIC processing of the Landsat images from paths 32/33, row 31 for the North Platte and South Platte NRDs application are described below. Figure 1 illustrates the area covered by the Landsat scenes, and includes most of the Nebraska Panhandle, a portion of south-east Wyoming, and part of north-east Colorado.

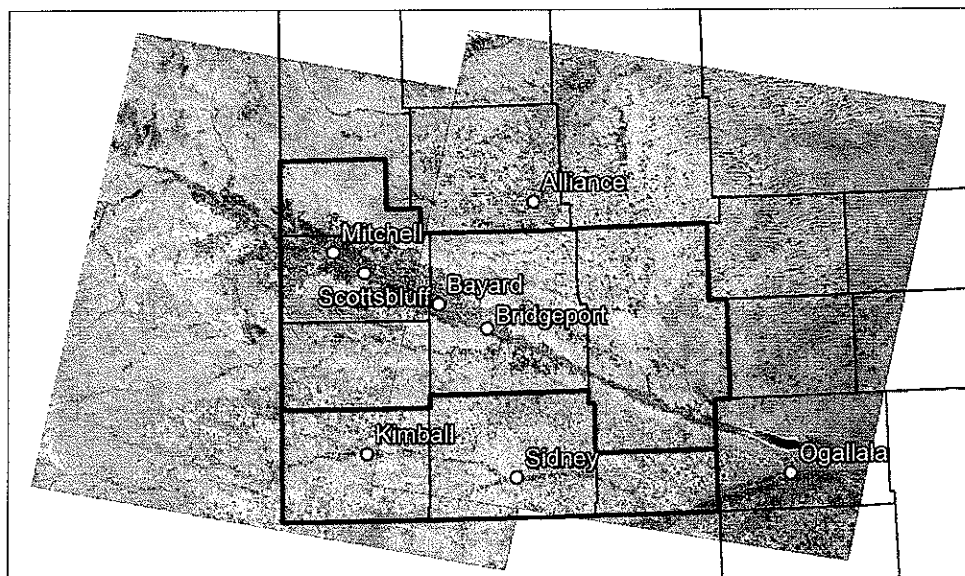


Figure 1 Example of the extent of the Landsat images for path 33 row 31 (8/11/2002) and for path 32 row 31 (9/5/2002) showing the county boundaries (black lines) and the boundaries of the North Platte and South Platte Natural Resource Districts (NRDs) (blue lines)

Digital Elevation Model

The Digital Elevation Model (DEM) used was obtained from the EROS Data Center Seamless Data Distribution System (<http://seamless.usgs.gov/>) national elevation dataset (NED). The DEM data were downloaded as GeoTiff format in 1 arc second (30 meter) resolution. The extent of the DEM encompassed an area larger than the extent of Landsat paths 32-33 and row 31 (figure 1). Because of limitations on spatial extent due to file size, the data were downloaded as smaller map sections of the overall study area. These smaller map sections were then mosaicked, or stitched together in order to provide a single, seamless dataset. The mosaicked DEM image was then reprojected to the same map projection as that of the Landsat

imagery using the nearest neighbor resampling method. The DEM used for 2002 is shown in Figure 2.

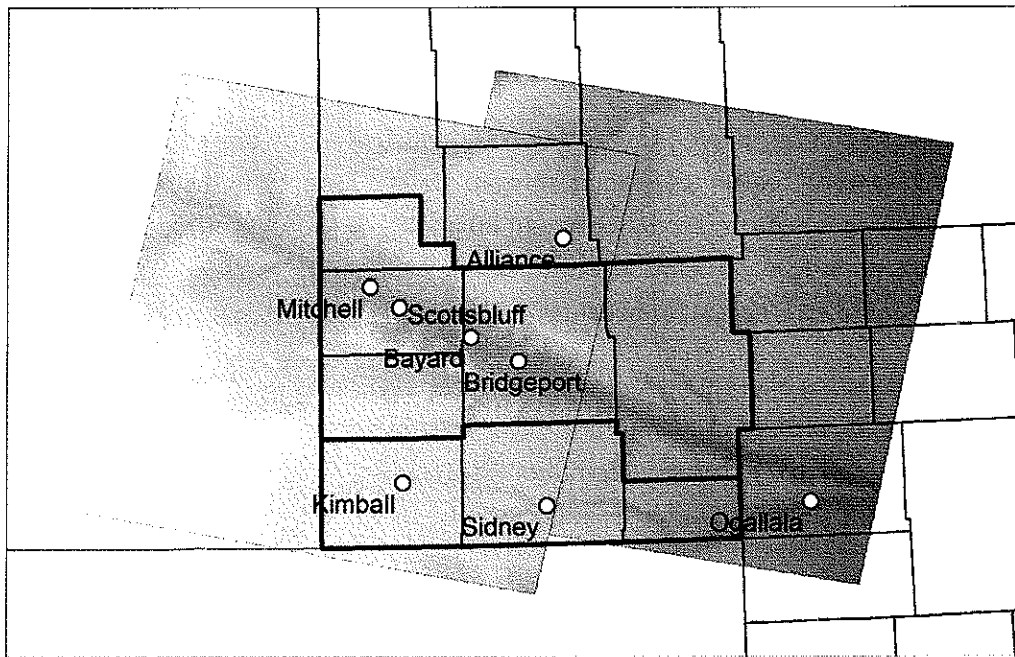


Figure 2. Example of the DEM used for path 32-33 in 2002. Lighter shades indicate higher elevation and darker shades represent lower elevation. County boundaries (black lines) and the boundaries of the North Platte and South Platte NRDs (blue lines) are shown.

Land Use Map

Three options of land use maps at 30 m resolution were considered. The three maps have been produced for different applications and purposes.

1. COHYST land use maps

The Cooperative Hydrology Study (COHYST) was carried out in order to improve the understanding of the hydrological and geological conditions, and to address endangered species issues along the Platte River watershed. One of the outcomes from COHYST was the generation of land use maps for the study area. The land use maps were based on Landsat 5 satellite imagery and a classification was done for the years 1997, 2001 and 2005. The study area stretched between Columbus, NE in the east and the western border of Nebraska near Scottsbluff. The land use classes developed for COHYST were primarily focused on agricultural land cover patterns and identifying individual crop types.

The area being studied in this project is Kimball, Cheyenne and Deuel Counties (South Platte NRD) and Banner, Morrill, Scotts Bluff, Garden and the south portion of Sioux Counties (North Platte NRD) The SP-NRD and NP-NRD study area is almost entirely covered by the COHYST land use maps except the far NE corner of Garden County.

The classification system employed in the COHYST land use maps are shown in Table 1 The primary objective when creating the land use map was to identify individual crop types. The classification accuracy is reported to be between 80 and 82 %. More information about COHYST, the land use maps and the classification system can be found on:

<http://www.calmit.unl.edu/cohyst/index.shtml>.

A land use map covering the entire state for the year 2005 was prepared by CALMIT in 2007. The classification followed the principles and classification system as employed during the 2001 COHYST land use mapping. For more information see:

<http://www.calmit.unl.edu/2005landuse/index.shtml>.

2. NE GAP land use map

The Nebraska Gap Analysis Program (NE GAP) land use classification is part of a nationwide effort seeking to “identify the degree to which all native plant and animal species and natural communities are or are not represented in our present-day mix of conservation lands”. GAP maps are produced by each state based on guide lines established by the USGS Biological Resources Division. One of the primary objectives during the NE GAP was to identify and distinguish between natural vegetation. The Nebraska GAP map used in conjunction with the METRIC application for the Nebraska Panhandle was developed by CALMIT at UNL in 2005 using Landsat imagery acquired from 1991-1993. More information about the Nebraska GAP project can be found at <http://www.calmit.unl.edu/gap/>. Land use classes for the Nebraska GAP land use map are shown in Table 1

3. NLCD land use map

The USGS generated the 2001 National Land Cover Database (NLCD) based on numerous data sources including, Landsat 5 and 7 imagery collected from 2001, DEM, GAP data, and National Agricultural Statistics Service (NASS) cropland data. The land use classes occurring in Nebraska are shown in Table 1. The NLCD land cover classification is identical for the United States and the classification lacks detail (e.g., vegetation type for agricultural land use, and areas with natural vegetation). More information about the land use system can be found at:

<http://landcover.usgs.gov/usgslandcover.php>.

4 Generation of a composite land use map

Due to need to maintain the greatest amount of detail in land cover maps used in METRIC, a composite map was generated combining the strengths of all three land use maps. For areas outside of the Nebraska state boundary, the NLCD data were used. While the NLCD data are accurate, it lacks the added detail describing land use classes. While the NLCD map describes the land use of, for example, rangeland as “grassland”, the NE GAP map describes the same land use class into six different categories. Because of this, detail is lost when using the NLCD map compared to the GAP and COHYST maps.

This same reasoning applies to the COHYST and GAP classifications. The COHYST map has a greater amount of detail (describes more land use classes) for agricultural areas, whereas the GAP map has a greater amount of detail for natural vegetation areas. Because of this, the Nebraska GAP map was used for non-agricultural classes and the COHYST map was used for agricultural classes.

Due to the different land use systems having the same values for different classes, NE GAP and NE COHYST values were changed. For the GAP data, a value of 100 was added to each class. For the COHYST data, a value of 120 was added to each class. Land use classes for non-agricultural classes in the COHYST data were not used in the new composite land use map and agricultural land use classes in the GAP map were not used. The land use composite map for 2002 is shown in Figure 3.

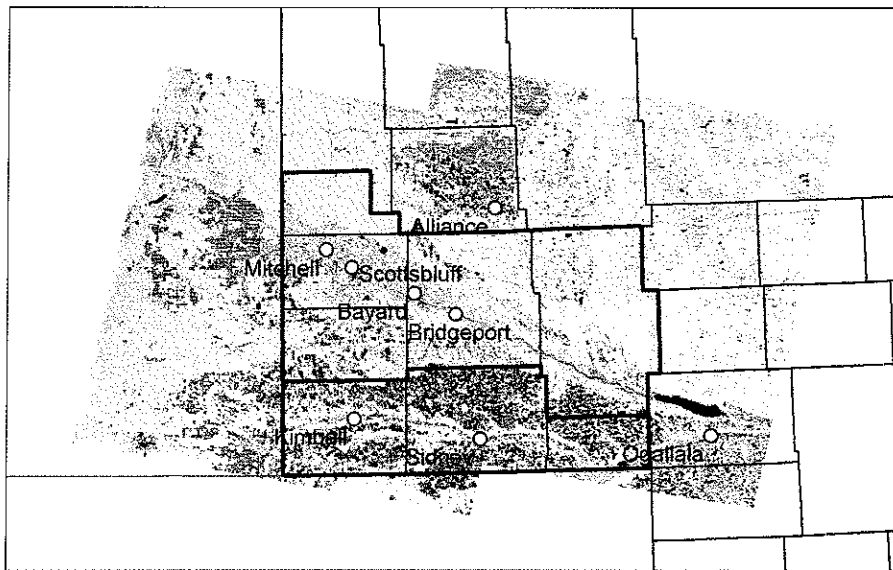


Figure 3 The land use composite map used in the METRIC application for 2002. County boundaries (black lines) and the boundaries of the North Platte and South Platte NRDs (blue lines) are shown.

Table 1. Land use classes of NLCD, Nebraska GAP, and COHYST with original class values and new class values.

| New Class Value | Original Class Value | Class Name | Data Set | Year |
|-----------------|----------------------|--------------------------------------|-----------|-----------|
| 0 | 0 | Background | NLCD | 2001 |
| 11 | 11 | Water | NLCD | 2001 |
| 21 | 21 | Developed, open space | NLCD | 2001 |
| 22 | 22 | Developed, low density | NLCD | 2001 |
| 23 | 23 | Developed, medium density | NLCD | 2001 |
| 24 | 24 | Developed, high density | NLCD | 2001 |
| 31 | 31 | Barren land | NLCD | 2001 |
| 41 | 41 | Deciduous forest | NLCD | 2001 |
| 42 | 42 | Evergreen forest | NLCD | 2001 |
| 43 | 43 | Tall trees | NLCD | 2001 |
| 52 | 52 | Shrub | NLCD | 2001 |
| 71 | 71 | Grassland | NLCD | 2001 |
| 81 | 81 | Pasture/hay | NLCD | 2001 |
| 82 | 82 | Cultivated crops | NLCD | 2001 |
| 90 | 90 | Woody wetlands | NLCD | 2001 |
| 95 | 95 | Emergent herbaceous wetland | NLCD | 2001 |
| 101 | 1 | Ponderosa Pine Forests and Woodlands | NE GAP | 1991-1993 |
| 102 | 2 | Deciduous Forest/Woodlands | NE GAP | 1991-1993 |
| 103 | 3 | Juniper Woodlands | NE GAP | 1991-1993 |
| 104 | 4 | Sandsage Shrubland | NE GAP | 1991-1993 |
| 105 | 5 | Sandhills Upland Prairie | NE GAP | 1991-1993 |
| 106 | 6 | Lowland Tallgrass Prairie | NE GAP | 1991-1993 |
| 107 | 7 | Upland Tallgrass Prairie | NE GAP | 1991-1993 |
| 108 | 8 | Little Bluestem-Gamma Mixedgras | NE GAP | 1991-1993 |
| 109 | 9 | Western Wheatgrass Mixedgrass Pr | NE GAP | 1991-1993 |
| 110 | 10 | Western Shortgrass Prairie | NE GAP | 1991-1993 |
| 111 | 11 | Barren/Sand/Outcrop | NE GAP | 1991-1993 |
| 0 | 12 | Agricultural Fields | NE GAP | 1991-1993 |
| 113 | 13 | Open Water | NE GAP | 1991-1993 |
| 0 | 14 | Fallow Agricultural Fields | NE GAP | 1991-1993 |
| 115 | 15 | Aquatic Bed Wetland | NE GAP | 1991-1993 |
| 116 | 16 | Emergent Wetland | NE GAP | 1991-1993 |
| 117 | 17 | Riparian Shrubland | NE GAP | 1991-1993 |
| 118 | 18 | Riparian Woodland | NE GAP | 1991-1993 |
| 119 | 19 | Low Intensity Residential | NE GAP | 1991-1993 |
| 120 | 20 | Commercial/Industrial/Transporta | NE GAP | 1991-1993 |
| 121 | 1 | Irrigated Corn | NE COHYST | 2005 |
| 122 | 2 | Irrigated Sugar Beets | NE COHYST | 2005 |
| 123 | 3 | Irrigated Soybeans | NE COHYST | 2005 |
| 124 | 4 | Irrigated Sorghum (Milo, Sudan) | NE COHYST | 2005 |
| 125 | 5 | Irrigated Dry Edible Beans | NE COHYST | 2005 |
| 126 | 6 | Irrigated Potatoes | NE COHYST | 2005 |
| 127 | 7 | Irrigated Alfalfa | NE COHYST | 2005 |
| 128 | 8 | Irrigated Small Grains | NE COHYST | 2005 |
| 0 | 9 | Range, Pasture, Grass (Brome, Ha | NE COHYST | 2005 |
| 0 | 10 | Urban Land | NE COHYST | 2005 |
| 0 | 11 | Open Water | NE COHYST | 2005 |
| 0 | 12 | Riparian Forest and Woodlands | NE COHYST | 2005 |
| 0 | 13 | Wetlands | NE COHYST | 2005 |
| 134 | 14 | Other Ag Land (farmstead, feed | NE COHYST | 2005 |
| 135 | 15 | Irrigated Sunflower | NE COHYST | 2005 |

| | | | | |
|-----|----|--------------------------|-----------|------|
| 136 | 16 | Summer Fallow | NE COHYST | 2005 |
| 0 | 17 | Roads | NE COHYST | 2005 |
| 138 | 18 | Dryland Corn | NE COHYST | 2005 |
| 139 | 19 | Dryland Soybeans | NE COHYST | 2005 |
| 140 | 20 | Dryland Sorghum | NE COHYST | 2005 |
| 141 | 21 | Dryland Dry Edible Beans | NE COHYST | 2005 |
| 142 | 22 | Dryland Alfalfa | NE COHYST | 2005 |
| 143 | 23 | Dryland Small Grains | NE COHYST | 2005 |
| 144 | 24 | Dryland Sunflower | NE COHYST | 2005 |

APPENDIX D

Treatment of Cloud Cover in Satellite Imagery

Landsat satellites capture images every 16 days, providing 2-4 images per month. However, due to frequent cloud cover less imagery is often available. METRIC is unable to estimate ET in imagery with cloud covered areas, including cloud shadows, jet contrails, smoke, and other major atmospheric phenomena. The ET_rF estimates for these areas do not represent ET_rF values at the land surface due to the cooler temperatures measured by the satellite sensor for cloud and cloud shadows and can lead to overestimation of ET. Because of this, these areas with cloud cover must be manually identified and digitally removed, or masked out.

Cloud identification was carried out visually for each image based on different band combinations in the original Landsat image. Areas of cloud cover were then manually traced, including areas of up to a kilometer cloud and cloud shadow areas to ensure any atmospheric influences are not included.

The methodology for cloud filling was carried out on 15 of 26 Landsat images (table 1). The cloud filling approach used linear interpolation based on ET_rF and NDVI to borrow values from previous available and next available cloud-free ET_rF images (figure 1). The interpolation is adjusted based on a weighted temporal distance between images.

Table 1. Dates and Landsat path/row of imagery in which cloud filling method was applied

| Date | Path/Row | Date | Path/Row |
|------------|----------|-----------|----------|
| 4/6/2002 | 32/31 | 5/15/2005 | 33/31 |
| 5/8/2002 | 32/31 | 5/31/2005 | 33/31 |
| 7/27/2002 | 32/31 | 7/2/2005 | 33/31 |
| 4/13/2002 | 33/31 | 7/10/2005 | 33/31 |
| 5/15/2002 | 33/31 | 8/19/2005 | 33/31 |
| 5/31/2002 | 33/31 | | |
| 6/8/2002 | 33/31 | | |
| 7/18/2002 | 33/31 | | |
| 9/4/2002 | 33/31 | | |
| 10/14/2002 | 33/31 | | |

In addition, the cloud filling method adjusted for differences in background ET_rF values between interpolated images. In order to do this, the FAO-56 K_e evaporation model was run on a daily basis using precipitation and ET_r inputs to estimate daily evaporation from wet soil. The K_e estimated for each image date is assigned as the background ET_rF for bare soil in that image. In

the following description, image $i-1$ is referred to as image 1, image i is referred to as image 2, and image $i+1$ is referred to as image 3.

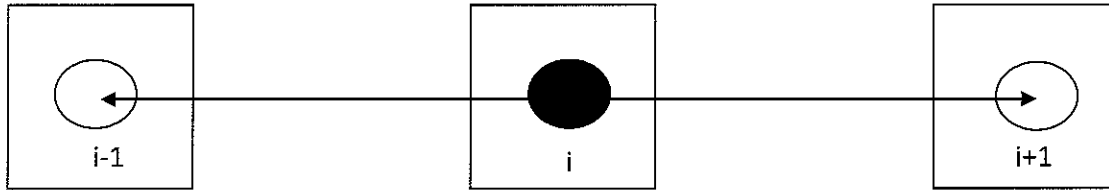


Figure 1. Cloud filling approach. Let ‘ i ’ be the image having cloud masked areas being filled from adjacent images (image 2). Let ‘ $i-1$ ’ (image 1) be the image earlier than image i . Let ‘ $i+1$ ’ (image 3) be the image later than image i .

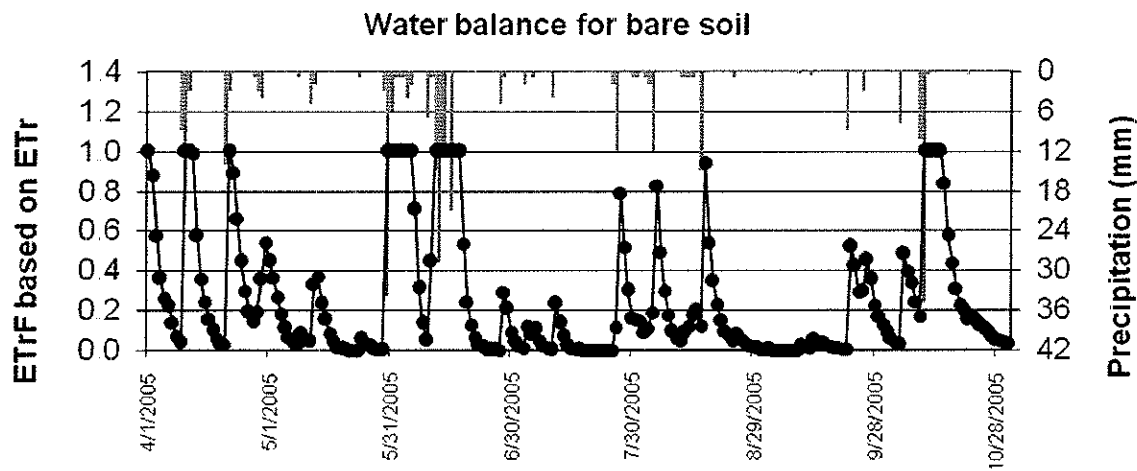


Figure 2. Soil water balance for upper 0.125 m of soil calculated from meteorological data from Scottsbluff AWDN station for 2005.

From the daily soil evaporation model, bare soil ET_{rF1} , ET_{rF2} , and ET_{rF3} were determined (figure 2). We plotted these values of ET_{rF} vs. NDVI, using NDVI representing bare soil conditions which is normally $\sim 0.15-0.2$ (figure 3). Values for ET_{rF} vs. NDVI representing full vegetation cover were plotted as well. Full cover ET_{rF} values are generally 1.05 in METRIC and full cover NDVI values are generally 0.8 (Allen et al., 2010). The reader should note that the full-cover point of ET_{rF} vs. NDVI is common to all three images.

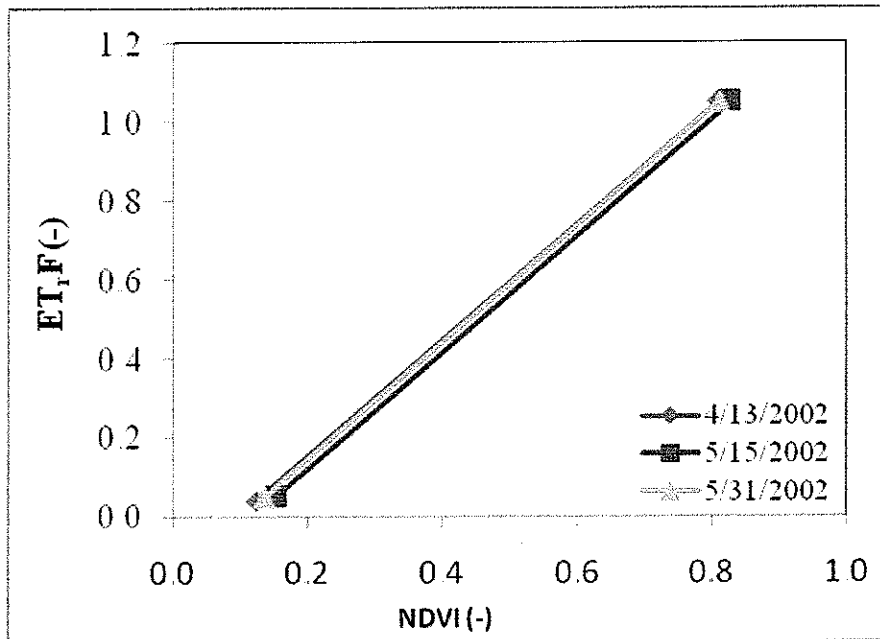


Figure 3. The relationship between ET,F vs $NDVI$ for Landsat images 4/13, 5/15, and 5/31 for. The background ET,F values represent ET,F from bare soil. The ET,F at full ground cover is 1.05.

After placing the four points on the plot, equations describing a relationship between ET,F and $NDVI$ for each image can be determined as:

$$ETrF1 = a1 + b1 NDVI$$

$$ETrF2 = a2 + b2 NDVI$$

$$ETrF3 = a3 + b3 NDVI$$

where

$$b1 = (ETrF_{full\ cover} - ETrF1) / (NDVI_{full\ cover} - NDVI_{bare\ soil})$$

$$a1 = ETrF_{full\ cover} - b1 NDVI_{full\ cover}$$

(1)

(2a)

$$b2 = (ETrF_{full\ cover} - ETrF2) / (NDVI_{full\ cover} - NDVI_{bare\ soil})$$

$$a2 = ETrF_{full\ cover} - b2 NDVI_{full\ cover}$$

(2b)

$$b3 = (ETrF_{full\ cover} - ETrF3) / (NDVI_{full\ cover} - NDVI_{bare\ soil})$$

$$a3 = ETrF_{full\ cover} - b3 NDVI_{full\ cover}$$

(2c)

These relationships correspond to expected average ET,F given $NDVI$ under rain fed conditions. Increased evaporation from irrigation cannot be detected. The differences between $ET,F1$ and $ET,F2$ and between $ET,F3$ and $ET,F2$ represent the amount of adjustment that was made to the $ETrF1$ and $ETrF3$ values borrowed from image 1 and image 3. The adjustment is greatest for

bare soil conditions and reduces to 0 for full ground cover conditions. The ET_rF_2 is estimated from ET_rF_1 and ET_rF_3 as (Allen, 2010):

$$ET_rF_2 = \frac{\Delta t_2 (ET_rF_1 + a_2 - a_1 + [b_2 - b_1]NDVI_1) + \Delta t_1 (ET_rF_3 + a_2 - a_3 + [b_2 - b_3]NDVI_3)}{\Delta t_1 + \Delta t_2}$$

where Δt_1 is the time difference between image i-1 and image i and Δt_2 is the time difference between image 1 and image 2. The $NDVI_1$ and $NDVI_3$ are the NDVI values borrowed from the two source images

The result of this cloud filling method will be a complete filled-in image for ETrF on day 'i' where values for all pixels are similar to the previous precipitation for that image. Note that any ETrF for a pixel in image 1 or 3 that is in excess of the ETrF predicted by the NDVI based equations may be due to irrigation effects. These effects will remain in the ETrF value as it is interpolated to image 2. This transfer is beneficial, for the most part, since irrigation impacts will remain embedded in the particular pixel. However, the process assumes that the irrigation effects are similar among the images for any particular pixel (Allen, 2010).

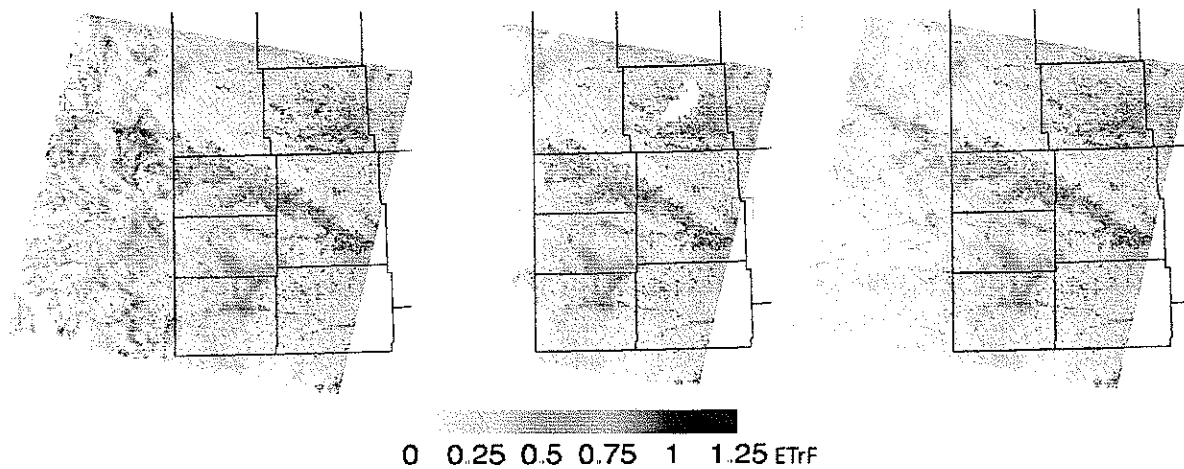


Figure 4. Sequence showing cloud filling process for July 10, 2005. The left image shows the cloud contamination (high ET_rF values and white areas) near the left edge of the image. The center image shows the area that was masked out in white (left part of image and area near top right corner). The right image shows the filled-in cloud area carried out using the cloud filling method.

References

Allen, R. 2010. Procedures for adjusting METRIC-derived ETrF images for background evaporation from precipitation events prior to cloud filling and Interpretation of ET between image dates. Internal memo, University of Idaho 11 pages

APPENDIX E

FAO 56 modified water balance using ArcGIS 9.x

Parikshit Ranade and Ayse Irmak

Purpose:

The purpose of this document is to illustrate, in detail, the procedure for running a modified FAO 56 water balance using ArcGIS 9.x. The modified FAO 56 water balance (MFWB) is used to create spatial grids of daily water balance parameters. This document illustrates the procedure of acquisition, creation, processing, storage of raw spatial data required to run MFWB in ArcGIS9.x. Various scripts and tools are required to perform these tasks in ArcGIS 9.x.

System Requirements:

Windows PC/Mac with ArcGIS 9.x version (with spatial analyst extension)

Microsoft® .NET Framework, version 2.0

ArcGIS Tools and scripts

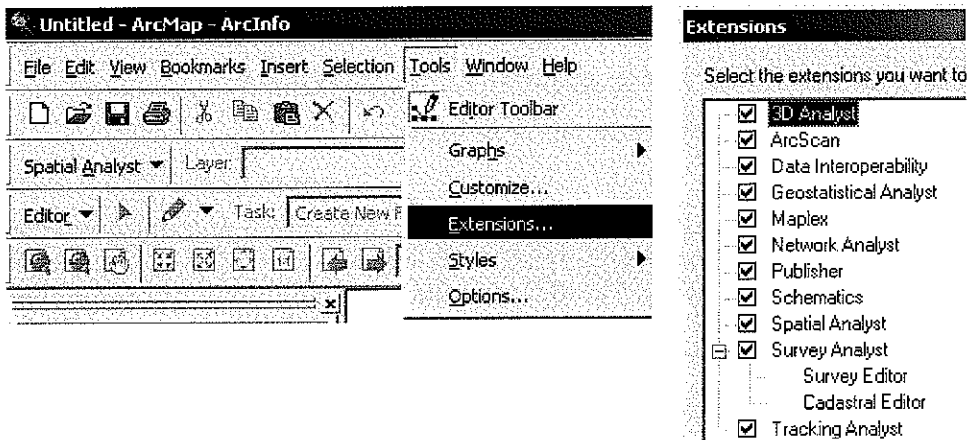
- *NRCS Soil Data Viewer* – Custom ArcGIS tool will be used to create soil data layers from SSURGO database.
- *HIS tools* - Perform various preprocessing tasks and run MFWB model in ArcGIS 9.x.


Getting ArcGIS ready

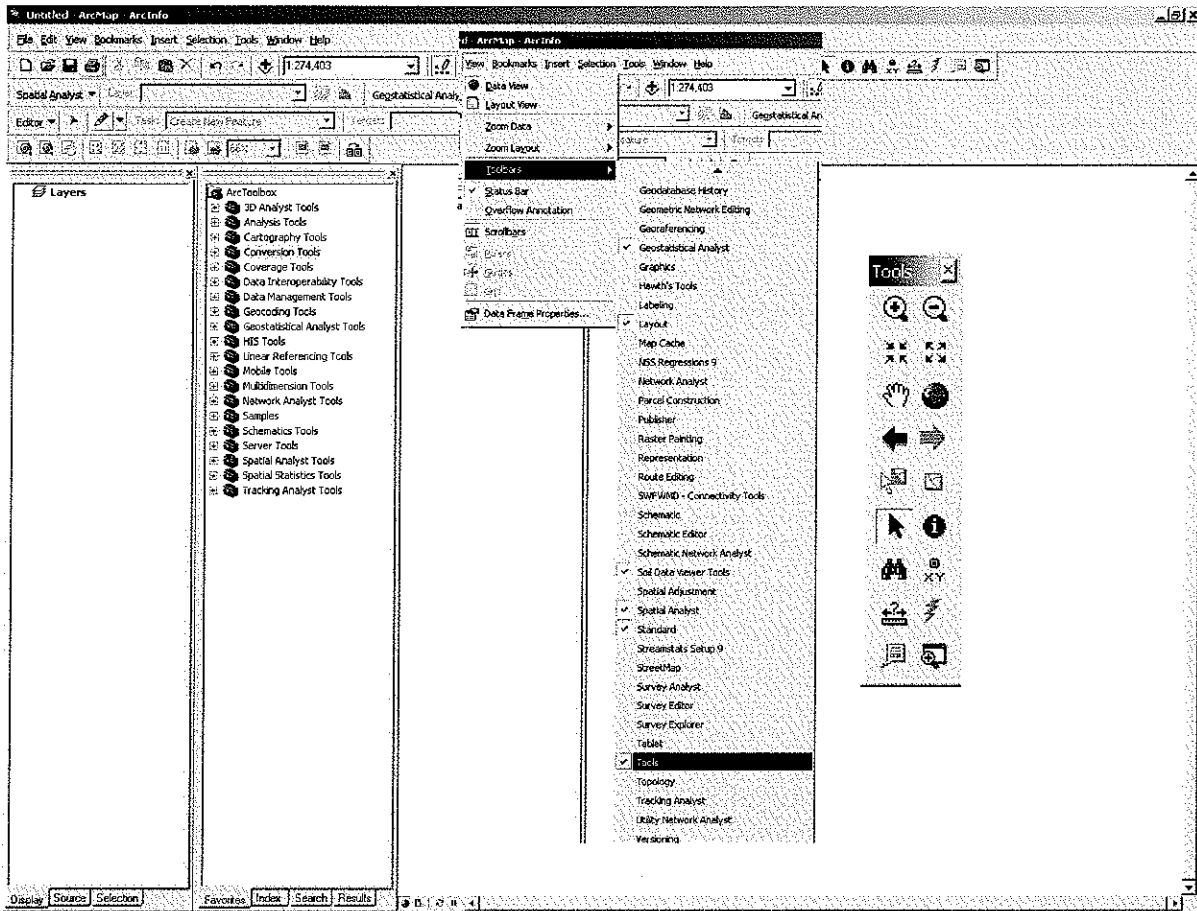
If the user is new to ArcGIS desktop software, it is recommended that one go through the tutorial 'getting started' and 'ArcMap'


(<http://webhelp.esri.com/arcgisdesktop/9.2/index.cfm?TopicName=Tutorials>) Also visit <http://resources.esri.com> for more information

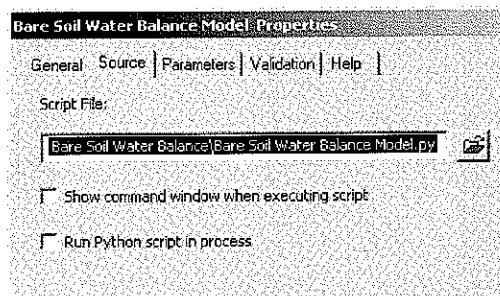
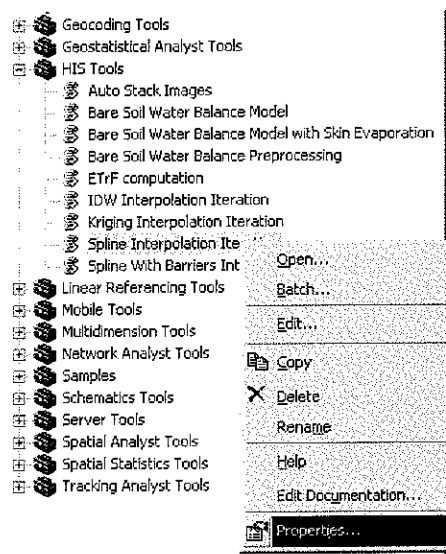
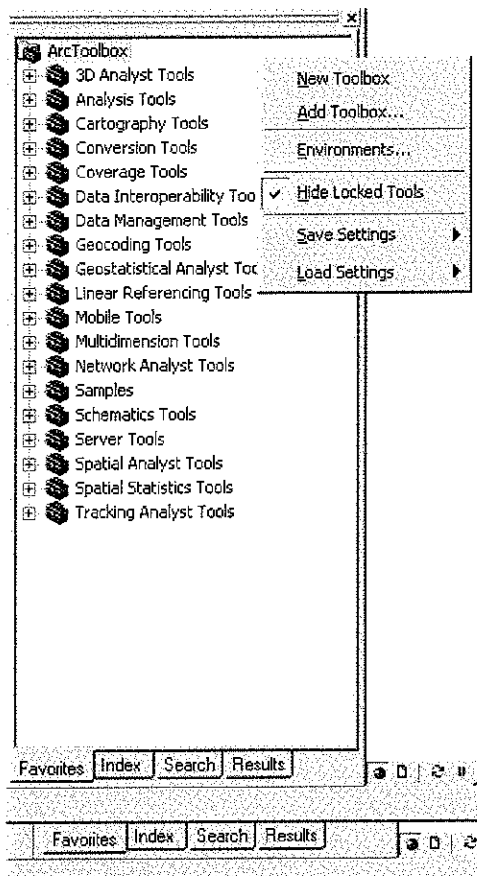
Open ArcMap. Make sure required extensions are enabled. Go to **Tool\Extensions**. Check '**Spatial analyst**' and '**Geostatisticalanalyst**'.



Download the Soil data viewer (<http://soils.usda.gov/sdv/download.html>) compatible with the ArcGIS version. Install Soil data viewer (make sure ArcGIS is closed when you install the soil data viewer. Actual use of the tool will be illustrated in following sections of the document. Make sure to close ArcGIS program while you install the Soil Data Viewer tool Refer to “**Soil Data Viewer 5.x User Guide**” for detail. Go to **View\Toolbar\Soil Data Viewer Tools**. Symbol  will appear on the screen which is your Soil Data Viewer toolbar. In the coming section we will learn how to use this tool



Now let's bring the HIS toolbox in ArcGIS. Click on  ArcToolbox symbol to open the ArcToolbox. Right click anywhere in ArcToolbox area and click on "Add Toolbox". Browse to the folder where you have saved **HIS Tools.tbx** file. Expand the HIS tool toolbox to explore the scripts and tools. Right click on each script/tool. **Go to properties\source, check if you have right pathname for Python file for script.** If the file path is wrong or does not exist you will get the error message -"**ERROR 000576: Script associated with this tool does not exist.**"



Spatial data creation

All the data required to run MFWB model should be in ArcGIS compatible raster and vector format. Weather and soil data can be downloaded from various sources including local/state and national agencies. See appendix for more information. **It is important to have all the spatial data in same coordinate system to avoid error.**

Weather

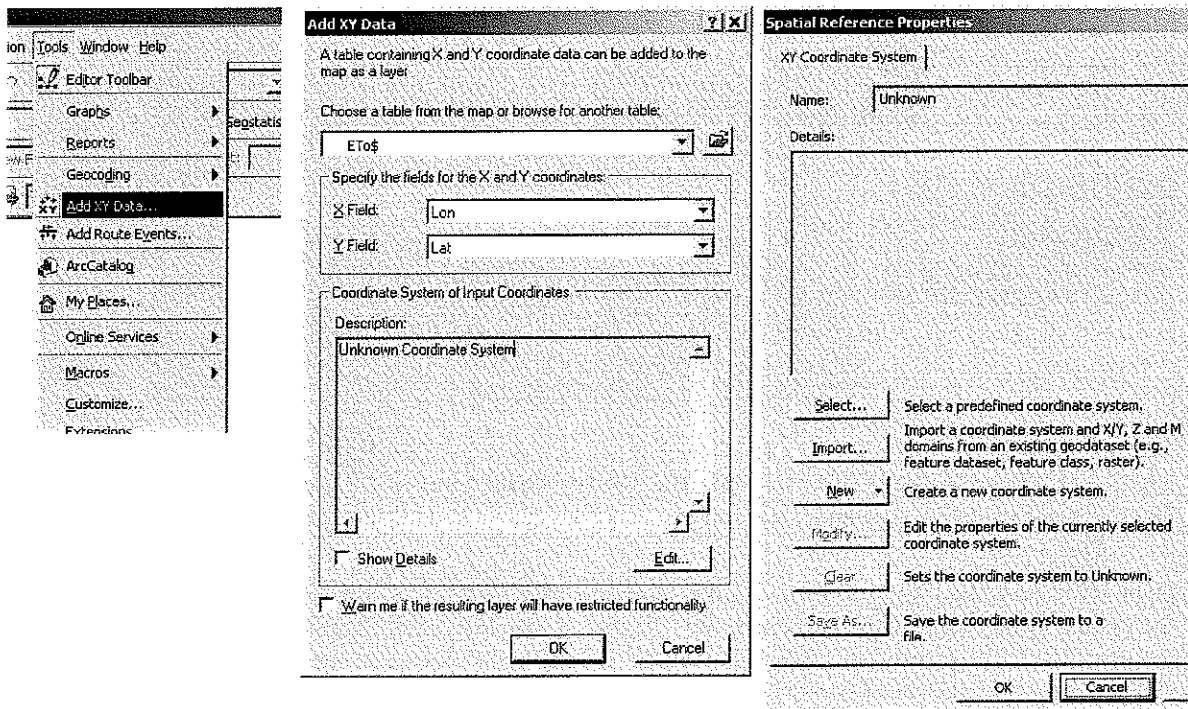
We require precipitation and rainfall data for the daily time step. The data can be obtained from National Climate Data Center (<http://www.ncdc.noaa.gov/>) or High Plains Regional Climate Center (<http://www.hprcc.unl.edu/>) or any other source. Reference evapotranspiration (ET_r) can be computed from the weather data using various methods. Refer to the RefETI program developed at the University of Idaho for more information on computation of ET_r (<http://www.kimberly.uidaho.edu/ref-et/>).

Data can be processed in Microsoft Excel sheet to bring it into the following format. Each row should contain the information for single point (weather station) including latitude, longitude and precipitation/ET_r data. **It is required that daily data in Excel is in chronological order** i.e. Jan 2nd cannot be before Jan 1st. These column headings are referred to as 'Field Names' in ArcGIS. It is good practice to include Station ID and Elevation information as well for each weather station. Save this file in both Excel 2003 and 2007 format. If you using ArcGIS9 1 you need to save it in dbf format.

| | A | B | C | D | E | F | G | H | I | J |
|----|------------|-----------------|----------|-----------|-------|-------|-------|-------|-------|-------|
| 1 | Station ID | Name | Latitude | Longitude | 1-Jan | 2-Jan | 3-Jan | 4-Jan | 5-Jan | 6-Jan |
| 2 | 1 | KEARNEY | 40.72 | -99.02 | 21.8 | 17.0 | 0.8 | 0.0 | 0.0 | 0.0 |
| 3 | 2 | MINDEN | 40.52 | -99.05 | 30.0 | 20.3 | 0.0 | 0.0 | 0.0 | 0.0 |
| 4 | 3 | SHELTON | 40.73 | -98.75 | 14.7 | 6.9 | 0.5 | 0.0 | 0.0 | 0.0 |
| 5 | 4 | HOLDREGE 4N | 40.50 | -99.35 | 7.9 | 9.9 | 0.0 | 0.0 | 0.0 | 0.0 |
| 6 | 5 | SMITHFIELD | 40.58 | -99.67 | 1.0 | 0.3 | 0.0 | 0.0 | 0.0 | 0.0 |
| 7 | 6 | GRAND ISLAND | 40.88 | -98.50 | 13.0 | 5.6 | 0.3 | 0.0 | 0.0 | 0.0 |
| 8 | 7 | LEXINGTON | 40.77 | -99.73 | 15.5 | 0.0 | 0.0 | 0.0 | 0.0 | 0.0 |
| 9 | 8 | COZAD | 40.97 | -99.95 | 41.7 | 0.0 | 0.0 | 0.0 | 0.0 | 0.0 |
| 10 | 9 | CLAY CENTER(SC) | 40.57 | -98.13 | 25.4 | 12.7 | 0.8 | 0.0 | 0.0 | 0.0 |
| 11 | 10 | GOTHENBURG | 40.95 | -100.18 | 28.1 | 0.0 | 0.0 | 0.0 | 0.0 | 0.0 |
| 12 | 11 | MERNA | 41.45 | -99.77 | 29.0 | 0.0 | 0.0 | 0.0 | 0.0 | 0.0 |
| 13 | 12 | ORD | 41.62 | -98.93 | 33.8 | 11.2 | 0.0 | 0.0 | 0.0 | 0.0 |
| 14 | 13 | CENTRALCITY | 41.15 | -97.97 | 21.3 | 4.3 | 3.8 | 0.0 | 0.0 | 0.0 |
| 15 | 14 | CURTISUNSTA | 40.63 | -100.50 | 15.8 | 0.0 | 0.0 | 0.0 | 0.0 | 0.0 |

Now we will import this data in ArcGIS point shapefile. Go to Tools\Add XY data. Choose the excel sheet path, latitude (Y) and longitude (X) correctly. Click on the 'Edit' button to select appropriate coordinate system. **It is advisable to use UTM coordinate system to have distance units in meters. Make sure to convert coordinates to UTM coordinate system before you add it to excel sheet. See appendix for more information on coordinate conversion**

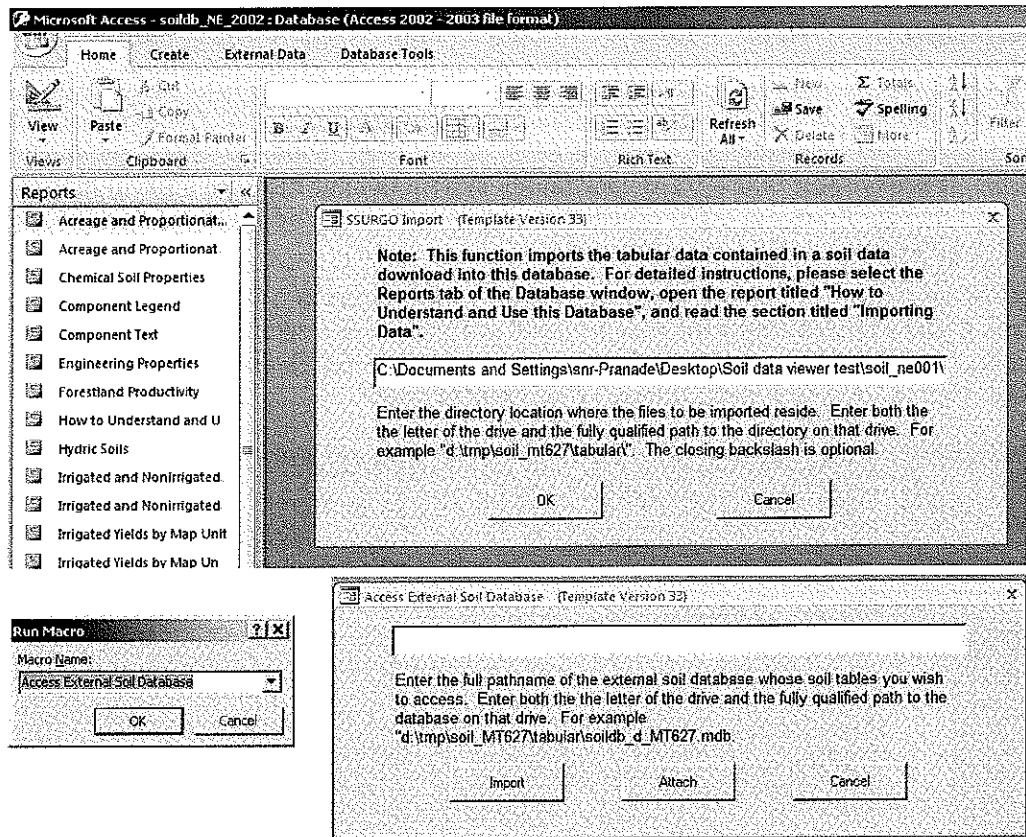
You can select the appropriate UTM zone and datum using 'select' button or 'import' it from another ArcGIS file with UTM coordinate system. Now you will see your data displayed in ArcGIS. Right click on the layer, click **Data\Export Data...** to save it as point shapefile. Make sure to export '**All features**' and use coordinate system same as '**this layer's source data**'.





Soil

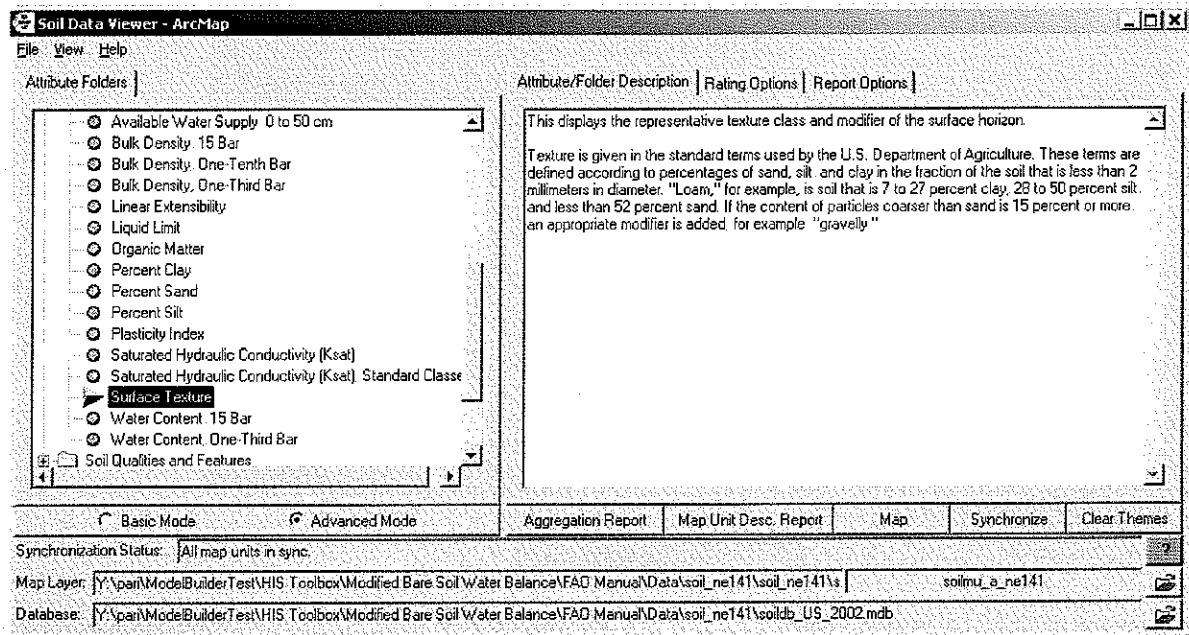
Soil data can be obtained from detail Soil Survey Geographic (SSURGO) or more general State Soil Geographic (STASGO). SSURGO data can be downloaded from soil data mart (<http://soildatamart.nrcs.usda.gov/>) for each county. Dataset for entire state can be downloaded from Geospatial data gateway (<http://datagateway.nrcs.usda.gov/>). Procedure for creating SSURGO soil data maps using Soil Data Viewer is explained in below.

First import the tabular SSURGO data into Microsoft access using inbuilt Macros. Make sure your Microsoft access security is set to allow the Macro content (otherwise you will see the message “Action failed”. If macro is not automatically enabled go to **Database tools/Run Macro Run “Access External Soil Database”**. Type the full folderpath where tabular county SSURGO data (in text file) is saved. Import tabular data for each county you want to work with.

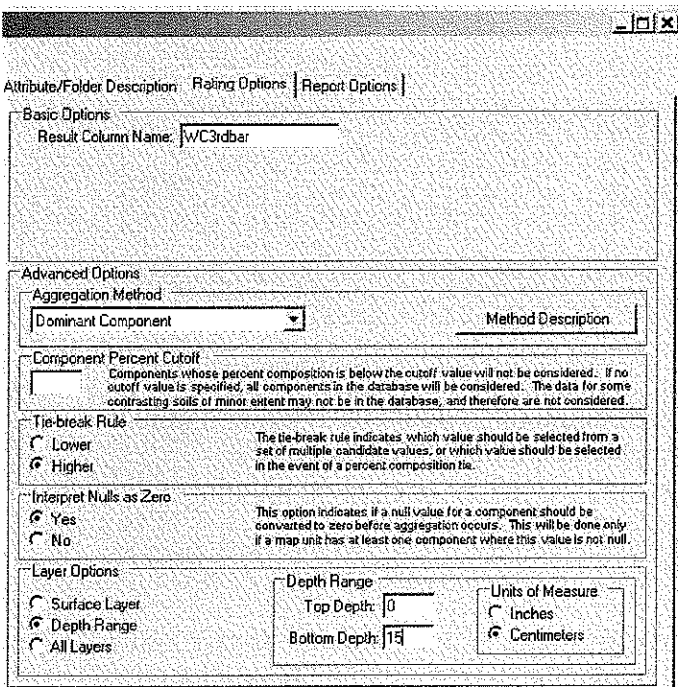


Open ArcGIS, go to View\Toolbars\Soil Data Viewer Tools. Symbol  will appear on the window. Open shapefile containing county soil survey polygons from “spatial” folder in county SSURGO data.

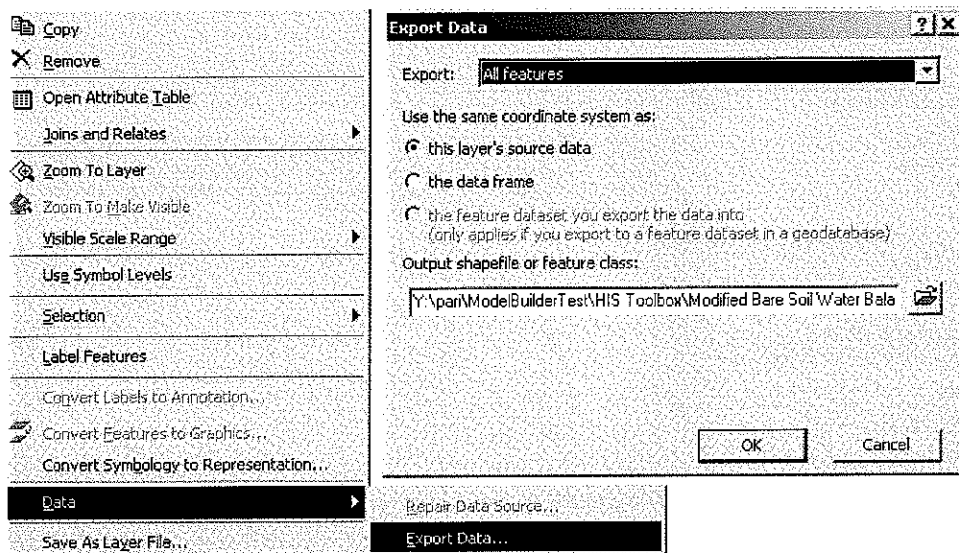
Open  Soil Data Viewer Tool. Choose corresponding “Database” for “Map Layer”. Map Layer is the spatial data you just have opened and Database is the Microsoft Access data with imported soil tabular data. Always use the “Advanced Mode” in soil data viewer to see detail soil properties. We need Surface texture, water content-15 bar (field capacity), water content-one third bar (wilting point) from physical soil properties



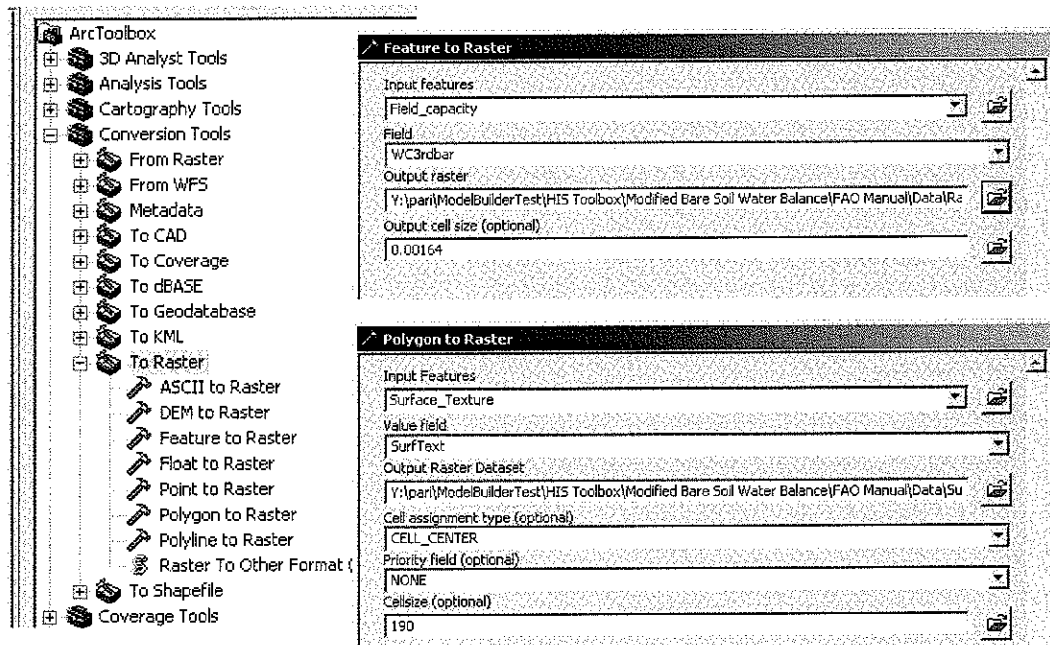
For more information refer to **Soil Data Viewer 5.x Online User Guide**. Choose appropriate “Rating Options”. Choose the Depth Range equal to depth of bare soil layer (Ze).



Click “Map”. You will see the “Layer” of the soil property in ArcGIS. This is temporary layer; export the data (Right click on the layer) to shapefile. Make sure you export “All features”.

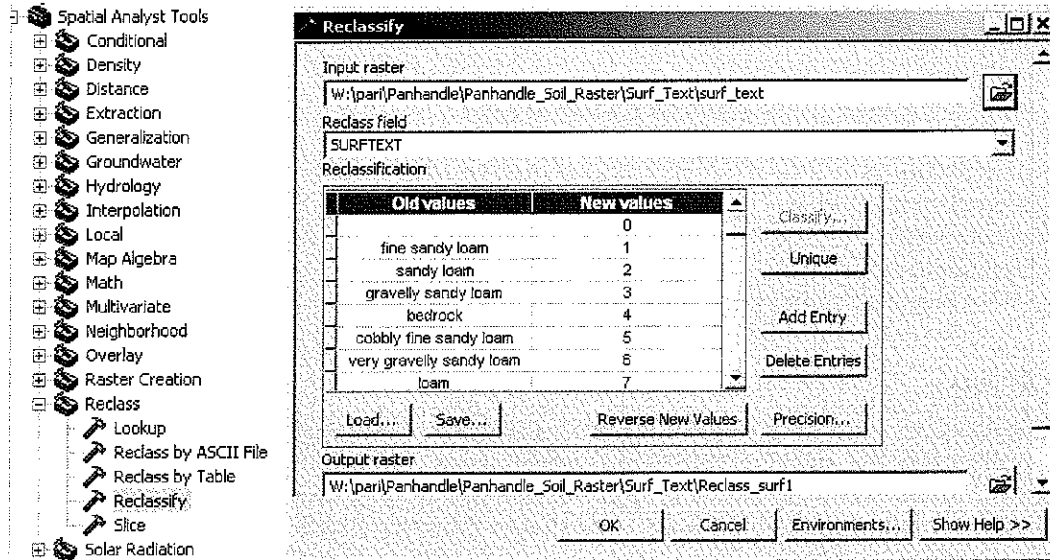


Now we have to save it as a raster. You can use “Feature to Raster” or “Polygon to Raster” tool under ArcToolbox\Conversion Tools\To Raster. Be sure to specify the cell size for output raster data.



Now we will create readily available water (REW) raster. We can reclassify “Surface Texture” raster. Use any of the Reclass tools under ArcToolbox\Spatial Analyst\Reclass. Reclassify tool is shown as an example. Choose the surface texture raster as Input Raster, surfTex as a reclass field. Old values should show the surface texture classes and new values should be integer starting from zero. You can edit the new values field and change it to REW values for corresponding texture class. Most important thing to remember is that **only integer values will be allowed as new values**. Even if you type floating point values, they will automatically be converted to integers. One way to go around it is to

multiply REW values by 1000 or so and divide reclassified raster later by same multiplier (1000 or so). You can also load the table containing old and new values. Use Spatial Analyst - Raster Calculator to perform mathematical and logical operations on raster data. Go to **view\Toolbars\Spatial Analyst**. Spatial analyst toolbar will appear on the window.



Useful tools for processing spatial data in ArcGIS

ArcToolbox\Spatial Analyst

- Interpolation
- Extraction
- Map Algebra
- Overlay

ArcToolbox\Conversion Tools

- To Raster
- To Shapefile

ArcToolbox\Analysis Tools

- Extract
- Overlay

ArcToolbox\Data Management Tools\ Projections and Transformations

- Feature
- Raster

View\Toolbars\Spatial Analyst

- Raster Calculator
- Options

View\Toolbars\Editor

View\Toolbars\Tools

View\Toolbars\Geostatistical Analyst

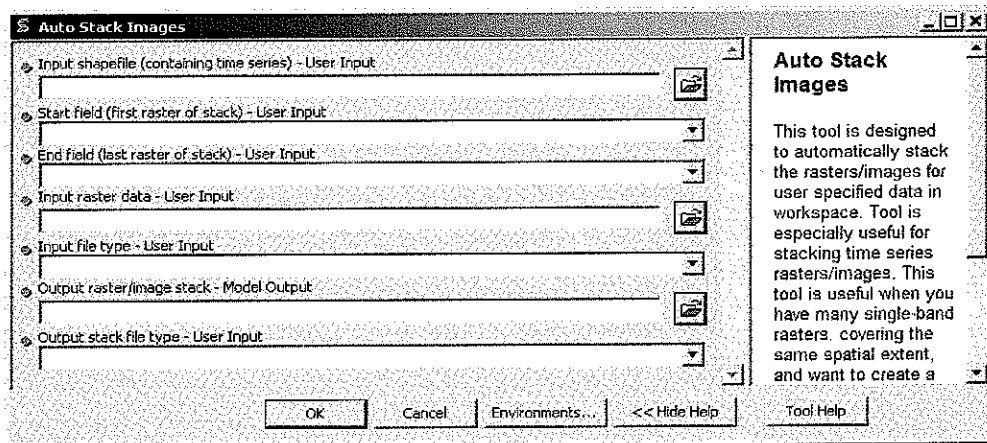
For more information about the above tools refer to ArcGIS help.

HIS toolbox - List of scripts

1. Auto Stack Images
2. Bare Soil Water Balance Model
3. Bare Soil Water Balance Model with Skin Evaporation
4. Bare Soil Water Balance Preprocessing
5. ETrF computation
6. IDW Interpolation Iteration
7. Kriging Interpolation Iteration
8. Spline Interpolation Iteration
9. Spline With Barriers Interpolation Iteration

Auto Stack Images -

This tool is designed to automatically stack the rasters/images for user specified data in workspace. Tool is especially useful for stacking time series rasters/images. This tool is useful when you have many single-band rasters, covering the same spatial extent, and want to create a multiple-band raster dataset. Tool uses shapefile fields as guideline to select raster filepaths. The Tool is flexible and allows conversion from various raster/image formats.

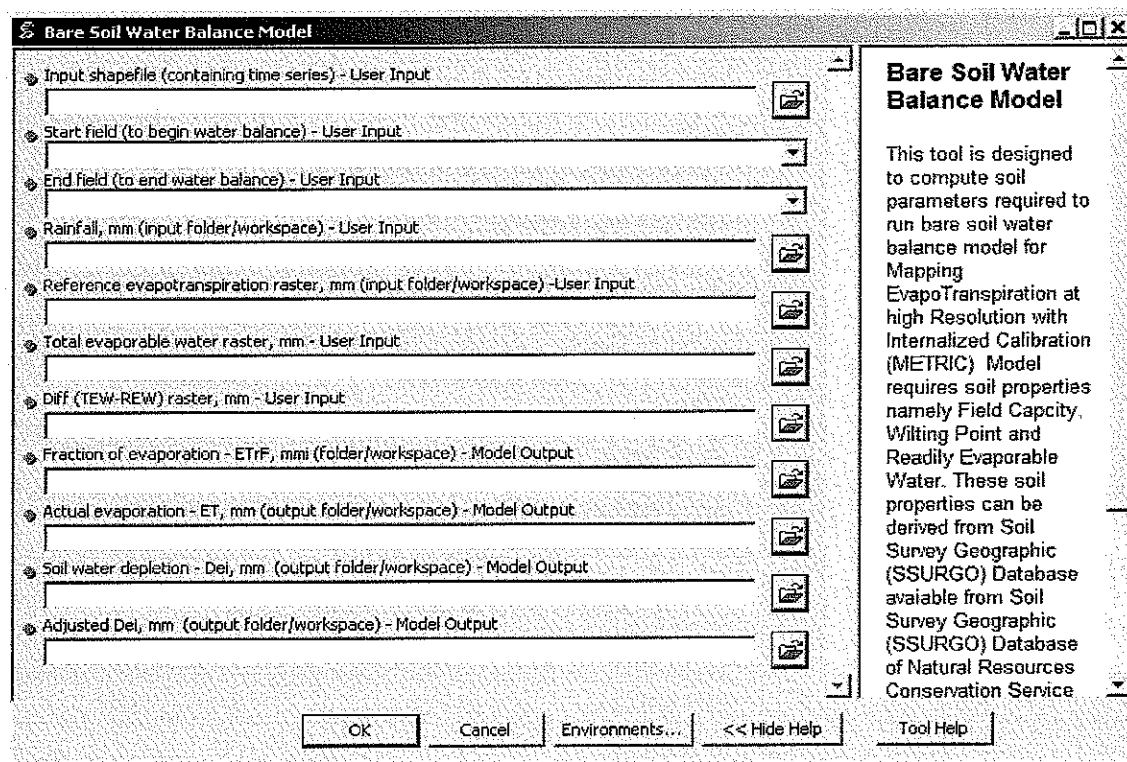


| Parameter | Data Type | Description |
|-------------------|------------|--|
| Input shapefile | Geodataset | Shapefile should contain the list of fields corresponding to raster names which are to be stacked. This could be typically a time series data of climate variable and field names may be DoY, Day or Julian date etc. User should note that shapefile fields should not contain any extensions such as .img, .jpg, .tif etc. |
| Start field | Field | The shapefile field name corresponding to the first raster/image to be stacked. |
| End field | Field | The shapefile field name corresponding to the last raster/image to be stacked. |
| Input raster data | Folder | The input raster datasets/workspace. The folder/workspace where the input rasters are saved with the corresponding field name from the input shapefile. Input rasters can have various raster/image formats. |

| | | |
|------------------------|--------------------|--|
| Input file type | File Type | Input file extension is the raster dataset file format Specify the file extension: bmp for BMP, img for an ERDAS IMAGINE file, jpg for JPEG, jp2 for JPEG 2000, png for PNG, tif for TIFF, or GRID for ArcGIS GRID. |
| Output stack | Raster | The filename of image/raster stack without extension |
| Output stack file type | Raster data format | When storing the raster dataset in a file format, you need to specify the file extension: .bmp for BMP, img for an ERDAS IMAGINE file, jpg for JPEG, jp2 for JPEG 2000, png for PNG, tif for TIFF, or GRID for ArcGIS GRID When storing a raster dataset in a geodatabase, no file extension should be added to the name of the raster dataset. A raster dataset stored in a geodatabase can be compressed; you can specify a compression type and compression quality. |

Bare Soil Water Balance Model -

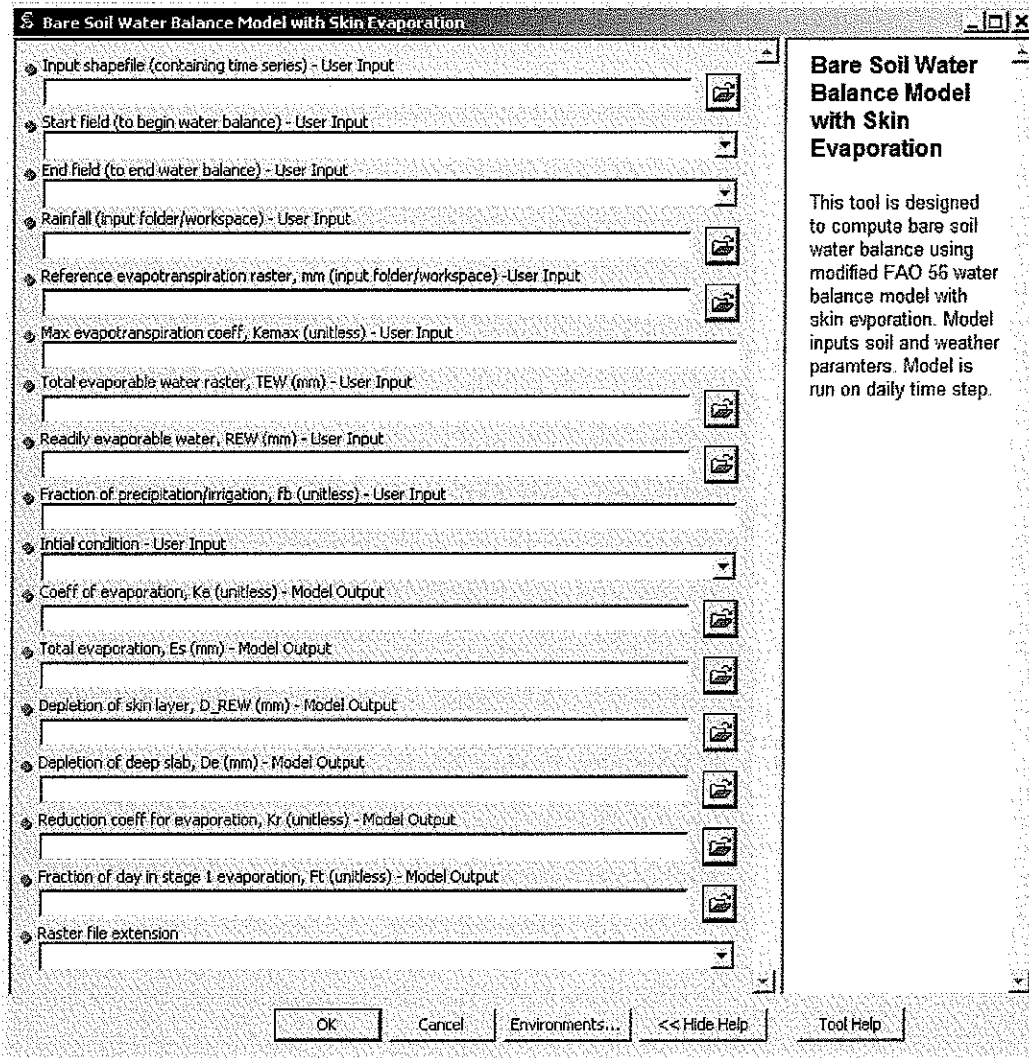
This tool is designed to compute soil parameters required to run bare soil water balance model for Mapping EvapoTranspiration at high Resolution with Internalized Calibration (METRIC) Model requires soil properties namely Field Capacity, Wilting Point and Readily Evaporable Water. These soil properties can be derived from Soil Survey Geographic (SSURGO) Database available from Soil Survey Geographic (SSURGO) Database of Natural Resources Conservation Service (NRCS). SSURGO data is available in form of Access Database and Shapefiles. Data can be easily processed in ArcGIS 9 x using the Soil Data Viewer Tool developed by USDA-NRCS



| Parameter | Data Type | Description |
|--------------------------------|----------------|---|
| Input shapefile | Geodataset | Shapefile should contain the list of fields for which daily bare soil water balance model has to be run (typically DoY, Day or Julian date etc). These names should correspond to the daily variables (ETr and rainfall) that user needs to input. Also corresponding outputs will also be saved with the same names as shapefile fields (i.e. daily Deiadj, ETrFi and ET rasters) |
| Start field | Field | The time period (field in the shapefile) from which bare soil water balance is to be initialized It is important to have previous day's soil water depletion is saved in the Deiadj folder with corresponding field name. |
| End field | Field | The time period (field in the shapefile) at which bare soil water balance is to be stopped. |
| Rainfall | Folder | Folder location where rainfall raster for each time step (field in shapefile) is saved with corresponding name. It is important to save all the rainfall rasters under the same folder with corresponding name and not under different subfolder. This is required for automation of reading rainfall rasters |
| Reference evapotranspiration | Folder | Folder location where reference evapotranspiration raster for each time step (field in shapefile) is saved with corresponding name. It is important to save all the reference evapotranspiration rasters under the same folder with corresponding name and not under different subfolder. This is required for automation of reading rainfall rasters |
| Total evaporable water raster | Raster dataset | Total evaporable water (IEW) refers to water holding capacity of the bare soil layer (~ 10 - 15cm deep) |
| Diff (IEW-REW) raster | Raster dataset | This is not a scientific term. It is computed to reduce computational time and power. It is arithmetic difference between IEW and REW (readily evaporable water). This parameter can be computed using soil data from SSURGO/STATSGO and bare soil preprocessing tool in ArcGIS9.X Also use Soil data viewer to analyse SSURGO data in ArcGIS |
| Fraction of evaporation - ETrF | Folder | The evaporation process at the bare soil surface is divided into two stages: an energy limiting stage (Stage 1) and a falling rate stage (Stage 2). Stage 1 is when layer is very wet. In this stage, the evaporation is limited only by the energy availability at the land surface. Stage 2 is in a drier condition, and there is no readily evaporable water (REW) but the soil holds some evaporable water. In stage 1 ETrF is assumed to be 1. In stage 2 ETrF is computed by equation, $ETrF = (IEW - Dei-1) / (IEW - REW)$ |
| Actual evaporation - EI | Folder | Actual evaporation, EI is the total amount of evaporation from bare soil layer at the end of the day and is expressed in mm. |
| Soil water depletion - Dei | Folder | Soil water depletion, Dei is the total amount of water depleted from the bare soil layer at the end of the day and is expressed in mm. |
| Adjusted Dei | Folder | Soil water depletion, Dei is adjusted within the upper and lower limit. Upper limit of soil water depletion is total evaporable water. Lower limit of soil water depletion is zero. |

Bare Soil Water Balance Model with Skin Evaporation -

This tool is designed to compute bare soil water balance using modified FAO 56 water balance model with skin evaporation. The Model inputs soil and weather parameters. The Model is run on a daily time step.

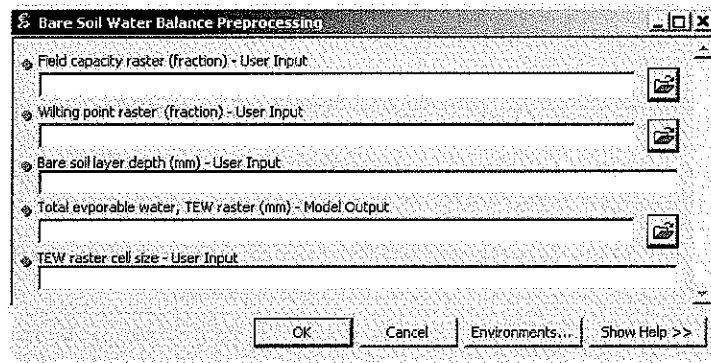


| Parameter | Data Type | Description |
|-----------------|------------|--|
| Input shapefile | Geodataset | Shapefile should contain the list of fields for which daily bare soil water balance model with skin evaporation has to be run (typically DoY, Day or Julian date etc). These names should correspond to the daily variables (ETr and rainfall) that user needs to input. Also corresponding outputs will also be saved with the same names as shapefile fields (i.e. daily De, Ke, Kr, Ft, Drew and Es rasters). |
| Start field | Field | The time period (field in the shapefile) from which bare soil water balance with skin evaporation is to be initialized. |
| End | Field | The time period (field in the shapefile) at which bare soil water balance with |

| | | |
|--|------------------|---|
| | | skin evaporation is to be stopped |
| Rainfall | Folder | Folder location where rainfall raster for each time step (field in shapefile) is saved with corresponding name. It is important to save all the rainfall rasters under the same folder with corresponding name and not under different subfolder. This is required for automation of reading rainfall rasters. |
| Reference evapotranspiration raster | Folder | Folder location where reference evapotranspiration raster for each time step (field in shapefile) is saved with corresponding name It is important to save all the reference evapotranspiration rasters under the same folder with corresponding name and not under different subfolder. This is required for automation of reading reference evapotranspiration |
| Max evapotranspiration coeff | Folder | Ke max is the maximum evaporation coefficient when the surface is wet (i.e., the rate during stage 1 drying) Ke max is generally assumed to be 1.2 for the grass reference ET _o and 1.0 for the alfalfa reference ET _r |
| Total evaporable water raster, IEW | Raster Dataset | Total evaporable water (TEW) refers to water holding capacity of the bare soil layer (~ 100 - 150 mm deep). |
| Readily evaporable water, REW | Raster Dataset | Readily evaporable water is water that can be depleted during energy limiting stage of soil evaporation. REW is a function of soil and plant type. For computation purposes REW can be simply derived based on surface soil texture |
| Fraction of precipitation/irrigation, fb | Folder | fb is the fraction of the precipitation and irrigation from a specific time step (day) that is assumed to be evaporated during that same time step If rainfall/irrigation events are assumed to occur later in a day, then fb = 0 If rainfall/irrigation events are assumed to occur early in a day, then fb = 1 If timing of rainfall/irrigation events during the day is unknown, then the recommended value for fb is 0.5 |
| Initial condition | String | Initial condition refers to the condition (dry/wet) of the bare soil zone before the starting day of water balance computation. Initial condition is used to compute the depletion in the bare soil water layer (D _e) and depletion of the skin layer (D _{rew}) at the end of the day before the starting day of water balance computation. |
| Coeff of evaporation, Ke | Float | Ke is the coefficient of evaporation Ke = total evaporation, ES / reference evapotranspiration, ET _r |
| Total evaporation, Es | Folder | Total evaporation is the total amount of evaporation from the bare soil layer at the end of the day. |
| Depletion of skin layer, D_REW | Folder | D _{rew} is the depletion of the skin layer at the end of the last day. |
| Depletion of deep slab, De | Folder | D _e is the depletion of the bare soil layer at the end of the day. |
| Reduction coeff for evaporation, Kr | Float | K _r is the reduction coefficient for evaporation in the total slab, and is computed following FAO-56 $K_r = \min\left(\frac{IEW - D_{e,i} - 1}{IEW - REW}, 1\right)$ |
| Fraction of day in stage 1 evaporation, Ft | Folder | Portion of the day that is in stage 1 (energy limiting stage). $F_t = \frac{REW - D_{rew,i}}{K_{max} * ET_r}$ |
| Raster file extension | Raster file type | Choose file extension for all the output rasters. When storing the raster dataset in a file format, you need to specify the file extension: .bmp for BMP, .img for an ERDAS IMAGINE file, .jpg for JPEG, .jp2 for JPEG 2000, .png for PNG, .tif for TIFF, or .grid for ArcGIS GRID |

Bare Soil Water Balance Preprocessing

This tool is designed to compute soil parameters required to run bare soil water balance model for Mapping EvapoTranspiration at high Resolution with Internalized Calibration (METRIC). The Model requires soil properties namely Field Capacity, Wilting Point and Readily Evaporable Water. These soil properties can be derived from the Soil Survey Geographic (SSURGO) Database available from the Soil Survey Geographic (SSURGO) Database of the Natural Resources Conservation Service (NRCS). SSURGO data are available in the form of Access Database and Shapefiles. Data can be easily processed in ArcGIS 9.x using the Soil Data Viewer Tool developed by USDA-NRCS.



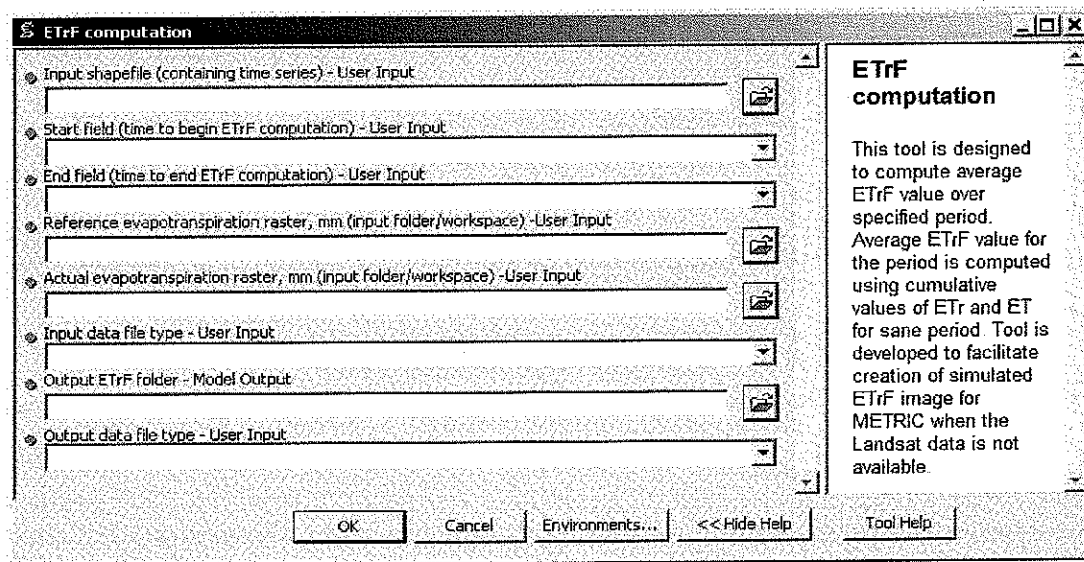
| Parameter | Data Type | Description |
|----------------------------|----------------|---|
| Field capacity | Raster Dataset | Field capacity is the maximum volume of water which soil can hold in its pores after excess water has been drained away. In this state of a soil the only water that remains is water retained by the soil particles through surface tension. |
| Wilting point | Raster Dataset | Permanant wilting point is the soil water content at the stage where the plant dies |
| Bare soil layer depth | Double | Soil depth the depth of bare soil layer. It is usually assumed around 100 - 150 mm |
| Total evporable water, TEW | Raster Dataset | TEW is another way of descibing soil water holding capcity. It can be computed using the formula $TEW = (FC - WP) * Ze$, where Ze is depth of bare soil layer |
| TEW raster cell size | Double | Cell size is spatial resoulution of the TEW raster/image. |

ETrF computation

This tool is designed to compute average ETrF value over a specified period. The Average ETrF value for the period is computed using cumulative values of ETr and ET for the same period. The Tool is developed to facilitate creation of a simulated ET1F image for METRIC when Landsat data are not available.

| Parameter | Data Type | Description |
|-----------------|------------|--|
| Input shapefile | Geodataset | Shapefile should contain the list of fields for which average ETrF has to be computed (typically DoY, Day or Julian date etc). These names should correspond to the variables (ETr and ET) that user needs to input. |
| Start field | Field | Beginning of the time period (field in the shapefile) for which average ETrF has |

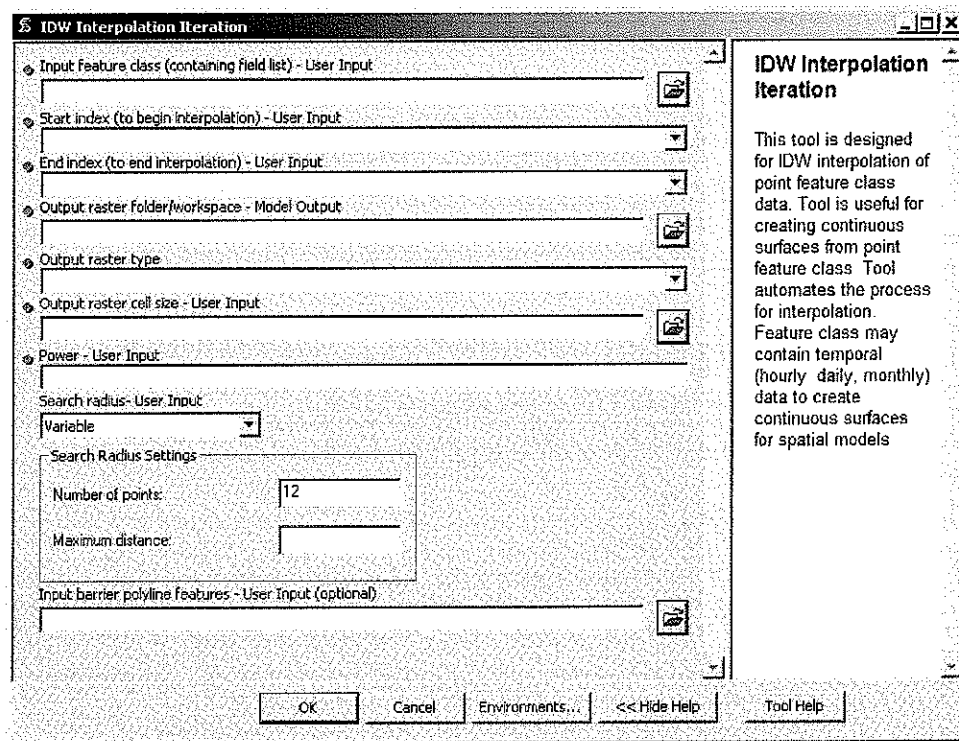
| | | |
|-------------------------------------|------------------|--|
| | | to be computed. |
| End field | Field | End of the time period (field in the shapefile) for which average ETrF has to be computed. |
| Reference evapotranspiration raster | Folder | Folder location where reference evapotranspiration raster for each time step (field in shapefile) is saved with corresponding name It is important to save all the reference evapotranspiration rasters under the same folder with corresponding name and not under different subfolder This is required for automation of reading rainfall rasters |
| Actual evapotranspiration raster | Folder | Folder location where actual evapotranspiration raster for each time step (field in shapefile) is saved with corresponding name. It is important to save all the actual evapotranspiration rasters under the same folder with corresponding name and not under different subfolder This is required for automation of reading rainfall rasters |
| Input data file type | Raster data type | When storing the raster dataset in a file format, you need to specify the file extension: .bmp for BMP, img for an ERDAS IMAGINE file, jpg for JPEG, jp2 for JPEG 2000, png for PNG, tif for TIFF, or no extension for GRID |
| Output ETrF folder | Folder | Folder where model results will be saved. The raster data includes summation of ET _r and summation of ET and average ETrF for selected period |
| Output data file type | Raster data type | When storing the raster dataset in a file format, you need to specify the file extension: .bmp for BMP, img for an ERDAS IMAGINE file, jpg for JPEG, jp2 for JPEG 2000, png for PNG, tif for TIFF, or no extension for GRID. |



IDW Interpolation Iteration

This tool is designed for IDW interpolation of point feature class data. The Tool is useful for creating continuous surfaces from point feature class. The Tool automates the process for interpolation. Feature class may contain temporal (hourly, daily, monthly) data to create continuous surfaces for spatial models.

| Parameter | Data Type | Description |
|---------------------------------|-------------------|---|
| Input feature class | Geodataset | The input point features containing the z-values to be interpolated into a surface raster. |
| Start index | Field | The initial value of the z-value range to be interpolated into raster using IDW. |
| End index | Field | The end value of the z-value range to be interpolated into raster using IDW. |
| Output raster folder/workspace | Folder | The output folder/workspace where interpolated raster data will be saved. Each raster will be saved with the name corresponding to the z-value it is created from. |
| Output raster type | Raster dataset | When storing the raster dataset in a file format, you need to specify the file extension: bmp for BMP, .img for an ERDAS IMAGINE file, .jpg for JPEG, .jp2 for JPEG 2000, .png for PNG, .tif for TIFF, or no extension for GRID. |
| Output raster cell size | Cellsize | The cell size at which the output raster will be created. |
| Power | Power | The exponent of distance. Controls the significance of surrounding points on the interpolated value. A higher power results in less influence from distant points. It can be any real number greater than zero, but the most reasonable results will be obtained using values from 0.5 to 3. The default is 2. |
| Search radius | Radius | Defines which surrounding points will be used to control the raster. There are two options: VARIABLE and FIXED. Variable is the default. VARIABLE {number_of_points} {maximum_distance} <ul style="list-style-type: none"> {number_of_points} — An integer value specifying the number of nearest input sample points to be used to perform interpolation. The default is 12 points. {maximum_distance} — Specifies the distance, in map units, by which to limit the search for the nearest input sample points. If the number of points for the VARIABLE option cannot be satisfied within that maximum distance, a smaller number of points will be used. FIXED {distance} {minimum_number_of_points} <ul style="list-style-type: none"> {distance} — The distance, in map units, specifying that all input sample points within the specified radius will be used to perform interpolation. The default radius is five times the cell size of the output raster. {minimum_number_of_points} — An integer defining the minimum number of points to be used for interpolation. If the required number of points is not found within the specified radius, the search radius will be increased until the specified minimum number of points is found. The default is zero. |
| Input barrier polyline features | Polyline features | Polyline features to be used as a break or limit in searching for the input sample points. |

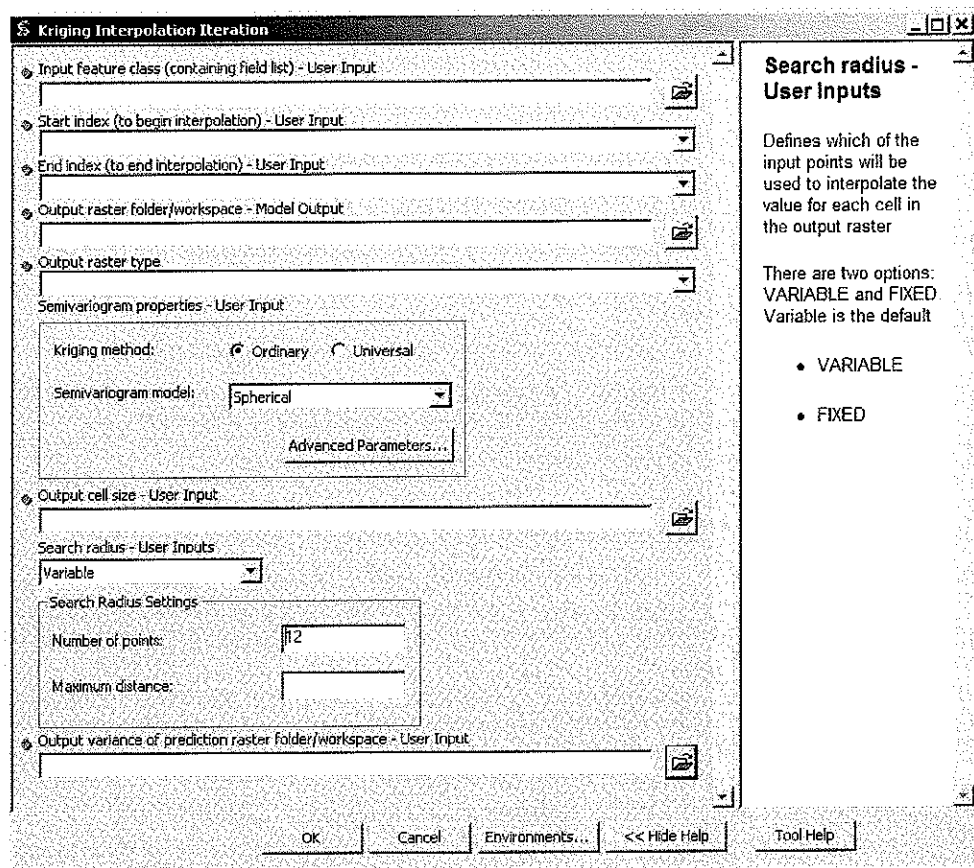


Kriging Interpolation Iteration

This tool is designed for spline interpolation of point feature class data. The Tool is useful for creating continuous surfaces from point feature class. The Tool automates the process for interpolation. Feature class may contain temporal (hourly, daily, monthly) data to create continuous surfaces for spatial models.

| Parameter | Data Type | Description |
|--------------------------------|------------------|--|
| Input feature class | Geodataset | The input point features containing the z-values to be interpolated into a surface raster |
| Start index | Field | The initial value of the z-value range to be interpolated into raster using kriging |
| End index | Field | The end value of the z-value range to be interpolated into raster using kriging |
| Output raster folder/workspace | Folder | Folder location where raster for each time step (field in shapefile) is saved with corresponding name User should note that all the rasters will be created under this folder with common 'Info' folder. User will have to use ArcCatalog to move or copy the individual rasters. |
| Output raster type | Raster data type | When storing the raster dataset in a file format, you need to specify the file extension: .bmp for BMP, img for an ERDAS IMAGINE file, jpg for JPEG, jp2 for JPEG 2000, png for PNG, tif for TIFF, or no extension for GRID |
| Semivariogram properties | Semivariogram | Semivariogram model to be used. <ul style="list-style-type: none"> • SPHERICAL — Spherical semivariogram model. This is the default • CIRCULAR — Circular semivariogram model • EXPONENTIAL — Exponential semivariogram model |

| | | |
|--------------------------------------|----------|---|
| | | <ul style="list-style-type: none"> • GAUSSIAN — Gaussian (or normal distribution) semivariogram model • LINEAR — Linear semivariogram model with a sill • LINEARDRIFT — Universal kriging with linear drift. • QUADRATICDRIFT — Universal kriging with quadratic drift. |
| Output cell size | Cellsize | <p>These advanced parameters must be enclosed in double quotation marks along with the semivariogram model option.</p> <ul style="list-style-type: none"> • Lag size — The default is the output raster cell size • Major range — Represents a distance beyond which there is little or no correlation. • Partial sill — The difference between the nugget and the sill • Nugget — Represents the error and variation at spatial scales too fine to detect. The nugget effect is seen as a discontinuity at the origin. |
| Search radius | Radius | <p>The cell size at which the output raster will be created</p> <p>Defines which surrounding points will be used to control the raster. There are two options: VARIABLE and FIXED. Variable is the default.</p> <ul style="list-style-type: none"> • VARIABLE {number_of_points} {maximum_distance} <ul style="list-style-type: none"> {number_of_points} — An integer value specifying the number of nearest input sample points to be used to perform interpolation. The default is 12 points {maximum_distance} — Specifies the distance, in map units, by which to limit the search for the nearest input sample points. If the number of points for the VARIABLE option cannot be satisfied within that maximum distance, a smaller number of points will be used. • FIXED {distance} {minimum_number_of_points} <ul style="list-style-type: none"> {distance} — The distance, in map units, specifying that all input sample points within the specified radius will be used to perform interpolation. The default radius is five times the cell size of the output raster {minimum_number_of_points} — An integer defining the minimum number of points to be used for interpolation. If the required number of points is not found within the specified radius, the search radius will be increased until the specified minimum number of points is found. The default is zero. |
| Output variance of prediction raster | Folder | Optional output raster where each cell contains the predicted semi-variance values for that location |

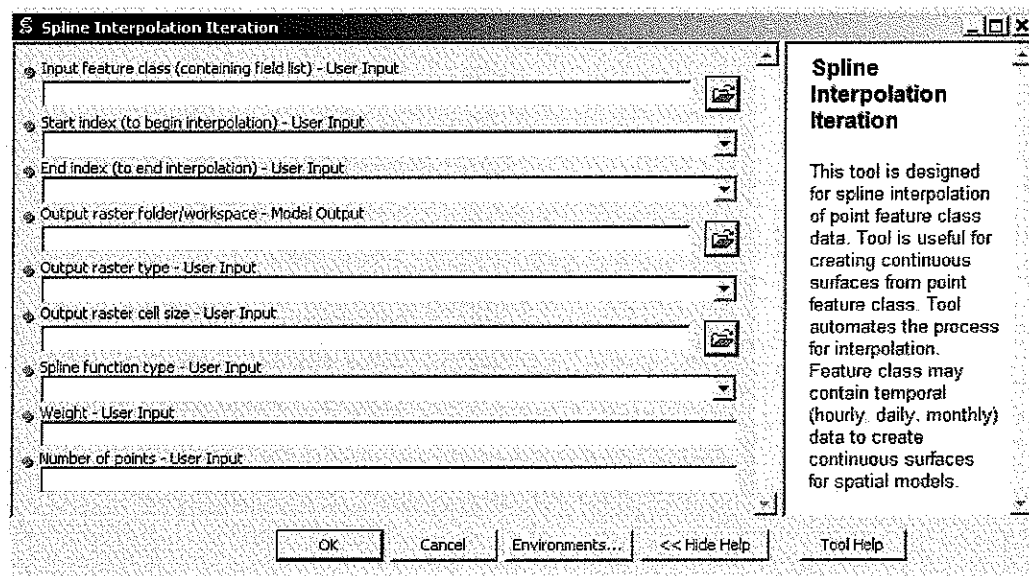


Spline Interpolation Iteration

This tool is designed for spline interpolation of point feature class data. The Tool is useful for creating continuous surfaces from point feature class. The Tool automates the process for interpolation. Feature class may contain temporal (hourly, daily, monthly) data to create continuous surfaces for spatial models

| Parameter | Data Type | Description |
|--------------------------------|------------------|---|
| Input feature class | Geodataset | The point feature containing the z-values to be interpolated into a surface raster |
| Start index | Field | The initial value of the z-value range to be interpolated into raster using spline |
| End index | Field | The end value of the z-value range to be interpolated into raster using spline. |
| Output raster folder/workspace | Folder | The output folder/workspace where interpolated raster data will be saved. Each raster will be saved with the name corresponding to the z-value it is created from User should note that all the rasters will be created under this folder with common 'Info' folder. User will have to use ArcCatalog to move or copy the individual rasters |
| Output raster type | Raster data type | When storing the raster dataset in a file format, you need to specify the file extension: .bmp for BMP, img for an ERDAS IMAGINE file, .jpg for JPEG, .jp2 for JPEG 2000, .png for PNG, .tif for TIFF, or no extension for GRID. |

| | | |
|-------------------------|----------|--|
| Output raster cell size | Cellsize | The cell size at which the output raster will be created. It could be any integer value depending upon the user need |
| Spline function type | String | The type of spline to be used <ul style="list-style-type: none"> REGULARIZED — Yields a smooth surface and smooth first derivatives TENSION — Tunes the stiffness of the interpolant according to the character of the modeled phenomenon |
| Weight | Double | Parameter influencing the character of the surface interpolation. When the REGULARIZED option is used, it defines the weight of the third derivatives of the surface in the curvature minimization expression. If the TENSION option is used, it defines the weight of tension. The default is 0.1 |
| Number of points | Long | Number of points per region used for local approximation |

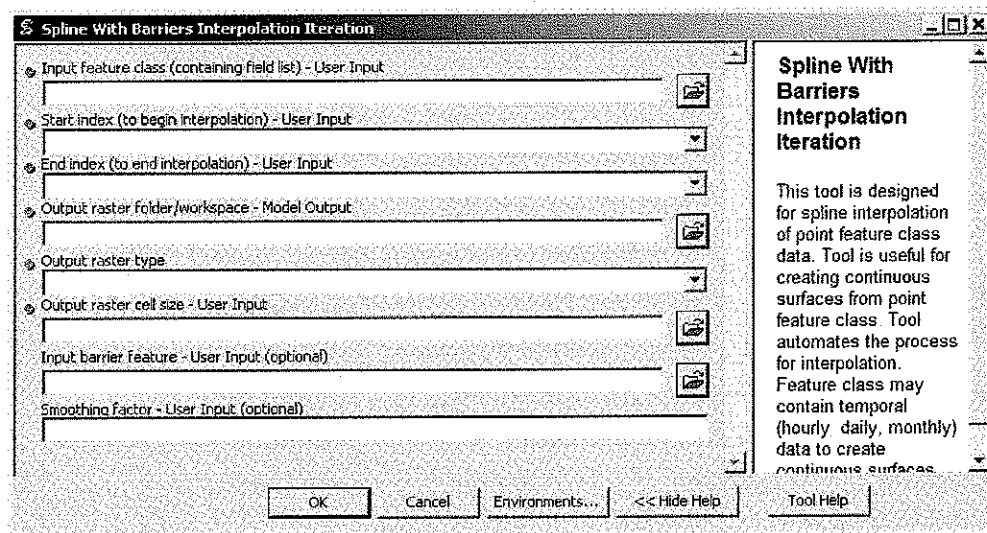


Spline with Barriers Interpolation Iteration

This tool is designed for spline interpolation of point feature class data. The Tool is useful for creating continuous surfaces from point feature class. The Tool automates the process for interpolation. Feature class may contain temporal (hourly, daily, monthly) data to create continuous surfaces for spatial models

| Parameter | Data Type | Description |
|--------------------------------|----------------------|---|
| Input feature class | Composite Geodataset | The point feature containing the z-values to be interpolated into a surface raster |
| Start index | Field | The initial value of the z-value range to be interpolated into raster using spline. |
| End index | Field | The end value of the z-value range to be interpolated into raster using spline. |
| Output raster folder/workspace | Folder | The output folder/workspace where interpolated raster data will be saved. Each raster will be saved with the name corresponding to the z- |

| | | |
|--------------------------------------|----------------------|--|
| | | value it is created from. |
| Output raster type | String | When storing the raster dataset in a file format, you need to specify the file extension: bmp for BMP, img for an ERDAS IMAGINE file, jpg for JPEG, jp2 for JPEG 2000, png for PNG, tif for TIFF, or no extension for GRID |
| Output raster cell size - User Input | Analysis cell size | The cell size at which the output raster will be created. It could be any integer value depending upon the user need. |
| Input barrier feature | Composite Geodataset | Polyline features to be used as a break or limit in searching for the input sample points. |
| Smoothing factor | Double | Parameter influencing the smoothing of the output surface. No smoothing is applied when the value is zero and the maximum amount of smoothing is applied when the factor equals 1. The default is 0.0 |



References

- Tasumi, M. 2003. Progress in operational estimation of regional evapotranspiration using satellite imagery. Ph.D. Dissertation, University of Idaho, Moscow, ID, p. 144 - 146
- Allen Richard. 2010. Modification to the FAO-56 Soil Surface Evaporation Algorithm to Account for Skin Evaporation during Small Precipitation Events.

Further reading

- Useful Internet Sites for GIS and Water Resources - available at <http://www.ce.utexas.edu/>
- ArcGIS webhelp - <http://resources.arcgis.com>
- Getting started with writing geoprocessing scripts - <http://webhelp.esri.com>
- ESRI Developer Network (EDN) - <http://edn.esri.com/>

APPENDIX F

Adjustment of ET_rF for Background Evaporation

Frequently, a Landsat image is processed on a date where previous rainfall has caused the evaporation from bare soil to exceed that for the surrounding monthly period. For our purposes, it is the goal that the final ET image represents the average evaporation conditions for the month. In order to achieve this, the 'background' evaporation of the processed image can be adjusted to better reflect that for the month or other period that it is to represent (Allen, 2010). Daily maps of spatially distributed soil evaporation are needed to apply this adjustment. The methods for the generation of soil evaporation maps are described in Appendix E.

Full adjustment for background evaporation is made for areas of completely bare soil, represented by $NDVI = NDVI_{bare\ soil}$, and no adjustment is made for surface areas fully covered by vegetation, represented by $NDVI = NDVI_{fullcover}$ (Allen, 2010). NDVI values in between bare soil and full cover are adjusted linearly. The following methodology description is taken from a white paper written by the University of Idaho (Allen, 2010). The METRIC generated ET_rF map can first be adjusted to a 'basal' condition, where the evaporation estimate is free of rainfall induced evaporation, but still may contain any irrigation induced evaporation:

$$(ET_r, F_i)_b = ET_r, F_i - (ET_r, F_{background})_i \left(\frac{NDVI_{fullcover} - NDVI_i}{NDVI_{fullcover} - NDVI_{baresoil}} \right) \quad (1)$$

where $(ET_r, F_{background})_i$ is the background evaporation on the image date (i) for bare soil, computed using the FAO-56 two-stage evaporation model. The $(ET_r, F_{background})_i$ can be spatially distributed across the image by applying the evaporation model with spatially distributed precipitation, reference ET, and soil properties (Allen, 2010).

Then, an adjusted ET_rF is computed for the image date that reflects background evaporation averaged over the surrounding period:

$$(ET_r, F_i)_{adjusted} = (ET_r, F_i)_b + (ET_r, F_{background})_i \left(\frac{NDVI_{fullcover} - NDVI_i}{NDVI_{fullcover} - NDVI_{baresoil}} \right) \quad (2)$$

where $\overline{(ET, F_{background})}$ is the average evaporation from bare soil due to precipitation over the averaging period (e.g., one month), calculated as:

$$\overline{(ET, F_{background})} = \frac{\sum_i^n (ET, F_{background})_i}{n} \quad (3)$$

Equations 11 and 12 can be combined as:

$$(ET, F_i)_{adjusted} = ET, F_i + \left(\overline{(ET, F_{background})} - (ET, F_{background})_i \right) \left(\frac{NDVI_{fullcover} - NDVI_i}{NDVI_{fullcover} - NDVI_{baresoil}} \right) \quad (4)$$

with limits $NDVI_{bare\ soil} \leq NDVI_i \leq NDVI_{full\ cover}$.

The results of this bare soil evaporation adjustment will be to preserve any significant evaporation stemming from irrigation and any transpiration stemming from vegetation, but with adjustment to evaporation stemming from precipitation from that on the image date to that of the surrounding time period (Allen, 2010).

References

Allen, R. 2010. Procedures for adjusting METRIC-derived ET,F images for background evaporation from precipitation events prior to cloud filling and Interpretation of ET between image dates. Internal memo, University of Idaho. 11 pages.

APPENDIX G

Estimation of Monthly and Seasonal Evapotranspiration

a) The METRIC algorithms to estimate land surface energy fluxes

Evapotranspiration estimation in METRIC is based on the principle of energy conservation. The model ignores minor energy components, and considers only vertical fluxes (horizontal advective flux is not explicitly included) to estimate latent heat (LE) as a residual in the energy balance (EB) equation [Allen et al., 2010].

$$R_n - H - \lambda E - G \approx 0 \quad (1)$$

where R_n is the net radiation, G is the soil heat flux, H is the sensible heat flux, and λE is the latent heat flux. The units for all the fluxes are in watts per meter squared (W m^{-2}).

Net radiation from a clear sky is estimated by balancing net shortwave and longwave components of the radiation budget:

$$R_n = R_{s\downarrow}(1 - \alpha_s) + R_{l\downarrow} - R_{l\uparrow} - R_{l\downarrow}(1 - \epsilon_o) \quad (2)$$

where α_s is shortwave albedo of the surface (dimensionless) for all pixels. It can be calculated by integrating satellite spectral reflectance values from the shortwave bands 1–5 and 7 of Landsat satellites. $R_{s\downarrow}$ is incoming shortwave radiation (W m^{-2}); $R_{l\downarrow}$ and $R_{l\uparrow}$ are incoming and outgoing longwave (thermal) radiation (W m^{-2}), respectively; ϵ_o is the surface emissivity (dimensionless). For more information regarding R_n and G , refer to Tasumi et al. [2005].

Clear sky incoming shortwave radiation ($R_{s\downarrow}$) is estimated from:

$$R_{s\downarrow} = S_c \cos \theta d_r \tau_{sw} \quad (3)$$

where S_c is the solar constant (1367 W m^{-2}); θ is the solar incidence angle, d_r is the inverse relative sun-earth distance, and τ_{sw} is the atmospheric transmissivity. The d_r is calculated from:

$$d_r = 1 + 0.033 \cos\left(\frac{2\pi}{365}J\right) \quad (4)$$

where J is the day of the year.

The τ_{sw} in Equation [3] may be calculated from a datum elevation using:

$$\tau_{sw} = 0.75 + 2 \times 10^{-5} (Z) \quad (5)$$

where Z is the datum elevation (m)

Incoming longwave radiation (Rl_{\downarrow}) is estimated from the Stephan-Boltzman law:

$$Rl_{\downarrow} = \varepsilon_a \sigma T_i^4 \quad (6)$$

where σ is the Stephan-Boltzman constant ($5.67 \times 10^{-8} \text{ W m}^{-2} \text{ K}^{-4}$); T_i is the incident near surface air temperature (K); and ε_a is the atmospheric emissivity, calculated from:

$$\varepsilon_a = 0.85(-\ln \tau_{sw})^{0.09} \quad (7)$$

Outgoing longwave radiation (Rl_{\uparrow}) is similarly calculated as:

$$Rl_{\uparrow} = \varepsilon_o \sigma T_s^4 \quad (8)$$

where ε_o is the surface emissivity (dimensionless). T_s is the radiometric surface temperature. When leaf area index (LAI) is less than three, $\varepsilon_o = 0.95 + 0.01 \text{ LAI}$. When LAI is greater than or equal to three $\varepsilon_o = 0.98$. LAI is calculated using the Soil Adjusted Vegetation Index (SAVI):

$$SAVI = \frac{(1+L)(\rho_{t,4} - \rho_{t,3})}{(1 + \rho_{t,4} + \rho_{t,3})} \quad (9)$$

$$\begin{aligned} LAI &= 11 * SAVI^3; & \text{for } SAVI \leq 0.817 \\ LAI &= 6; & \text{for } SAVI > 0.817 \end{aligned} \quad (10)$$

where $\rho_{t,3}$ and $\rho_{t,4}$ are at-satellite reflectances for Landsat bands 3 and 4, respectively L is a constant for SAVI.

Soil heat flux (G) can be expressed as a portion of net radiation that depends on radiometric surface temperature (T_s) and LAI. Equation 11 suggests that the G/R_n ratio increases with higher rates of T_s and decreases with LAI.

$$\frac{G}{R_n} = (1.80(T_s - 273.16)/R_n + 0.084) \quad (\text{if } LAI < 0.5) \quad (11b)$$

$$\frac{G}{R_n} = 0.05 + 0.18 e^{-0.521 LAI} \quad (\text{if } LAI \geq 0.5) \quad (11b)$$

The Normalized Difference Vegetation Index (NDVI) is calculated as follows:

$$NDVI = \frac{(\rho_{t,4} - \rho_{t,3})}{(\rho_{t,4} + \rho_{t,3})} \quad (12)$$

Sensible heat flux (H) is determined using a heat and momentum flux equation on a pixel by pixel basis (eq 13).

$$H = \rho_{air} C_p \frac{b + aT_{s\ DEM}}{r_{ah}} \quad (13)$$

where ρ_{air} is air density (kg m^{-3}); C_p is air specific heat ($1004 \text{ J kg}^{-1} \text{ K}^{-1}$); r_{ah} is the aerodynamic resistance to heat flow (s m^{-1}) determined using iterative Monin Obukhov air stability corrections; a and b are coefficients calibrated for each image; and $T_{s\ DEM}$ is the surface radiometric temperature (K) that has been 'de-lapsed' to account for elevation.

Values for H are computed according to $T_{s\ DEM}$. This is done using the " dT vs. $T_{s\ DEM}$ " function where dT is the difference between the air temperature very near the surface (at 0.1 m above the zero plane displacement height, d , plus height for roughness, z_{om}) and the air temperature at 2 m above the zero plane displacement height plus z_{om} . METRIC assumes a linear change in dT with subsequent change in $T_{s\ DEM}$. The linear equation for dT vs. $T_{s\ DEM}$ ($dT = a + bT_{s\ dem}$) is established by using the dT values at two anchor conditions ("hot" and "cold") within the image. The linearity assumption is based on the field research demonstrated by Wang et al (1995), Bastiaanssen (1995), Franks and Beven (1997a,b), and Franks and Beven (1999). The dT is used because of the difficulties in estimating surface temperature accurately from the satellite due to uncertainties in air temperature (T_{air}), atmospheric attenuation, contamination, and radiometric calibration of the sensor (Bastiaanssen et al., 1998a,b; Allen et al., 2007a, b). Assuming neutral atmospheric conditions, initial values for the friction velocity (u^*) and r_{ah} are computed, following with H . Then, u^* and r_{ah} are computed again using the Monin-Obukhov theory for stability correction. The corrected r_{ah} is then used to compute a new dT function and a new value for H . This iteration is repeated until dT and r_{ah} at the anchor pixels stabilize.

Selection of anchor pixels (hot and cold) in Landsat imagery was performed following recommendations found in Allen et al (2010). For the 'hot' anchor pixel, a daily soil water balance model was used to determine whether any residual evaporation existed from exposed soil at the time of each satellite image due to recent rainfall events. The residual evaporation was then considered when assigning a value for ET for the 'hot' pixel, where the hot anchor pixel was generally a bare soil condition located within about 20 km of the weather station. The

FAO-56 (Allen et al., 1998) soil evaporation model was used to estimate residual evaporation from the upper 0-125 m soil layer.

The cold anchor pixel was selected from an area of homogeneous grassland similar to a well-watered alfalfa meadow where H (and dT) was assumed to be zero and all available energy was consumed by λLE . In METRIC[®], the function for H (eq. 14) at the cold pixel is expressed as:

$$H_{cold} = Rn - G - 1.05ET_r \quad (14)$$

where ET_r is the reference ET based on alfalfa as a reference crop using the standardized ASCE Penman-Monteith equation for alfalfa (ET_r) following the procedures given in ASCE-EWRI (2005). Once all components of the energy balance (Rn , G , and H) have been calculated, λLE can be derived for each pixel as the residual of equation 1.

b) Fraction of Reference ET (ET_rF) and Daily Evapotranspiration

The integration of LE over time in METRIC was split into two steps. The first step was to convert the instantaneous value of LE into daily ET_{24} values by holding the reference ET fraction constant (Allen et al., 2007b). An instantaneous value of ET (ET_{inst}) in equivalent evaporation depth is the ratio of LE to the latent heat of vaporization (λ):

$$ET_{inst} = 3600 \frac{LE}{(\rho_w \lambda)} \quad (5)$$

where 3600 is the time conversion from seconds to hour, and ρ_w is water density ($\sim 1000 \text{ Mg m}^{-3}$).

The reference ET fraction (ET_rF) is defined as the ratio of instantaneous ET (ET_{inst}) for each pixel to the alfalfa-reference ET calculated using the standardized ASCE Penman-Monteith equation for alfalfa (ET_r) following the procedures given in ASCE-EWRI (2005):

$$ET_rF = \frac{ET_{inst}}{ET_r} \quad (6)$$

ET_rF serves as a surrogate for K_c (basal crop coefficient) and has been used with 24-hour ET_r in order to estimate the daily ET at each Landsat pixel:

$$ET_{24} = ET_rF \times ET_{r-24} \quad (7)$$

where ET_{24} is the daily value of actual ET (mm d^{-1}), ET_{r-24} is 24 hour ET_r for the day of the image and calculated by summing hourly ET_r values over the day of image. The procedures outlined in ASCE-EWRI (2005) were used to calculate parameters in the hourly ET_r .

For rangeland, once the instantaneous R_n , G , and H are determined, the instantaneous evaporative fraction (Λ) was calculated as:

$$\Lambda = \frac{\lambda ET}{R_n - G} \quad (8)$$

The daily actual ET (ET_c) was estimated as:

$$ET_c = \frac{86400\Lambda(R_{n24} - G_{24})}{\rho_w \lambda} \quad (9)$$

where, ET_c is the daily crop ET (mm day^{-1}), R_{n24} is the daily net radiation calculated on a daily time step (W m^{-2}), G_{24} is the daily soil heat flux (W m^{-2}), λ is the latent heat of vaporization (J kg^{-1}), and ρ_w is the density of water (kg m^{-3}).

c) Estimating daily ET_r between satellite image dates using a cubic spline

The daily estimates of ET_r for the satellite overpass dates were extrapolated between image dates using a cubic spline model. The cubic spline model used for the extrapolation has been described by Allen et al. (2010) and Trezza et al. (2008). The spline creates a smooth curve for ET_r between images to simulate the day-to-day development of vegetation

The spline estimates the ET_r value for each day of a month (such as e.g. the month of June) based on the ET_r values estimated for the image date(s) for that month plus two image dates earlier than the month and two image dates later than the month.

There were not two independent ET_r images available prior the months of April and May to be used for the splining of the ET_r . At this early period of the growing season, crop development is stagnant or very slow, and changes in vegetation cover are small.

Because the first satellite image date was at the end of April, producing an estimate of the monthly ET_r for April is somewhat challenging since no information was available for the beginning of the month. Because of the cold temperatures experienced in this area, very little crop development is expected to occur until May. The ET_r and ET estimates for April were scaled from bare soil evaporation as estimated using the daily gridded evaporation model, which in most cases gives a reasonable estimate of the ET during the non-growing season

portion of the year. The evaporation from bare soil represents 'average' bare soil conditions regarding drainage, soil type and texture for the particular soil type. As a consequence, additional uncertainty in the ET_rF and ET estimates for April may exist for fields with soil and drainage properties different from those for the soil type simulated, and for fields covered by a layer of senesced plant material, mulch or having a relatively dense cover of green plant cover. Users are cautioned to consider these factors on a field-to-field basis before using the estimates of ET_rF and ET for the month of April. A similar approach was employed when estimating the ET for the month of October 1997.

d) Estimating monthly ET

Daily values of ET were calculated on a pixel by pixel basis for each image by:

$$ET_{daily} = ET_rF_{daily} \times ET_{r_daily} \quad (10)$$

Where ET_{daily} is the daily evapotranspiration (mm/day), ET_rF_{daily} are the daily ET_rF values, and ET_{r_daily} are daily values of alfalfa based reference evapotranspiration (mm/day). ET_{r_daily} data are maps encompassing the entire study area. They were produced with AWDN weather station data using the University of Idaho RefET software. The generation of ET_{r_daily} maps is described in Appendix A.

Daily values ET were then summed to monthly totals as:

$$ET_{month} = \sum_{i=m}^n ET_{daily} \quad (11)$$

Where ET_{month} is total monthly ET , and m and n are the first and last day of the month.

The monthly average fractions of ET_rF_{month} were calculated as:

$$ET_rF_{month} = \frac{ET_{month}}{ET_r_{month}} \quad (12)$$

Where ET_{month} is the monthly ET estimate and ET_r_{month} is monthly ET_r , generated by summing the values of the daily ET_r maps for that month. Results of METRIC derived monthly estimates for the Nebraska Panhandle for 2002 and 2005 are shown in Figures 1-8. As a sample, the monthly and seasonal ET_r from the Scottsbluff AWDN station for 2002 and 2005 is shown in Table 2

Table 2. Monthly, seasonal (April through October), and annual ET_r (inches) estimated from the 2002 and 2005 Scottsbluff AWDN station.

| Month | 2002 ET_r (inches) | 2005 ET_r (inches) |
|---------------------|----------------------|----------------------|
| January | 3.03 | 1.40 |
| February | 3.58 | 2.67 |
| March | 3.59 | 4.67 |
| April | 7.38 | 5.38 |
| May | 8.48 | 7.68 |
| June | 11.18 | 8.17 |
| July | 11.39 | 9.83 |
| August | 8.54 | 7.04 |
| September | 5.73 | 6.03 |
| October | 3.26 | 3.81 |
| November | 2.68 | 3.25 |
| December | 2.13 | 1.89 |
| April-October Total | 55.96 | 47.94 |
| Year Total | 70.97 | 61.82 |

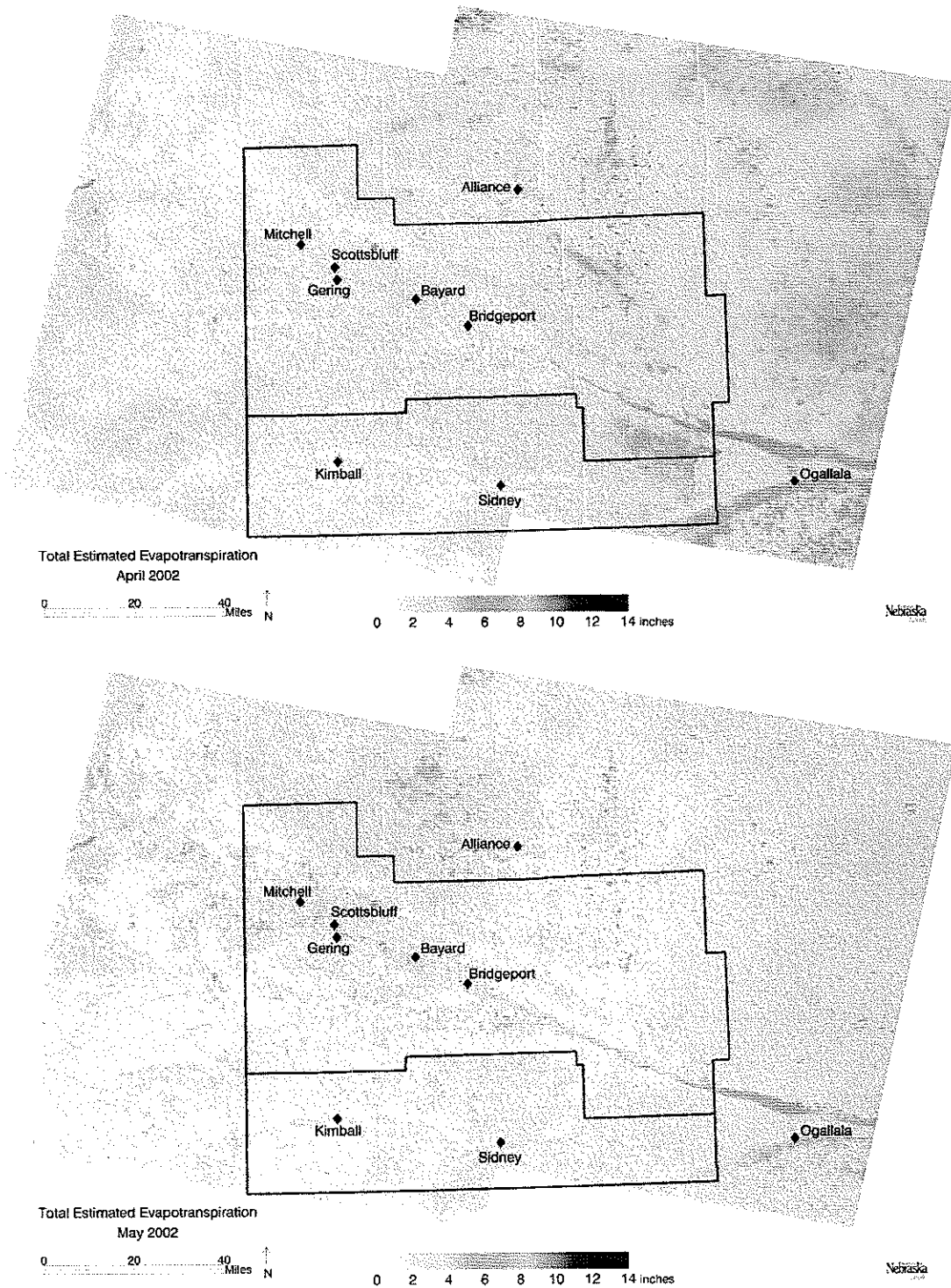


Figure 1. Monthly ET generated from METRIC for Landsat path 32-33, row 31 for 2002. Blue lines indicate North Platte and South Platte boundaries.

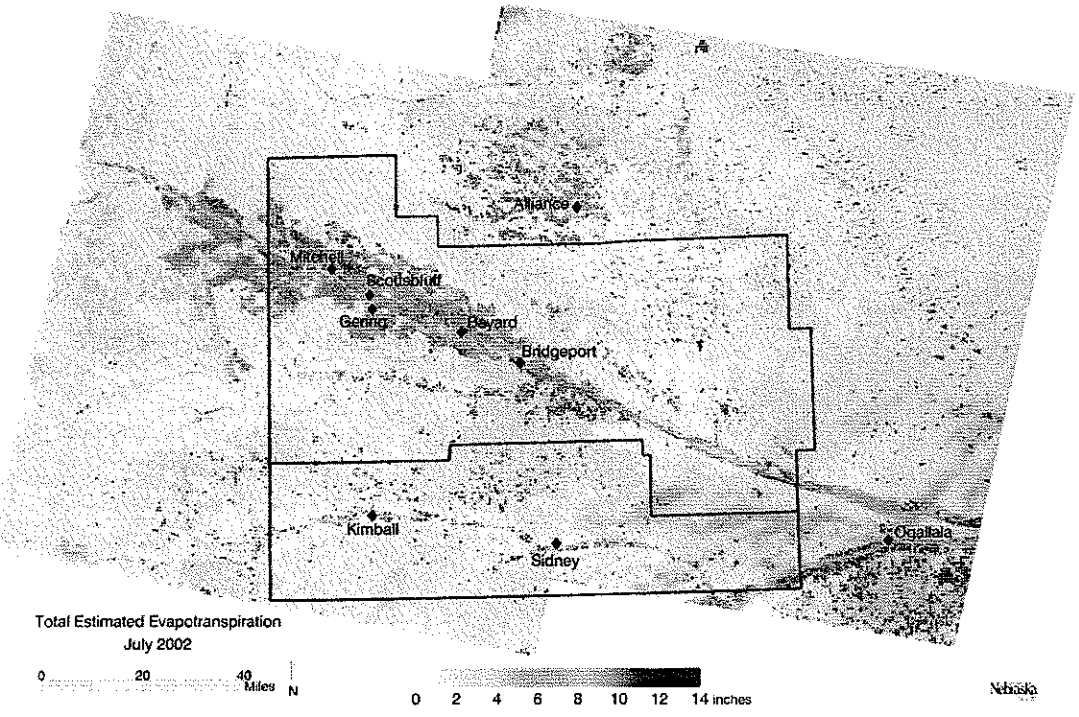
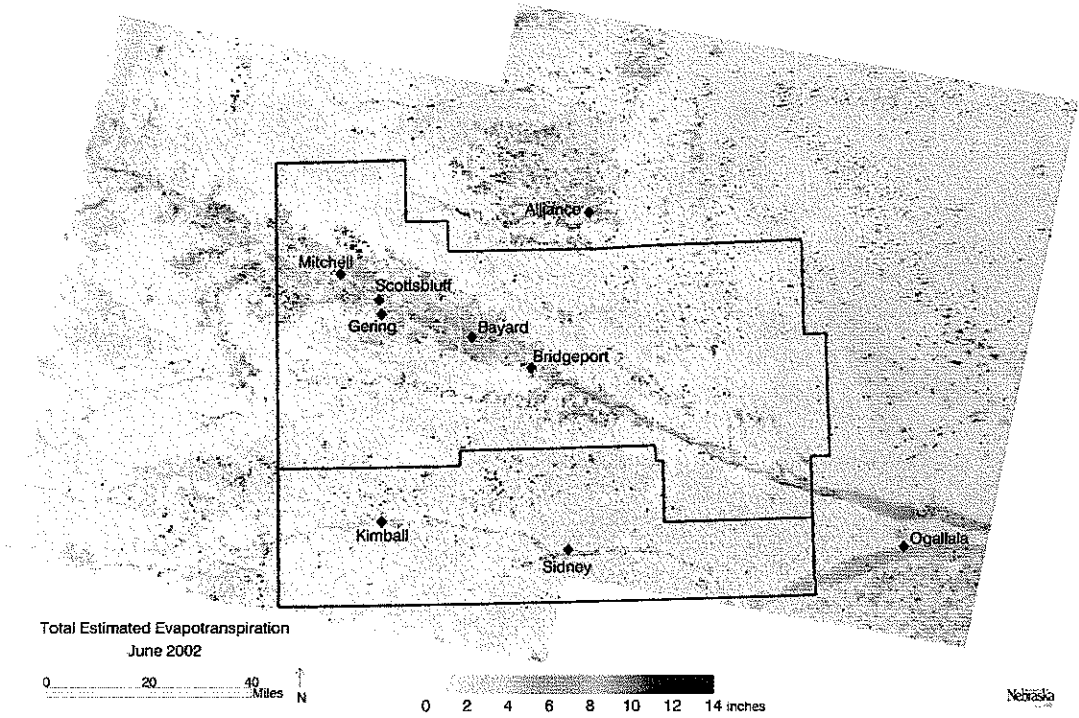


Figure 2. Monthly ET generated from METRIC for Landsat path 32-33, row 31 for 2002. Blue lines indicate North Platte and South Platte boundaries.

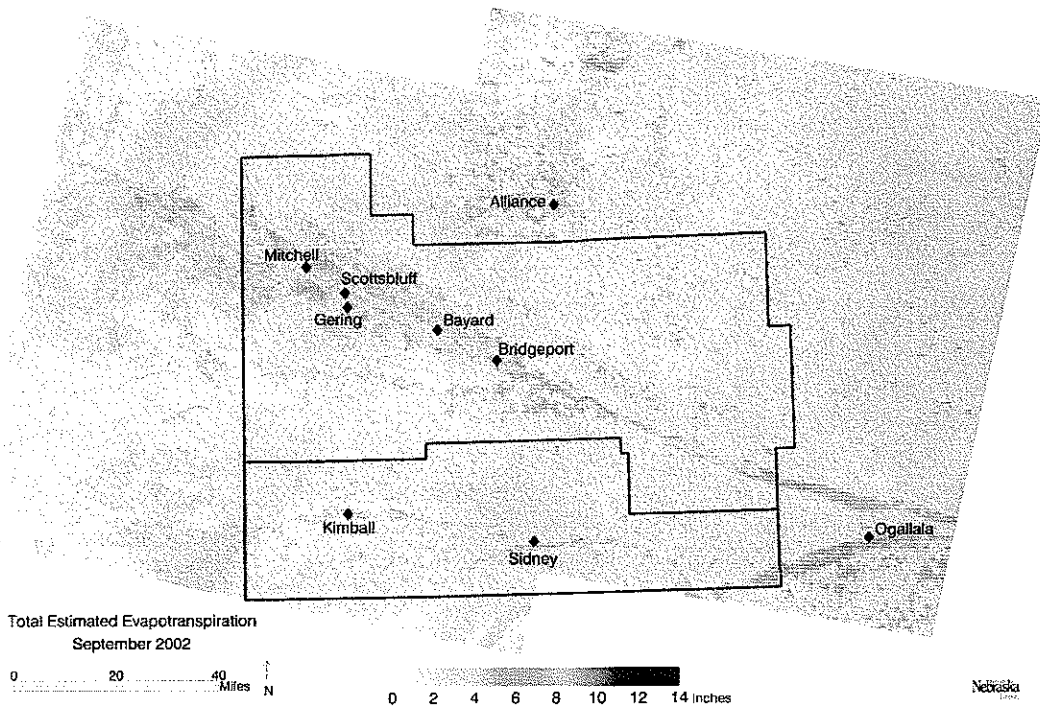
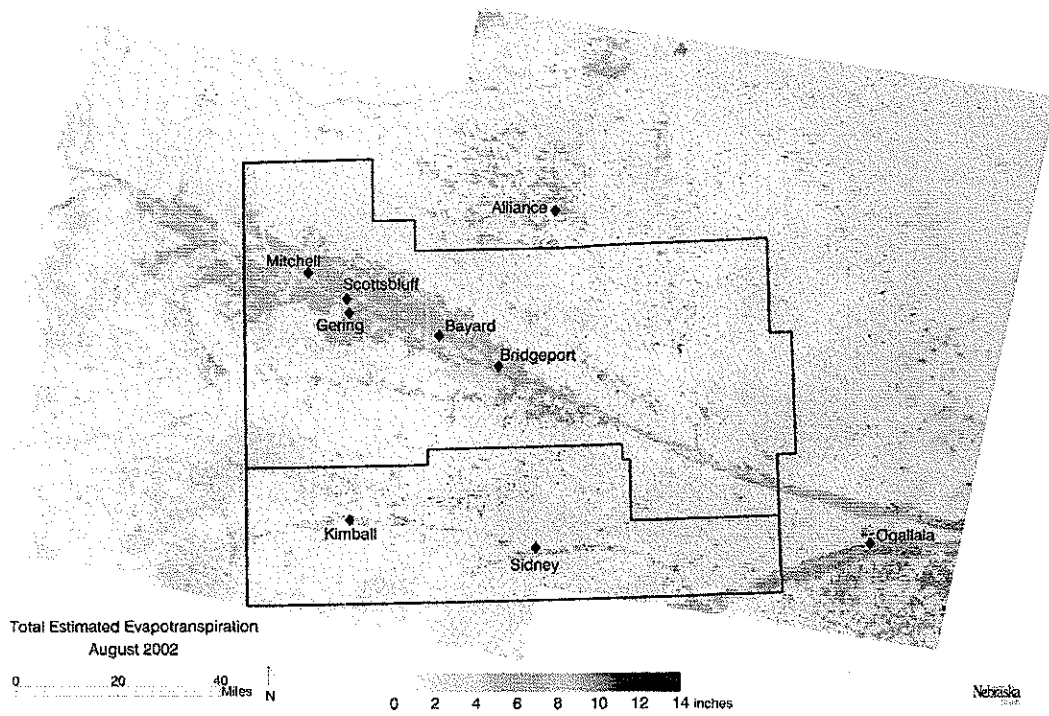


Figure 3. Monthly ET generated from METRIC for Landsat path 32-33, row 31 for 2002. Blue lines indicate North Platte and South Platte boundaries.

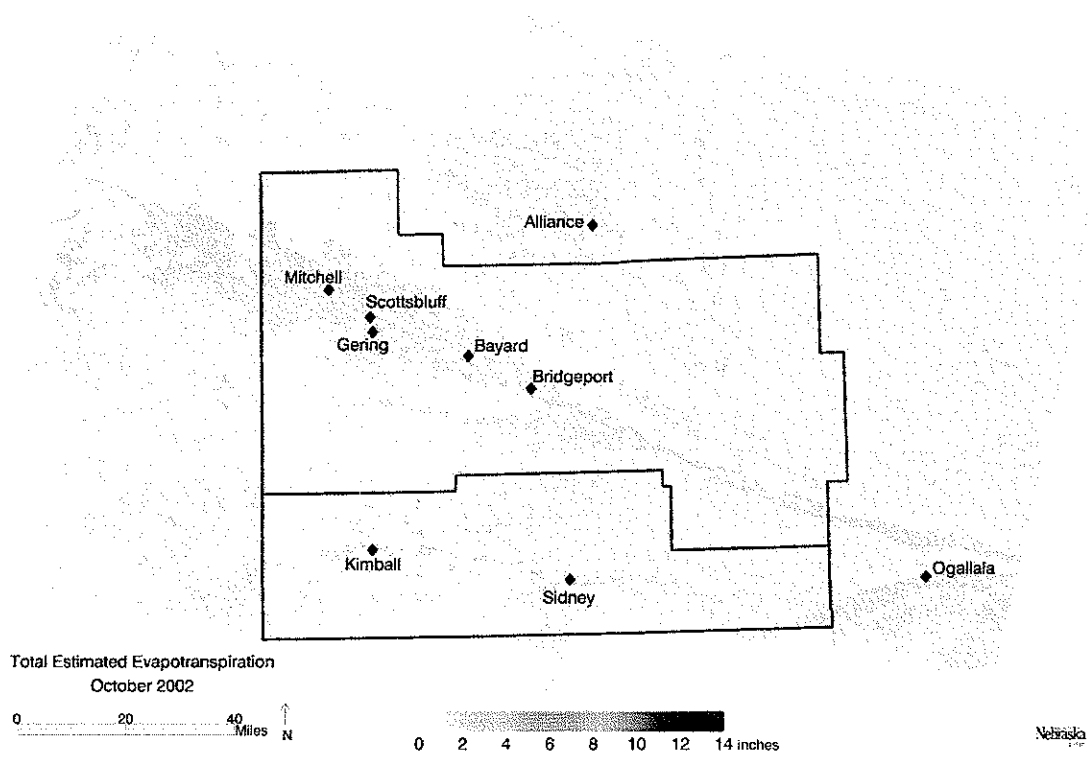


Figure 4. Monthly ET generated from METRIC for Landsat path 32-33, row 31 for 2002. Blue lines indicate North Platte and South Platte boundaries.

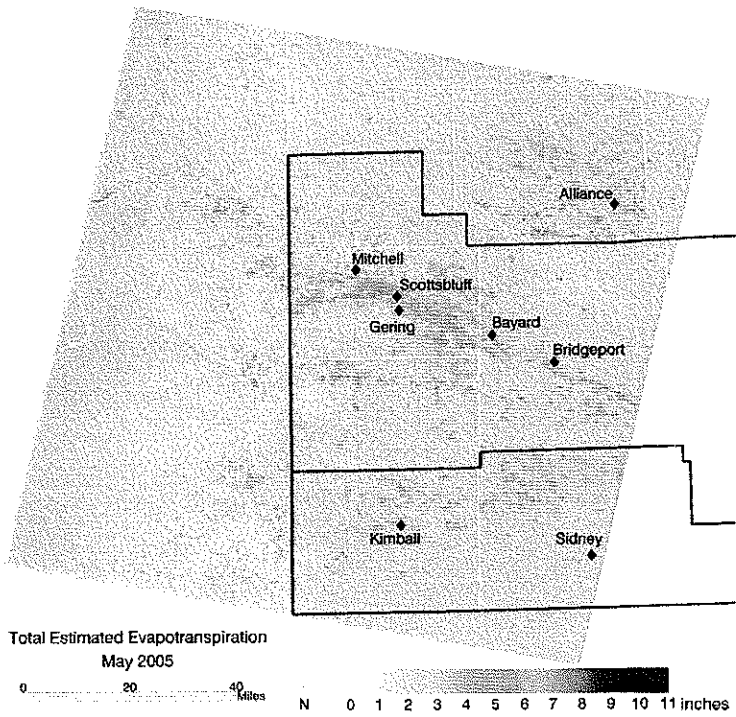
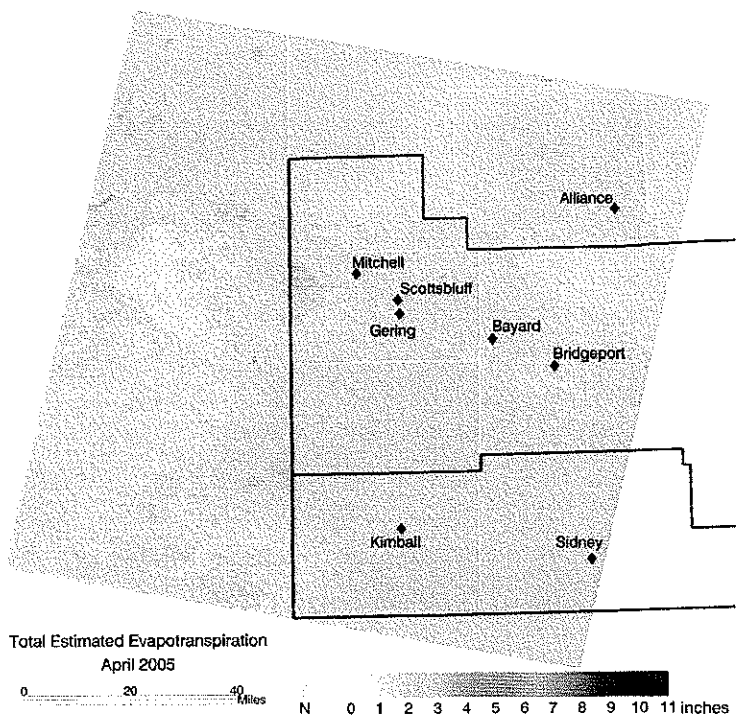


Figure 5. Monthly ET (April and May) generated from METRIC for Landsat path 33, row 31 for 2005. Blue lines indicate North Platte and South Platte boundaries.

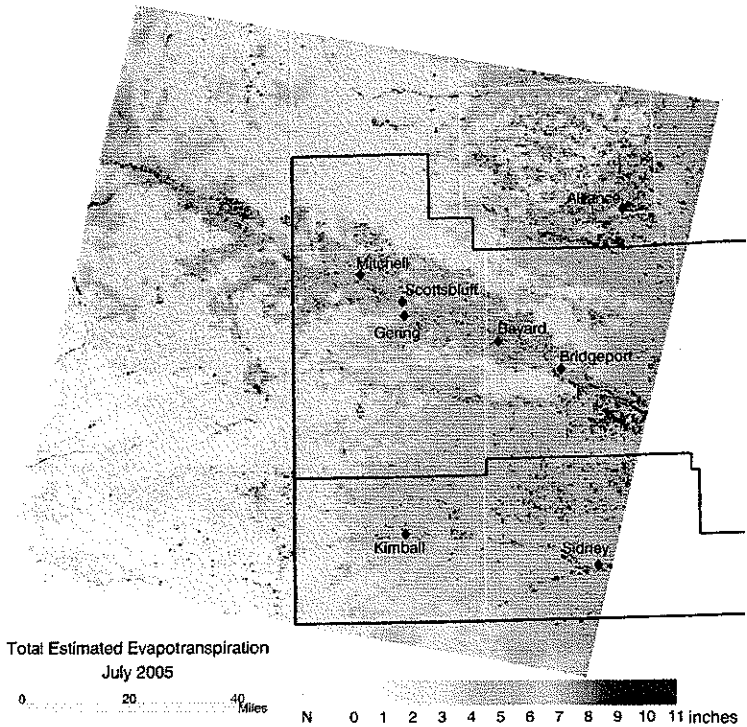
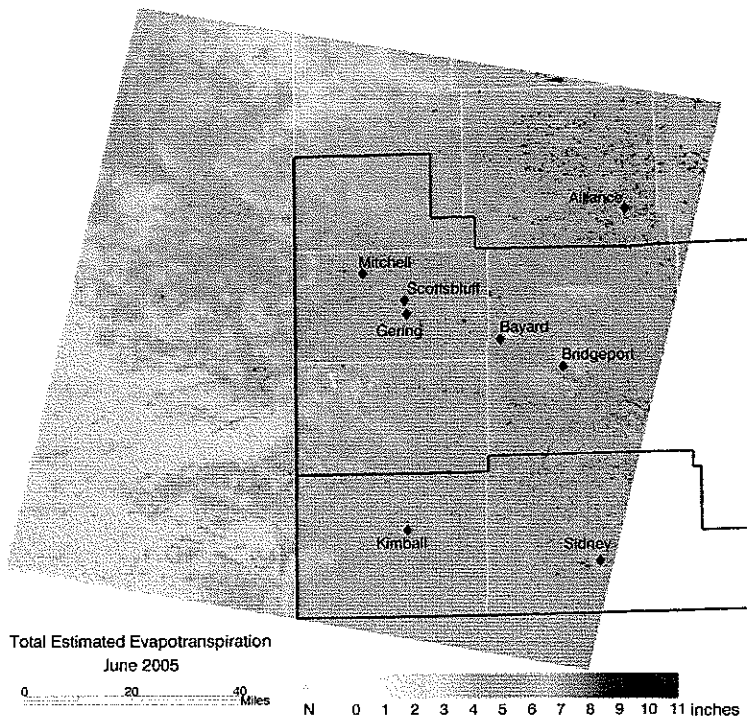


Figure 6 Monthly ET (June and July) generated from METRIC for Landsat path 33, row 31 for 2005. Blue lines indicate North Platte and South Platte boundaries.

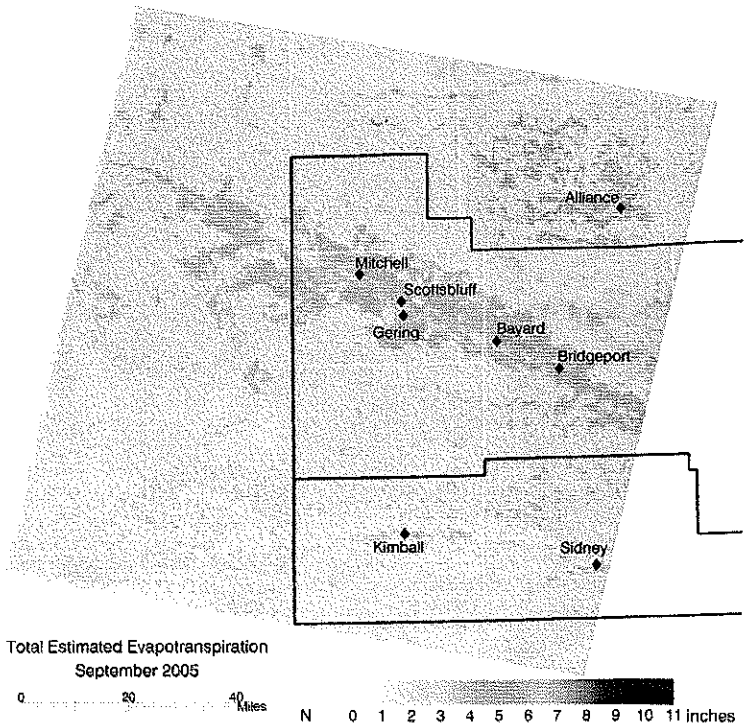
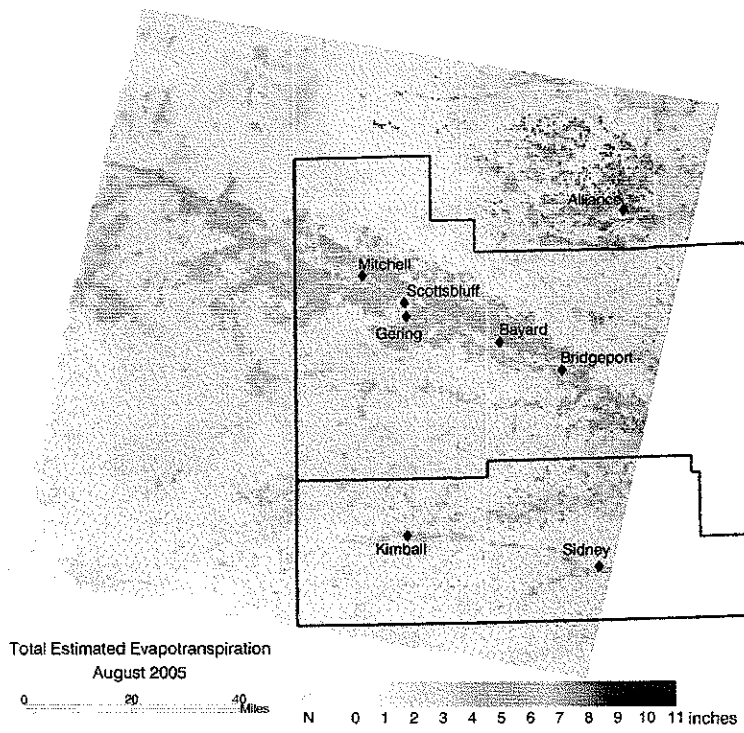


Figure 7. Monthly ET (August and September) generated from METRIC for Landsat path 33, row 31 for 2005. Blue lines indicate North Platte and South Platte boundaries

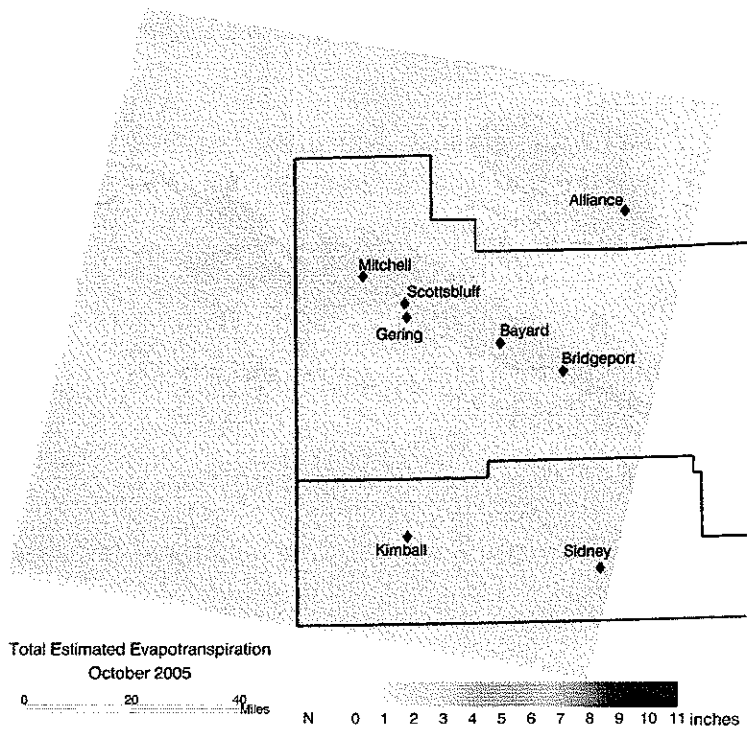


Figure 8. Monthly ET (October) generated from METRIC for Landsat path 33, row 31 for 2005. Blue lines indicate North Platte and South Platte boundaries.

Treatment of negative ET_{r,F}.

In some cases, due to statistical uncertainty and insufficient model calibration, some land use types may take on slightly negative values in the final ET_{r,F} map generated at each satellite image date due to uncertainties in the energy balance computations. During the calibration process, very dry desert areas are normally considered to have an ET_{r,F} close to zero. Due to the heterogeneity of the desert areas (slight differences in soil characteristics, vegetation and similar) the ET_{r,F} values will hover around zero, with some ET_{r,F} values slightly above zero while others are slightly below zero. When spatially averaged over a medium to large area, variations will tend to cancel out.

In the ET_{month} products generated from METRIC, a floor was applied so that negative values were set to zero. When generating the seasonal ET estimates from the monthly ET estimates, a possible negative estimate of ET in one month may somewhat counteract a positive ET estimate the following month which may lead to an overall underestimation in seasonal ET. Because for some land use types, such as desert where the negative ET values are countered by positive ET

values when viewed over a larger area (e.g. several km²), this may lead to a slight positive bias in the estimates

No floor was used when generating the $ET_{rF_{month}}$ product; hence the negative values are included in the $ET_{rF_{month}}$ maps. This will allow the user to avoid creating a bias from dry desert or similar areas when summarizing the values over a larger area.

e) Estimation of Seasonal ET and ET_{rF}

The seasonal estimate (April through October) of total ET, ET_{season} and seasonal ET_{rF} , $ET_{rF_{season}}$ were calculated as:

$$ET_{season} = \sum_{i=m}^n ET_{month} \quad (13)$$

Where ET_{season} is cumulative seasonal ET, and m and n are the first (m=4) and last (n=10) months of the season. $ET_{rF_{season}}$ was calculated as:

$$ET_{rF_{season}} = \frac{ET_{season}}{ET_{r_{season}}} \quad (14)$$

Where $ET_{r_{season}}$ is the seasonal ET_r acquired by summing the maps of total ET_r for each month. Results of the seasonal estimation of ET for 2002 and 2005 are shown in Figure 9 and Figure 10.

The primary focus in the application of METRIC in the south-west portion of the Nebraska Panhandle was to estimate the ET from irrigated and non-irrigated agricultural land (including range land). The ET_{month} and ET_{season} estimates from other land cover types such as for asphalt roads (including rural roads) have a high degree of uncertainty compared to other urban structures. The ET from a road is normally very low as the surface is almost impermeable so there is very little residual ET once the surface is dry. Excess water during precipitation events will either run off the road (often through storm drains) or removed by traffic, reducing the annual evaporation from the road surface to as little as 10 % of the precipitation.

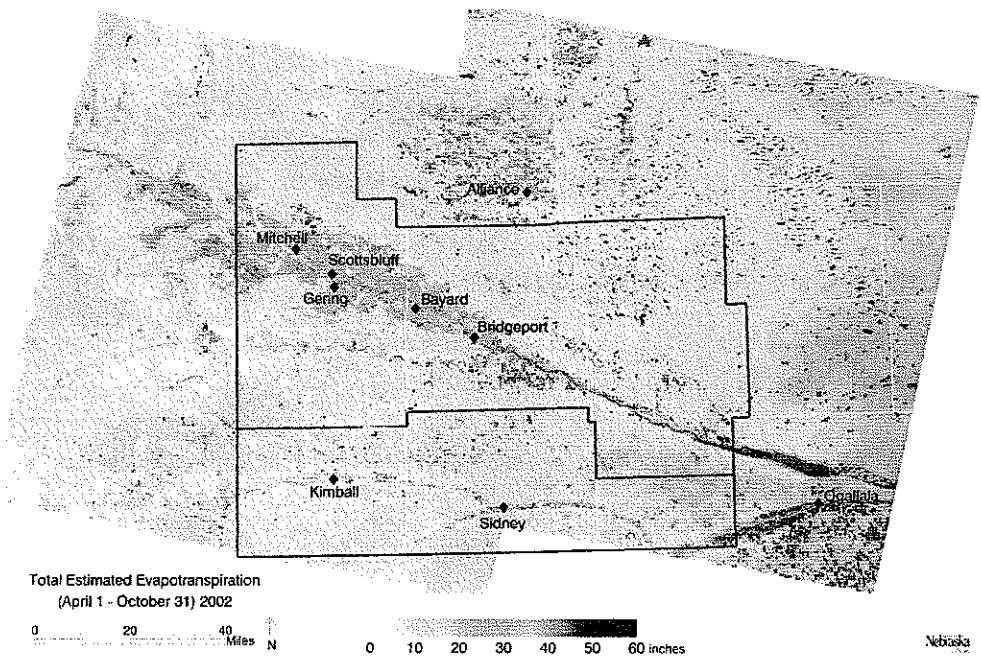


Figure 9 Total growing season (April through October) ET for 2002 Landsat path 32-33, row 31. Values are in inches.

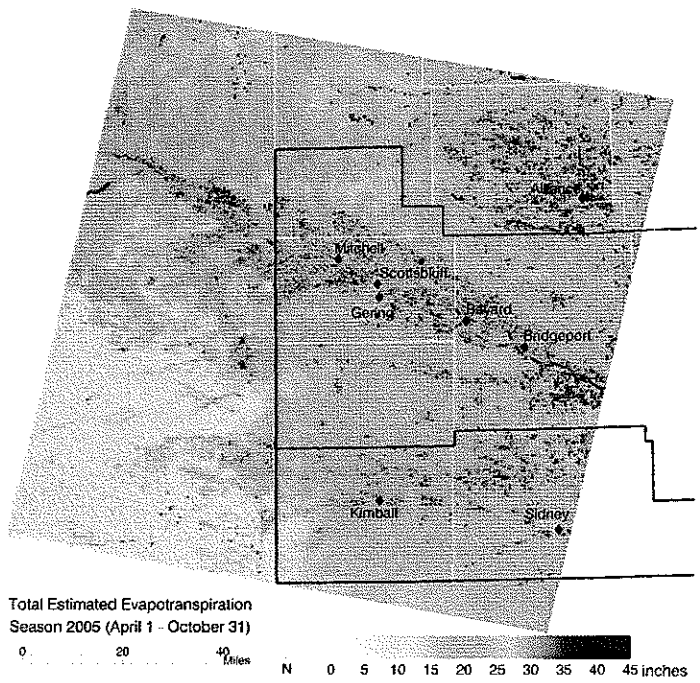


Figure 10 Total growing season (April through October) ET for 2005 Landsat path 33, row 31. Values are in inches

References

Allen, R.G. (2009). "Methodology for adjusting METRIC-derived ET_F Images for Background Evaporation from Precipitation Events prior to Cloud filling and Interpretation of ET between Image Dates." Note. University of Idaho, Kimberly R&E Center, Kimberly, Idaho. 11 pp.

Allen, R.G., Tasumi, M., Trezza, R., Kjaersgaard, J.H. (2010). "METRIC Applications Manual." Version 2.0.6. University of Idaho, Kimberly, Idaho. 164 pp.

Tasumi, M., Trezza, R., Allen, R.G. 2005. Operational aspects of satellite-based energy balance models for irrigated crops in the semi-arid U.S. *Irrigation and Drainage Systems*, 19: 355-376.

Trezza, R., Allen, R.G., Garcia, M. (2007). "Methodology for Cloud Gap Filling in METRIC." University of Idaho, Kimberly, Idaho. 7 pp.

Trezza, R., Allen, R.G., Garcia, M., Kjaersgaard, J.H. (2008). "Using a Cubic Spline to Interpolate between Images." University of Idaho, Kimberly, Idaho. 9 pp.

APPENDIX H

'Value-added' products from METRIC Evapotranspiration and Crop Coefficient Maps

Rick Allen¹, Ayse Irmak², Gary Hergert³, Jeppe Kjaersgaard¹, Ian Ratcliffe²
22 October, 2010, revised 24 October, 2010, Feb. 5, 2011.

The North Platte and South Platte Natural Resources Districts (NRD) and USDA-NRCS have funded work by the University of Nebraska and University of Idaho to produce monthly and growing season evapotranspiration (ET) over major areas of the North Platte and South Platte NRDs for years 1997, 2002 and 2005. These ET maps show water consumption at 30 m detail that can provide useful information for assessing:

- field to field variability in ET
- crop to crop variability in ET
- spatial variation in ET regionally
- crop coefficients specific to the Panhandle area
- water consumption by water source
- water consumption by user group
- water consumption by location
- differences among years caused by
 - precipitation differences
 - relative ET demands caused by weather differences
 - cropping patterns
- impacts of types of agriculture and irrigation systems
- impacts of land use.

The above information is useful for designing programs for managing overall water consumption within the NRD's and for preparing hydrologic and conformance reports. The value added products listed above can be derived from Geographical Information Systems (GIS). These systems are designed to organize and present spatial information and lend themselves to improved visualization of water consumption information. Current (GIS) capabilities of the two NRD's should be sufficient to derive water consumption products from the METRIC products.

The following is a detailed list of GIS based products that can be created within the NRD's by GIS specialists. The University of Nebraska can provide guidance on the creation of these products:

¹ University of Idaho, Kimberly, Idaho

² University of Nebraska, Lincoln

³ University of Nebraska, Scottsbluff

1. **Crop water use (CWU)** from irrigated lands
 - using GIS, CWU can be quantified in terms of
 - total ET from a land parcel
 - ET of irrigation water (that ET that is above the ET component of natural precipitation)
 - The CWU can be in the form of spatial maps or presented as means and variances of CWU aggregated over larger areas
 - CWU from ground-water (GW) vs. surface-water (SW) sources
 - CWU by crop type
 - CWU by land use
 - CWU by Year (1997, 2002, 2005)

2. **CWU from nonirrigated land** including natural vegetation such as riparian systems.
 - CWU from riparian systems and how it varies as a function of
 - location
 - vegetation density
 - vegetation type
 - understory
 - depth to ground water
 - invasive species control
 - CWU by location and type of rangeland
 - CWU (and ground-water recharge) by type of fallow farming (continuous vs. every other year)

3. **Crop Coefficients** during peak periods and over annual periods
 - by crop
 - by Year (1997, 2002, 2005)
 - Aggregated spatially across the NRD
 - Aggregated spatially by Water Source or by Stream Basin
 - by NRD or sub-NRD or water source
 - to provide spatial contrast in relative water use
 - to indicate differences among relative water use (i.e., Kc) among years
 - due to relative water supply
 - due to implementation of any curtailment programs or policies

4. **Crop Coefficients** for monthly and shorter periods. Crop coefficient (Kc) information has been created from the METRIC procedure on a monthly basis. When combined with spatial information on crop types (i.e., crop classifications) for the three years processed, Kc data can be sampled by crop type. Kc curves can be created by averaging among many fields having the same crop type and then splining between Landsat image dates (Tasumi et al., 2005; Singh and

Irmak, 2009⁴). For example, the following figure 1 shows a crop coefficient curve developed for dry beans in the Twin Falls, Idaho vicinity using METRIC produced ET from year 2000. Several hundred bean fields were sampled and averaged (grey symbols and curve). The METRIC derived Kc curve is compared in the figure with Kc based on a standard Kc curve produced by the US Bureau of Reclamation Agrimet⁵ system that is traceable to lysimeter-based Kc data collected by Wright 1981⁶) and is compared to Kc by Allen and Robison (2007)⁷ that is based on the 'dual Kc' method where evaporation from wet soil is considered separately from transpiration and where estimates were made all twelve months of the year, including during the nongrowing season. The agreement among the three independent systems of Kc's is relatively good, indicating that the Agrimet and Allen-Robison curves are appropriate for the area. If the older published Kc curves were substantially different due to differences in assumed planting dates, or variety of crop, or water management, etc., they

⁴ Tasumi, M., R G Allen, R. Trezza, J. L. Wright. 2005. Satellite-based energy balance to assess within-population variance of crop coefficient curves, *J Irrig. and Drain. Engrg*, ASCE 131(1):94-109

http://www.kimberly.uidaho.edu/water/papers/remote/ASCE_JIDE_2005_Tasumi%20et%20al_p94.pdf

Singh R., and A. Irmak. 2009. Estimation of Crop Coefficients Using Satellite Remote Sensing *J Irrig. and Drain Eng.*, ASCE 135(5): 597-608.

⁵ <http://www.usbr.gov/pn/agrimet/>

⁶ Wright, J. L. (1981). Crop coefficients for estimates of daily crop evapotranspiration. *Irrig. Sched. for Water and Energy Conserv. in the 80's*, Am. Soc. of Agr. Engrs., Dec. 18-26.

⁷ Allen, Richard G. and Clarence W. Robison, 2007 ***Evapotranspiration and Consumptive Irrigation Water Requirements for Idaho***, Research Technical Completion Report, Kimberly Research and Extension Center, University of Idaho, Moscow, ID. <http://www.kimberly.uidaho.edu/ETIdaho/>

could be adjusted using the METRIC-based Kc curves.

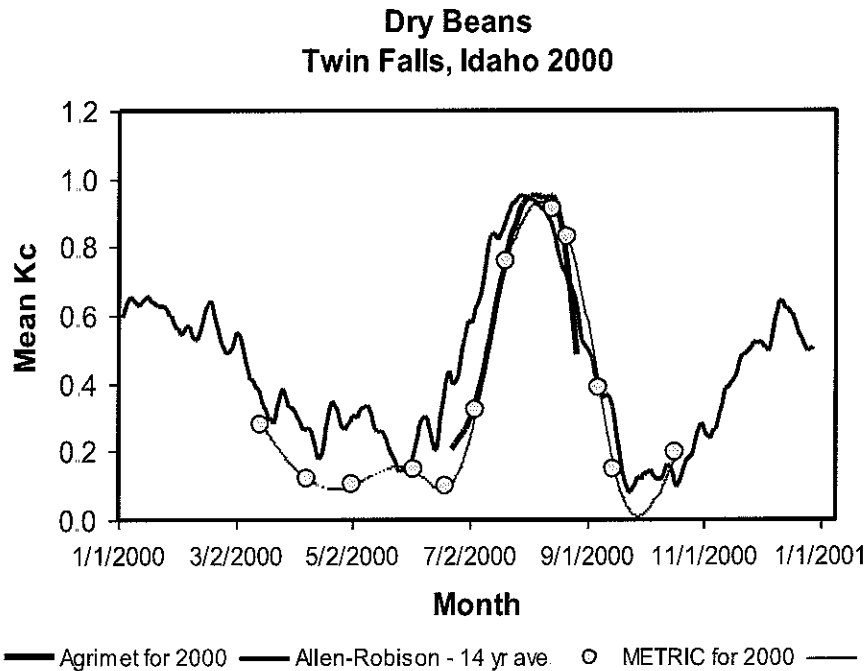


Figure 1. An average crop coefficient curve (grey symbols) developed for dry beans in the Twin Falls, Idaho vicinity using METRIC produced ET from year 2000. Also shown are Kc from a standard Kc curve published by the US Bureau of Reclamation Agrimet⁸ system and a Kc curve simulated from Kc tables by Allen and Robison (2007)⁹

The following figure 2 shows a sampling of Kc from about 700 corn fields in southcentral Idaho, where the Kc was derived from METRIC ET. In the figure, each vertical line represents a satellite image date and each small blue point represents the Kc of one field. The large black circles represent the average Kc on each satellite image date over all fields. Large variation in Kc early in the year was caused by wetness of individual fields.

⁸ <http://www.usbr.gov/pn/agrimet/>

⁹ Allen, Richard G. and Clarence W. Robison, 2007 *Evapotranspiration and Consumptive Irrigation Water Requirements for Idaho*, Research Technical Completion Report, Kimberly Research and Extension Center, University of Idaho, Moscow, ID. <http://www.kimberly.uidaho.edu/ETIdaho/>

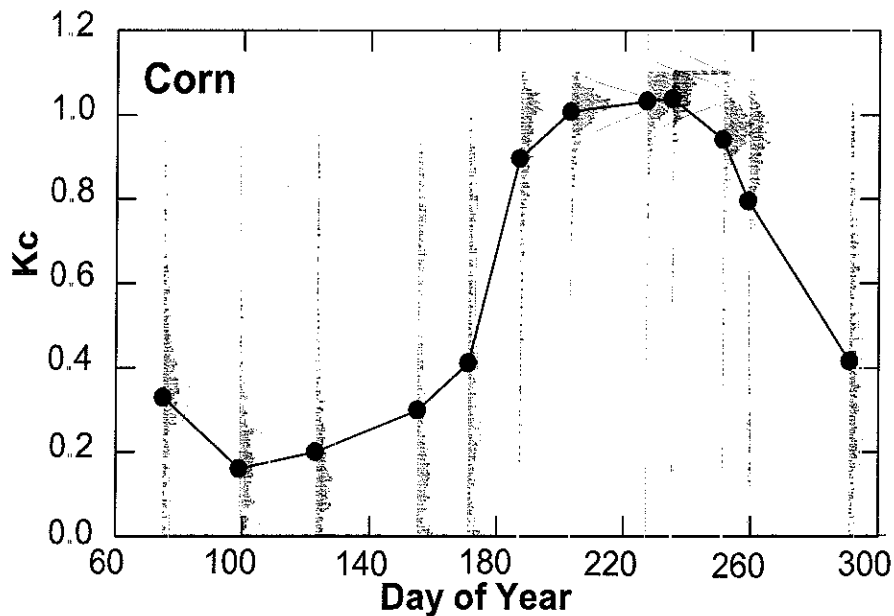


Figure 2. Kc on individual satellite image dates (vertical lines) and averaged Kc curve for the year (solid black symbols and curve) for southcentral Idaho as determined from METRIC ET.

5 Ground water Recharge

- Groundwater recharge (R) can be estimated from a water balance for an area as

- $R = P + I - ET - SRO$

where P = Precipitation, I = Irrigation and SRO = surface runoff, for time periods long enough that soil water storage can be neglected.

The ET can be based on the METRIC products

- by directly using METRIC for the years processed
 - by using ET from METRIC to calibrate a Kc x Reference ET method that can then be applied during nonMETRIC years. The Reference ET is based on weather data.
- The recharge estimate can be expressed on a growing season or annual basis (the annual basis is preferred to account for evaporation of P during wintertime. (However, METRIC based ET is generally not available for wintertime due to clouds.) Wintertime ET can be estimated from daily water balance models using precipitation and reference ET as inputs (for example, Allen and Robison, 2007 in Idaho and Hay et al., UNL in Nebraska). In addition, computer models that estimate daily evaporation from bare soil were prepared for the study area using gridded precipitation

and soil type data during the METRIC applications and can be made available.

The graphic shown in Figure 3 is an image of $ET - P$ during April – October, 1997. Because impacts of irrigation were not included, the image only shows estimated recharge in nonirrigated areas (expressed as negative $ET - P$). Irrigation areas stand out as positive $ET - P$. Figure 3 was taken from a presentation made at a remote sensing conference in Jackson, Wyo. in September 2010 (slide 19). The ppt is at: <http://www.kimberly.uidaho.edu/~rallen/Nebraska/>

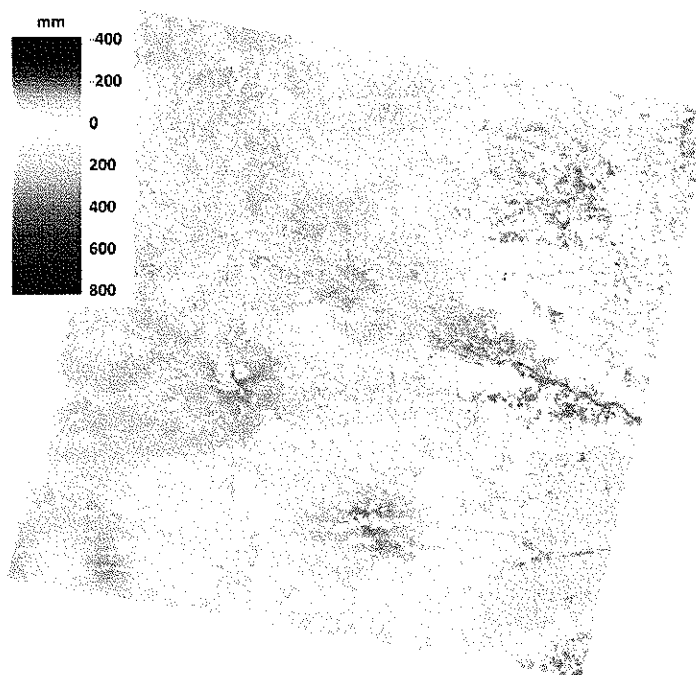


Figure 3. Growing Season (April 1 – October 31) evapotranspiration minus precipitation for 1997 for the south-west corner of the Nebraskan Panhandle. Positive values for $ET - P$ generally occur for irrigated areas where ET is supplied by irrigation in addition to P. Areas of negative $ET - P$ indicate areas of potential ground-water recharge.

One cautionary point in any analysis of $ET - P$ (or $P - ET$) where ET is taken from METRIC, is that the maps used for P need to be 'congruent' with the maps for P used in creating the METRIC product. In other words, it is beneficial if any biases in the precipitation products or grids, caused by interpolation or measurement biases, also appear in the ET estimate. This is important when calculating recharge as the difference between P and ET, where biases in R need to be minimized.

In the UI and UNL applications of METRIC, a gridded soil water balance / evaporation model was operated on a daily basis using maps of P for all three years and the estimated evaporation was used during the METRIC ET process for interpolation among satellite image dates to incorporate evaporation from rainfall events. Therefore, the ET maps from METRIC are 'biased' toward the particular precipitation maps utilized in the process model, so that recharge estimates should be less biased.

Annex A of this paper is a summary of how ET and recharge have been estimated in applications of a MODFLOW ground water model on the eastern Snake River Plain of Idaho. METRIC ET was used during those applications to calibrate crop coefficient x reference ET based methods that were, in turn, applied to other years.

- 6 Impacts of cultural practices on ET:
 - o no- or low-tillage cultivation vs. tillage cultivation
 - o pre irrigation vs. no pre-irrigation
 - o high plant population or narrow rows vs. low plant populationThese comparisons will require field by field information that is not available via remote sensing.
- 7 Variation in CWU by soil type.
- 8 Variation in CWU by basin: for example, Pumpkin Creek Basin vs. North Platte Valley (where annual allocations are currently 12 and 18 inches, respectively)
9. Comparison of CWU from METRIC with estimates by COHYST, etc.

Additional examples of spatial aggregation and expression of ET-based information are provided by the following illustrations. A number of other types of graphics are possible.

Performance of Irrigation Canal Companies

ET from METRIC can be aggregated over service areas of canal companies and then divided by measured diversions to determine 'performance' factors. The following figure shows an example for the Twin Falls Canal Company in Idaho, where precipitation over the service area was added to diversions to obtain an estimate of total water supply.

The second part of the figure shows a service area-wide crop coefficient, K_c .

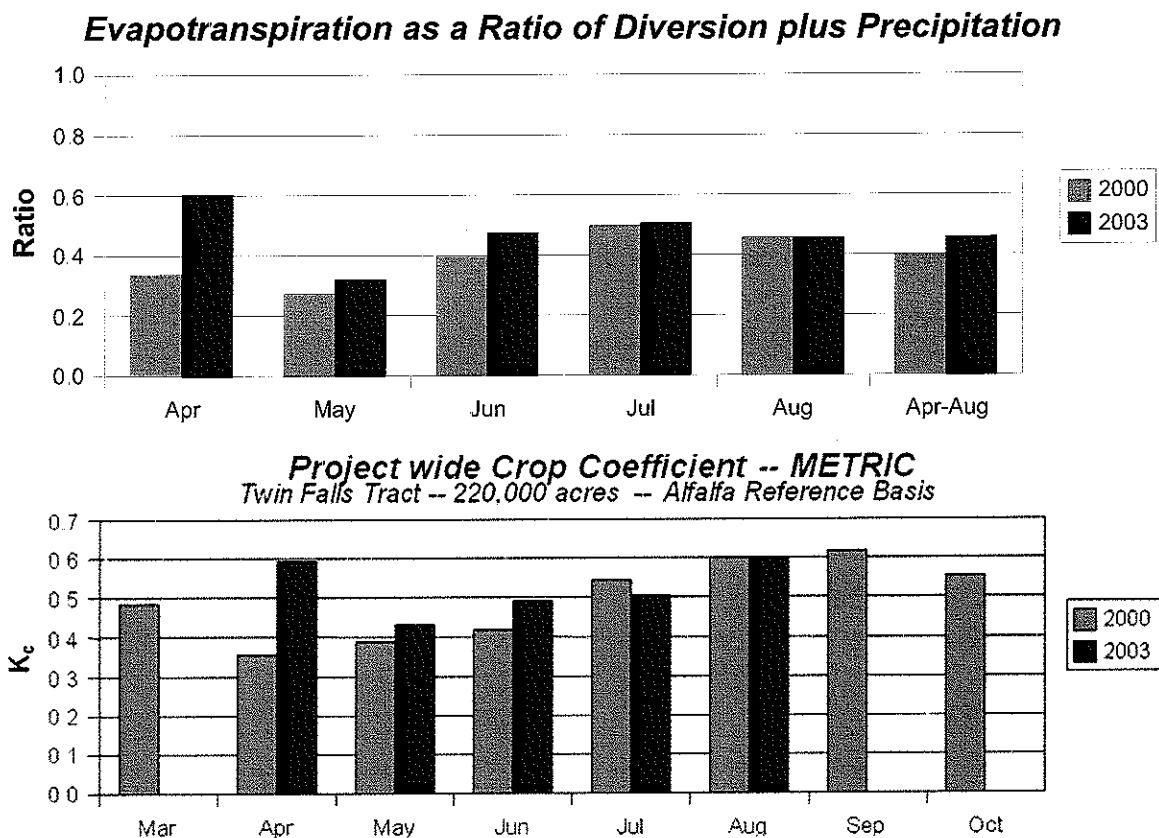


Figure 4. "Performance" of the 202,000 acre Twin Falls Canal Company tract of southcentral Idaho (top) expressed as the ratio of ET to the sum of canal diversions plus precipitation. Sept-Oct. 2003 ET data were not available due to clouded images. The bottom image shows a tract-averaged crop coefficient by month (alfalfa reference basis) (Allen and Robison, UI internal report, 2005). Diversions plus diversions less ET are anticipated to return to the fresh water system as surface return flow and as ground-water recharge.

Evidence of Curtailment of Irrigation or Retirement/Buyout of Water Rights.

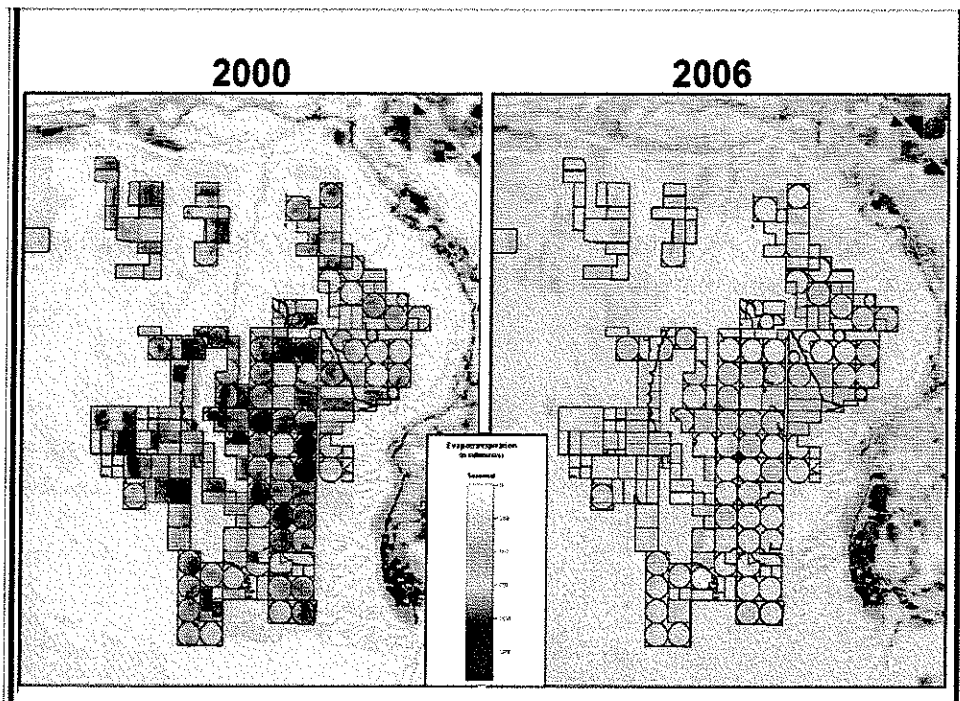


Figure 5. Growing Season (April – October) Evapotranspiration from the “Bell Rapids Mutual Irrigation Company” lands (~25,000 acres) during year 2000 and in year 2006, one year after selling rights to their water to the State of Idaho for Salmon Recovery. The ET in 2006 was from residual soil water storage. Water rights polygons are overlaid onto the ET map. Graphic from W. Kramber, IDWR 2009, pers. commun., ET data from Allen et al., UI, 2009.

Aggregation of ET by hydrologic basin .

Ground water modeling as well as surface water hydrologic water balances are often assessed on the basis of hydrologic unit (HUC). ET from METRIC can be aggregated over hydrologic units for use in water balances, estimation of recharge and sustainable ground-water depletions. An example is shown for the Tampa Bay, Florida area in Fig. 6.

A similar aggregation of ET for portions of the Imperial Irrigation District, showing contrasts between different years, is shown in Figure 7.

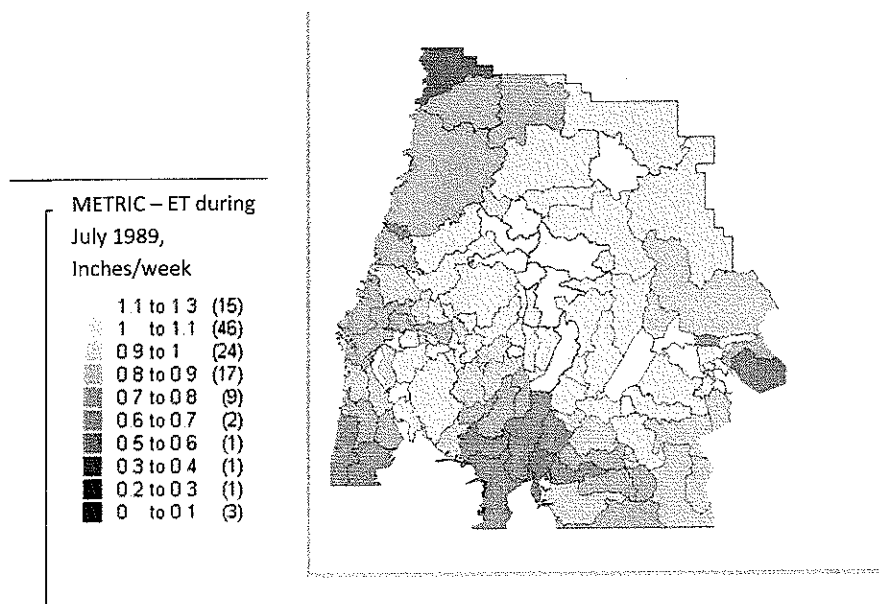


Figure 6. ET derived from METRIC and Landsat for the watershed source area of the city of Tampa Bay, Florida, aggregated by hydrologic unit. Data by R.Allen for Tampa Bay Water, 2002.

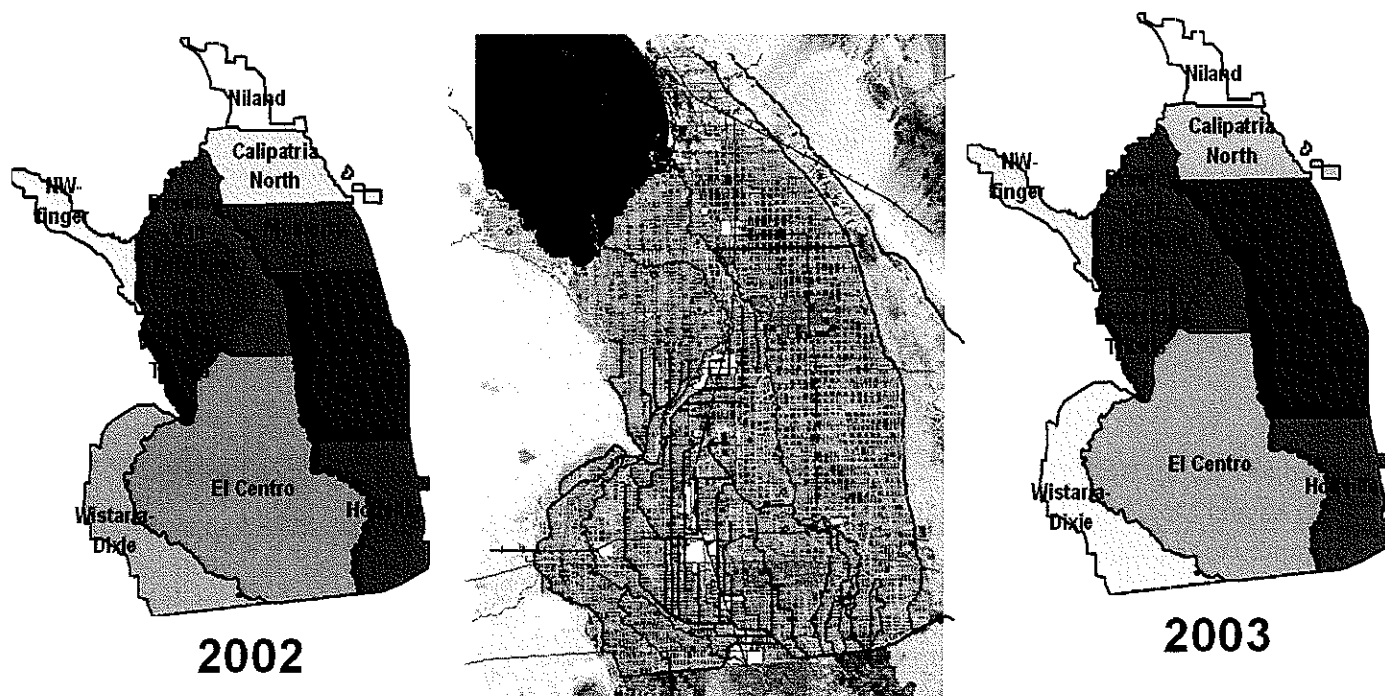


Figure 7. Relative depths of winter ET for vegetables, aggregated by Irrigation Management Area, within the Imperial Irrigation District of California. Data via METRIC by Allen et al., 2003.

Annex A.

Description on how Evapotranspiration is used in the Idaho Snake River Plain Aquifer Ground Water Model

Rick Allen, University of Idaho

Based on excerpts from a report by D. M. Cosgrove, B. A. Contor, G. S. Johnson. 2006. Enhanced Snake Plain Aquifer Model: final report. Idaho Water Resources Research Institute, University of Idaho, submitted to the Idaho Department of Water Resources (available at http://www.if.uidaho.edu/%7ejohnson/FinalReport_ESPAM1_1.pdf)

with some updates from material provided by B. A. Contor in January 2011.

The eastern Snake River Plain aquifer has a water volume the size of Lake Erie and supports nearly 2 million acres of irrigated agriculture. The aquifer is recharged by irrigation percolation; canal, stream, and river losses; subsurface flow from tributary valleys; and precipitation directly on the plain. The aquifer discharges to the Snake River, springs along the Snake River and to ground-water pumping, primarily for irrigation. Incidental aquifer recharge from irrigation is a significant component of the water budget and has varied as irrigation practices have evolved. The 1980 water budget of the USGS (Garabedian, 1992) shows that surface water irrigation contributes more than 50 percent of the total recharge to the aquifer. Historically, recharge from surface water irrigation increased as more land was brought into production up to the 1970s. Since the 1970s, a gradual conversion to sprinkler irrigation methods reduced the amount of incidental recharge from irrigation.

A transient version of the Eastern Snake River Plain Aquifer Model (ESPAM) has 44 6-month stress periods. The transient model is necessary to capture natural variation in water supply from year to year.

Recharge on Irrigated Lands

Irrigated agriculture having water supply from the river contributes a net recharge to the aquifer (surface-water irrigation) and ground-water pumping creates a net discharge from the aquifer (ground-water irrigation). Estimation of net recharge to the aquifer from surface-water irrigated lands requires measurement of surface water diversion, irrigation return flow, canal leakage, precipitation and evapotranspiration. The calculation is as follows:

Field Delivery from the river = Diversions - Canal Leakage - Return Flows

Net Recharge (surface) = (Field Delivery + Precipitation) – (ET x Adjustment Factor)

Ground-water pumping rates have only been measured since the mid-1990s on the ESRP. The measurement methods are not consistent throughout the plain, so measurement data are not reliable. Additionally, the data that do exist record gross pumpage and not net extraction. The lack of historical ground-water pumping measurement data and the lack of consistency in the measured data require an alternative method of estimating net discharge from ground-water irrigation. Net discharge from the aquifer from ground-water irrigated lands is estimated using evapotranspiration, offset by available precipitation. The rationale behind this method of estimation is that any ground water which is pumped in excess of crop demand (ET) will infiltrate back into the aquifer. The calculation is:

Net Discharge from aquifer due to pumping = (ET x Adjustment Factor) - Precipitation

When the precipitation exceeds the demand, there will be a net recharge to the aquifer on ground-water irrigated lands. When demand exceeds precipitation, there will be a net discharge.

The following section describes the approach used to estimate ET for the 2006 report when only one year of METRIC ET data were available

Crop Mix

Knowledge of the mix of grown crops is necessary for the estimation of ET. Differences in crop mix can change average ET by as much as ten percent, which translates into 1.7×10^{10} ft³ (400,000 AF), or approximately seven percent of the aquifer water budget, assuming two feet of ET on 2,000,000 irrigated acres and a 6,000,000 acre-foot aquifer budget. The final crop mix used for the ESPAM was calculated based on data from several sources of crop statistics data, as discussed below.

The primary data source is the National Agricultural Statistics Service (NASS) crop report data, which are based on county-wide surveys of farm operators. These data are available in three formats for the study area. These are the Published Estimates Data Base On Line (USDA, 2000), the US Agricultural Census (USDA, 1992, 1997) and the Idaho Agricultural Statistics (Idaho Department of Agriculture, 1981 - 2002) reports. The Published Estimates Data Base On Line (PEDB) version provides county-wide acres planted and harvested, by crop. These reports do not include alfalfa hay for the earlier years of the study, so 1982 and 1987 values from the US Agricultural Census (Ag Census) version of the NASS data for alfalfa were used. The Idaho Agricultural Statistics (IAS) report was used to fill in gaps in the PEDB potato data. The Agricultural Census reports provide more detailed results, including details of irrigated and nonirrigated acreage by county, for the years 1982, 1987, 1992, and 1997.

The IAS report is compiled from NASS data and includes yearly values for irrigated and non-irrigated acreage, by county, for major crops. As of the time of this study, the IAS data were available for years 1980 through 2001. Many of the county agents interviewed

recommended the NASS/IAS data

Growing season evapotranspiration was estimated primarily using an alfalfa reference ET scaled by crop coefficients. The alfalfa reference ET is available for each NOAA weather station within the ESRP. Allen (2002) evaluated five different ET calculation methods. The Kimberly-Penman Alfalfa Reference method was chosen as most suitable for the modeling application (Allen, 2003). This method was developed with Idaho empirical data and of the five methods is the most directly comparable to the reference ET reported in Estimating Consumptive Irrigation Requirements for Crops in Idaho (Allen and Brockway, 1983) data and to Agrimet (U.S. Bureau of Reclamation, 2003) estimates.

The selected data series provides only reference ET, but calculation of crop ET also requires crop coefficients (Kc values). Coefficients for individual crops were extracted from the original Allen and Brockway (1983) data by dividing individual crop ET by reference ET, for each weather station each month. The original data only include typically grown crops for each location. To avoid calculating zero ET if an atypical crop is grown, Kc values for all crops were assigned to all weather stations. Missing values were supplied from nearby stations. The variation of Kc between weather stations for any given crop is low (Allen, 2003). Because the data for each county include values for all typically grown crops, missing values represent rarely-grown crops. Therefore, this substitution will affect only a few acres within any stress period and has a very low potential of introducing error. An average Kc value was determined for each county which was an average, weighted according to the proportion of crops, from the nearest NOAA station data. This was performed for each model stress period.

ET estimation for this project included a remote sensing analysis of ET using the **METRIC** algorithm (Allen and others, 2002; Allen and others, 2005; Morse and others, 2000) for the 2000 growing season. METRIC results were used to calculate ET adjustment factors. ET adjustment factors allow adjustment of ET to account for deviations from a perfectly managed crop such as a) water shortage, b) crop disease or c) post-harvest watering. ET adjustment factors may also reflect differences in ET due to source of irrigation water or method of application. Unique ET adjustment factors were evaluated for a) sprinkler or furrow application, b) ground water or surface water source and c) irrigation entity. The METRIC analysis indicated that the Kimberly-Penman estimates of ET are consistent with crops which are furrow-irrigated, but that crops irrigated with sprinklers have approximately 5% higher ET. For the ESPAM calibration, ET adjustment factors were set at 1.0 for all furrow application and at 1.05 for all sprinkler application. For more information regarding ET adjustment factors, the reader is referred to ESPAM Design Document DDW-021.

Though crops do not actively transpire in the winter time, evaporation and sublimation continue. For the ESPAM, winter-time ET is based on experiment data collected over several years at Kimberly, Idaho.

(Wright, 1993). The average winter ET from the Wright study is reported in Table 8 taken from the Cosgrove et al. 2006 report

Table 8. Six-year average of measured lysimeter winter ET for Kimberly, Idaho.

| Month | Average ET, mm/day | Average ET, ft/month |
|----------|--------------------|----------------------|
| November | 0.7 | 0.069 |
| December | 0.4 | 0.041 |
| January | 0.6 | 0.061 |
| February | 1.0 | 0.093 |

The Idaho Recharge Calculation Tool.

The operation of the Fortran recharge tool implicitly adjusts for changes in ground-water use on mixed-source lands, by the process used to calculate net recharge. Within the tool, full irrigation requirement (consumptive use minus precipitation) is applied to all irrigated lands as an aquifer extraction. On lands with surface-water supplies, net surface-water application is applied as aquifer recharge, offsetting the required irrigation extraction. For each stress period and each surface-water irrigation entity, the net depth of surface-water application is calculated based on the diversion and return data for that stress period. The application depth is based on the full acreage of surface-water only parcels and a portion of the acreage (based on the source fraction described above) of mixed-source parcels. Then, within each model cell, the stress period- specific application depth is applied as an aquifer recharge. The applied water is pro-rated to mixed-source and surface-water-only parcels based on the source fraction. Where application exceeds irrigation requirement (surface-water-only parcels) a net recharge is inferred. Where irrigation requirement exceeds application (mixed-source parcels) a net withdrawal is inferred. On mixed-source parcels, in years with high surface-water supplies, the difference between irrigation requirement and surface-water supply is small and small amounts of net ground-water pumping on these mixed lands are represented in the model water budget. When surface-water supplies are low, the difference is large and large amounts of ground-water pumping are represented.

